WATER COMPATIBLE MOLECULARLY IMPRINTED POLYMERS
FOR THE RECOGNITION OF
BIOLOGICALLY ACTIVE COMPOUNDS IN AQUEOUS MEDIA

Dissertation

Dipl-Chem. Panagiotis Manesiotis

Universität Dortmund, Institut für Umweltforschung

Oktober 2005

WATER COMPATIBLE MOLECULARLY IMPRINTED POLYMERS FOR THE RECOGNITION OF BIOLOGICALLY ACTIVE COMPOUNDS IN AQUEOUS MEDIA

Dem Fachbereich Chemie der Universität Dortmund

zur Erlangung des akademischen Grades eines

Doktor der Naturwissenschaften

(Dr. rer. nat.)

vorgelegte Dissertation

von:

Dipl-Chem. Panagiotis Manesiotis

geboren am 28.03.1979

in Korinthos, Griechenland

Betreuer : Priv. Doz. Dr Börje Sellergren

Koreferrent: Univ.-Prof. Dr Christof M. Niemeyer

Universität Dortmund, Institut für Umweltforschung

Oktober 2005

Acknowledgements

Throughout my work that led to this doctoral thesis I had the opportunity and pleasure to meet, collaborate and interact with several persons, whose contribution made life, the universe and… everything, a better place to be. These persons I would like to thank in this short foreword…

(*Karl* and *Maria-Anna* as well), *Issam Lazraq*, *Dr Eric Schillinger*, *Dr Jeroen Verhage* (otherwise known as "Μήτσος"), *Filipe Vilela*, *Bettina Hofmann* and *Kim Schwarzkopf* (the "apprentices").

Prof. Dr Klaus K. Unger and the "Ungerverse" from *Johannes Gutenberg Universität Mainz*, where everything started, for the great welcome and quick incorporation in the group. Especially, *Jakob T. Mossing*, who made the first steps in the riboflavin/uracil project and spent a lot of time in bringing me up to speed before leaving, *Dr Vassilis Stathopoulos*, who spent only a small period of time in Mainz, but made a lot of difference in the general understanding of things and the way days go by (e.g. φραπέ και τάβλι), *Dr Sandra Pati*, for being a great friend and for a great guided tour of Rome, and *Dr Bernd Mathiasch* for introducing me to NMR spectroscopy in practice and for all the help he offered with NMR titrations.

Dr Anthony Rees, *Dr Ecevit Yilmaz*, *Brian Boyd* and *Christian Svensson* from *MIP Technologies*, Sweden, for a greatly educating week in Lund and for the flawless collaboration in the development of the riboflavin imprinted polymer.

Prof. Gianluca Ciardelli and the Biomedical Research group in Pisa, for a great week in Italy, in scientific and recreational matters. Especially, *Davide Silvestri*, my main collaborator there, for the introduction to membrane science, and *Alfonsina Rechichi*, whose stay in Dortmund for two weeks forced for me to finally understand the grafting techniques.

Dr Paul Hughes and *Dr Eric Brouwer* from *Heineken Technical Services*, Zoeterwoude, the Netherlands, for the perfect cooperation and the donation of beer samples (usually in large volumes) for mainly research purposes. Cheers!

Last, but certainly not least, *Despina Economopoulou*, my beloved girlfriend, whose support throughout my doctoral work was invaluable, my family, farther *Georgios*, mother *Vasiliki*, sister *Katerina*, and all my friends for the moral support and tolerance all these years… Σας ευχαριστώ πολύ!

Table of Contents

1 Zusammensfassung

Ihm Rahmen meiner Dissertation habe ich mich mit dem Design, der Synthese und der Evaluierung molekular geprägter Polymeren (Molecularly Imprinted Polymers), welche wasserlösliche, biologisch relevante Substanzen binden können, beschäftigt.

Dabei werden verschiedene Ansätze auf dem Weg zur Erkennung ausgewählter biologisch aktiven Substanzen diskutiert. Das Hauptaugenmerk lag auf der Entwicklung geprägter Materialien zum selektiven Entfernen von Riboflavin, einem wasserlöslichen Vitamin des B Komplexes (B_2) aus einer komplexen Matrix, zumeist Lebensmitteln, ohne Auswirkung auf die Zusammensetzung des Produktes. Der erste Projektteil wurde finanziert von Heineken Technical Services (Zoeterwoude, Niederlande) mit der Aufgabenstellung, Riboflavin selektiv aus Bier zu entfernen, um im Rahmen fortlaufender Untersuchungen die Rolle des Riboflavin auf die Geschmackstabilität zu verstehen.

Um ein erfolgreich geprägtes Material für das gewählte Zielmolekül zu erhalten, ist die Wahl eines geeigneten funktionellen Monomers oder eine Kombination solcher wichtig, um somit ein Optimum an Bindungsstärke zu erzielen und so zu einer großen Zahl an selektiven Bindungsstellen zu gelangen. Das Monomer wurde ausgewählt aus verschiedenen synthetisierten Substanzen für die Erkennung von Uracil, respektive dem in organischen Lösungsmittel löslichen 1-Benzyluracil, welches die gleichen Akzeptor-Donor-Akzeptor-Wasserstoffbrücken ausbilden kann wie Ribolflavin. Die Monomere wurden mittels ^{1}H-NMR-Titrationsexperimenten und Evaluierung der zugehörigen Polymersysteme getestet und somit konnten die besten für das Target Ribolfavin ausgewählt werden.

Riboflavin gehört zu den wasserlöslichen Vitaminen aber ist unlöslich in den im Imprinting üblicherweise verwendeten Lösungsmitteln. Dies machte eine Substitution des Originalmoleküls notwendig, wobei das Analogon die nahezu gleiche Größe, Form und Funktionalität besitzen sollte aber signifikant besser löslich sein muß in Lösungsmitteln, wie Acetonitril, Chloroform, Toluol usw.

Anfängliche Versuche mit käuflichen Flavinderivaten ergaben aufgrund der zu großen Unterschiede zu Riboflavin nur schlechte Ergebnisse. Anschließend wurden über eine vierstufige Synthese verschiedenen Alkylflavine als Templatkandidaten hergestellt. Trotz der stark verbesserten Löslichkeit zeigten die geprägten Polymere wiederum nur unzureichende Eigenschaften. Die Lösung dieses Problems ergab sich schließlich durch einen käuflichen Riboflavintetraester, dem Tetrabutyrate, welches zur Synthese einer kleinen Serie verschiedener Tertraalkylester inspirierte. Die Evaluierung der hergestellten Polymere zeigte, daß das kleinste Derivat, das Tertraacetat von Riboflavin, als Riboflavin-analoges Templat in Frage kam.

Bis zu diesem Punkt wurden alle Polymere mit dem gängigsten Vernetzer im molekularen Prägen, dem Ethylenglykoldimethacrylat, hergestellt. Da die Bemühungen darin bestanden, Materialien für den Einsatz in wasserreichen Medien mit minimaler unspezifischer Bindung herzustellen, wurde versucht in neuen Materialien die verbesserten Bindungsstellen aus dem beschriebenen rationelle Design mit einem wasserkompatiblen Rückgrad zu verbinden.

Als erste Möglichkeit kam das weit verbreitete hydrophile Comonomer 2-Hydroxyethylmethacrylat in Frage. Zwar konnte damit die unspezifische Bindung leicht reduziert werden, allerdings wurden auch die Erkennungseigenschaften minimiert. Die Alternative, der hydrophile Vernetzer Pentaerythritoltriacrylat, der zugleich dazu führt, daß das Polymerrückgrat hauptsächlich aus Vernetzereinheiten besteht, erwies sich dann als erfolgreich. Die so hergestellten Polymere zeigten nicht nur eine sehr geringe unspezifische Bindung, sondern auch einen starken Anstieg der Bindungscharakteristika und der Selektivität. Dies konnte dann in Anwendungen bei der Extraktion von Riboflavin aus Multivitaminproben, Milch und Bier gezeigt werden. ITC-Experimente (Isothermal Titration Calorimetry) indizierten, das diese synthetischen Materialien dem natürlichen Riboflavinrezeptor, einem Protein, überlegen sind.

Weitere Optimierungsversuche mit Polymerisationen bei niedrigeren Temperaturen und mit anderer hydrophiler Vernetzer zeigten keine signifikante Verbesserung. In einem Versuch die Bindungsstelle des natürlichen Rezeptors nachzuahmen, wurde eine Serie aromatischer Comonomere eingesetzt. Dabei soll die Bindung im Protein durch einen

Tryptophanrest nachgeahmt werden, der mit dem Riboflavin π-π-Wechselwirkungen eingeht. Leider führte dies zu einer Erhöhung der unspezifischen Bindung, was eine Verwendung ausschließt.

In einem abschließenden Schritt sollte eine weitere Hydrophilisierung des bisher optimalen Materials durch teilweise Hydrolyse der nicht umgesetzten Doppelbindungen des Vernetzers zu weiteren Hydroxylgruppen erfolgen. Tatsächlich erfolge eine Erniedrigung der unspezifischen Bindung und eine Erhöhung der Retentionszeit des Riboflavins auf dem geprägten Polymer. Dieser Effekt wurde durch Frontalanalyse bestätigt, womit sich das Potential der teilweisen Hydrolyse für die Erzeugung wasserkompatibler geprägter Polymere bestätigte.

Parallel zu diesem Hauptprojekt, konnte ich meine erworbene Expertise in NMR- und UV-basierten Untersuchungen von funktionellen Monomeren auf weitere laufende Projekte innerhalb des Arbeitskreises anwenden. Das Ziel was insbesondere die Erkennung der Glutaminsäure durch die Bindung der Carboxylatgruppe über Harnstoff-basierte Monomere und deren Auslese durch ^{1}H-NMR- und UV-Titrationen. Der stärkste Wirt wurde erfolgreich für die Synthese molekular geprägter Polymere mit gesteigerter Enantioselektivität eingesetzt. Dabei konnte mit einem Monomer auch eine Farbänderung bei der Bindung/Abspaltung beobachtet werden.

Zusammenfassend ist zu sagen, dass im Rahmen dieser Arbeit durch Optimierung der Polymermatrix und durch Maßschneidern der Bindungseigenschaften der funktionellen Monomere eine verbesserte Bindungsstärke und Selektivität im geprägten Polymer erzielt werden konnte. Wenn man die bekannten Vorteile der geprägten Polymere, wie die Robustheit sowie die thermische und chemische Stabilität mitberücksichtigt, konnte gezeigt werden, dass durch rationelles Design, geprägte Materialien mit einzigartigen Eigenschaften zugänglich sind.

2 Summary

This thesis describes the design, synthesis and evaluation of molecularly imprinted polymers (MIPs) targeting water soluble compounds of biological importance.

Throughout this manuscript, the approaches taken towards the recognition of the selected biologically active compounds will be discussed. The main effort was focused towards the development of an imprinted material that would be able to selectively remove riboflavin, a water-soluble vitamin of the B complex (B_2), from complicated, mainly food matrices, without otherwise affecting the composition of the product. The initial stage of the research was sponsored by Heineken Technical Services (Zoeterwoude, The Netherlands), whose main interest was the selective removal of riboflavin from beer, as part of the continuing effort to understand the role of riboflavin in beer flavour instability.

In order to achieve a successful imprinting of a selected target, it is important to choose the proper functional monomer (or combination thereof), which will provide the optimum binding strength that will eventually lead to an increased number of selective binding sites in the resulting polymer. The monomer for this particular target was selected by a parallel route during this work, namely the screening of different synthesised host monomers for the recognition of uracil, in particular an organic solvent soluble derivative of uracil, 1-benzyluracil, which possesses exactly the same hydrogen bond Acceptor – Donor – Acceptor triad as the one present in riboflavin. A series of monomers were tested, by means of ^{1}H-NMR titration experiments and evaluation of the corresponding polymers, and the best ones were selected for targeting riboflavin.

However, riboflavin, belonging to the water-soluble vitamins group, is not soluble to any of the organic solvents used in molecular imprinting. Therefore, there was need for substitution of the original target with an analogue molecule of as similar size, shape and functionality as possible, but with significantly higher solubility in solvents commonly used in molecular imprinting, e.g. acetonitrile, chloroform, toluene etc. Initial attempts included a commercially available flavin-like molecule, phenyl flavin, which soon proved

to be a poor choice, due to significant shape and size differences to riboflavin. Then, a four step synthetic protocol towards the synthesis of template candidates was developed, leading to several substituted alkyl flavins. The solubility was significantly improved, however, the structure of these molecules prove to be once again not optimal for them to be successful replacements for riboflavin in the imprinting process. The riddle was finally solved with the discovery of a commercially available riboflavin tetra-ester, riboflavin tetrabutyrate, and the thus inspired synthesis of a series of different alkyl tetra-esters. Evaluation of the synthesised materials has proven that the smaller synthesised analogue, namely the tetraacetate ester of riboflavin, was the best substitute for the targeted vitamin.

Up to this point, all polymers were synthesised based on the most commonly used cross-linker in molecular imprinting, ethyleneglycol dimethacrylate (EDMA), a cross-linking monomer that comprises both rigidity and moderate hydrophilic/hydrophobic character. However, the aim was to synthesise materials capable of operating in highly aqueous environments, with minimal to none non-specific binding. Efforts were focused towards the generation of materials that encompass both the enhanced binding sites generated with the aforementioned rational design, and a water-compatible polymer backbone. Towards this purpose, the use of a commonly used hydrophilic monomer, 2-hydroxyethyl methacrylate (HEMA), as co-monomer was first undertaken. Although the non-specific binding, as estimated by the binding of riboflavin on the control polymers, was marginally reduced, the recognition properties of the imprinted polymers were diminished. Thus, the use of a hydrophilic cross-linking monomer was decided as an alternative, supported by the fact that the polymer backbone is built mainly by cross-linker units. Pentaerythritol triacrylate (PETRA) was chosen as the first candidate, which prove to be a very successful selection, since the polymers produced by using it as cross-linker, not only exhibited significantly less non-specific binding, but also a dramatic increase in the binding characteristics and selectivity, as it has been shown by application of these materials in the extraction of riboflavin from multivitamin samples, milk and beer. Furthermore, Isothermal Titration Calorimetry (ITC) experiments indicated that the synthesised material outperformed the natural receptor of riboflavin, the Riboflavin Binding Protein.

Further optimisation attempts included polymerisation at lower temperatures and the use of other hydrophilic cross-linkers, but no significant improvement was achieved. In an attempt to mimic the binding site of the natural receptor, where the binding is facilitated by the presence of a tryptophan moiety offering π-π interactions with the iso-alloxazine structure of riboflavin, a series of aromatic monomers was included in the synthetic protocol, leading to an increase in the non-specific binding thus prohibiting the use of the materials for the designated purpose. A final step towards the further hydrophilisation of the optimal so far materials was through partial hydrolysis of the remaining unreacted double bonds of the cross-linker that should release more hydroxyl groups thus increasing the hydrophilic character of the polymers. Indeed a significant decrease in the non-specific binding was achieved, while the retention times for riboflavin on the imprinted polymers increased. The effect was confirmed by frontal analysis, highlighting the potential of this partial hydrolysis treatment for achievement of highly water compatible imprinted polymers.

In parallel to this main project, the expertise obtained in NMR and UV – based screening of functional monomers, was applied in an ongoing project within the working group, namely the recognition of amino acids, glutamic acid in particular, by targeting the carboxylic acid moiety. Thus, a series of amido-pyridines (for the recognition of the carboxyl group) and urea-based monomers (for the recognition of carboxylate anions) were screened by means of ^{1}H-NMR and UV titrations and the strongest hosts were successfully applied in the synthesis of molecularly imprinted polymers which exhibited enhanced enantio-selectivity and furthermore, in the case of urea-based monomers, they were optically active and displayed significant change in their colour upon binding/release of the template.

Concluding, throughout this work, it has been shown that by optimising the polymer matrix and by tailoring the binding properties of the functional monomers used in molecular imprinting, it is possible to achieve enhanced binding strength and selectivity, comparable to these of natural receptors. Taking into account the known advantages of imprinted polymers, e.g. robustness, thermal and chemical stability, it has been shown that by rational design, imprinted materials with unique properties are readily accessible.

3 Introduction

«*Τα πάντα ρει και ουδέν μένει*»; "*Everything is on the move, nothing is constant*".[1] *Heraclitus*, the famous Greek philosopher of the 6th century BC, used these words to portray his observation that the world around us is constantly changing. Many centuries later, in 1859, *Charles R. Darwin* published one of the most controversial but also influential books ever, that was meant to shape the modern world and our perception about life. In "*The origin of species*" Darwin suggested that nature is a dynamic system which through constant change is evolving and trying to reach perfection. The basis of evolution, and of life itself, is the constant effort to adapt to the surrounding environment, a process he called "*Natural Selection*".[2] In the molecular scale, it is the interactions between biomolecules, and the recognition that plays the main role in these interactions that is responsible for our existence. In other words, *molecular recognition*, the communication between molecules, and the vast number of consequences following the recognition event, is an essential part of life as we know it. The formation of cell membranes is based upon the interactions between phospholipids and proteins, organised in a way that protects the intracellular space but also allows the bi-directional flow of information. The DNA double helix, discovered by *J.D. Watson* and *F.H.C. Crick* in 1953,[3] is another marvellous example that underlines the importance of interactions between simple building blocks for our life. While single molecules base their existence on strong covalent bonds, complexes like the ones mentioned above are normally maintained by weaker binding forces, leading to dynamic, flexible systems that have the possibility of rapid organisation between different units, a process essential for a large number of natural processes such as DNA replication, enzymatic catalysis, protein biosynthesis and eventually to evolution itself.

Inspired by such marvellous examples of *molecular recognition* provided by nature, chemists have dedicated significant effort in mimicking these properties of natural systems[4] and utilise them in a series of different processes, including the synthesis of artificial receptors, highly specific catalysts and drug development. This trend caused the birth of the field and

term of *supramolecular chemistry*,[5] to describe the interactions taking place not within the same molecule or atom, a field which was extensively explored by chemists in the 19th century, but between different molecules, when they are found in close proximity.[6]

Traditional organic chemistry, studies mainly the creation and destruction of covalent bonds, the strength of which is responsible for keeping individual molecules together. However, the latter, mainly due to their robustness and the huge energetic barrier that prevents their creation and breakage at physiological conditions are not handy for the generation of flexible, reversible and dynamic systems such as the ones required by nature. This is why life has based its very existence mostly on weak forces between molecular species such as hydrogen bonds, ion pairing, and hydrophobic interactions. These forces are weak when considered individually however in a complex system, such as a cell membrane or an enzyme, a big number of such weak interactions are combined resulting many times in an end effect similar to the one of covalent bonds. Adding the adjustability and the possibility for correction in a very complex system further highlights the advantages of such systems.

How can we obtain such materials and use their benefits for our research? Scientists from different disciplines have worked out different methods that meet their needs, based on their background and expertise:

The first is to turn to biology, harnessing the immune system to raise an antibody to the compound of interest. This is now a routine exercise and there are numerous companies that can do it for a moderate fee, though antibodies are still too expensive for most applications in the chemical industry. Furthermore, objections raised by animal protection associations and environmental agencies, are pushing research away from the use of animals for such purposes.

A second possibility is to design and build a receptor molecule from scratch; chemists have synthesised a wide range of structures, including cages, bowls, clefts and crowns, from readily available precursors.[7-10] However, the time and expenses related to the synthesis of such artificial receptors, as well as the synthetic effort required, are often prohibiting, leading researchers to look for alternative solutions to their need for selective recognition.

Such an alternative is the preparation of *Molecularly Imprinted Polymers,* [11, 12] capable of combining the advantages of synthetic plastics, such as low cost, durability and robustness, with the recognition properties of natural receptors. Taking into account the ease of preparation without need for advanced synthetic skills explains the exponential growth in the number of researchers involved in the field of Molecular Imprinting within the last 20 years.

3.1 Molecular Imprinting

3.1.1 …explained in a few words

Molecular Imprinting exploits the simple, but elegant, principle of using elements of the target molecule to create its own recognition site. This is achieved allowing a template, e.g. an analyte of interest or an analyte closely related to it, to form complexes in solution with one or more polymerisable receptors that have the possibility to interact with this template in one or more ways, e.g. hydrogen bonds or ionic interactions. Then, a highly cross-linked polymeric matrix is formed around the template–functional monomer complexes by adding an excess of cross-linking monomer, thus "freezing" these interactions in such an arrangement that would allow subsequent re-binding of any analyte that has the correct size, shape and functionality to match the requirements of the so-called *binding site* (Figure 3.1). Thus, molecularly imprinted materials possessing binding sites with affinity comparable to the ones of natural receptors and with higher chemical and physical stability than their natural counterparts are readily accessible.
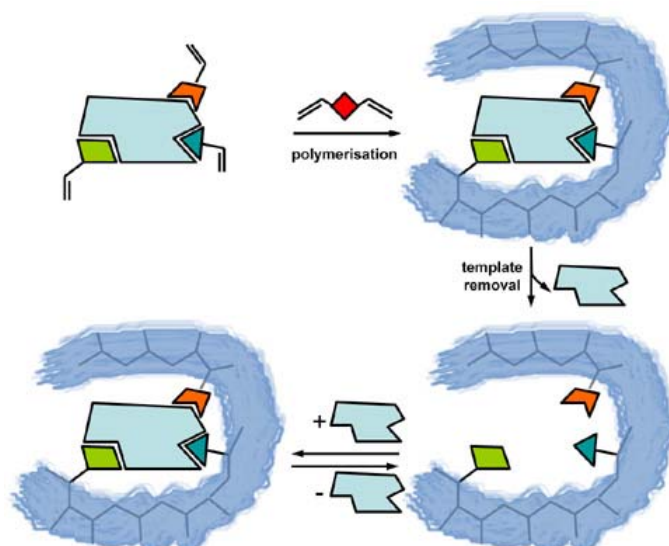
Figure 3.1   The principle of Molecular Imprinting

3.1.2   What are the potential targets?

A search in the recent literature reveals the diversity of templates used in Molecular Imprinting. These range from small molecules such as drug substances,[13] amino acids,[14-16] steroid hormones,[17-19] or metal ions[20-23] to larger molecules such as peptides[24-26] or proteins.[27-29]

Regardless of the size and shape of the template molecule, in order to achieve a successful imprint, it is necessary that the latter possesses at least one, preferably a combination of, functional groups that can be complexed by an available functional monomer. The probability that such groups exist increases of course with the size of the target molecule. However, there is an upper boundary to the size of a template, imposed by limitations in solubility and diffusion of the template in and out of the polymer matrix. This is the main reason why surface and scaffold imprinting techniques have so far been more successful in the recognition of biological macromolecules.[30]

3.1.3   MIPs vs. Host-Guest chemistry

By a first look, Molecular Imprinting can be considered a technique closely related to guest-host chemistry. Nonetheless, there is a significant difference between the two approaches towards molecular recognition; in host-guest

chemistry the aim is to prepare a synthetic host which comprises a series of functional groups placed in a particular order and in well defined positions, in one single molecule. The chemical effort required in order to achieve such a receptor unit is usually excessive. Imprinting overcomes this problem by holding the recognition elements in place, owing to their interactions with the template, while they are connected to a macromolecular scaffold *via* growing polymer chains. This allows the pathways between neighbouring groups in the recognition site to be of virtually any length through the cross-linked matrix, precisely matching the template's requirements. An analogy can be made with the structure of antibodies, where amino acid residues at the binding site are brought together by folding the protein chain. *Linus Pauling* once speculated that antibodies were synthesised to complement the "template" antigen. This insight proved to be incorrect, but was the first description of molecular imprinting.[31]

The synthetic effort required *en route* to an artificial recognition element has been the main reason for which most researchers involved in the field of molecular imprinting have limited their palettes of building blocks available for the creation of their artificial locks to the commercially available ones. However, although one could envisage a lot of potential combinations of building blocks just considering what one can find in the chemical catalogues, the very few examples of working groups,[32-34] including the one in which this project was carried out,[15, 16, 35-37] that have invested time and effort in the design of functional monomers, often inspired by outstanding examples from supramolecular chemistry, show that the effort is greatly rewarding.

3.1.4   *Thesaurus of terms used in Molecular Imprinting*

As the term states by itself, Molecular Imprinting makes use of molecules in order to generate imprints of the latter capable of subsequently recognising the same or closely related analytes. Throughout the years since the first report of the technique in 1972 as *enzyme-analogue built polymers* by the group of *G. Wulff*,[38] a number of creative expressions have been used to describe this technique including among others, "*host-guest polymerisation*",[39] "*template polymerisation*",[40, 41] creation of "*footprints*"[42]

and preparation of "*specific adsorbents*".[43] The term used today is fairly attributed to the group of *K. Mosbach*,[44] one of the most active groups in the field.

The terms used to name the different components employed in Molecular Imprinting technology emanate, as one would expect, from fields directly related to the technique. The term *template* is used in supramolecular chemistry to describe the blueprint on which a receptor is based. The rest of the terms used originate from polymer science. The monomer, or *functional monomer*, is the building block responsible for the introduction of functionality into the polymer matrix, complementary to the functionality present in the template molecule. The *cross-linker* is the component in excess in most polymerisation protocols, and being a di- or tri- functional monomer, it ensures rigidity and robustness of the final material. Being the component in excess it also determines the hydrophobic/hydrophilic character of the polymer as well as its swelling properties. In the traditional imprinting protocol, the materials are produced by solution polymerisation, meaning that the presence of a solvent (*porogen*), is also necessary, not only in order to generate a homogenous pre-polymerisation mixture where the template-monomer equilibrium can take place, but also to assist in the production of a porous polymer network, accessible for both the removal of the template as well as the re-binding of the analytes of interest. Finally, since most molecular imprinting protocols are based on free-radical polymerisations, a free-radical *initiator* is added, selected based upon the choice of thermal or photochemical polymerisation.[45]

3.1.5 Approaches to Molecular Imprinting

Depending on the background and expertise of each group involved in the field of Molecular Imprinting, a number of different approaches have been developed. Throughout the years since the initial reports, two main approaches to Molecular Imprinting may be distinguished. The *covalent* approach, developed by *G. Wulff* and co-workers,[38] where template-monomer complex is actually prepared in one or more separate steps prior to polymerisation by reversible covalent bonds. After polymerisation, these

reversible bonds are selectively cleaved and the recognition process takes place based on their re-formation upon contact of the template with polymer matrix. In an early example, D-glyceric-(p-vinylanilide)-2,3-o-p-vinylphenyl-boronate and divinylbenzene were co-polymerised and subsequent hydrolysis of the glycerate moiety revealed binding sites exhibiting enantio-selectivity for D-glyceric acid. The *non-covalent* approach, the most popular of the two due to its simplicity and multitude of combinations, was developed mainly by *K. Mosbach* and co-workers.[39, 46] Here, the pre-arrangement between the template and the monomer(s) is formed by non-covalent, or (weak) metal coordination interactions and subsequent recognition is dependent on these interactions. A third "hybrid" approach has been developed by the group of *M. Whitcombe*, taking advantage of a combination of these approaches.[47] This *semi-covalent* approach, makes use of strong covalent bonds in the imprinting step (as in the covalent approach), while non-covalent interactions are employed in the recognition process after cleavage of the template from the polymer. In a bibliographic example, the ester of 4-vinylphenol with cholesterol was used as a template. After co-polymerisation of the template with excess of cross-linker, the carbonate-bond was cleaved. The template was then washed out of the polymer to reveal binding sites containing a phenolic residue oriented in a manner that allows specific rebinding via non-covalent interaction with the hydroxyl group of cholesterol.

Each of the aforementioned approaches has their advantages and disadvantages. Choosing the proper approach depends to a great extent on the template at hand, as well as the applications in which these materials are requested to operate. The covalent and semi-covalent approaches have shown so far the best potential in generating well-defined homogenous binding sites with high affinity for their templates. Evidently, major limitations are imposed on these approaches since there are only a limited number of compounds or compound families that can be functionalised in a way that allows subsequent incorporation of them in a polymer matrix and reversible cleavage of their covalent bonds to the polymer chains. Additionally, there are only a few chemical reactions that can be utilised for the synthesis of such polymerisable templates, e.g. boronic esters, ketals or Schiff bases. Finally, the slow kinetics of rebinding, especially in the covalent approach, renders

these materials impractical for uses in chromatographic applications or solid phase extractions. Essentially, the same situation is true for the use of metal-coordination interactions, and therefore these approaches have enjoyed their principal success in rather specific systems.

The non-covalent approach is generally regarded as being of more versatile nature and can be applied to almost any type of template, since there is a large number of commercially available functional monomers with diverse functionality ranging from acidic (acrylic and methacrylic acid), basic (2- and 4-vinyl pyridine, 2-(diethylamino)ethylmethacrylate) or neutral (acrylamide, methacrylamide), hydrophilic (2-hydroxyethyl methacrylate) or hydrophobic (styrene, naphthyl methacrylate). On the other hand, since the forces stabilising the complexes between templates and monomers are usually very weak, the imprinting process usually leads to very heterogeneous materials, with a distribution of binding affinities ranging from very strong (well defined binding sites, fewer in number) to very weak (less defined binding sites, majority). Additionally, the number of parameters that need to be considered in this approach is larger, temperature of polymerisation, concentration of template and monomers, polarity of porogenic solvent being the most important of them. In spite of the above drawbacks, this approach has attracted the greatest number of researchers, and the majority of applications currently presented in literature comply with this technique.

In order to overcome the heterogeneity problem, researchers have embarked in the use of solid supports and immobilised templates in combination with a non-covalent imprinting step. Some remarkable examples were demonstrated by the group in which this work was carried out, including the immobilisation of small peptide sequences on silica beads and polymerisation of the monomer mixture in the pores of the silica support, which when followed by dissolution of the latter leads to the generation of replica particles containing well defined binding sites capable of recognising the template as well as larger peptides that contain the same terminal sequence.[26, 48]

3.1.6   Morphologies of Molecularly Imprinted Polymers

Up to this date, most imprinting protocols are based on solution polymerisation that leads to the generation of a monolith, which is subsequently washed, crushed and sieved in order to yield particles of different size depending on the intended application (e.g. 25-36μm for HPLC evaluation; 50-100μm for SPE protocols). However, partly due to the need for more homogenous particle size distributions and partly due to the need for higher yields of useful particles, several different configurations have been developed and used, that can be divided in three major categories: protocols leading to polymer beads, films or membranes and finally *in-situ* polymerisations in HPLC or capillary columns for direct use in chromatography. Here a few examples will be presented in order for the reader to obtain an overview of the methods used, except for the bulk polymerisation method, which has been employed throughout this project, and will be described in the following chapters.

3.1.6.a   Imprinted polymer beads

Almost all techniques used for the preparation of polymer beads have been adapted to the generation of imprinted polymer beads. Thus, MIPs have been prepared by suspension,[49-51] emulsion,[52, 53] dispersion,[54, 55] precipitation[56] polymerisation or by grafting/coating of imprinted polymers on preformed silica[48, 57] or polymer microspheres.[58]

A. Mayes and co-workers[59] have developed a suspension polymerisation technique based on the use of a liquid perfluorocarbon as the dispersing phase. This non-polar dispersant stabilises the interactions between functional monomers and templates required for the recognition process during molecular imprinting. Their method produced polymer beads, with almost quantitative yield, which were used after only a simple washing step. In this case, an acrylate polymer with perfluorocarbon and poly-(oxyethylene) ester groups was used to stabilise an emulsion of functional monomer, cross-linker, template, initiator, and porogenic solvent in perfluoro-(methylcyclohexane). The average bead size ranged between 50 and 5μm depending on the amount of stabilising polymer.

P. A. G. Cormack and co-workers,[56] have recently reported on the synthesis of theophylline-imprinted and non-imprinted mono-disperse, spherical, polymer particles of about 5*µ*m in diameter prepared in one step by precipitation co-polymerisation of divinylbenzene and methacrylic acid. The particles were applied to HPLC and SPE separations and showed high selectivity for theophylline.

Finally, *M. Whitcombe* and co-workers[58] produced sub-micrometer surface-imprinted particles by a two-stage aqueous emulsion polymerisation with a poly(divinylbenzene) shell over a cross-linked poly(styrene) core. The second stage polymerisation was performed in the presence of a polymerisable surfactant and pyridinium 12-(cholesteryloxycarbonyloxy)dodecanesulfate, which acted both as a surfactant and as a template. Removal of the template left hydrophobic cavities on the surface of charged particles or particles bearing benzyl alcohol groups, dependent on the protocol adopted.

3.1.6.b Films and membranes

Imprinted films and membranes[60] have been so far generated by direct casting on a surface or a device and mostly used for separation or sensor applications. Recently, *V. M. Rotello* and co-workers reported on a molecular sensor for recognition of hexachlorobenzene in water. This was based on a thin molecularly imprinted polymer thin film attached to a quartz crystal microbalance. The materials were optimised by controlling the heterogeneity of cross-linking and using appropriate electron-rich complements to the electron-deficient hexachlorobenzene and the final films were unambiguously capable to distinguish hexachlorobenzene from small molecules of similar sizes and structures.[61]

M. Ulbricht and co-workers prepared a sulfonated polysulfone and then blended it with cellulose diacetate. This blend was used as the matrix polymer for the preparation of molecularly imprinted polymer membranes *via* phase inversion from a casting solution containing a template and polyethylene glycol as pore forming agent. Solvent, polymer blend composition and total polymer concentration were optimised and the effects of the latter parameters onto pore structure were studied by membrane water uptake and specific

surface area measurements. Results of template rebinding during filtration through MIP as well as control membranes provided evidence for surface imprinting of the porous membranes.[62]

Membranes have also been prepared by synthesising imprinted polymers inside the pores of a porous membrane that acts as a solid support,[63] or gluing the polymer particles together using a particle binding agent obtaining, for example, coated glass plates similar to those used in thin layer chromatography.[64]

3.1.6.c   Monolithic MIPs for use in chromatography

The traditional grinding and sieving process that is employed in the synthesis of imprinted polymers results in a high degree of irregularity of the particles thus produced. In combination with the broad particle size distribution, packing these materials into columns can be somewhat tedious, especially when capillary columns are used. In order to avoid capillary packing, several different imprinting formats devoted to the capillary format have been developed.[65] These can be roughly categorised in three main groups; monolithic MIPs, surface grafted MIPs and nanoparticle MIPs. The monolithic format can either be synthesised in situ or constructed by entrapment of prefabricated MIP particles in different types of matrices.[66, 67] The surface grafted polymer format allows immobilisation of the MIP stationary phase as a coating on the inside of the capillary for open-tubular CEC applications[68, 69] or on silica particles that subsequently can be packed into capillaries.[70, 71] The third format, i.e. the nanoparticle MIP, is used in a partial filling application of CEC.[19, 59, 72]

Furthermore, monolithic MIPs have been prepared for use in HPLC columns.[73] *H. Zou* and co-workers reported on the preparation of molecularly imprinted monolithic stationary phases that achieved liquid chromatographic separation of amino-acid enantiomers and diastereomers. In order to achieve this, they used low polar porogenic solvents, e.g. toluene and dodecanol, which resulted in molecularly imprinted monolithic stationary phases with good flow-through properties and high resolution.

3.1.7 Applications of Molecularly Imprinted Polymers

During the last years, a great deal of research has been dedicated in understanding of the mechanism of formation of Molecularly Imprinted Polymers.[74] However, the majority of researchers are exploring the potential fields of applications of MIPs. These can be categorised in four main areas, namely chromatography, including solid phase extractions, immunoassay type of applications, catalysis and sensing. In the following paragraphs, a few examples will be given in order to demonstrate the use of MIPs in these fields.

3.1.7.a Chromatography

Here, the imprinted polymer is used as the stationary phase for separation and/or isolation of analytes of interest.[75] This application is based on the fact that the imprinted polymer has a better retention for the template molecules than others. Thus, injecting a mixture of analytes containing the template used at the imprinting step on an imprinted polymer column should lead to discrimination of the template (elutes last, with significant peak tailing) and the irrelevant analytes (elute with the solvent front or near it with sharp symmetric peaks). An area that has attracted particular interest is enantio-separations using *Molecularly Imprinted Chiral Stationary Phases* (MICSPs). Such materials have been developed and successfully applied for the resolution of enantiomeric compounds including amino acids[76] and derivatives thereof,[77-80] peptides[78, 81] and commercial drugs.[82-84]

A related area of application is solid-phase extraction,[85-87] where the imprinted polymer is used as a "sponge" to concentrate the molecule of interest. Thus, following an adsorption step when all analytes present in a sample are loaded on the SPE cartridge, non-specifically bound molecules are washed of in the so-called "*molecular recognition step*" while the imprinted compound stays bound in the binding sites. Finally, in the washing step the selectively bound analyte is washed out of the column in its pure form.

3.1.7.b   Immunoassays

Possibly the most cited publication related to imprinted polymers is related to the application of MIPs as substitutes for antibodies.[88] *G. Vlatakis et al.*[89] demonstrated the use of MIPs in a radio-labeled ligand-binding assay, using theophylline as the template. Their assay measured accurately drug levels in human serum, with results comparable to those obtained using the well established immunoassay technique based on antibodies. *Molecularly Imprinted Assays* (MIAs) have also been developed for pesticides, e.g. atrazine[90, 91], drugs, e.g. diazepam[92] and hormones such as cortisol[93] and estradiol.[19]

3.1.7.c   Catalysis

Here, molecularly imprinted polymers are used as enzyme mimics. The most remarkable examples come from the group of *G. Wulff*.[94] In one of the latest reports, molecularly imprinted polymers mimicking the active site of carboxypeptidase A were synthesised and their catalytic activity was determined by investigating the rate of hydrolysis of different carbonates in aqueous environments. Using Zn^{2+} or Cu^{2+} as the cations present in the binding site, they achieved a near 3200-fold increase in the catalytic activity with diphenyl carbonate as the substrate when zinc cations were used, and more than 8000-fold increase when zinc was replaced by copper cations.[95, 96]

3.1.7.d   Sensors and biosensors

Sensing devices are one of the most common applications of imprinted polymers due to their ease of preparation and the robustness of the final materials which can be re-used for an almost unlimited number of measurements.[97] The MIP is here used as the recognition element directly conjugated with the transducer. The signal transferred to this transducer can either emanate from the binding event itself, thus leading to a change in the physicochemical properties of the system (mass, capacitance), from a specific property of the analyte, e.g. fluorescence, electrochemical activity, or from the

imprinted polymer whereby the signal is produced by reporter groups in the vicinity of the binding site.

The first category includes the most common sensor format used so far, the *Quartz Crystal Microbalance* (QCM). The group of *F. Dickert* has demonstrated particular activity in this area with remarkable examples of imprinting proteins and viruses and subsequent detection of them using the sensing system.[98, 99] Taking advantage of the fluorescence activity of the template *K. Mosbach et al.* have developed a fibre-optic detection based sensor for dansyl-L-phenylalanine.[100] Finally the group of *T. Takeuchi* has reported on a receptor for 9-ethyladenine with a porphyrin moiety placed at the binding centre, leading to selective quenching of the polymer fluorescence upon binding of the template.[101] During this work an example of the use of fluorescent functional monomers has been demonstrated, whereby the fluorescence of a pyridine or pyrimidine based imprinted polymer decreases upon binding with 1-benzyluracil.[37]

As artificial receptors, MIPs have also been used to screen combinatorial chemical libraries, where compounds that are closely related to a known ligand could be easily identified by their relative binding strength to the imprinted polymers. Even though there have, until now, only been a few preliminary reports that demonstrated the feasibility of the approach,[102-104] it is expected that MIPs will find applications in drug screening and development, in particular for the initial screening of large libraries.

3.1.8   Conclusions and perspective of MIPs

Molecular Imprinting is a relatively young research branch yet it has attracted significant interest in the fields of analytical and bio-analytical chemistry, as well as in catalysis and sensing techniques. This is mainly due to its simplicity, versatility and cost effectiveness escorted by the robustness and reliability of the produced materials.

Nonetheless, a few very important issues remain unresolved, namely reduction of the non-specific binding and increased water-compatibility as well as generation of more homogenous materials for use in analytical applications. Although significant attempts towards the resolution of the latter

have been recently reported, mainly employing the use of solid supports (e.g. silica beads) as the cast around which the imprinted polymer is formed, MIPs remain generally hydrophobic polymeric materials, with limited water-compatibility which restricts their application to organic rich media. This issue has been successfully addressed during this doctoral work, as will be shown in the following chapters, by using designed functional monomers and modifying the polymer matrix, allowing selective recognition of the imprinted compounds in highly aqueous environments.

3.2 The templates selected for this study

In order to address the issue of water-compatibility and non-specific binding, a series of hydrophilic compounds, or compounds abundant in aqueous environments, were selected as targets in this study, the main aim being the selective recognition of the latter in their natural environment with a potential application in *in-vivo* analysis and isolation.

Here the characteristics of the main target compounds, whose recognition is discussed in this doctoral thesis, will be presented in order to point out their significance in biological processes and the importance of the achievements that will be presented in the following chapter.

3.2.1 Uracil and its biological importance

Uracil is an organic base of the pyrimidine family. It was isolated from herring sperm and also produced in a laboratory in the early 1900s. When combined with ribose with a glycosidic linkage, uracil forms the nucleoside uridine, which in turn can be phosphorylated with one to three phosphoric acid groups, yielding respectively the three nucleotides UMP (uridine monophosphate), UDP (uridine diphosphate), and UTP (uridine triphosphate). The analogous nucleosides and nucleotides formed from uridine and deoxyribose occur only very rarely in living systems; such is not the case with the other pyrimidines.

The nucleotide derivatives of uracil perform important functions in cellular metabolism, particularly in carbohydrate metabolism; UTP acts as a coenzyme in the biosynthesis of sucrose in plants, lactose and glycogen in

mammals, and chitin in insects. It can also readily donate one of its phosphate groups to adenosine diphosphate (ADP) to form adenosine triphosphate (ATP), an extremely important intermediate in the transfer of chemical energy in living cells. Since the uracil nucleotides contain only ribose and not deoxyribose, UTP is the source of uridine only in ribonucleic acid (RNA); there is no uridine in deoxyribonucleic acid (DNA). Its involvement in the biosynthesis of RNA demonstrates that uracil is important in the translation of genetic information. A few laboratory derivatives of uracil have been designed as experimental anti-metabolites for use in cancer chemotherapy, e.g. 5-fluorouracil.
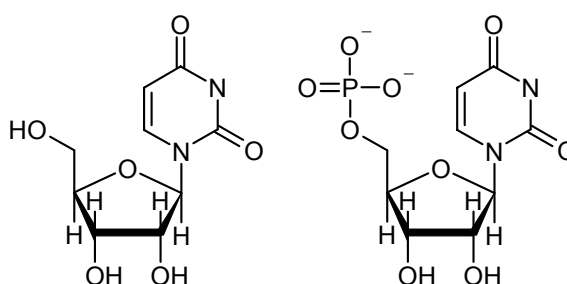
Scheme 3.1:   Structures of Uridine and Uridine monophosphate (UMP)

Being a molecule of such biological importance, uracil has attracted the attention of several research groups who have attempted to selectively recognise it by means of molecular imprinting.

Examples include the work of *Spivak* and *Shea*,[105] who used HPLC in order to evaluate the binding affinity and selectivity of EDMA – MAA based imprinted co-polymers against RNA and DNA bases. The synthesised materials showed specific binding for adenine, cytosine, and guanosine derivatives. These bases contain a 2-aminopyridine substructure previously found important for the binding and specificity of polymers imprinted with 9-ethyladenine.[106] Thymine and uracil derivatives, which do not contain the 2-aminopyridine substructure, exhibited little specific binding to the imprinted polymers. The magnitude of the binding affinity for each of the nucleoside derivatives to its own imprinted polymer was found to follow the order A > G > C > T, U.

Furthermore, *Takeuchi et al.*[107] used the anti-tumour active compound 5-fluorouracil (5-FU) as a target molecule and synthesised imprinted polymers

using 2,6-bis(acrylamido)pyridine and/or 2-(trifluoromethyl)acrylic acid as functional monomers and observed selectivity for 5-FU over the selected 5-FU derivatives. Simultaneous use of both functional monomers led to improvement of affinity and separation factors for 5-FU.

Finally, *Kobayashi et al.*,[108] selected uracil as template for the synthesis of molecularly imprinted membranes based on poly(acrylonitrile-co-methacrylic acid) [P(AN-co-MAA)] by phase inversion. In their study, FT-IR and ^{1}H-NMR were used in order to characterise the polymer-template interaction as well as Scanning Electron Microscopy (SEM) and Atomic Force Microscopy (AFM) in order to obtain information regarding the morphology of the imprinted membranes. The membranes showed permeation selectivity for uracil over dimethyluracil and caffeine, as measured by means of bound analyte on the membrane (bound uracil: 7.9μmol/g; dimethyluracil: 0.6μmol/g; caffeine: 0.8μmol/g).

3.2.2 Riboflavin and its natural receptor

Riboflavin is an essential vitamin in human nutrition occurring in a wide variety of food products. In the body riboflavin is transformed into two active coenzymes, flavin mononucleotide (FMN) and flavin adenine dinucleotide (FAD). These two active flavins are directly involved as coenzymes with oxidases and dehydrogenases for the hydrolysis of fatty acids and the degradation of amino acids or pyruvic bases. Second, flavins can transfer electrons or protons from a donor to an acceptor, important in the Krebs cycle and the respiratory chain.[109]
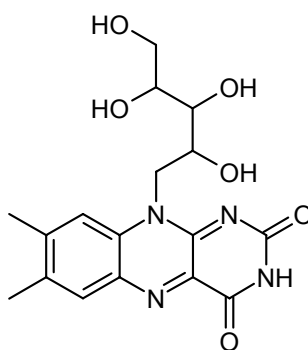
Scheme 3.2:   Structure of riboflavin

23

While riboflavin is relatively stable towards heat and acidic pH, in the presence of alkalis and light it decomposes to lumiflavin, a more oxidative agent that contributes to the decomposition of vitamin C. The photo reduction of riboflavin is responsible for the break-down of the bitter iso-alpha acids in the presence of sulphur source, which leads to the well known "sun-struck" flavour of white wine, champagne, milk and beer exposed to sunlight. In order to prevent development of such undesired flavours, these products are stored preferably in bottles that are dark, non transparent to light, in the cases of beer and wine, or plastic/paper in the case of milk.

In addition, it has been postulated that apart from the role in "sun-struck" flavour formation, riboflavin and other flavins[110] are also involved in the formation of reactive oxygen species in beer and thus contribute to the formation of stale flavour in general. Hence, the photosensitising properties of flavin entities have a negative impact on the stability of beer flavour and, consequently, the selective removal of these flavins from beer could be a strategy toward improving the robustness and quality of beer flavour.[111]
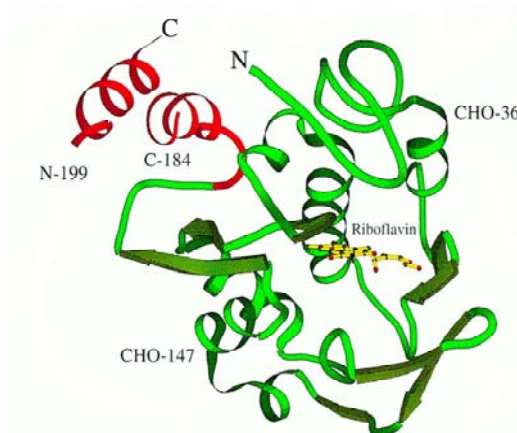
Figure 3.2   *Ribbon diagram of the riboflavin binding protein (**RfBP**)*

The natural receptor of riboflavin is the riboflavin binding protein (**RfBP**) which is a globular monomeric protein of ~30 kDa. Apo-**RfBP** binds riboflavin in a 1:1 ratio, with high affinity: K_d ~ 1.3nM (at pH 7.0, 25°C). The binding of riboflavin to apo-**RfBP** is nearly independent of pH between pH 6 and 9 but rapidly declines with decreasing pH below pH 6. At the pH of beer, which is ~4.2, the K_d amounts to ~1.6μM.[112] The binding of riboflavin to apo-**RfBP** almost completely quenches riboflavin fluorescence, due to stacking of the

riboflavin iso-alloxazine ring with aromatic side chains in the riboflavin binding site of **RfBP** between the parallel planes of Tyr75 and Trp156.[113]

So far, official methods for quantification of riboflavin in food samples are based usually on HPLC measurement and microbiological assays. Alternative methods involve electrochemical or fluorescent characteristics of flavins for standard solutions,[114-116] biological fluids,[117, 118] and pharmaceutical tablets[119] but none for food matrixes. In addition to these approaches, methods based on biological properties of riboflavin through its binding with **RfBP** from egg white have been investigated.[120, 121]

Recently, an assay for quantification of riboflavin in milk-based products has been developed using the principle of *Surface Plasmon Resonance* (SPR) with on-chip measurement. The quantification was done indirectly by measuring excess of **RfBP** that remains free after complexation with riboflavin molecules originally present in the sample solution.[109]

However, none of the aforementioned methods has the potential of a large scale preparative application. Thus, it is still of great interest for the food industry, and the brewing industry in particular, to develop a robust, water compatible material with the ability to selectively bind and remove riboflavin from food and beverage matrices, without otherwise affecting the respective product.

3.2.3 *Glutamic acid and related compounds*

Glutamic acid plays a critical role in proper cell function, but it is not considered an essential nutrient in humans because the body can manufacture it from simpler compounds. In addition to being one of the building blocks in protein synthesis, it is the most widespread neurotransmitter in brain function, as an excitatory neurotransmitter and as a precursor for the synthesis of GABA in GABAergic neurons. Glutamate activates both ionotropic and metabotropic glutamate receptors. Free glutamic acid cannot cross the blood-brain barrier in appreciable quantities; instead it is converted into L-glutamine, which the brain uses for fuel and protein synthesis.

One of the most well known glutamate containing structures is methotrexate (abbreviated MTX; formerly known as amethopterin), an antimetabolite drug

used in treatment of cancer and autoimmune disease. It was originally used, as part of combination chemotherapy regimens to treat many kinds of cancers. It is still the mainstay for the treatment of many neoplastic disorders including acute lymphoblastic leukaemia.

Methotrexate bases its activity in the inhibition of the metabolism of folic acid. In particular, it inhibits dihydrofolate reductase (DHFR), an enzyme that is part of the folate synthesis metabolic pathway, which catalyses the conversion of dihydrofolate to the active tetrahydrofolate. Folic acid is needed for the *de novo* synthesis of the nucleoside thymidine, required for DNA synthesis. Methotrexate, therefore, inhibits the synthesis of DNA, RNA, thymidylates, and proteins.
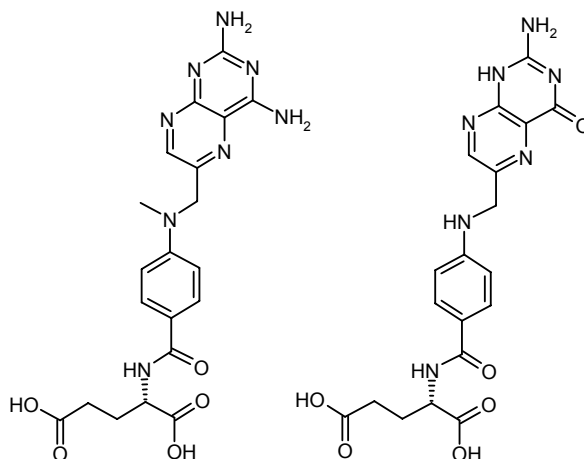
Scheme 3.3: *Structures of methotrexate (left) and folic acid (right)*

The aforementioned example of carboxylate and carboxylic acid activity and biological role underlines the importance of this class of compounds. It is thus of no great surprise that significant research effort has been directed towards the recognition of such molecules by both monomeric and polymeric receptors, molecularly imprinted polymers being a particularly attractive approach, especially for larger compounds with diverse functionality. In a recent study, *Spivak* and co-workers performed a survey of commercially available amine-based monomers for binding and selectivity of carboxylate and phosphonic acid templates.[122] The results of the study show an interesting trend in the nature of the interaction between the functional monomer and the template, where higher selectivity is generally observed for MIPs containing aromatic amine-based functional monomers even though

higher affinities are achieved by the aliphatic amine monomers, highlighting the influence of binding group directionality and monomer flexibility on MIP selectivity.

As part of the continuing effort towards the recognition of the carboxylate functionality and inspired by some remarkable examples from the field of supramolecular chemistry, a series of urea based monomers were synthesised during this doctoral work, and their binding properties were evaluated both in solution and in the solid state, as functional monomers incorporated in glutamic acid imprinted polymers.

4 Results and Discussion

4.1 Scope of the Work

In recent years, Molecular Imprinting has emerged as a very attractive alternative to natural receptors.[11, 12] However, this relatively new technology has to deal with some essential issues, which nature has already addressed through the millions of years since the emergence of life as we know it, the most important of them being water compatibility.

Most natural processes take place in aqueous environments, even if in some cases the local environment is shielded from water and appears very hydrophobic (e.g. enzyme active-centres, cell membranes, etc.). In contrast, Molecularly Imprinted Polymers are traditionally prepared using organic, non-water-compatible, components, which oblige the employment of organic solvents during their synthesis. As a result, MIPs are generally very hydrophobic and when required to operate in highly aqueous media, like biological or environmental samples, their selectivity diminishes, giving rise to non-specific binding of other matrix components. Therefore, in most cases, a sample pre-treatment step is required, during which most of the interfering hydrophobic compounds have to be removed, by means of consecutive extractions with organic solvents, or, in some cases, intermediate organic solvent equilibration steps during a solid phase extraction cycle, which help the selectivity of MIPs to be revealed. All these result in making the application of MIPs time consuming and less environmentally friendly. Recent work undertaken in the working group where the present work was carried out has resulted in water-compatible MIPs obtained by high-throughput synthesis and experimental design. The best performing materials were up-scaled and in subsequent evaluation they revealed high selectivity for their template, bupivacaine, and very low non-specific binding, allowing their use for direct extraction of the local anaesthetic from blood plasma samples.[123]

Additionally, with few exceptions,[32-34] the use of commercially available functional monomers in Molecular Imprinting has been favoured, despite the fact that they are able to provide only weak interactions with the template molecule. Generally, this means that a large excess of functional monomer is

used in order to ensure maximum complexation of the template. However, non-complexed functional monomer units will be present and, during polymerisation, these will be distributed randomly throughout the polymer matrix. This leads to functionality capable of substrate binding being placed outside the templated sites. This is one of the major causes of the non-specific binding observed with non-covalent MIPs.

One approach to improve this situation involves the preparation of functional monomers which provide relatively strong and stoichiometric interactions with a given template. If the monomer-template interactions are sufficiently strong, stoichiometric use of the monomer should lead to a high concentration of complexes in the pre-polymerisation solution. This would then be transformed into a high yield of imprinted sites in the final polymer.[124] As the majority of functional monomer would be employed in complexes, there should be a concomitant, drastic reduction in the degree of non-specific binding in the obtained imprinted polymer.

Scope of this work is to create hydrophilic Molecularly Imprinted Polymers that have high selectivity for their template and are able to maintain it even when applied in aqueous samples with complicated matrices, taking advantage of the benefits offered by designed polymerisable hosts. Two main compound groups have been selected for this study, namely imide functionality containing molecules (uracil, riboflavin) and carboxylic acids and the anions thereof (glutamic acid, methotrexate).

The approaches taken towards the selective recognition of the aforementioned targets, as well as the achievements of this doctoral research will be presented in this section.

4.2 Imprinting of Uracil derivatives

The main target of this doctoral work was to develop Molecularly Imprinted materials that would have the ability to selectively recognise riboflavin. Nevertheless, initial efforts were diverted towards the recognition of an organic solvent soluble uracil derivative, namely 1-benzyluracil (**1-BU**). Uracil is one of the four RNA nucleotide bases and possesses a hydrogen bond Acceptor – Donor – Acceptor (A-D-A) triad identical to the one present in riboflavin; it was therefore a reasonable choice as model compound for the initial tests and screening of functional monomers. It also provided a temporary solution to the solubility problem that was faced with riboflavin, since an easy and efficient synthetic route towards 1-benzyluracil is available in the literature.[125] In the following paragraphs the screening of functional monomers for the recognition of the imide moiety, including some novel monomers, the synthesis of imprinted polymers and the evaluation thereof will be discussed.

4.2.1   1st generation of monomers for the recognition of uracils

Recognition of uracil derivatives was based on the imide moiety with the A-D-A hydrogen bond triad. At the first instance, three functional monomers were synthesised[126] and their binding strength towards **1-BU** was first measured by means of ^{1}H-NMR titrations. In Scheme 4.1 the proposed binding modes of the 3 monomers with **1-BU** are displayed.
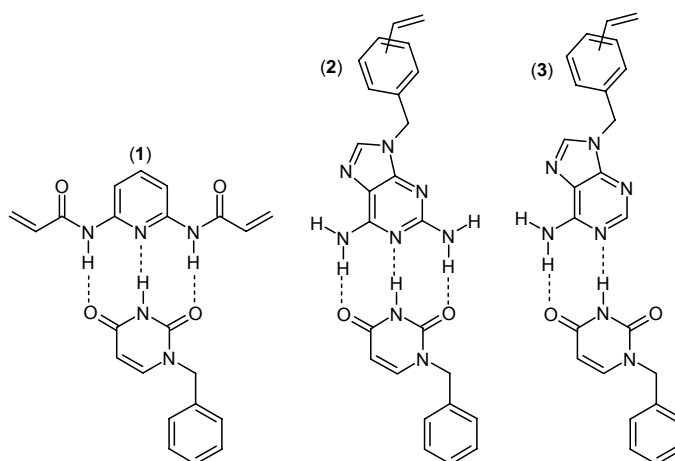
Scheme 4.1

2,6-bis(acrylamido)pyridine (**1**) has been used in the past for the recognition of uracils[127] and for the imprinting of barbiturates.[34] It offers a hydrogen bond triad complementary to the one found in uracil, based on two amide protons (donors) and the pyridine nitrogen (acceptor). 9-(3/4-vinylbenzyl)-2,6-diaminopurine (**2**) was synthesised by modification of a published method[128] and possesses also a hydrogen bond triad, however, this is based on two amino groups and a purine ring nitrogen. Monomer **3**, 9-(3/4-vinylbenzyl)adenine, is based on the base-pair partner of thymine in nucleic acids, therefore could be expected to participate in hydrogen bond interactions with uracil molecules, despite the fact that it can only offer a two-point binding. At this point it has to be noted that adenine can complex to uracil/thymine in two possible modes; the Watson-Crick mode[3] (as drawn above) and the Hoogsteen mode,[129] which is mainly found in crystals. However, the latter mode is significantly weaker and is therefore neglected during the calculations of the association strength. In order to test the binding strength of this first generation of monomers, ^{1}H-NMR titrations were performed in $CDCl_3$ and the binding isotherms are overlaid in Figure 4.1. The full titration data for these and all the other ^{1}H-NMR titration experiments are presented in § 8.5 of the Appendix.
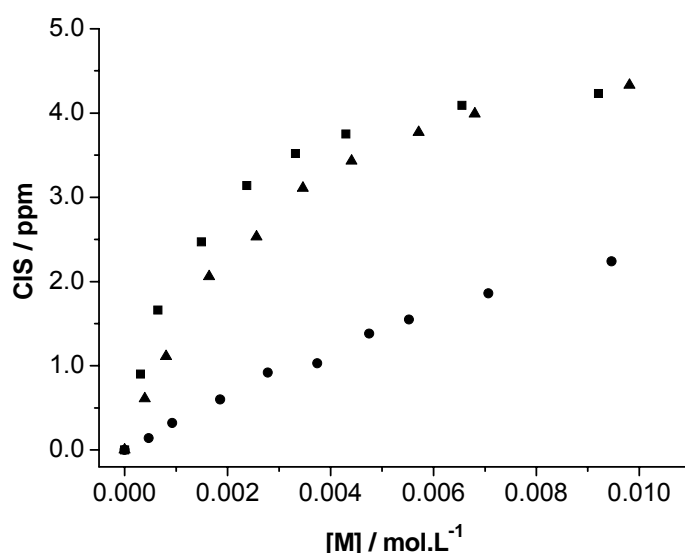

Figure 4.1:   *Binding isotherms obtained by ^{1}H-NMR titrations of monomers* **1** *(■),* **2** *(▲) and* **3** *(●) with* **1-BU** *(**1-BU** imide proton followed).*

The data obtained by the titrations were fitted to the 1:1 binding isotherm (see § 8.4) and the apparent association constants were derived, as shown on Table 4.1.

Monomer	K_{app} (M^{-1})	$\Delta\delta_{max}$ (ppm)
1	757±28	4.23
2	320±16	4.33
3	53±7.5	2.24

*Table 4.1:   Apparent association constants and maximum CISs for the binding of the 1st generation monomers to **1-BU***

As expected, the order of binding strength is according to the number of potential H-bonds offered by each receptor monomer. Thus, monomer **3**, with only two potential H-bonds from the ring N and the single amino- group present in the molecule, shows the weakest affinity to **1-BU**. Adding one amino group to the monomer structure (**2**) increases the binding constant by almost an order of magnitude. Moving away from the purine core and replacing the amino group H-bond donors with amides connected to a pyridine ring (monomer **1**), increases the binding strength by more than a factor of 2.

4.2.2 1st generation of MIPs against 1-benzyluracil

The monomers described above were used to synthesise Molecularly Imprinted Polymers against **1-BU**. Due to the limited solubility of monomer **3** mainly, a ratio of template: monomer: cross-linker of 1: 2: 400 was decided. The detailed recipe is shown on Table 4.2.

| Polymer	Template **1-BU**	Functional Monomer	Cross-linker (EDMA)
P1a	0.01g / 0.05mmol	**1** - 0.022g / 0.1mmol	3.8mL / 20mmol
P2	0.01g / 0.05mmol	**2** - 0.027g / 0.1mmol	3.8mL / 20mmol
P3	0.01g / 0.05mmol	**3** - 0.025g / 0.1mmol	3.8mL / 20mmol

Table 4.2

For each imprinted polymer, a corresponding control polymer was synthesised in a similar manner, but with omission of the template (**P$_N$x**). Chloroform (5.6mL) was used as porogenic solvent. The polymerisation was carried out at 40°C for 24h and ABDV (1% w/w of total monomers) was used as the free radical initiator.

After the polymerisations were completed, the polymers were extracted with methanol using the Soxhlet apparatus, followed by crushing and sieving to obtain particles with size 25-50μm, which were sedimented and then packed into HPLC columns for evaluation in the chromatographic mode (for details on the polymer preparation see § 6.4.2 of the Experimental Part). Particles of the same size were used also for equilibrium batch rebinding experiments.

4.2.3 Chromatographic evaluation of the 1st generation MIPs

In order to assess the binding strength of the synthesised MIPs, a series of different analytes was injected sequentially on the respective packed columns and the retention times for each analyte were recorded. Additionally, comparing the retention times of the template (**1-BU**) and the other injected analytes, conclusions can be drawn regarding the selectivity of the materials. In order to facilitate the further discussion, the structures of the injected analytes are depicted in Scheme 4.2. 1-cyclohexyluracil (**CHU)** is another uracil derivative that was used in this study as a closely structurally related analyte. 1,3-dibenzyluracil (**1,3-DBU**) is a by-product of the synthesis of **1-BU**, and serves as a valuable control analyte since its imide proton is substituted by a second benzyl group, therefore the primary binding moiety has been blocked. 3-Azido-3′-deoxythymidine (**AZT**) is a thymine based anti-cancer drug (zidovudine).
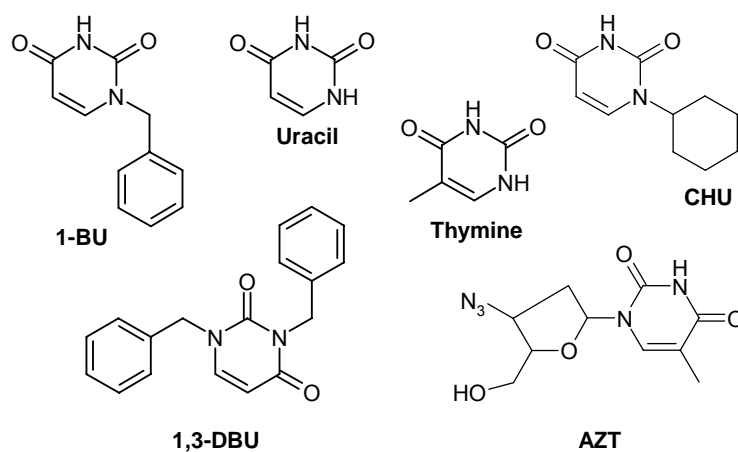
Scheme 4.2

The retention factors (k_{MIP}) calculated for the 1st generation of materials (in 100% acetonitrile) are displayed in Figure 4.2. As a measure of imprinting selectivity, k_{MIP}/k_{NIP} values (imprinting factors) are displayed in Figure 4.3. k_{MIP} indicates the retention factor of the analytes on the imprinted (MIP) columns and k_{NIP} the corresponding retention factor on the non-imprinted (NIP) columns.
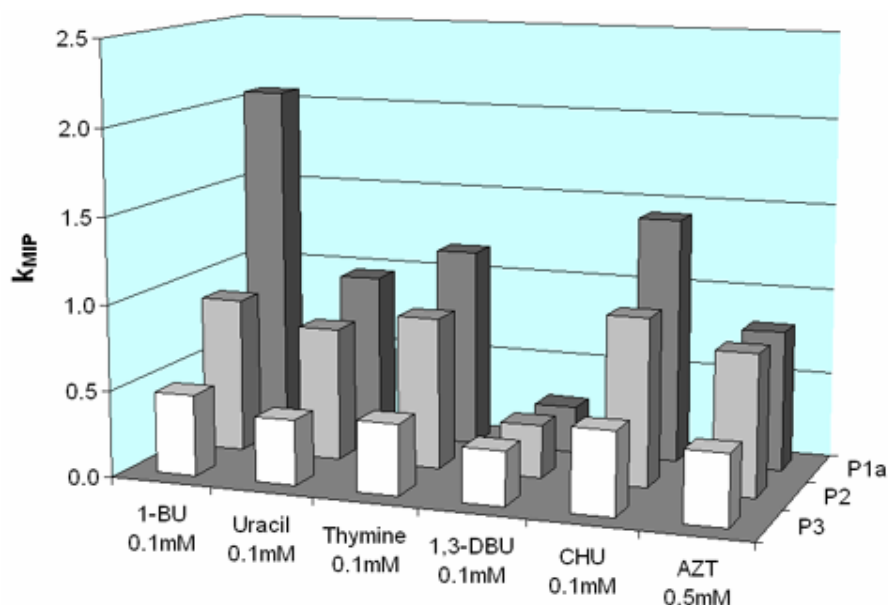
Figure 4.2: k_{MIP} values of the different analytes on the corresponding MIPs
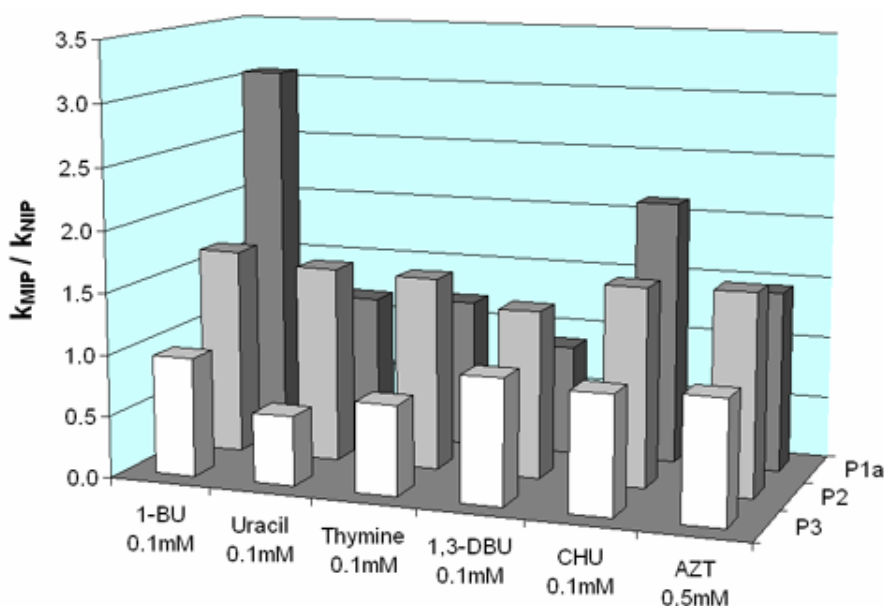
Figure 4.3: k_{MIP}/k_{NIP} *values of the different analytes*

All measurements were performed on a HP1050 Liquid Chromatograph. The injection volume was 5µL, the flow rate 1mL/min and detection was performed using a Diode Array Detector (DAD) recording chromatograms at 260nm.

For polymers prepared with **3** as the functional monomer (**P3**), little or no change in the retention behaviour of the analytes is observed on either the MIP or the NIP, since all k_{MIP}/k_{NIP} values are ≤ 1. This is consistent with the lack of imprinting effect observed for the template molecule and the weak solution association exhibited by this monomer.

For polymers prepared with **2** as the functional monomer (**P2**), little shape selectivity is observed for the template over different 1-substituted uracils or for un-substituted uracils. However, the retention behaviour of **1,3-DBU**, where a hydrogen-bonding site has been removed (compared to **1-BU**), is clearly different.

Finally, the retention behaviour of the different analytes on the polymers prepared from **1** (**P1a**) show the largest differences. Thus, we observe signs of shape selectivity on changing the substituent at the 1-position of uracil (k_{MIP} for **1-BU** versus k_{MIP} of **CHU** and k_{MIP} of **AZT**). Moreover, removing or adding hydrogen-bonding sites to the analyte adversely affects the retention behaviour, with **1,3-DBU** being extremely weakly retained.

The study of the first generation of monomers for the recognition of uracils clearly demonstrates that the strength of the interaction between the template and functional monomer in a solution mimicking the pre-polymerisation solution is directly translated into the subsequently prepared MIPs. Furthermore, it points out that monomer **1** should be the basis for the development of stronger receptor monomers for the recognition of uracils.

4.2.4   2nd generation of monomers for the recognition of uracils

In order to achieve further improvement of the binding strength, efforts were directed towards the synthesis of bis-amide based functional monomers with improved basic character of the ring nitrogen atom. Increased basicity should lead to an enhancement of the H-bond accepting properties of the host monomer.

4.2.4.a   Towards novel imide receptor monomers

Two possible routes were proposed for the generation of improved imide receptors. The first route consisted of a 7-step synthetic procedure and was considered not worthwhile since, according to the literature,[130] the overall yield was considerably low and in this case an easily accessible, inexpensive functional monomer was pursued.

The second route was based on the use of pyrimidines instead of pyridines as the core of the functional monomer. By substitution of the *para-* to the ring N1 position with an electron donating group, the basicity of the aforementioned ring N should increase, therefore the H-bond acceptor character should be superior. The synthetic protocol comprised of the nucleophilic substitution of the 6-chloro group in 2,4-diamino-6-chloropyrimidine by piperidine (**4**) or an ethoxy- group (**5**). This route was regarded as significantly less time/effort consuming thus, the two novel monomers that should fulfil the sought requirements were synthesised.[37] The initially proposed binding mode of the two monomers is displayed in Scheme 4.3.
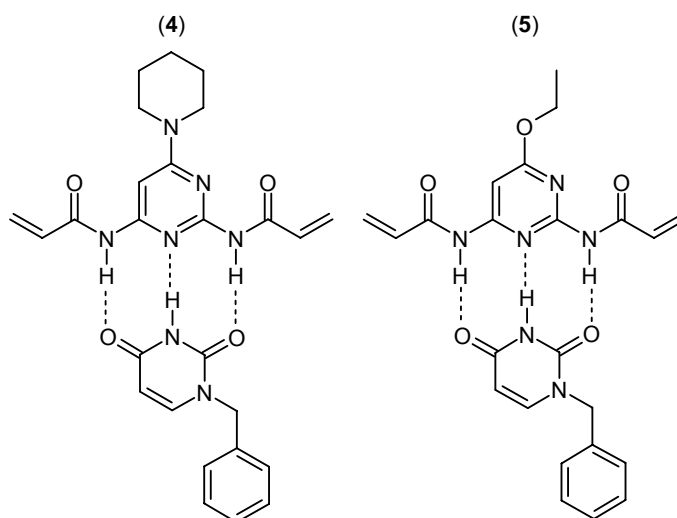
Scheme 4.3

4.2.4.b   *Monomer evaluation in solution*

The association constants between the novel monomers and the model compound **1-BU** were measured by means of ^{1}H-NMR titrations in CDCl$_3$. The respective binding isotherms derived from the ^{1}H-NMR titration experiments are overlaid in Figure 4.4 together with the one obtained for monomer **1**, for direct comparison.
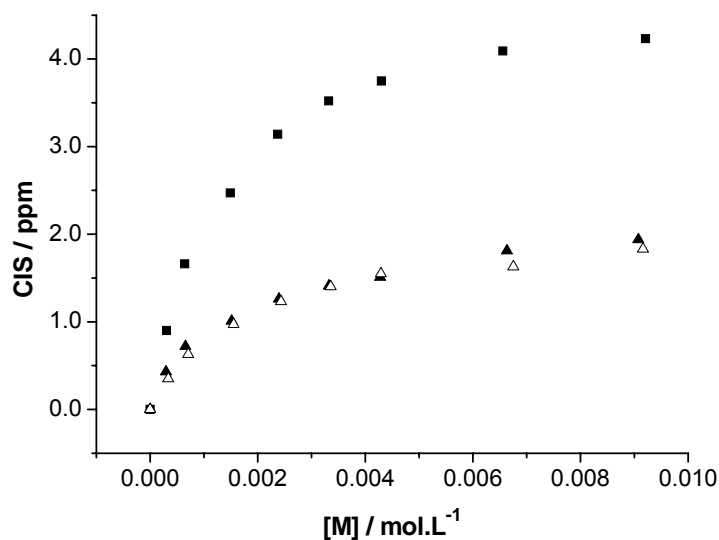
Figure 4.4:   *Binding isotherms for the titration of **1-BU** with monomers **1** (■), **4** (▲) and **5** (△) (**1-BU** imide proton followed).*

The data were fitted to the 1:1 binding isotherm and the results are presented in Table 4.3.

Monomer	K_{app} (M^{-1})	$\Delta\delta_{max}$ (ppm)
4	596±85	1.94
5	561±37	1.83

Table 4.3:   *Apparent association constants and maximum CISs for the binding of the 2nd generation monomers to **1-BU***

Unexpectedly, the apparent association constants for both monomers were significantly lower than the one measured for **1**, but in the same range with each other. However, the maximum shifts of the uracil imide protons when titrated with monomers **4** and **5** were also significantly lower than the one observed upon titration with monomer **1**. Further characterisation of the novel monomers was necessary in order to fully understand the differences in their performances.

4.2.4.c   Why are these monomers so different?

Although the difference in the maximum shifts measured between monomers **1** and **4** or **5** could be attributed to the dissimilar magnetic environment, the magnitude of the difference suggested other causes. Thus, it was suggested that strong self-association of monomers **4** and **5** would lead to similar behaviour and subsequently to a "false" saturation curve.

Indeed, compounds similar to **4** are known to self-associate[131] as shown in Scheme 4.4, where the amide at position 2 adopts an energetically unfavourable *cis*-conformation due to repulsion of the carbonyl oxygen by the N3 ring nitrogen.
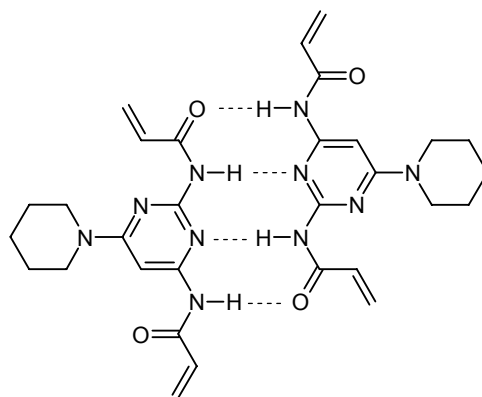
Scheme 4.4

Comparing the individual NMR spectra that were recorded in CDCl$_3$ with the ones recorded in DMSO-d$_6$, another interesting effect was observed, namely the fact that while the vinyl protons *c* and *d* (Scheme 4.5) appeared as quartets in DMSO-d$_6$ at 6.6-6.7 ppm, they appeared at 6.6-6.7 and 7.2-7.3 ppm in CDCl$_3$ (Figure 4.5).
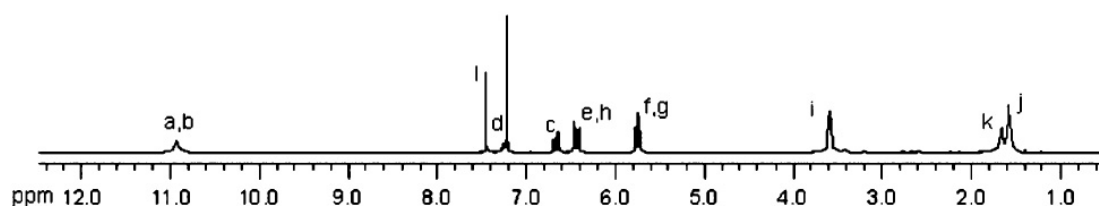
Figure 4.5: ^{1}*H-NMR spectrum of monomer 4 in CDCl$_3$*

This downfield shift of *d* is likely due to weak hydrogen bonding with the ring N3 and the corresponding vinyl proton. This would stabilise a *cis*-conformation of the amide group and place the vinyl group nearer to the piperidine ring.
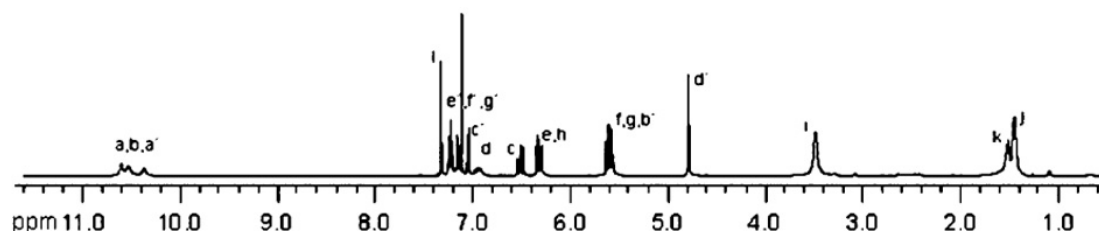
Figure 4.6: ^{1}*H-NMR spectrum of a 1:1 mixture of 4 and 1-BU in CDCl$_3$*

A closer examination of the ^{1}H-NMR spectrum of an equimolar mixture of **4** and **1-BU** in CDCl$_3$ (Figure 4.6) reveals several interesting factors. While in the spectrum of the monomer alone (Figure 4.5) the amide protons appear as

one broad peak, the presence of **1-BU** induces a split in the signals of the amides (*a, b*), indicating the existence of an additional complex species at this concentration.
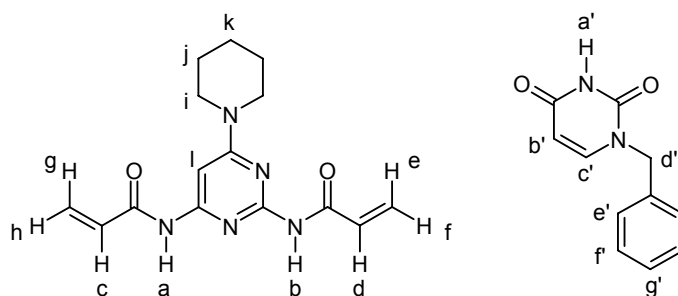
Scheme 4.5

Supporting this effect is the fact that vinyl proton *d* that was strongly shifted downfield (7.2-7.3 ppm), seems to return upfield towards the other vinyl protons (6.9-7.0 ppm), possibly indicating an induction of the *trans*-conformation and a disruption of the self-association of the monomer upon binding with **1-BU**. Finally, addition of **1-BU** leads to significant downfield shifts of the piperidine *i* protons whereas the vinyl protons *d* and *f* and amide protons *a* and *b* shifted upfield.

proton	start δ (ppm)	Δδ (ppm)	
		1	**4**
Ha'	7.99	+4.19	+1.940
Hb'	5.66	+0.06	+0.040
Hc'	7.13	+0.15	+0.050
Hd'	4.90	+0.08	+0.020
He',f',g'	7.34	+0.05	+0.015

Table 4.4:   *Complexation-Induced Shifts observed in the titration of **1-BU** with **1** or **4***

proton	δ (ppm) **4**		Δδ (ppm) **4+1-BU**	Δδ (ppm) **4** *dilution*
Hj	d	1.578	+0.003	0.00
Hk	d	1.658	-0.008	-0.01
Hi	s	3.589	+0.023	0.00
Hf,g	m	5.745	-0.016	+0.02
He,h	m	6.438	+0.002	0.00
Hc	q	6.660	-0.035	-0.12
Hd	q	7.228	-0.18[a]	-0.05
Hl	s	7.444	-0.005	-0.01
Ha,b	s	10.930	-0.25[b]	-1.00

Table 4.5: *Complexation-Induced Shifts of **4** observed in an equimolar mixture of **1-BU** and **4** (5 mM each in CDCl$_3$) compared to **4** alone and upon dilution of **4** from 10 to 0.8 mM. ([a] Broadened quartet; [b] signal appeared as two peaks at 10.65 and 10.72 ppm)*

The extent of the shifts of protons *d* and *f* were larger but in the same direction as those observed in the dilution experiment of **4** (see § 4.2.4.e). Of particular interest is the relatively large upfield shift of vinyl proton *d* which supports the hypothesis that **1-BU** destabilises the *cis*-amide conformation (Table 4.5).

4.2.4.d 2D-NOESY investigation of the complexes

2D-NOESY spectroscopy was employed in order to further investigate the structure of the complexes formed between monomer **4** and **1-BU**. Thus, standard solutions containing a) monomer **4** and b) a stoichiometric mixture of monomer **4** and **1-BU** were prepared and scanned in the 2D-NOESY mode (see Scheme 4.5 for structures with labelled atoms).

The 2D-NOESY spectra are displayed in Figure 4.7 and Figure 4.8.
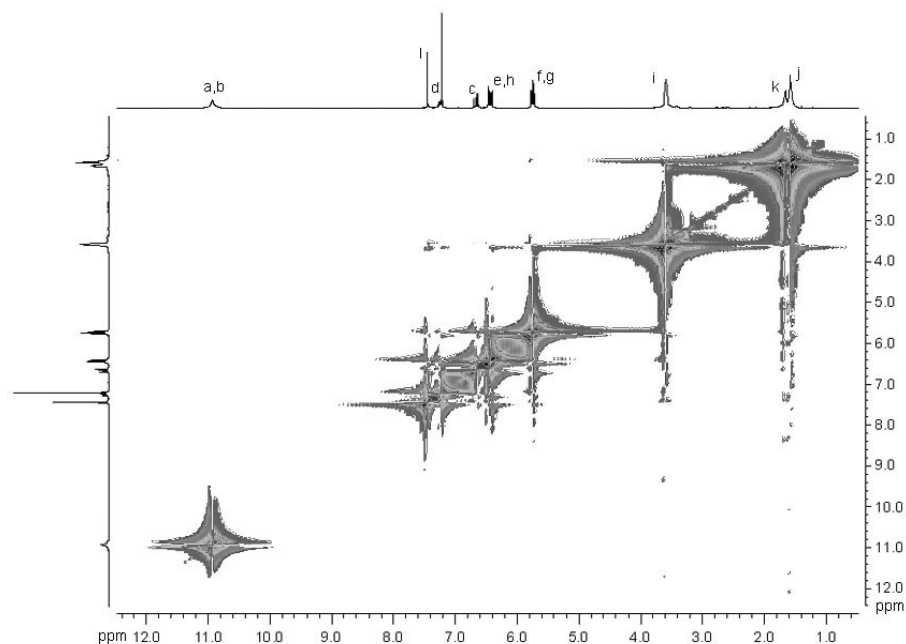
Figure 4.7: 2D-NOESY spectrum of **4** in CDCl₃
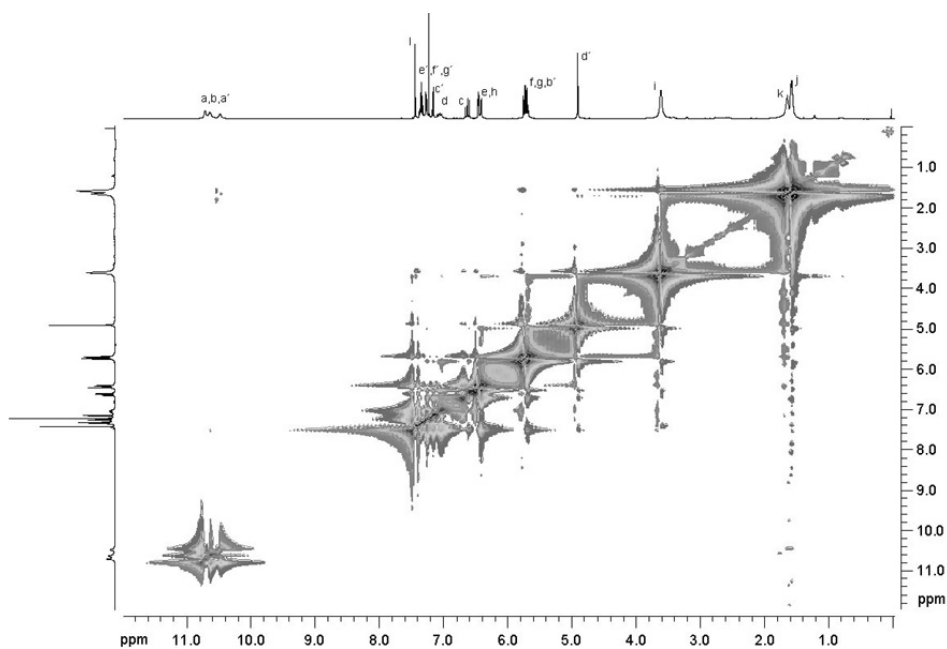
Figure 4.8: 2D-NOESY spectra of **4** with one equivalent of **1-BU** in CDCl₃

The 2D-NOESY spectrum of **4** (Figure 4.7) shows positive NOEs between the aliphatic carbons of the piperidine ring (*i, j, k*) and the corresponding vinyl protons (*d, e, f*), supporting the *cis*-amide conformation of monomer **4**.

In the equimolar mixture of **4** with **1-BU** (Figure 4.8) we find again the positive NOE signals indicating the proximity of the vinyl protons with the piperidine ring protons however, due to the weakness of the other signals, no further conclusions could be drawn.

4.2.4.e *^{1}H-NMR dilution studies*

In order to estimate the extent of the self-association of monomers **4** and **5**, ^{1}H-NMR dilution studies were carried out. Thus, nine solutions of each monomer were prepared in CDCl$_3$ and the corresponding NMR spectra were recorded. The shifts of the amide protons were plotted against the concentration of the respective sample and Figure 4.9 was created.
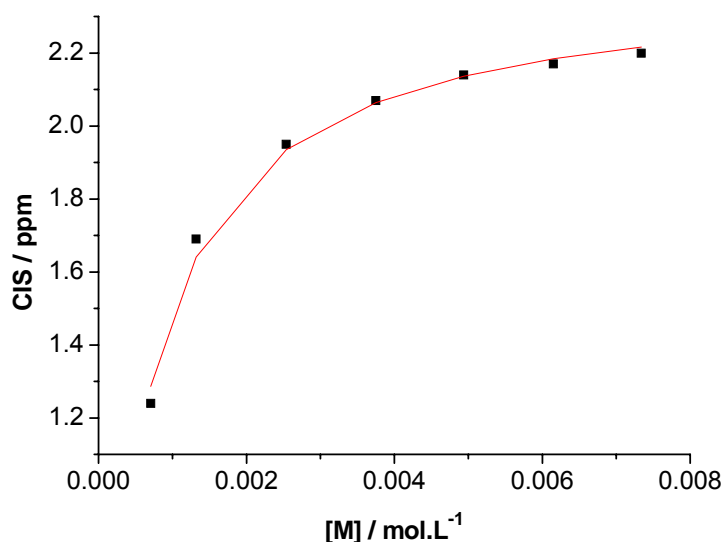
Figure 4.9: *Dilution study results and curve fit for monomer **4***

Unfortunately, in the case of monomer **5**, not enough points in the isotherm could be produced due to the low concentrations used and the low sensitivity of the NMR instrument available.

As the concentration of the solute decreases, the equilibrium of the self-association $(2S \rightleftharpoons S_2)$ is shifted towards the left, meaning that more of the solute molecules are found in the "free" state. Therefore, the shift of the amide protons observed in the dilute samples approaches the one of the monomer, since a minimum amount of dimers is present in solution.

The data points were fitted by non-linear regression using Origin$^{®}$ 7.0 to a 1:1 dimerisation model. A self-association constant of 731±51 M^{-1} was obtained, significantly higher than the ones previously reported in the literature for hexanoic acid (2-hexanoylaminopyrimidine-4-yl)amide (170 M^{-1}),[131] however expected, since the example studied there, should exhibit a weaker H-bond stabilisation of the *cis*-amide by the ring N3, as well as the electron releasing group at the 6 position.

At this point should be mentioned that a similar dilution experiment using monomer **1**, showed no shift of the amide protons upon dilution, indicating lack of self-association.

Having estimated the self-association constant for monomer **4**, it is possible to re-plot the data obtained by its titration with **1-BU**. Thus, the concentration of "free" monomer, meaning the concentration of monomer that is available for complexation with the template, is re-calculated using equation 4.1. Afterwards, assuming a maximum CIS, the concentration of free monomer [M] is calculated, and plotted against [M.T] (concentration of monomer complexed to the template) to give the final binding curve. In this case the CIS measured for monomer **1** is a good approximation for the maximum CIS of monomer **4** upon binding to **1-BU**.

The equation used for the re-calculation of [M] is:

$$\left[M\right] = -\frac{1}{4K_{S_2}} + \sqrt{\frac{1}{16K_{S_2}{}^2} - \frac{1}{2K_{S_2}}\left(\frac{\Delta\delta}{\Delta\delta_{\max}}T_t - M_t\right)} \qquad 4.1$$

Where, $\Delta\delta$ is the CIS of the imide proton of **1-BU**, $\Delta\delta_{max}$ the estimated maximum CIS of the imide proton of **1-BU**, T_t is the total concentration of template and M_t the total concentration of monomer.
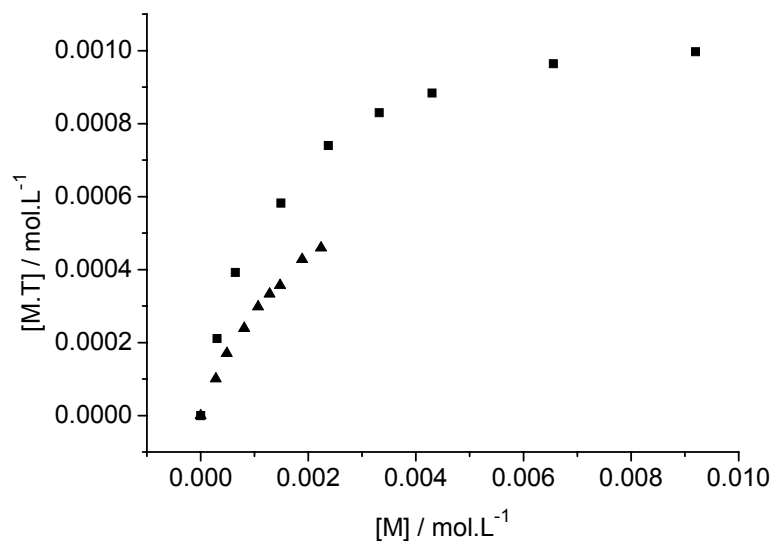
Figure 4.10: *Binding isotherms for **1** (■) and **4** (▲) corresponding to the data in Figure 4.4, assuming for **1** a 1:1 binding model and for **4** a 1:1 model with dimerisation of **4** (K_{S2} = 731M^{-1}, $\Delta\delta_{max}$ = 4.5 ppm; **1-BU** imide proton followed).*

However, as seen in Figure 4.10, the curve that is generated when taking into account the dimerisation of monomer **4** and assuming a maximum CIS equal to the one measured for monomer **1**, is far from reaching saturation, therefore the intrinsic association constant of **4** with **1-BU** can not be extracted by this method.

4.2.4.f   ATR-FT-IR study of the complexation

The presence of self-association is further supported from FT-IR investigations of monomer **4** and a stoichiometric mixture of it with **1-BU**. Thus, two solutions were prepared in $CHCl_3$; a 5mM solution of monomer **4** and a 5mM solution of **4** and **1-BU**. Both solutions were then transferred on the crystal of the ATR module and the spectra were recorded (32 scans) once the solvent was completely evaporated. As a control experiment, the same measurements were performed with monomer **1**, for which it has already been established by ^{1}H-NMR dilution studies that no self-association takes place in solution.
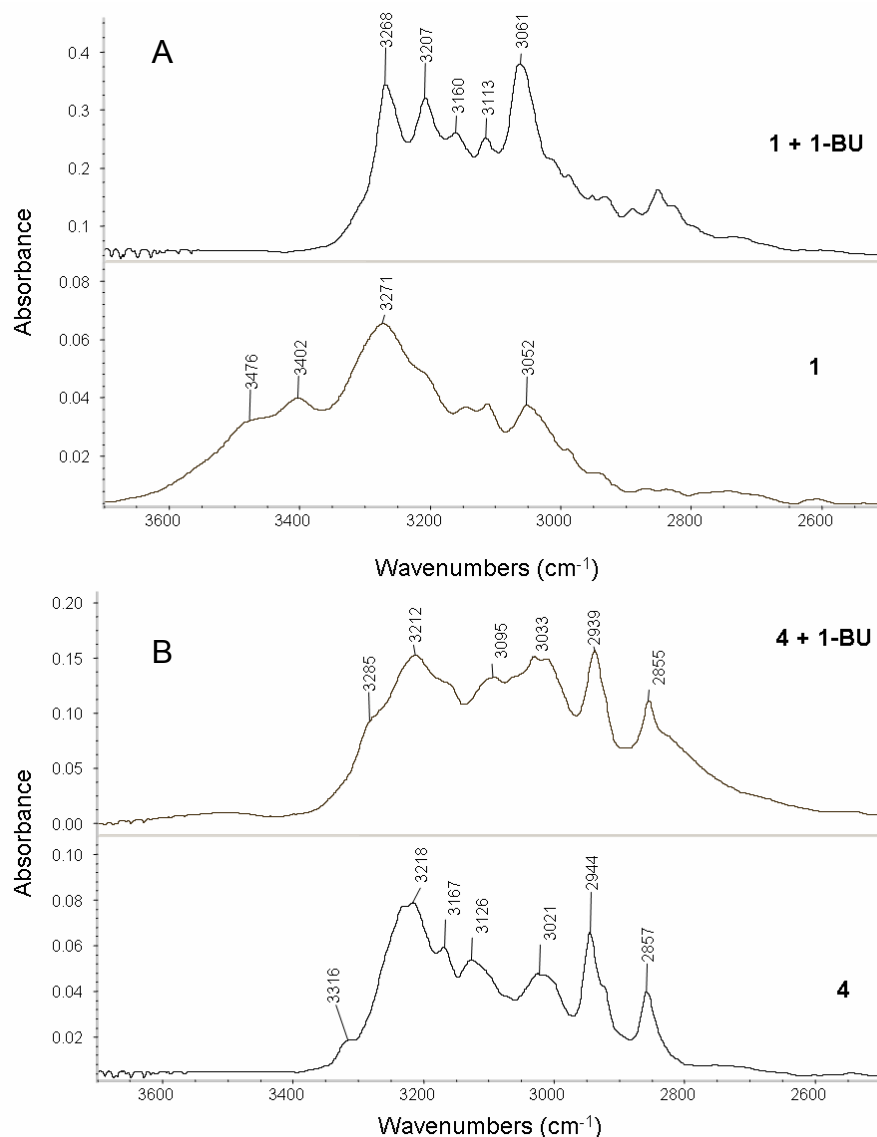
Figure 4.11: *FT-IR spectra of (A) **1** with and without **1-BU** and (B) **4** with and without **1-BU***

In the high frequency part of the spectra recorded with monomer **1**, the following peak assignments were made (Figure 4.11A): 3476, 3402 cm^{-1} CONH free, N-H stretch; 3271 cm^{-1} CONH associated, N-H stretch.

Similarly, for monomer **4** the following bands could be assigned (Figure 4.11B): 3316 cm^{-1} trans CONH associated, N-H stretch, 3218 cm^{-1} cis CONH associated, N-H stretch, 2954 cm^{-1} piperidine CH_2, C-H stretch (asym.), 2857 cm^{-1} piperidine CH_2, C-H stretch (sym).

The high-frequency region reveals stark differences in the positions of the bands corresponding to the NH stretching mode of the amide groups.[132] Whereas **1** exhibits bands at 3402 and 3476 cm^{-1}, corresponding to non-

associated NHs, **4** exhibits somewhat more intense bands below 3316 cm^{-1}, indicative of strong hydrogen bonds.

Although it is not possible to unambiguously assign the bands in the low-frequency region, it is notable that **4** showed bands at frequencies expected for *cis*-amides, whereas no such bands were found in the spectra of **1**. Furthermore, the bands of **4** were generally sharper than those of **1**. This indicates the presence of a defined structure showing little conformational ambiguity (Figure 4.12).

Upon addition of a stoichiometric amount of **1-BU**, the bands of **1** become sharper whereas those of **4** become broader. For **1** the sharpening of the bands is explained by the formation of a well-defined triple hydrogen bonded complex. Further support for this structure is the relatively intense NH bands and the apparent absence of bands corresponding to non-associated NH. Opposite to the complex between **1-BU** and **1**, addition of **1-BU** to **4** appears to result in a less defined structure. This is possibly caused by multiple amide bond conformations or interaction modes *vis-à-vis* **1-BU**. Studying more closely the high-frequency region, the NH stretch vibrations are found at lower frequencies (even extending below 2800 cm^{-1}) in the complex between **1-BU** and **4** than those found in neat **4** or in the **1-BU**-**1** complex. These spectral features indicate the presence of strongly hydrogen-bonded complexes.[132] Another important observation concerns the relative intensities of bands tentatively assigned to *cis* and *trans*- amide bonds. Addition of **1-BU** leads to an apparent weakening of the former indicating that the *trans*- conformation is favoured. This would be an expected result if **1-BU** competes for the same interaction sites of **4** as those involved in dimerisation.
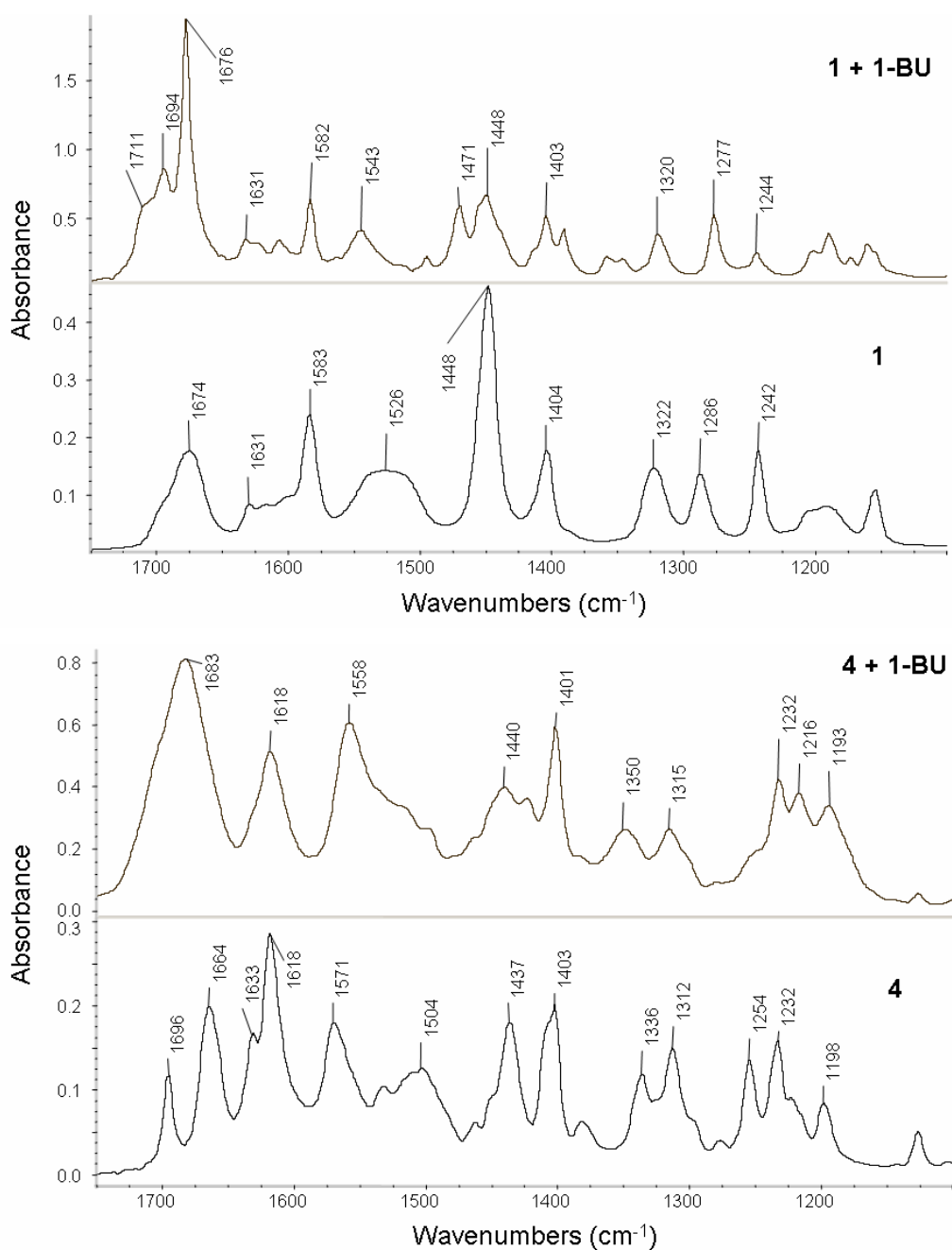
Figure 4.12:   Low frequency regions of the recorded FT-IR spectra

4.2.4.g   Fluorescence dilution studies of the monomers

As a final confirmation of the self-association of monomer **4**, an additional dilution study was performed, this time monitored by fluorescence spectroscopy. Thus, standard solutions of monomers **1** and **4** in CDCl$_3$ with concentrations ranging from 5×10^{-5} to 1×10^{-3}M were prepared and their fluorescence emission at 440nm (excitation at 270nm) was recorded.
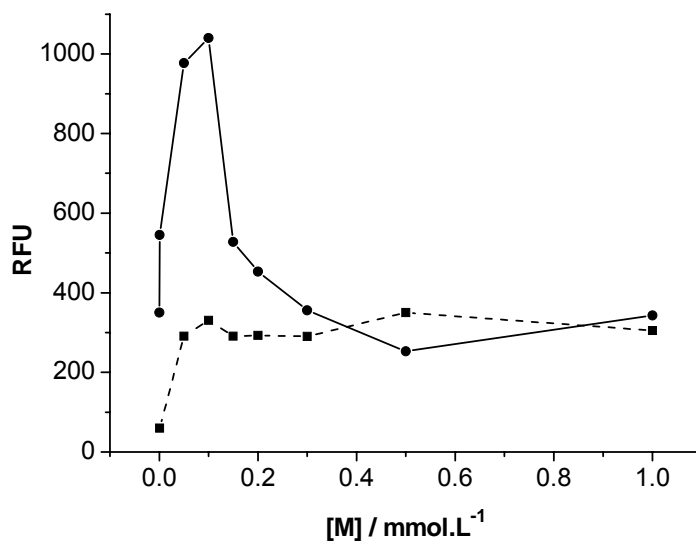
Figure 4.13: *Fluorescence intensity change upon dilution of monomers **1*** *(- -■- -) and **4** (—●—)*

The results plotted in Figure 4.13 are in perfect agreement with the expectations. Monomer **1** shows a linear decrease in its fluorescence below 0.05mM and then the fluorescence remains almost constant (out of the linear range) above 0.1mM. Inversely, monomer **4** shows a dramatic increase in its fluorescence between 0.5 and 0.1mM, indicating that more of the molecules are in the "free" state below this concentration, thus less self-quenching of the fluorescence occurs. Only in the range below 0.05mM there is linear correlation between concentration and fluorescence intensity.

4.2.5   2nd generation of MIPs against 1-benzyluracil

Monomers **1**, **4** and **5** were significantly more soluble in $CHCl_3$ than **2** and **3**, therefore a second recipe was worked out according to which higher concentrations of monomers and template would be used, leading to a higher concentration of imprinted sites in the resulting materials. The ratio of template to monomer was also decreased to 1:1.5, moving towards more stoichiometric imprints. Detailed recipes are shown in Table 4.6. For each imprinted polymer, a corresponding control polymer was synthesised in a similar manner, but with omission of the template (**P$_N$x**).

Polymer	Template 1-BU	Functional Monomer	Cross-linker (EDMA)
P1	0.041g / 0.2mmol	**1** - 0.066g / 0.3mmol	3.8mL / 20mmol
P4	0.041g / 0.2mmol	**4** - 0.091g / 0.3mmol	3.8mL / 20mmol
P5	0.041g / 0.2mmol	**5** - 0.079g / 0.3mmol	3.8mL / 20mmol

Table 4.6

$CHCl_3$ (5.6mL) was used again as porogenic solvent. The polymerisation was carried out at 40°C for 24h and ABDV (1% w/w of total monomers) was used as the free radical initiator.

After the polymerisations were completed, the polymers were extracted with methanol using the Soxhlet apparatus, followed by crushing and sieving to obtain particles with size 25-50μm, which were sedimented and then packed into HPLC columns for evaluation in the chromatographic mode. Particles of the same size were used also for equilibrium batch rebinding experiments and fluorescence monitored batch rebinding experiments.

4.2.6   Mode of monomer incorporation

Although the elemental analysis data indicated that the monomers had been stoichiometrically incorporated into the polymers, the question remained whether they were different concerning the conversion of the second vinyl group. The fluorescence spectral properties of **1** and **4** provided unique structural information concerning the mode of monomer incorporation in the polymer. Monomers **1** and **4** exhibited fluorescence emission at 435nm (on excitation at 270nm) (inserts on Figure 4.14) which could serve as a direct measure of the accessibility and microenvironment of the imprinted binding sites in the cross-linked polymers.[133]
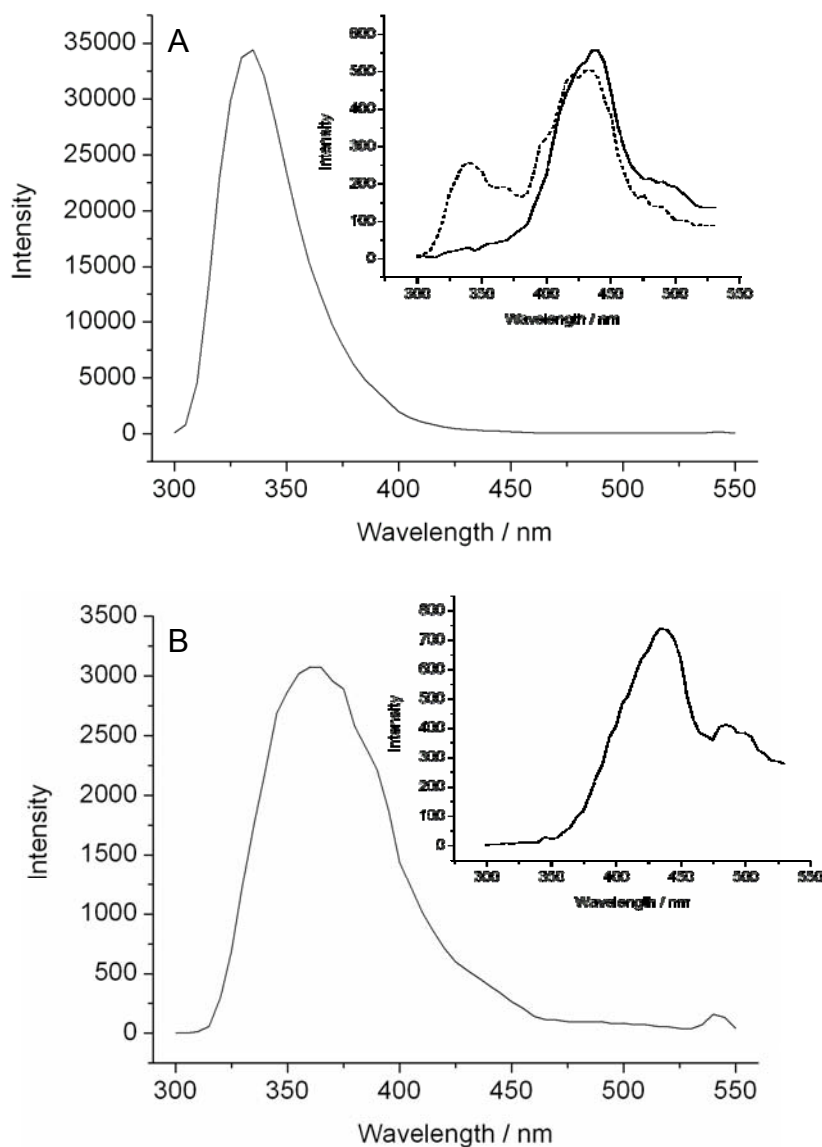
Figure 4.14:   *Emission spectra of (A)* **1** *(insert - solid line), control compound* **6** *(insert – dashed line) and* **7** *(main graph); (B)* **4** *(insert) and control compound* **8** *(main graph)*

As seen in Figure 4.15, the fluorescence spectra corresponding to polymers **P1** and **P4** prepared from monomers **1** and **4**, respectively, displayed emission maxima at *ca.* 340nm, corresponding to a blue shift of nearly 100nm compared to the free monomers. Furthermore, the emission intensity was observed to be at least an order of magnitude stronger than for the free monomers. Weaker intensities were also observed at higher wavelengths with a shoulder at 435nm. These spectral features could be informative about the mode of monomer incorporation in the polymer. The fluorescence emission spectra (λ_{ex} = 270nm) of unreacted monomer **1** (Figure 4.14A-insert) was

compared with those of the model compounds (see Scheme 4.6) corresponding to mono-reacted (**6**) (Figure 4.14A-insert) and completely reacted (**7**) monomers (Figure 4.14).
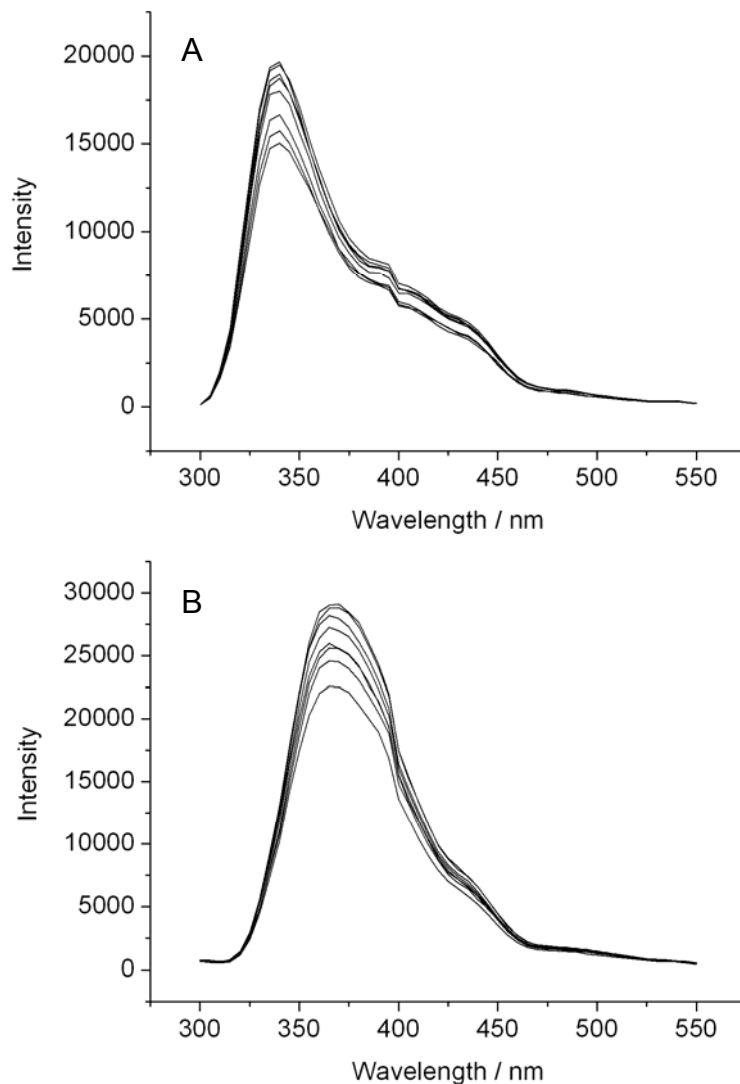
Figure 4.15:   *Fluorescence titration of (A)* **P1** *with* **1-BU** *and (B)* **P4** *with* **1-BU**

Whereas **1** showed a single broad and weak emission band at 435nm, the model compound **6** in addition exhibited a weak band at 340nm. However, model compound **7** showed a single and strong emission peak at 340nm which coincided with the emission spectra of the polymers. The same result was also obtained when comparing the spectra of **4** (Figure 4.14B-insert) and model compound **8** (Figure 4.14B).
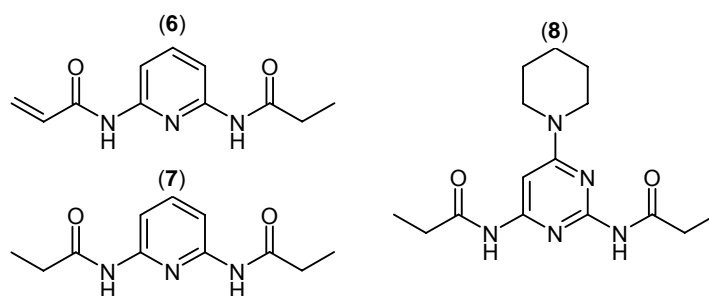
Scheme 4.6

These results suggest that the blue shift is predominantly due to a chemical change in the monomer emission properties upon polymerisation rather than micro-environmental effects. Based on these observations it is concluded that a significant portion of both monomers (**1** and **4**) has been doubly incorporated in the polymer. The large difference in emission intensity between the model compounds precludes a quantitative evaluation of the data.

4.2.7   Chromatographic evaluation of the 2nd generation MIPs

The synthesised materials were evaluated using HPLC. The group of injected analytes comprises molecules where there exist either additional sites for interaction with the pendant functionalities within the polymer matrixes (uracil (**U**) and 5-fluorouracil (**5-FU**)), a molecule where a hydrogen bonding site has been blocked (1,3-dibenzyl uracil (**DBU**)) and a molecule containing a different substituent at the 1-position (**AZT**).

All measurements were performed on a HP1050 Liquid Chromatograph. As mobile phase 100% acetonitrile was used. The injection volume was 5μL, the flow rate 1mL/min and detection was performed using a Diode Array Detector (DAD) recording chromatograms at 260nm.
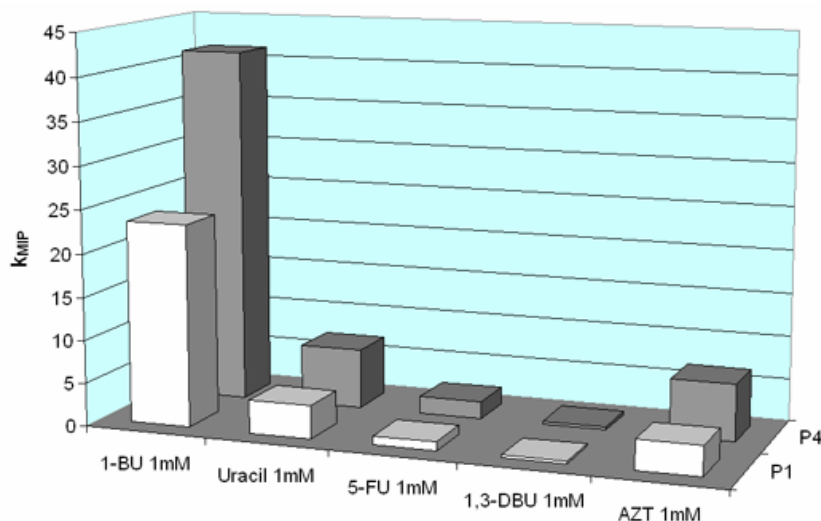
Figure 4.16: k_{MIP} *values of the different analytes on the corresponding MIPs (mobile phase: 100% MeCN)*
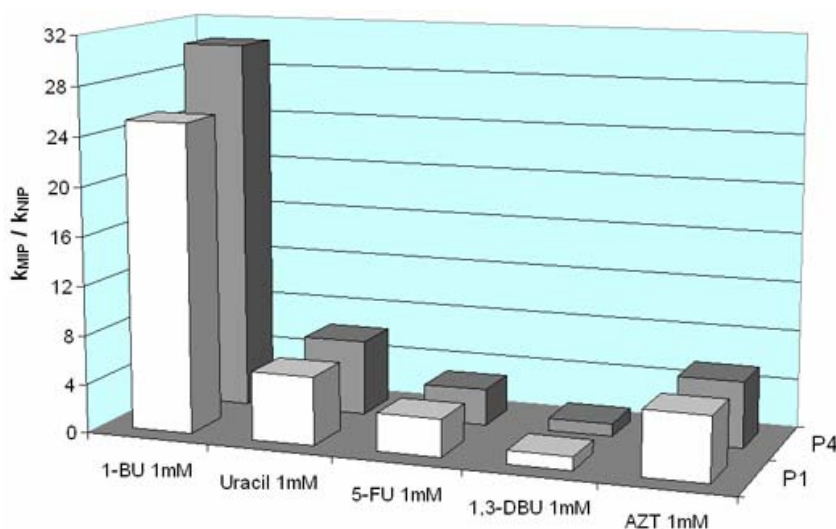
Figure 4.17: k_{MIP}/k_{NIP} *values of the different analytes*

Opposite to the expectations based on the solution-binding results, the polymers prepared using **4** (**P4**) exhibited stronger retention and higher imprinting factors (k_{MIP}/k_{NIP}) than those prepared using **1** (**P1**). As seen in Figure 4.16, the template molecule was nearly two times more retained on **P4** than on **P1**. On injection of the other, similar analytes onto the polymers, the difference between the MIP and NIP becomes even starker. While the retention of these analytes on the NIP are little different from that of the template molecule, the imprinted polymer shows a high degree of selectivity for its template (Figure 4.17).

The HPLC retention data, although demonstrating a clear improvement using **4**, are not sufficient for determining its origin. Since only one point on the isotherm is tested, the higher retention and imprinting factors obtained on **P4** may be due to a larger number of accessible sites, a higher intrinsic binding affinity of these sites or a combination of these effects.

4.2.8 Batch rebinding experiments

Equilibrium batch rebinding experiments were performed in order to gain an insight into the grounds of this unexpected performance of **P4**. Thus, 10mg of the corresponding material were weighed into HPLC vials and subsequently incubated with 1mL solutions of **1-BU** of increasing concentrations (0-1mM) in acetonitrile for 24 hours.

Then, an aliquot (200μL) of each supernatant solution was transferred to a well of a 96 well-plate and the UV absorbance was measured using a plate reader. The concentration of each of the supernatants was obtained with the help of a calibration curve, constructed previously. The amount of **1-BU** bound on each polymer was plotted against the concentration of free template in solution to generate Figure 4.18.
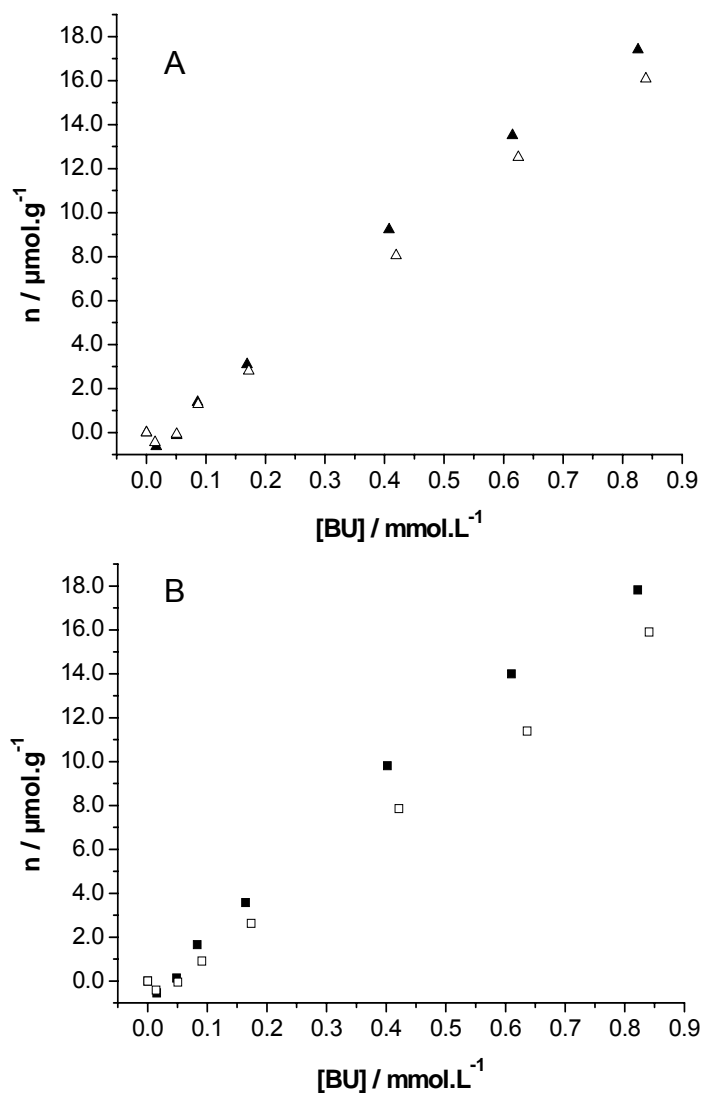
Figure 4.18:   *Isotherms for the adsorption of **1-BU** on (A) ▲ **P1**, △ **P$_N$1**; (B) ■ **P4** and □ **P$_N$4***

When considered individually, the isotherms described close to straight lines and none of the polymers exhibited visible saturation within the measured concentration interval. This shows that the non-specific adsorption was weak in acetonitrile although, as indicated by the slope of these curves, a significant number of such weak sites were present. When comparing the isotherms of the imprinted with the non-imprinted polymers, the former were steeper showing that the MIPs had adsorbed more **1-BU** at a given concentration of free **1-BU**. This difference was larger for **P4** than for **P1**, which appears more clearly from a plot of the differential adsorptions (Figure 4.19).
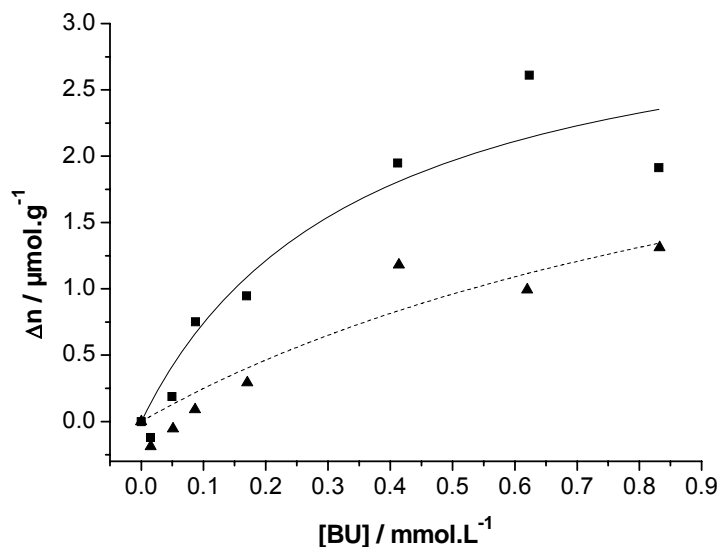
Figure 4.19:   *Differential plot (MIP-NIP) of **1-BU** adsorbed on:* ▲ ***P1** and* ■
                              P4

From the differential plot it is concluded that **P4** contains additional binding sites, which appear to be stronger and to exist in a greater abundance than those of **P1**.

4.2.9 Fluorescence monitored batch rebinding

Similar performance of the polymers was observed when the synthesised materials were incubated with different concentrations of the template and the equilibration process was monitored in real-time by fluorescence measurements. Thus, 10mg of polymer were weighed into the wells of a 96 well-plate and incubated with increasing concentrations of **1-BU** in acetonitrile. The plate was sealed to avoid evaporation of the solvent and was immediately transferred in the plate reader. The fluorescence intensity of each polymer (λ_{ex}= 270nm, λ_{em}= 340nm) was recorded at fixed intervals for at least one hour. At the end of the monitoring time, a full emission spectrum of each well, corresponding to a polymer incubated with different concentration of **1-BU**, was recorded (Figure 4.15).

4.2.9.a   Kinetic study of the binding

The recorded fluorescence intensities of each well were plotted against the time and Figure 4.20 was produced.
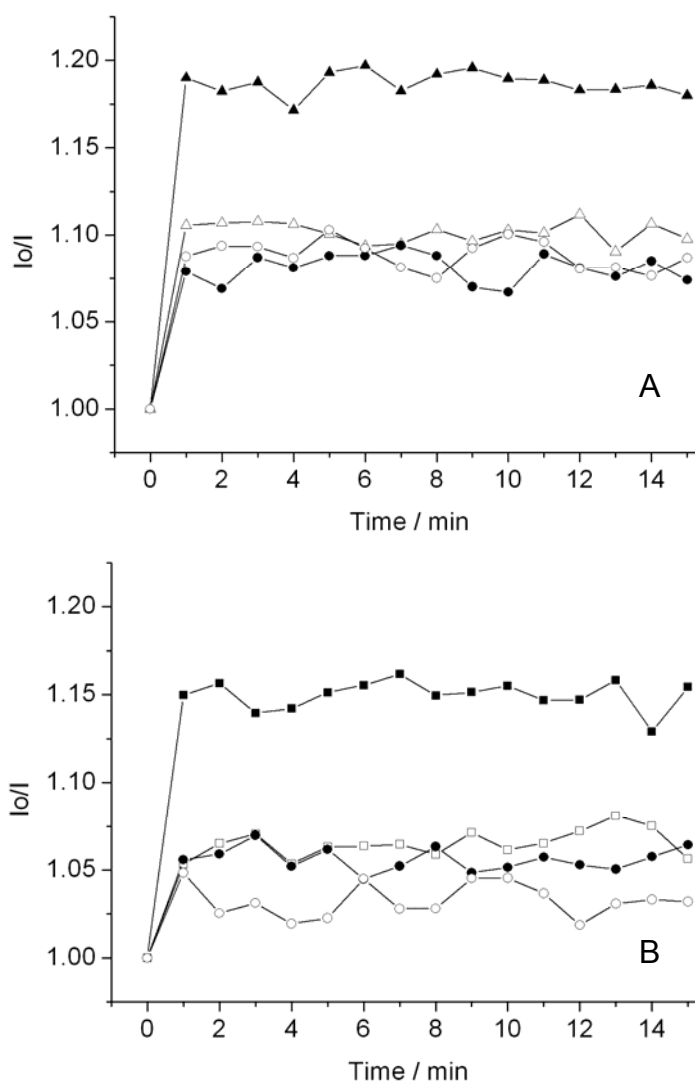
Figure 4.20:   *Fluorescence response upon binding of (A)* ***1-BU*** *on* ***P1*** *(▲),* ***1-BU*** *on* ***P_N1*** *(△),* ***1,3-DBU*** *on* ***P1*** *(●),* ***1,3-DBU*** *on* ***P_N1*** *(○); (B)* ***1-BU*** *on* ***P4*** *(■),* ***1-BU*** *on* ***P_N4*** *(□),* ***1,3-DBU*** *on* ***P4*** *(●),* ***1,3-DBU*** *on* ***P_N4*** *(○)*

The response of the polymers to the binding event was immediate and after the first minute, no significant changes in the fluorescence were observed. Additionally, when the same experiment was performed with **1,3-DBU**, instead of the **1-BU** itself, the change in fluorescence on **P1** and **P4** was minimal and in both polymers it coincided with the one measured for **P_N1** and **P_N4** respectively.

4.2.9.b   "Rebinding on the plate" measurements

In order to be able correlate the fluorescence quenching observed on each polymer with the amount of bound template, after the kinetic measurement was completed, an aliquot of the supernatant (100μL) was transferred to a neighbouring well and the UV absorbance (260nm) was measured, thus allowing a calculation of the free template and consecutively the concentration of **1-BU** bound on the polymer.
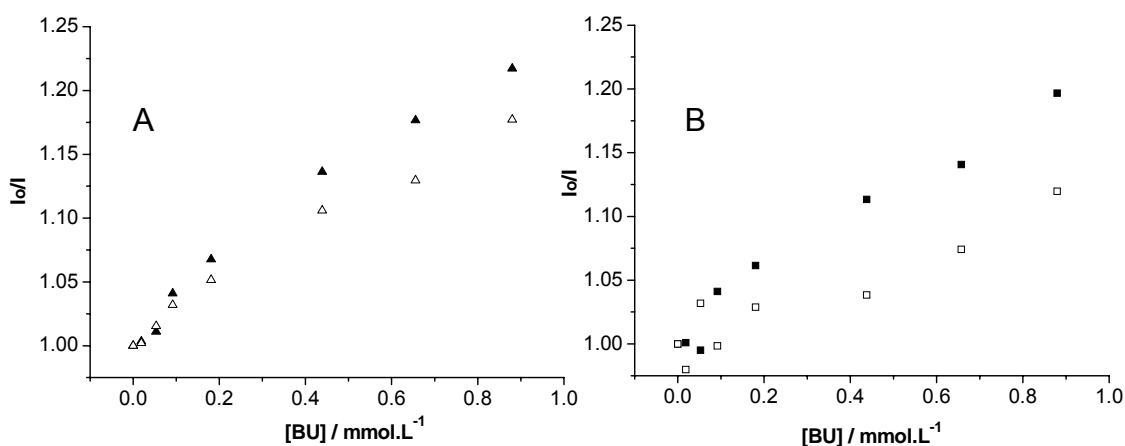
*Figure 4.21:   Stern-Volmer plots showing the fluorescence quenching upon addition of **1-BU** to a suspension of (A) **P1** (▲) and **P$_N$1** (△) and (B) **P4** (■) and **P$_N$4** (□)*

The fluorescence data reveal larger imprinting effects for **P4** than for **P1**, as reflected in the differential plots (Figure 4.22). The correlation between the differential Stern-Vollmer curves and the corresponding binding isotherms shows that a simple measurement of the fluorescence quenching reports on how much template is bound to the polymer.
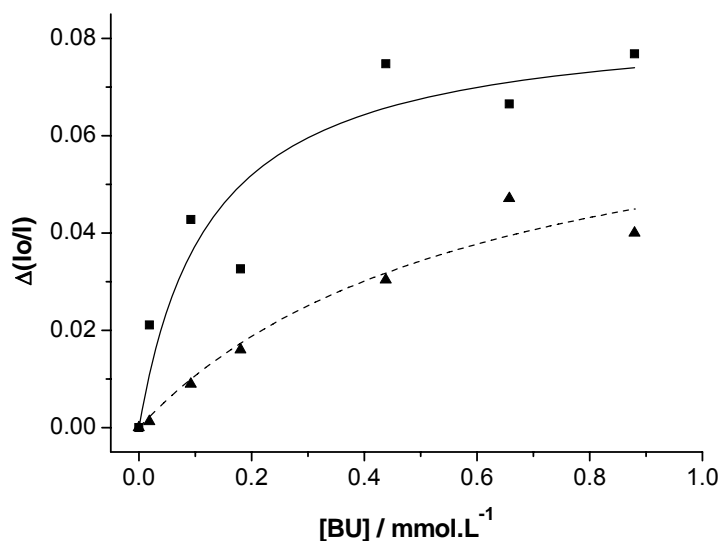
Figure 4.22: Differential binding plot corresponding to the data presented on Figure 4.21 for **P4** (■) and **P1** (▲)

4.2.10 Attempts to prevent dimerisation

Obviously, molecules incorporating the affinity enhancing features of **4** but unable to dimerise would be of significant interest. In an effort to prevent dimerisation model compounds **9** and **10** were synthesised (Scheme 4.7). These compounds exhibit more bulky amide substituents which could stabilise the amide *trans-* isomer and thus prevent dimerisation. Attempts to synthesise the methacrylamide version of **4** failed due to its unexpectedly high tendency to polymerise. This may in itself be an indication that also this molecule prefers the *cis-* isomer resulting in a less conjugated double bond.
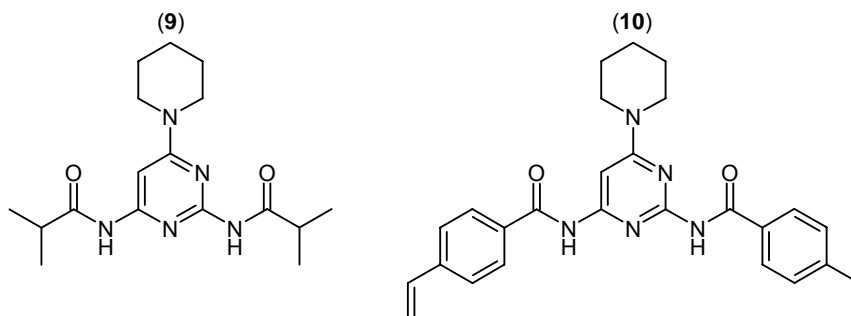
Scheme 4.7

Whereas **9** exhibited similar dimerisation behaviour as **4** judged from IR and NMR data, **10** alone showed IR spectra more similar to **1**. However, addition of **1-BU** to **10** did not lead to disappearance of the bands corresponding to free NH groups, indicating that these interacted weakly compared to **1** and **4**. This was further supported by the low chromatographic imprinting factors obtained for polymers prepared against **1-BU** using monomer **10**.

4.2.11 Conclusions

A series of functional monomers with the ability to recognise the imide moiety present in uracil have been synthesised and subsequently tested in solution and in the resulting imprinted polymers. Monomers **1** and **4** (Scheme 4.8) appeared to be the candidates concentrating the major advantages, namely sufficient solubility and relatively high association constants to **1-BU**.
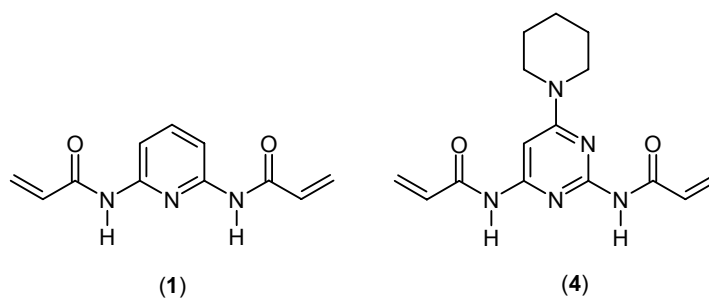
Scheme 4.8

Interestingly however, despite the apparently weaker binding of **1-BU** displayed by monomer **4** compared to monomer **1**, imprinted polymers made using **4**, exhibit increased imprinting effects reflected in higher retention and imprinting factors. These differences are attributed to the properties of the polymers to the binding mode presented by **4** and also its ability to dimerise (Scheme 4.9).

Thus, the lower apparent solution binding constant is likely the result of pronounced dimerisation of **4** masking the inherently stronger hetero-complex formation **4**:**1-BU**. These differences are carried through into the polymer matrix during the polymerisation step. Template removal exposes the high affinity D-A-D hydrogen bonding array of **4** whereas the dimers are locked up and are thereby poorly accessible. Possibly, **4** also exposes additional

interaction sites for **1-BU** but the exact nature of these is still unknown. Monomer **1** binds more weakly to **1-BU** but shows, on the other hand, no tendency to dimerise. The net effect should be the creation of weaker imprinted sites and more pronounced non-specific binding.
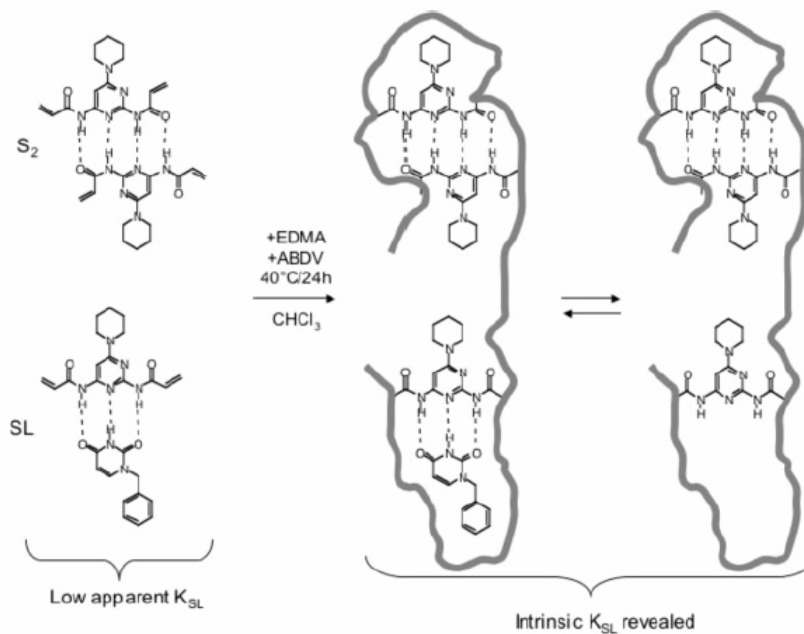
Scheme 4.9

An interesting property of the system is the correlation between the ligand binding with the extent of fluorescence quenching. Although fluorescence reporter groups have been incorporated in imprinted binding sites previously,[101, 134] the use of simple D-A-D monomers as combined binding and reporter groups has only recently been reported. The enhanced affinity *vis-à-vis* imides using **4**, seems promising for the future design of polymers for the separation and sensing of such guests.

4.3 Water compatible imprinted polymers for the recognition of riboflavin

Having obtained valuable information regarding the performance of the selected binding elements for the recognition of uracils, efforts were concentrated in the development of a water-compatible material for the selective binding of riboflavin in highly aqueous environments. The steps taken towards this direction will be discussed in the following paragraphs.

4.3.1 Solubility of riboflavin

Riboflavin (vitamin B_2) is a member of the B complex of water soluble vitamins, although its water solubility is marginal.[77, 135]
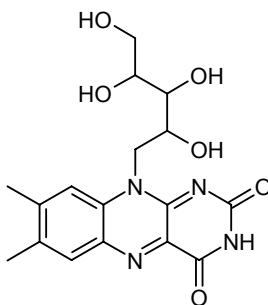
Scheme 4.10: Structure of riboflavin

Furthermore, as initial solubility studies showed, it is insoluble in most low-polar organic solvents used in molecular imprinting (e.g. acetonitrile, toluene, chloroform) and is only readily soluble in formic acid, DMSO and DMF. Thus, the first challenge faced during the effort to imprint riboflavin was the selection/synthesis of a soluble analogue that would provide similar size, shape and functional group arrangement with the original target, but would be sufficiently soluble in the aforementioned solvents commonly used in molecular imprinting.

4.3.2 Phenyl flavin and alkyl flavins

The first attempt was based on a one step synthesis of phenyl flavin (**PF**) (Scheme 4.11) from o-amino diphenylamine and alloxane monohydrate.[136]

However, this was shortly proven to be a poor choice since, apart from the different π-electron distribution and its highly hydrophobic character, its size and shape were far from similar to the one of riboflavin. The subsequently synthesised imprinted polymers against phenyl flavin indicated minimal selectivity and high non-specific binding for riboflavin in aqueous systems. Test experiments for the extraction of riboflavin from beer using these materials led to complete decolourisation of the product. This approach was thus abandoned and a different methodology was decided.
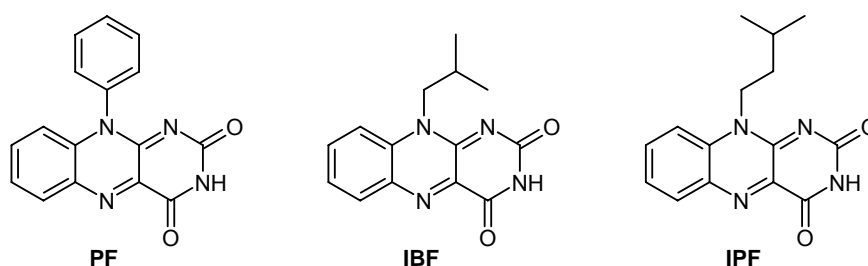
Scheme 4.11: Structures of phenyl flavin and the different alkyl flavins

Examining the structure of riboflavin, one can divide the molecule in two main structurally and functionally similar parts: the iso-alloxazine part, comprising the planar hydrophobic three ring system and the open sugar chain, a more flexible, hydrophilic part. Thus, it was considered that a potentially good template analogue candidate could contain the basic hydrophobic part of riboflavin, but a more organic soluble alkyl side chain, replacing the open ribose structure. A four step synthetic protocol for the synthesis of alkyl substituted flavins was adapted from a previously published procedure,[137] whereby starting from alkylation of the amino group of 2-nitroaniline using the corresponding alkyl bromide and subsequent reduction of the nitro-group followed by condensation of the product with alloxane, two alkyl substituted flavins were synthesised, with different size of alkyl chains, the isobutyl flavin (**IBF**) and the isopentyl flavin (**IPF**) (Scheme 4.11).

Once the new flavins were obtained, extensive solubility tests were performed, in order to determine whether the main objective of increasing the solubility was fulfilled. The solvents tested were chloroform and acetonitrile, the most commonly used solvents in molecular imprinting, and a mixture of water/ethanol : 95/5, a solvent system similar to the composition of beer. The

maximum concentrations achieved are displayed in Table 4.7 together with the corresponding solubility of riboflavin for direct comparison.

Solvent	Riboflavin	PF	IBF	IPF
chloroform	<0.1mM	1mM	**16mM**	8mM
acetonitrile	<0.1mM	1mM	5mM	6mM
water/ethanol : 95/5	1mM	<1mM	<1mM	<1mM

Table 4.7:   Solubility of riboflavin and its analogues

The maximum concentration obtained, namely **IBF** in chloroform, was approximately 5 times lower than the one usually required in molecular imprinting (~0.1M), but was sufficient for the initial tests.

In order to estimate the association constant between **IBF** and monomer **1** a ^{1}H-NMR titration was performed in $CDCl_3$ (Figure 4.23).
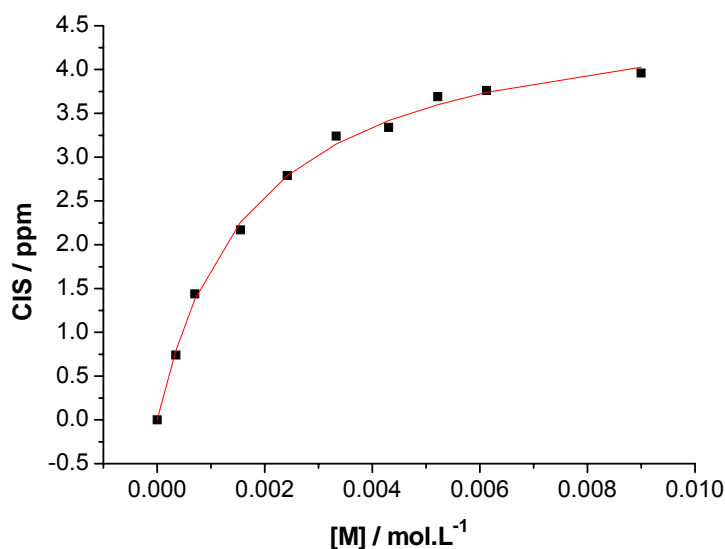
Figure 4.23:   Binding isotherm and curve fitting for the ^{1}H-NMR titration of **IBF** (1mM) with monomer **1** (0-10mM) in $CDCl_3$

The obtained association constant (570±35 M^{-1}) is in good agreement with the ones recorded for the uracil derivatives, indicating that **1** is a suitable functional monomer for the generation of MIPs against this flavin analogue. The small difference in the association strength can be attributed to the different magnetic and electronic environment between uracil and flavin.

4.3.3   IBF imprinted polymers

Molecularly imprinted polymers against **IBF** were synthesised using **1** as the functional monomer and EDMA as the cross-linker, as shown in Table 4.8.

Polymer	Template IBF	Functional Monomer 1	Cross-linker (EDMA)
PIBF	0.0544g / 0.2mmol	0.0657g / 0.3mmol	3.8mL / 20mmol
P$_N$IBF	-	0.0657g / 0.3mmol	3.8mL / 20mmol

Table 4.8:   *Composition of IBF imprinted polymers (5.6mL of CHCl$_3$ as porogen)*

Polymerisation was initiated thermally, using ABDV as the free radical initiator, and was allowed to proceed for 24h at 40°C. A control polymer (**P$_N$IBF**) was prepared in exactly the same manner, but with omission of the template. The synthesised polymers were washed using the Soxhlet apparatus and methanol as the solvent and subsequently crushed and sized into 25-50μm particles, which were finally packed in HPLC columns for evaluation in the chromatographic mode. The retention factors (*k*) obtained for the different analytes injected on the columns in 100% acetonitrile as mobile phase are displayed in Figure 4.24.
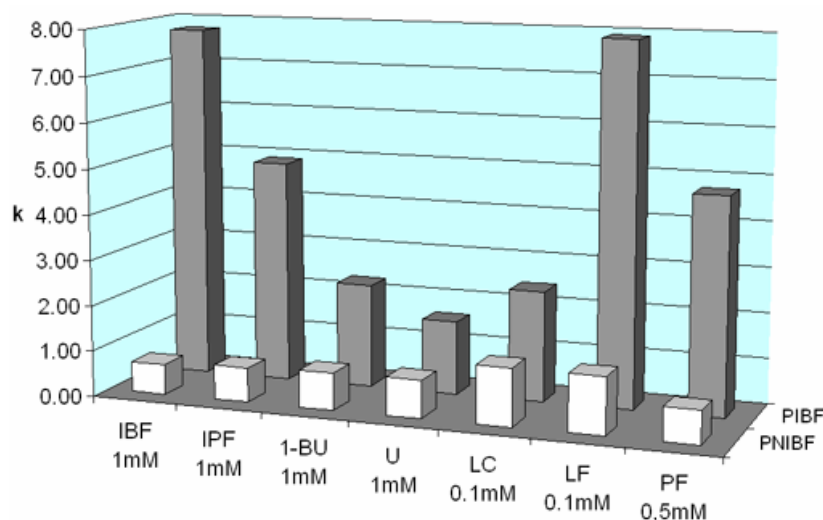
Figure 4.24:   *Retention factors of injected analytes on the **PIBF** and **P$_N$IBF** packed columns (mobile phase: 100% MeCN; injection: 5µL; flow rate: 1mL/min; detection: DAD @ 260nm)*

The library of injected analytes consists of the template **IBF**, the slightly larger template analogue **IPF**, uracil (**U**) and its derivative **1-BU**, phenyl flavin (**PF**) and the two major products of riboflavin decomposition, lumiflavin (**LF**) and lumichrome (**LC**) (Scheme 4.12).

LF   **LC**
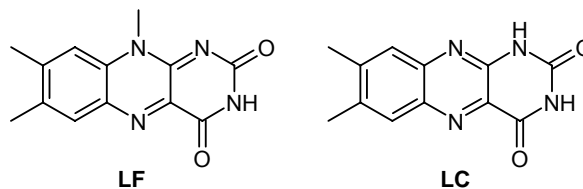
Scheme 4.12: Structures of lumiflavin and lumichrome

Observing Figure 4.24 it becomes clear that the synthesised imprinted polymer exhibits very good selectivity for its template over the other injected analytes, with the exception of **LF**, which has a very similar structure to **IBF** and is equally retained on the polymer. The structurally related **IPF** and **PF** are also retained but significantly less that the template. Uracil and **1-BU**, as well as **LC**, although they contain the same imide moiety, are very different to the imprint molecule and therefore are not strongly retained.
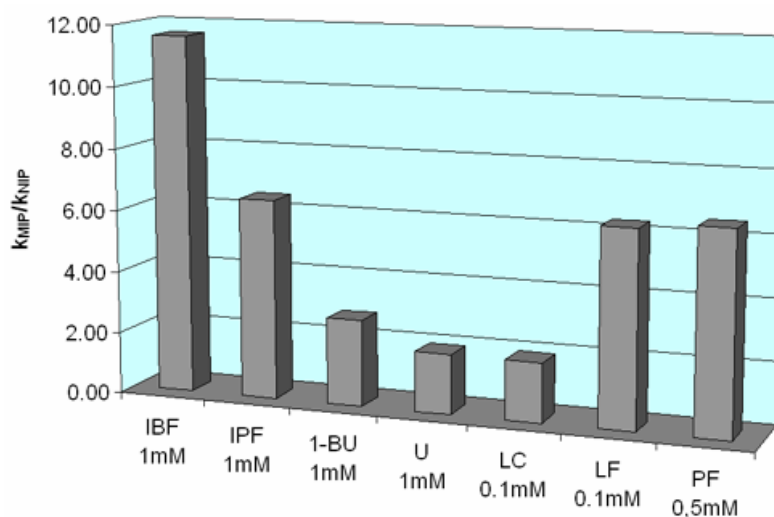
Figure 4.25: k_{MIP}/k_{NIP} values of injected analytes in 100% MeCN

Similarly, observing Figure 4.25, **IBF** is clearly the most selectively retained analyte, while the polymer appears to exhibit "group" selectivity for flavin based structures and low affinity for non-related structures, such as uracils.

Further evaluation of the binding characteristics of the **IBF** imprinted polymers towards the analyte of interest, riboflavin, was performed in aqueous mobile phases. Thus, the dependence of the retention time of **IBF** and riboflavin on the percentage of MeCN in a mobile phase consisting of 95% water and 5% ethanol was studied. In the case of **IBF**, the analysis was performed in the range 30-100% MeCN (Figure 4.26), while for riboflavin, due to solubility limitations, the range was between 10 and 50% MeCN (Figure 4.27).
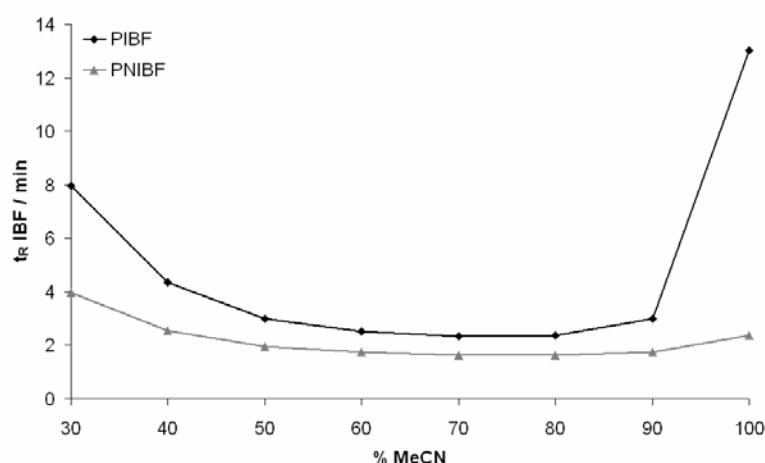
Figure 4.26:   Dependence of retention time of *IBF (0.5mM; 5µL) on the PIBF and P_NIBF packed columns (125mm x 4.6mm) on the percentage of MeCN in the mobile phase (H_2O/EtOH : 95/5)*

As seen in Figure 4.26, in pure organic mobile phase, the imprinted polymer, **PIBF**, exhibits maximum retention for **IBF**, while on the non-imprinted polymer, **P_NIBF**, the retention time is minimal. With the addition of only 10% aqueous mobile phase the difference in the retention between the two polymers diminishes, since a 70% drop in the retention on **PIBF** is observed. The situation remains unchanged until approximately 50% MeCN, after which point the increasing amount of water in the mobile phase leads to an increase in the non-specific hydrophobic binding, observed in both imprinted and non-imprinted polymers.

In the case of riboflavin a similar effect takes place. Unfortunately, the measurements could only be performed in a smaller range of organic phase content due to solubility limitations of riboflavin in MeCN. However, examining Figure 4.27, one can observe that while in high percentage of MeCN the

polymers exhibit no selectivity for riboflavin, in mostly aqueous systems, the imprinted polymer reveals its inherent affinity for the target analyte, despite the increased non-specific binding.
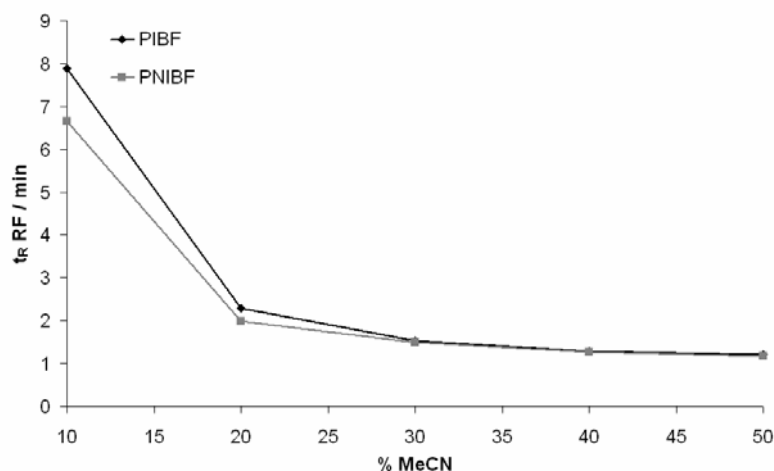
Figure 4.27:   *Dependence of retention time of riboflavin (0.5mM; 5µL) on the PIBF and P_NIBF packed columns (125mm x 4.6mm) on the percentage of MeCN in the mobile phase (H_2O/EtOH : 95/5)*

This is a first positive indication that with such systems it is possible to achieve selectivity in highly aqueous environments nevertheless, these results are far from satisfactory and further optimisation is needed.

4.3.4   Riboflavin tetra esters as template analogues

The imprinting effect can be greatly enhanced by introduction of larger number of binding sites in the matrix of an imprinted polymer. In order to achieve this, a higher concentration of template-monomer complexes needs to be present in the pre-polymerisation mixture, since these complexes are the precursors of the imprinted cavities in the resulting material. The complexation process is governed by the equilibrium between free and complexed monomer and template species. Shifting this equilibrium towards the complexed side requires an increased total concentration of the binding partners. In the studied case, monomer **1** is adequately soluble in the polymerisation solvent though further increase of its concentration is expected to lead to increased non-specific binding. It is therefore necessary to find a template analogue with higher solubility than that of **IBF**.

Inspired by the availability of a riboflavin tetra ester, namely riboflavin tetrabutyrate, in the chemical catalogues, a series of flavin alkyl esters was synthesised in order to investigate the dependence of the binding characteristics of the synthesised imprinted polymers on the alkyl chain length. The syntheses were performed in one step with relatively high yields. The series is presented in Scheme 4.13.

RfAc   **RfPr**   **RfBu**
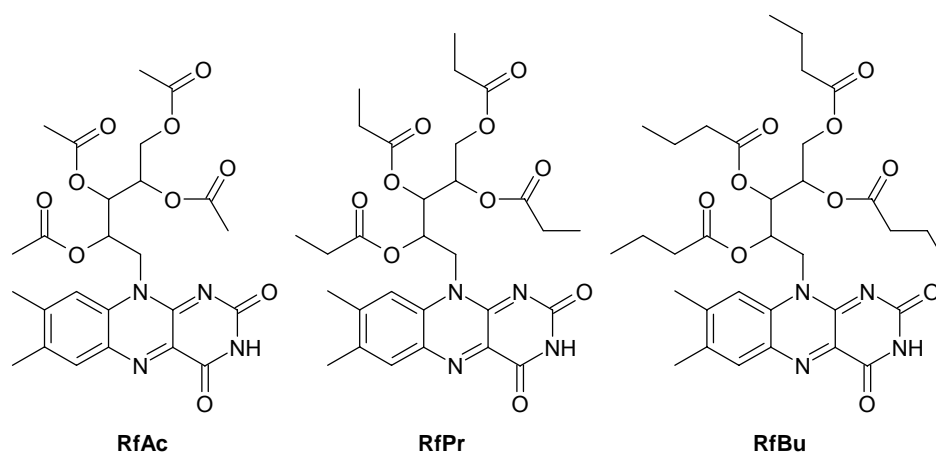
Scheme 4.13: Structures of the riboflavin tetra esters

Solubility studies of the synthesised and commercially available riboflavin tetra esters in chloroform have been carried out and the results are displayed in the following table.

Solvent	Riboflavin	RfAc	RfPr	RfBu
chloroform	<0.1mM	0.2M	0.6M	0.8M

Table 4.9

An at least 10-fold increase in the solubility of the template analogues compared to the one of **IBF** was achieved, which allowed the synthesis of imprinted polymers with the normally used concentration of template (0.1M).

4.3.4.a   *Riboflavin tetra ester imprinted polymers*

Molecularly imprinted polymers were synthesised in chloroform, using the above synthesised tetra esters as template analogues, **1** as the functional monomer and EDMA as the cross-linker in chloroform (Table 4.10). The

polymerisation was initiated thermally at 60°C using AIBN as free radical initiator and was allowed to proceed for 24 hours. After this time, the polymers were washed with methanol using a Soxhlet apparatus and subsequently crushed and sieved to collect particles between 25-50μm for further evaluation in the chromatographic or batch mode.

Polymer	Template	Functional Monomer *1*	Cross-linker (EDMA)
P(RfAc)	**RfAc** - 0.546g / 1mmol	0.218g / 1mmol	3.8mL / 20mmol
P(RfPr)	**RfPr** - 0.600g / 1mmol	0.218g / 1mmol	3.8mL / 20mmol
P(RfBu)	**RfBu** - 0.656g / 1mmol	0.218g / 1mmol	3.8mL / 20mmol
P$_N$	-	0.218g / 1mmol	3.8mL / 20mmol

Table 4.10: Composition of tetra ester imprinted polymers (5.6mL of CHCl$_3$ as porogen)

4.3.4.b   Chromatographic evaluation of the polymers

The sized particles were packed in HPLC columns (125mm × 4.6mm) in order to assess their binding properties. The retention times of several analytes in organic mobile phase (MeCN-1%CH$_3$COOH) was initially tested and the results are presented in Figure 4.28.

The use of riboflavin esters as templates leads to imprinted polymers with extremely high retention times for their respective templates thus, addition of 1% acetic acid in the mobile phase was necessary to reduce the retention times to a workable time frame.

Figure 4.28: *Retention factors of injected analytes on the tetra ester imprinted polymers packed columns (mobile phase: MeCN-1% CH₃COOH; injection: 5µL; flow rate: 1mL/min; detection: DAD @ 260nm)*

Examination of Figure 4.28 and Figure 4.29 reveals a series of interesting trends. Firstly, the tetra ester imprinted polymers show generally higher affinity for tetra esters than for other analytes. This is attributed to the similarities in shape and size between the three esters, which are starkly different than the smaller flavins or the uracil derivative. However, the polymers show interesting size exclusion effects, discriminating the increasingly bulky tetra esters depending on their size. Thus, the retention times of the tetra esters decrease on **P(RfAc)** as the size of the alkyl chain increases. This phenomenon is expected since the cavities present in **P(RfAc)** can easily accommodate **RfAc** but not the bigger **RfPr** or **RfBu**. On the **P(RfPr)**, the template is well retained, but the space available in the binding sites is enough for **RfAc** to be bound and too "tight" for **RfBu** to fit.

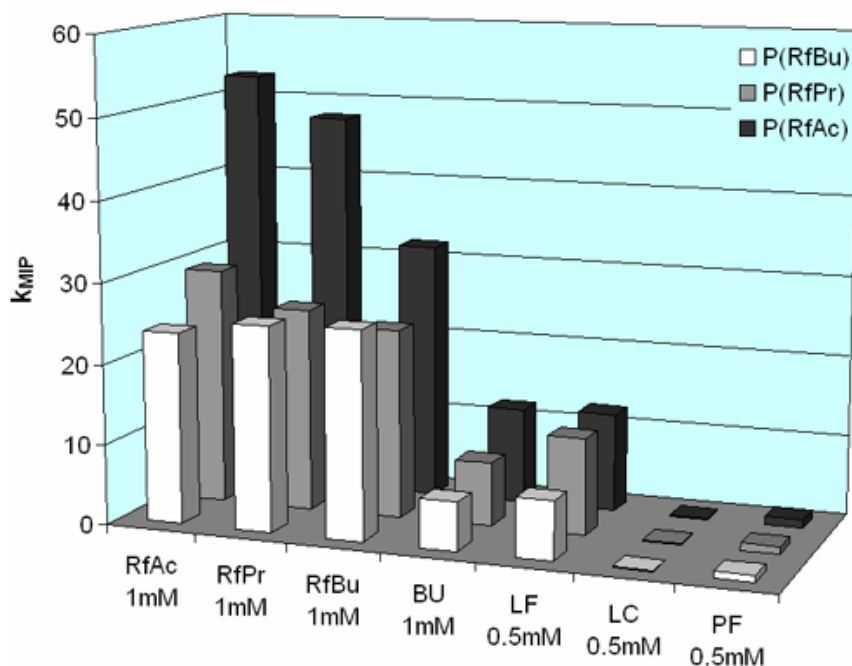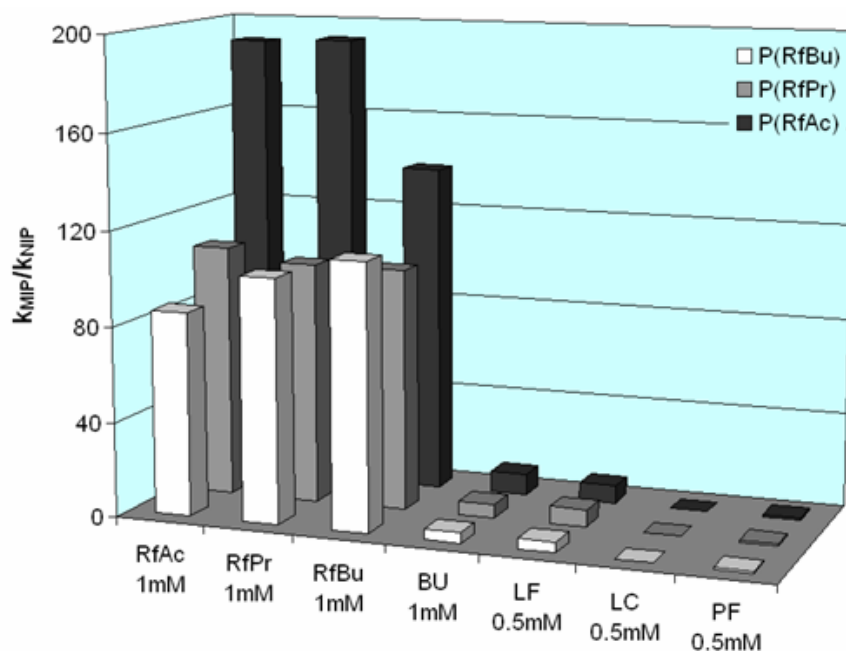*Figure 4.29:* k_{MIP}/k_{NIP} *values of injected analytes on the tetra ester imprinted polymers packed columns (mobile phase: MeCN-1% CH₃COOH; injection: 5μL; flow rate: 1mL/min; detection: DAD @ 260nm)*

Finally, on **P(RfBu)** the template is optimally bound in the cavities but the other two esters appear to be too small thus their binding is not facilitated by secondary "sticky" contacts to the walls of the binding sites, which appear to play a significant role to the binding event.

Another interesting fact is that **P(RfAc)** has significantly higher retention times for all three esters, compared to **P(RfPr)** and **P(RfBu)**, possibly due to higher number or quality of binding sites present in the polymer. This could be attributed to the fact that **RfAc**, being the smallest of the three esters, has a more defined structure in solution while the two increasingly bigger esters have higher flexibility and less defined structure, leading to poorer imprinting quality.

The large imprinting factors that these polymers exhibit arise from two effects, namely the pronounced retention of the riboflavin analytes on the imprinted polymers coupled with low retention on the control, non-imprinted polymer **P_N** (Figure 4.29). This observation suggests that the binding sites provided by the functional monomer units in **P_N** are located in areas of the polymeric matrix that cannot be accessed by the larger tetra ester analytes. This assumption is

supported by the comparatively stronger retentions of the smaller analogue analytes on $\mathbf{P_N}$.

4.3.4.c   Frontal Analysis of the tetra ester imprinted polymers

In order to further investigate the binding characteristics of the synthesised polymers, staircase frontal analysis experiments were performed. Thus, the columns used in the above chromatographic evaluation were loaded with step-wise increasing concentrations of their respective template in the used mobile phase (MeCN – 1% acetic acid) and the time until breakthrough of each "step" was recorded. Subsequent mathematic elaboration of the data (see § 6.5.46.5.3 in the Experimental Part) leads to the isotherms presented in Figure 4.30, where the amount of adsorbed analyte per unit of polymer mass (q / μmol.g^{-1}) is plotted against its concentration in the mobile phase (C / mmol.L^{-1}).

The results of the thermodynamic study of the polymers confirm the observations made in the dynamic mode. Hence, the non-imprinted polymer shows no significant binding for any of the three tested riboflavin tetra esters, while **P(RfPr)** and **P(RfBu)** perform almost identically. **P(RfAc)** appears to have the highest affinity for its template as well as a higher capacity.
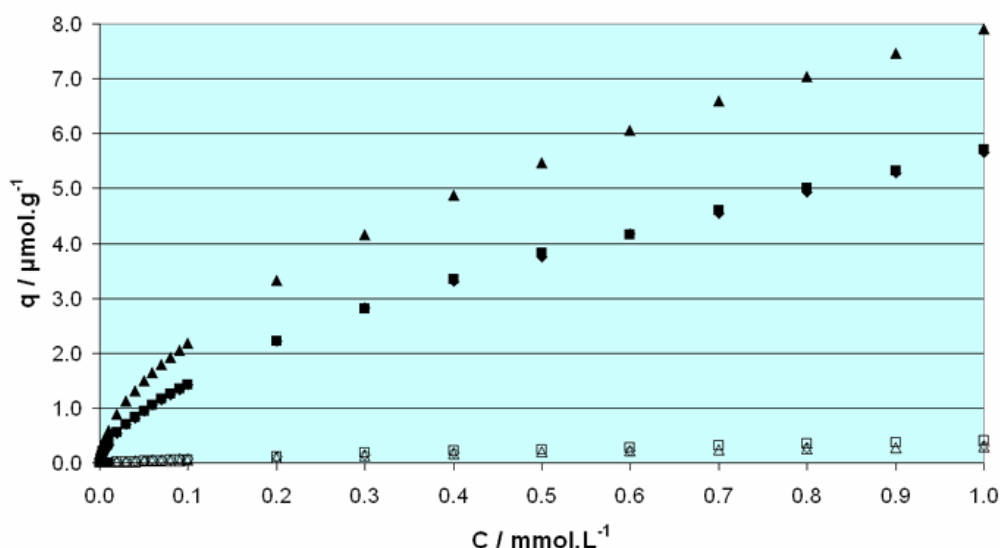
Figure 4.30:   *Binding isotherms obtained by frontal analysis: ▲ RfAc on P(RfAc); △ RfAc on P_N; ◆ RfPr on P(RfPr); ◇ RfPr on P_N; ■ RfBu on P(RfBu); □ RfBu on P_N*

The double logarithmic plot (Figure 4.31) of the data above is linear to a great extent, indicating that the latter can be fitted to the Freundlich isotherm (see Experimental Part § 6.5.4).
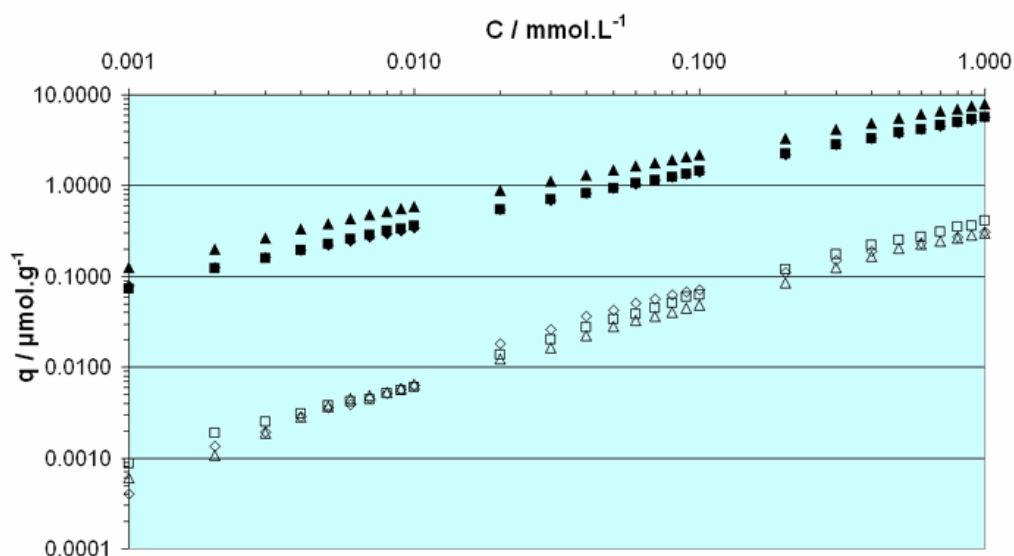
Figure 4.31: Log-Log plot of the data obtained by frontal analysis: ▲ **RfAc** on **P(RfAc)**; △ **RfAc** on **P_N**; ◆ **RfPr** on **P(RfPr)**; ◇ **RfPr** on **P_N**; ■ **RfBu** on **P(RfBu)**; □ **RfBu** on **P_N**

The parameters obtained by non-linear regression are displayed in Table 4.11.

Polymer	a	m	K_a (M^{-1})	N ($\mu mol.g^{-1}$)
P(RfAc)	3.9966	0.5586	2.60×10^4	1.13×10^{-1}
P(RfPr)	2.8517	0.5970	2.29×10^4	5.84×10^{-2}
P(RfBu)	2.8250	0.5961	2.29×10^4	5.82×10^{-2}
P_N	0.1582^a	0.7743	1.29×10^4	5.98×10^{-4}
	0.2058^b	0.7821	1.26×10^4	7.16×10^{-4}
	0.1596^c	0.6601	1.86×10^4	1.86×10^{-3}

Table 4.11: Fitting parameters of the frontal analysis data to the Freundlich isotherm ($q=a\times C^m$) and calculated average association constants and average number of binding sites (^{a}row corresponds to the isotherm of binding of **RfAc** on the **P_N**; ^{b} **RfPr** on the **P_N**; ^{c}**RfBu** on the **P_N**). Origin^{TM} 7.0 was used for the curve fitting.
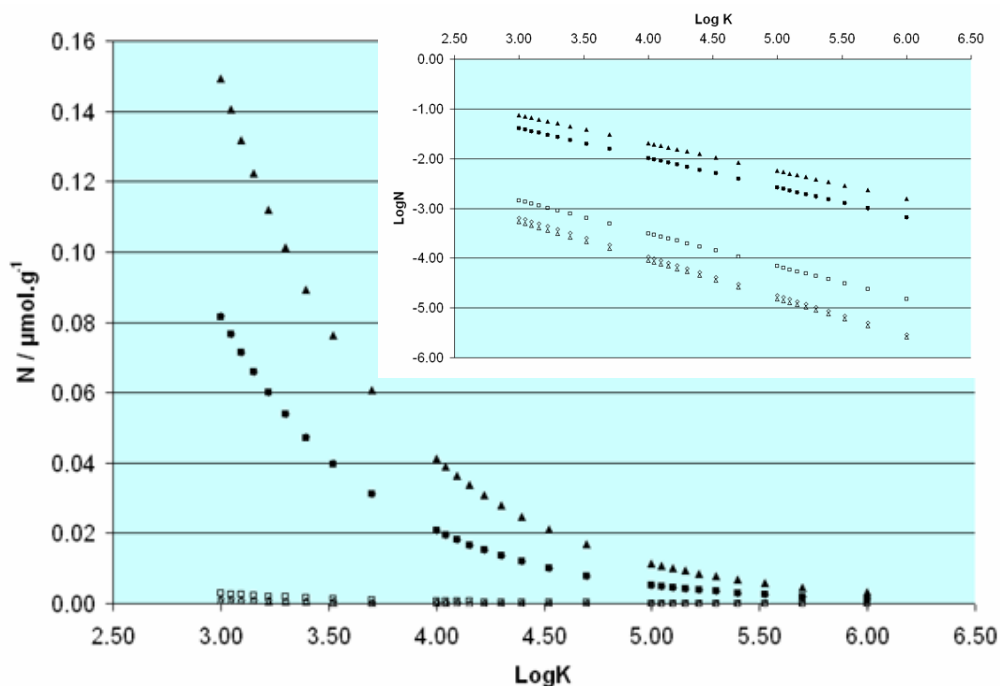
Figure 4.32: *Semi-log plot of the affinity distribution obtained by fitting of the frontal analysis data to the Freundlich isotherm (▲ **RfAc** on **P(RfAc)**; △ **RfAc** on **P$_N$**; ◆ **RfPr** on **P(RfPr)**; ◇ **RfPr** on **P$_N$**; ■ **RfBu** on **P(RfBu)**; □ **RfBu** on **P$_N$**); Insert: corresponding log-log plot*

The binding sites of **P(RfAc)** appear to be the most heterogeneous as indicated by parameter *m*, but also approximately double as many as the ones present in **P(RfPr)** and **P(RfBu)**, as shown by *N*, calculated by the affinity distribution analysis (Figure 4.32). The association constants for the binding of each imprinted polymer with its corresponding template are in the same order of magnitude, with the one calculated for **P(RfAc)** being marginally higher. Parameter *m* for **P$_N$** is significantly higher, indicative of more homogeneous material, a phenomenon generally observed for non-imprinted polymers. The affinity constants are also lower, but in the same order of magnitude however, the number of binding sites is at least 100 times smaller.

4.3.4.d Extension of the isotherms by batch rebinding

The performed frontal analysis experiments offer a valuable insight into the binding capability of the riboflavin tetra ester polymers however, the examined

concentration window is relatively small (0 - 1mM). This is mainly due to the limitation posed by the HPLC detector, which could only measure concentrations of tetra ester up to 1mM, even at 490nm, far from any local maxima in the tetra ester UV spectra. Concentrations higher than 1mM exceeded the upper limit of absorbance that could be measured by the instrument. In order to overcome this limitation and extend the studied concentration window, a batch rebinding experiment was designed, ranging from 0 - 20mM in the same mobile phase as the one used in the frontal analysis experiment.

Thus, 8×10mg of polymer were accurately weighed in equal number of HPLC vials (1.5mL) and were allowed to equilibrate with 500μL of increasingly concentrated solutions of the corresponding tetra ester. After 24h, an aliquot of each supernatant (100μL) was transferred to the wells of a 96 well-plate and the concentration of "free" analyte (C_f) was calculated measuring the UV absorbance of the solution at 260nm. The amount of analyte bound to the polymer per unit of polymer mass (q / μmol.g^{-1}) was calculated by subtraction. Finally, the binding isotherms were produced by plotting q *vs.* C_f (Figure 4.33).
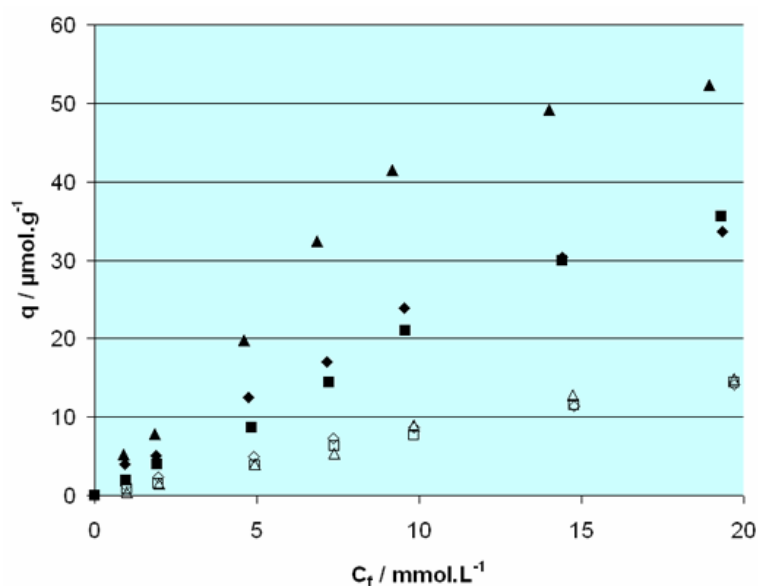
Figure 4.33:   Binding isotherms obtained by batch rebinding in MeCN – 1% acetic acid (▲ RfAc on P(RfAc); △ RfAc on P$_N$; ◆ RfPr on P(RfPr); ◇ RfPr on P$_N$; ■ RfBu on P(RfBu); □ RfBu on P$_N$)

Once again, the already made observations were confirmed. **P(RfAc)** shows the highest capacity and binding strength for its template, with **P(RfPr)** and **P(RfBu)** showing significantly lower affinity however, much higher than this of P_N, proving again the undisputed imprinting effect.

Concluding the thermodynamic study of the riboflavin tetra ester imprinted polymers, **P(RfAc)** clearly outperforms the other two synthesised polymers, not only showing stronger affinity to its template, but also more well defined binding sites. Whether these promising characteristics are directly translated in the binding of riboflavin in aqueous environments remains to be tested.

4.3.4.e   *Performance of the polymers in aqueous environments*

The potential of the so far synthesised polymers for selective recognition of riboflavin in aqueous samples was initially tested by chromatographic means. Hence, the columns used for the chromatographic and thermodynamic evaluation of the riboflavin tetra ester imprinted polymers were equilibrated with a mobile phase consisting of 5% ethanol in water; a mixture similar to the composition of beer. However, upon injection of a 0.5mM solution of riboflavin, the analyte was not eluted from the columns after more than 2 hours, indicating strong binding of the vitamin but also significant non-specific binding. In order to reduce the retention times to a reasonable time scale, increased amounts of acetonitrile were added to the mobile phase. 20% acetonitrile leads to very quick elution of riboflavin from all three columns, with a slightly higher retention factor measured on **P(RfAc)**.
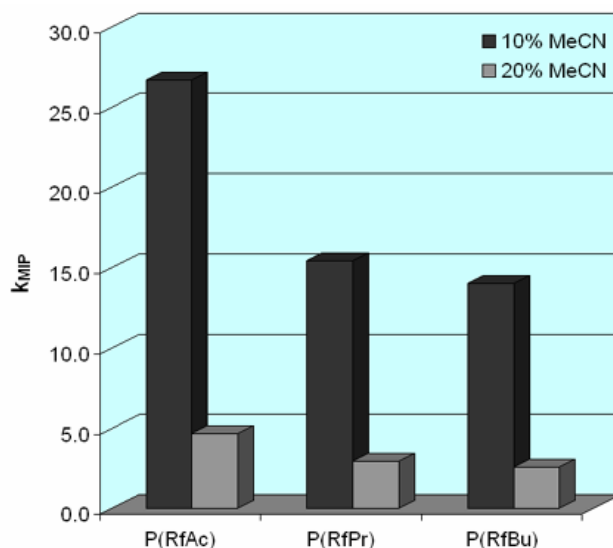
Figure 4.34:   *Retention factors of 0.5mM riboflavin on the tetra ester imprinted polymers packed columns (mobile phase: dark grey columns 10% MeCN – 90% (H_2O-5%EtOH), light grey columns 20% MeCN – 80% (H_2O-5%EtOH); injection: 5μL; flow rate: 1mL/min; detection: DAD @ 260nm)*

The difference becomes starker at 10% acetonitrile, at which composition the retention time of riboflavin on **P(RfAc)** is almost double than the ones on **P(RfPr)** or **P(RfBu)** (Figure 4.34). However, the level of non-specific binding observed on these polymers was relatively high regarding the desired applications.

4.3.4.f   *Proof of the Art – Using commercial monomers*

As a control of the importance of monomer **1** in the imprinting process, a batch of imprinted polymers against **RfAc** was synthesised using the traditional composition template : monomer : cross-linker 1 : 4 : 20, using methacrylic acid as the functional monomer (**P(RfAc)$_{MAA}$**). All other parameters were kept identical to the previously synthesised tetra ester imprinted polymers.

The selectivity of the obtained materials towards their template as well as riboflavin was evaluated in the chromatographic mode.
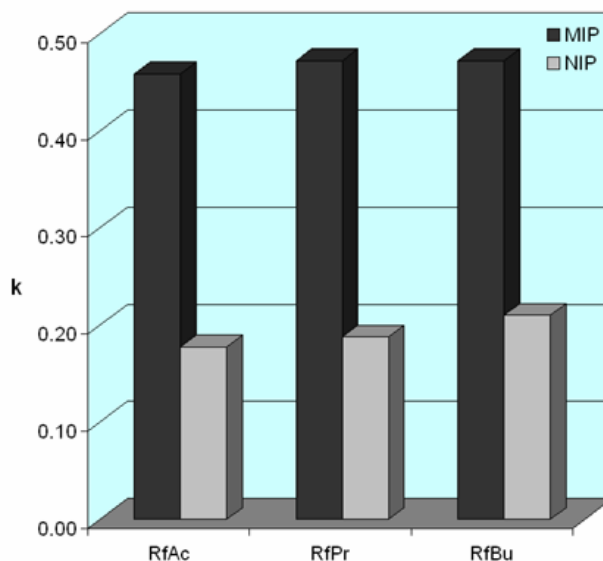
Figure 4.35: *Retention factors of the tetra esters on **P(RfAc)$_{MAA}$** imprinted polymers (mobile phase: MeCN-1% CH$_3$COOH; injection: 5µL; flow rate: 1mL/min; detection: DAD @ 260nm)*

As seen in Figure 4.35, a minimal imprinting effect can be observed, with the maximum retention time on the **P(RfAc)$_{MAA}$** observed for **RfBu** (~2 min). The polymer shows no selectivity for its template *vs.* the other larger tetra esters, suggesting that the difference in size of the tetra esters alone cannot lead to successful imprinting, establishing the importance of the appropriate functional monomer.

Similar behaviour is observed when the MAA-based polymers are tested in aqueous environments (Figure 4.36), where no retention or selectivity for riboflavin was displayed and the imprinting factors calculated being smaller than 1.
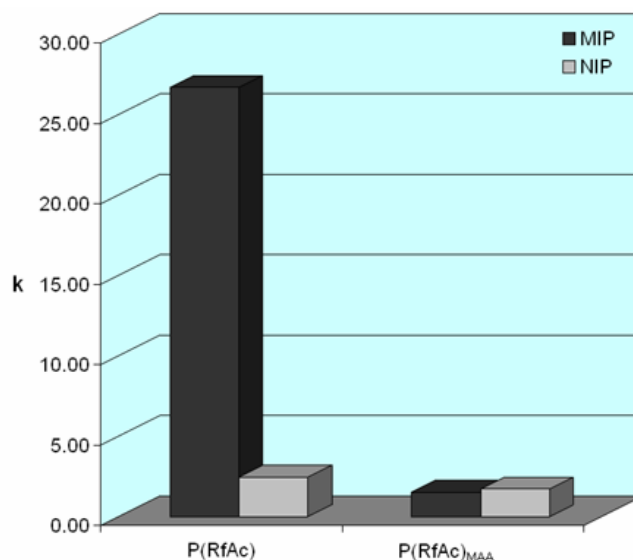
Figure 4.36: *Retention factors of 0.5mM riboflavin on **P(RfAc)** (inserted here for direct comparison) and **P(RfAc)$_{MAA}$** packed columns (mobile phase: 10% MeCN – 90% (H$_2$O-5%EtOH); injection: 5µL; flow rate: 1mL/min; detection: DAD @ 260nm)*

4.3.4.g Conclusions on the screening of the template analogues

Thus far, a series of riboflavin tetra esters with increasing size of the ester alkyl chain has been tested in order to determine which could play the role of the template analogue in the quest towards imprinted polymers that exhibit selectivity for riboflavin. From the very first tests, **RfAc** outperformed the other two tetra esters, since its use as template in the molecular imprinting process led to polymers with higher affinity and capacity for their template itself, as well as for riboflavin, even in highly aqueous environments, proving that the followed strategy could lead to rewarding results. **RfAc** has been selected as the best riboflavin analogue and from this point on it will be used as template of choice in the steps taken towards further optimisation of the imprinting system in order to reach the optimum material.

Having chosen a template analogue that fulfils all the initial requirements, most importantly solubility, the focus will be diverted towards the optimisation of other parameters involved in the imprinting process. Several different routes were followed, including polymerisation at lower temperatures, use of hydrophilic co-monomers and alternative cross-linkers.

4.3.5   Polymerisation at lower temperatures

One of the most important stages *en route* towards a successful imprinting process is the complexation between template and functional monomer, which takes place in the pre-polymerisation solution. As all equilibriums, this is also governed by the well known principle of *Le Châtelier*. While studying the association of template and monomer in solution, most measurements are performed at room temperature thus, the measured association constant is relevant only when the temperature of the experiment is quoted and the variation in its value is strongly dependent on the change in environmental parameters. On the other hand, free radical polymerisations are commonly initiated by elevated temperature. Hence, the number of monomer – template complexes in solution, before these are permanently "frozen" in the cross-linked polymer matrix, can be starkly reduced, leading to a smaller number of active binding sites in the resulting imprinted polymer.

In order to overcome this problem, more sensitive free radical initiators with initiation temperatures at 35°C can be used, but difficulties in handling of such reactive initiators makes them impractical. Alternatively, UV initiation at low temperatures (e.g. 0°C) can be used. However, in this study, the use of UV light is prohibited by the fact that the templates are light sensitive and break down easily even by exposure to daylight.

A molecularly imprinted polymer using the same composition to **P(RfAc)** has been synthesised, this time using ABDV as the free radical initiator, instead of AIBN, allowing the performance of the polymerisation at 40°C (**P(RfAc)$_{40}$**). The synthesised polymer was subsequently extracted with methanol using a Soxhlet apparatus, crushed and sieved in a size of 25-50μm, sedimented and packed in HPLC columns (125mm × 4.6mm) for further chromatographic evaluation.

Initially the polymer performance in organic environment was tested and the results are presented in Figure 4.37.
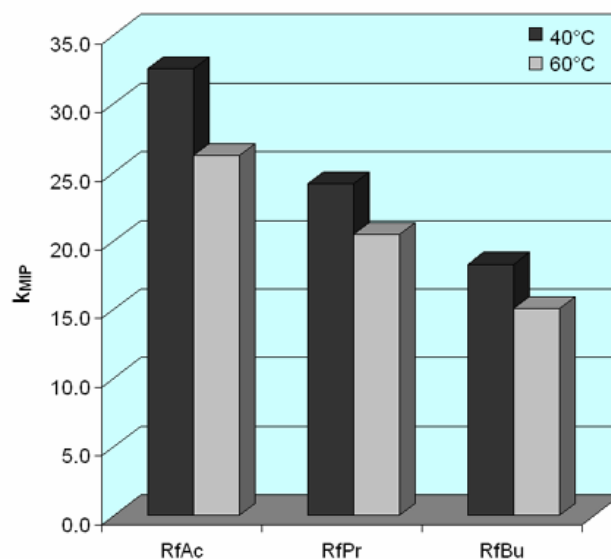
Figure 4.37: *Retention factors of the tetra esters on **P(RfAc)** and **P(RfAc)$_{40}$** imprinted polymers (mobile phase: MeCN-1% CH$_3$COOH; injection: 5µL; flow rate: 1mL/min; detection: DAD @ 260nm)*

Clearly, the polymers synthesised at lower temperature show longer retention times compared to the ones synthesised at 60°C. Furthermore, **P(RfAc)$_{40}$** displays enhanced selectivity towards the template **RfAc** compared to **P(RfAc)**.
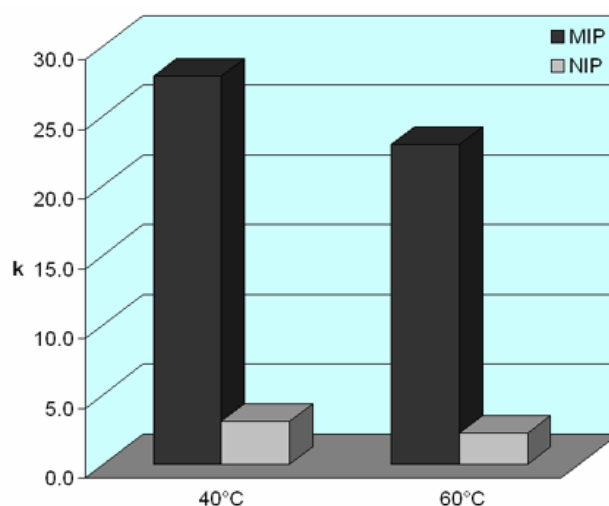
Figure 4.38: *Retention factors of 0.5mM riboflavin on **P(RfAc)** and **P(RfAc)$_{40}$** packed columns (mobile phase: 10% MeCN – 90% (H$_2$O-5%EtOH); injection: 5µL; flow rate: 1mL/min; detection: DAD @ 260nm)*

Further evaluation of **P(RfAc)$_{40}$** in an aqueous mobile phase reveals the positive effect of reduced temperature during the polymerisation, as the

retention times of riboflavin are significantly increased. Nevertheless, the retention time is also increased on the non-imprinted polymer, leading to an overall lower imprinting factor (9.0 on **P(RfAc)$_{40}$** and 10.0 on **P(RfAc)**), indicating that the effect of temperature in the polymerisation step can be positive or negative and to a great extent is system dependent.

4.3.6 Incorporation of hydrophilic co-monomers

In order to reduce the hydrophobic non-specific binding observed by the so far synthesised EDMA-based polymers, the incorporation of a hydrophilic co-monomer in the polymerisation mixture was decided, namely 2-hydroxyethyl methacrylate (HEMA), which has been successfully used in several imprinting protocols as hydrophilic agent.[123]
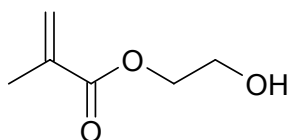
Scheme 4.14: Structure of 2-hydroxyethyl methacrylate (HEMA)

The following imprinted polymers (and the corresponding non-imprinted ones with omission of the template) were synthesised:

Polymer	RfAc	HEMA	Functional Monomer 1	Cross-linker (EDMA)
P(RfAc)$_{H5}$	0.546g 1mmol	0.61mL 5mmol	0.218g 1mmol	3.8mL 20mmol
P(RfAc)$_{H10}$	0.546g 1mmol	1.22mL 10mmol	0.218g 1mmol	3.8mL 20mmol

Table 4.12

The polymers were worked-up in the same manner as **P(RfAc)** and particles with size 25-50μm were packed into HPLC columns for chromatographic evaluation.

When tested in organic mobile phase, the HEMA containing polymers exhibited an unexpected performance (Figure 4.39). The retention times for all

tetra esters were almost diminished in comparison to **P(RfAc)** and they appeared smaller as the amount of HEMA in the polymer was increased. Some size selectivity can still be detected on **P(RfAc)$_{H5}$** and **P(RfAc)$_{H10}$**, but the effect is significantly suppressed.

*Figure 4.39:   Retention factors of the tetra esters on **P(RfAc)**, **P(RfAc)$_{H5}$** and **P(RfAc)$_{H10}$** imprinted polymers (mobile phase: MeCN-1% CH$_3$COOH; injection: 5µL; flow rate: 1mL/min; detection: DAD @ 260nm)*

The same dramatic decrease in retention time of riboflavin is observed in aqueous mobile phases (Figure 4.40).

Thus, the retention factor decreases by a factor of 3 when 5 equivalents of HEMA are included in the polymerisation mixture and factor of almost 10 when 10 equivalents of the hydrophilic co-monomer are added. Interestingly though, the retention time also decreases significantly on the non-imprinted polymers, indicating that some suppression of the non-specific binding occurs.

Figure 4.40: *Retention factors of 0.5mM riboflavin on **P(RfAc)**, **P(RfAc)$_{H5}$** and **P(RfAc)$_{H10}$** imprinted polymers (mobile phase: 10% MeCN – 90% (H$_2$O-5%EtOH); injection: 5μL; flow rate: 1mL/min; detection: DAD @ 260nm)*

The overall inferior performance of **P(RfAc)$_{H5}$** and **P(RfAc)$_{H10}$** is possibly due to the fact that incorporation of increasing amounts of a non cross-linking monomer, decreases the percentage of cross-linking of the resulting polymer thus, leading to less rigid and defined binding sites, which are known to generally possess poor recognition properties.

4.3.7 Use of alternative cross-linkers I – TRIM

The cross-linker is in most imprinted systems the component in excess and therefore defines to a great extent the structure, morphology and physicochemical characteristics of the material. Thus, changing the cross-linking unit in the so far optimum imprinting system could prove beneficial. At first the tri-functional cross-linker TRIM was used in place of EDMA.
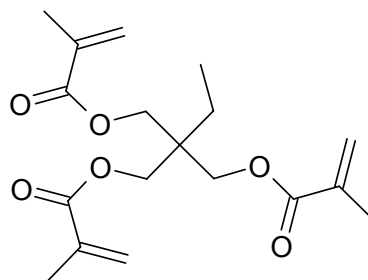
Scheme 4.15: Structure of trimethylolpropane trimethacrylate (TRIM)

In order to achieve a similar percentage of cross-linking in the final material, the ratio of monomer to cross-linker was changed to 1 : 12 instead of 1 : 20.

Polymer	RfAc	Functional Monomer 1	Cross-linker (TRIM)
P(RfAc)TRIM	0.546g / 1mmol	0.218g / 1mmol	3.8mL / 12mmol

Table 4.13

All other components were present at the same concentration (Table 4.13) and chloroform was used as the porogenic solvent.
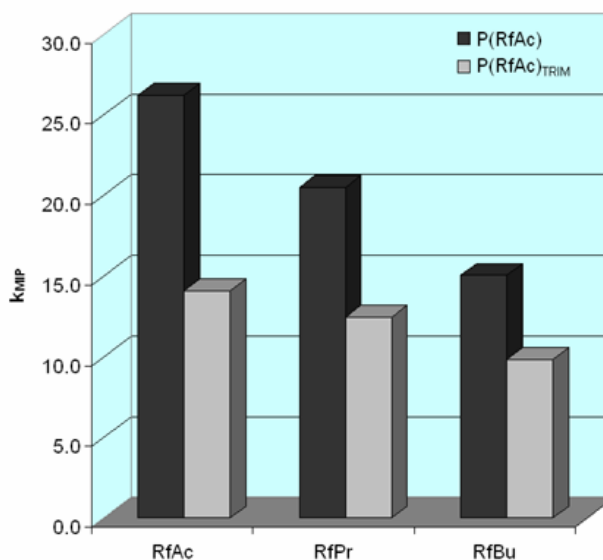
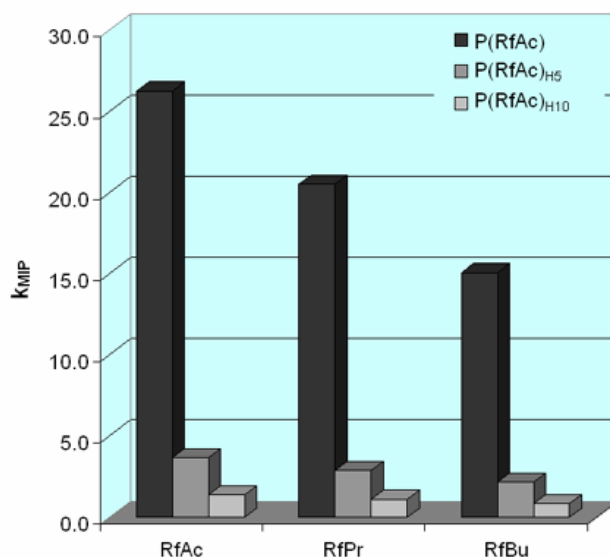*Figure 4.41:   Retention factors of the tetra esters on **P(RfAc)** and **P(RfAc)**$_{TRIM}$ imprinted polymers (mobile phase: MeCN-1% CH$_3$COOH; injection: 5µL; flow rate: 1mL/min; detection: DAD @ 260nm)*

87

Following work-up of the materials, particles of 25-50μm were packed in HPLC columns and the performance of the imprinted polymers was evaluated in the chromatographic mode. As seen in Figure 4.41, the use of TRIM leads to a dramatic decrease in the retention factors of all tested tetra esters and a diminishing in the selectivity of the polymer for its template.

Similarly, when tested in aqueous mobile phase (Figure 4.42), **P(RfAc)**$_{TRIM}$ shows significantly lower binding strength for riboflavin and increase in the non-specific binding. The latter effect is possibly due to the more hydrophobic character of the cross-linker and therefore of the resulting imprinted polymer, which induces hydrophobic binding in highly aqueous environments.
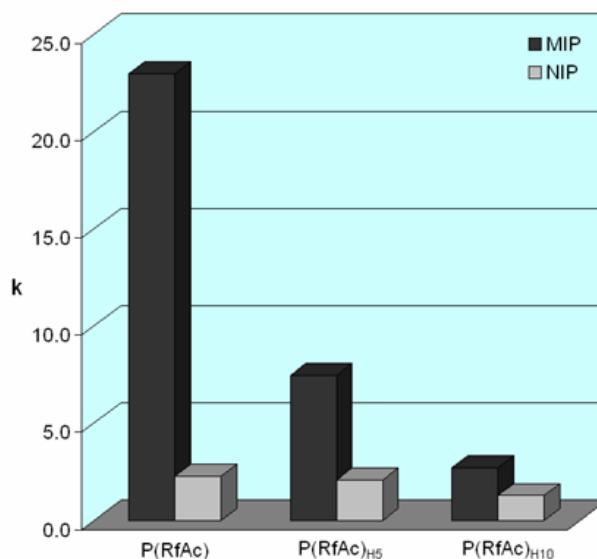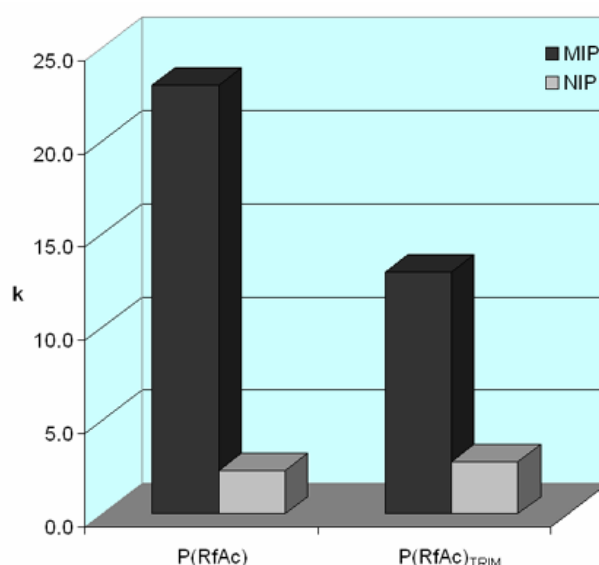

Figure 4.42: *Retention factors of 0.5mM riboflavin on* ***P(RfAc)*** *and* ***P(RfAc)***$_{TRIM}$ *imprinted polymers (mobile phase: 10% MeCN – 90% (H$_2$O-5%EtOH); injection: 5µL; flow rate: 1mL/min; detection: DAD @ 260nm)*

One possible explanation for the dramatic reduction of the binding strength of the imprinted polymers could be the rigidity of the cross-linker, which results in a stiff matrix that does not facilitate the transport of template molecules in and out or the binding sites. Additionally, permanent entrapment of template units in the polymer could lead to a reduction in the number of the available for interaction binding sites.

4.3.8   Use of alternative cross-linkers II – PETRA

Pentaerythritol triacrylate is a hydrophilic cross-linker with similar structure to this of TRIM. However, commercial grade pentaerythritol triacrylate is mainly a mixture of tri-and tetra-acrylate esters of pentaerythritol with some dimers and trimers containing an average of 3.3 acrylate groups per molecule.
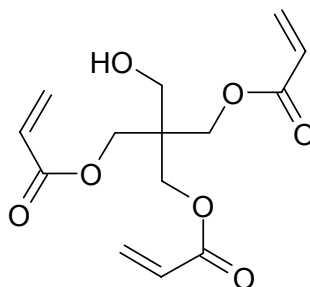
Scheme 4.16: Structure of pentaerythritol triacrylate (PETRA)

Industrially, PETRA is used in manufacturing coatings, inks and adhesives improving their resistance against weather, chemicals, water and abrasion. Thus, the combination of hydrophilic character and rigidity should prove beneficial for the resulting imprinted polymers. These advantages have been previously utilised in the synthesis of enantio-selective MIPs against amino-acid derivatives[138] and ephedrine.[139]

4.3.8.a   Synthesis of PETRA based imprinted polymers

The recipe displayed in Table 4.14 was used in order to synthesise molecularly imprinted polymers against **RfAc** using PETRA as cross-linker. Due to the significantly higher density of the cross-linker (~1.2 g/L), a lower volume of solvent was used in order to keep the ratio monomer / solvent volume constant, compared to the previously synthesised polymers. A control, non-imprinted polymer (**P$_N$'**) was synthesised in the same manner, with the omission of the template.

Polymer	RfAc	Functional Monomer 1	Cross-linker (PETRA)
P(RfAc)'	0.546g / 1mmol	0.218g / 1mmol	3.57g / 12mmol
PN'	-	0.218g / 1mmol	3.57g / 12mmol

Table 4.14:   Composition of P(RfAc)' polymers (3.5mL of CHCl₃ used as porogenic solvent; initiator: AIBN; T=60°C for 24h)

After polymerisation, the materials were washed with methanol, using a Soxhlet apparatus, crushed, sieved and particles of size 25-50μm were packed in HPLC columns (125mm × 4.6mm) for evaluation of their binding characteristics.

4.3.8.b   Chromatographic evaluation of the polymers

As seen in Figure 4.43, the PETRA based materials exhibit an exceptional improvement in the binding strength towards their template.
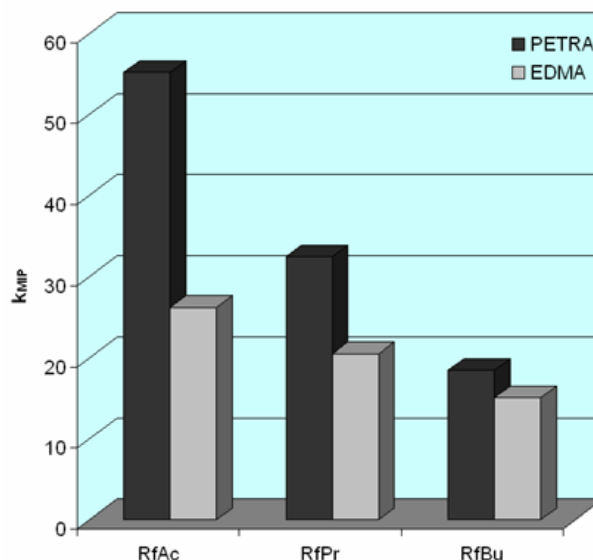
Figure 4.43:   Retention factors of the tetra esters on P(RfAc) and P(RfAc)' imprinted polymers (mobile phase: MeCN - 1% CH₃COOH; injection: 5µL; flow rate: 1mL/min; detection: DAD @ 260nm)

Specifically, the retention factor for RfAc is more than double compared to the one measured on the EDMA based polymer. Moreover, the selectivity of the polymers is significantly improved, since the relative increase in the retention factors for RfPr and RfBu is 60% and 20% respectively. Finally, indication of

the reduction in the non-specific binding on these materials is provided by the decrease by 50% in the retention factors measured for all analytes, which leads to imprinting factors in the range of 500.

4.3.8.c   Frontal analysis

In order to get more information about the binding strength and derive valuable thermodynamic parameters, frontal analysis experiments were performed with **P(RfAc)'**, in the same conditions as for **P(RfAc)**. The raw adsorption isotherms are presented in Figure 4.44.
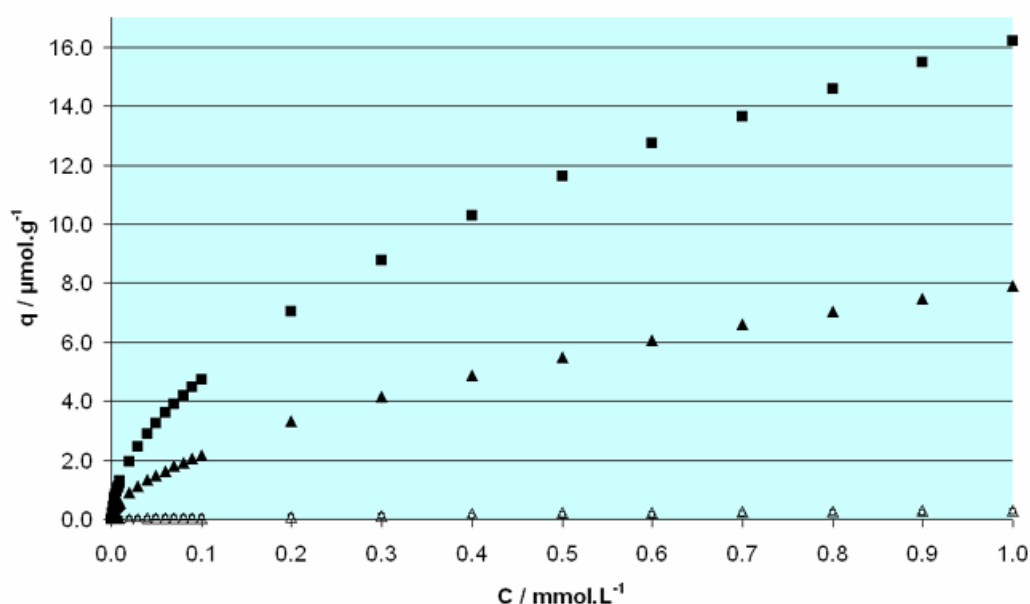
Figure 4.44:   *Binding isotherms obtained by frontal analysis:* ■ *RfAc on P(RfAc)';* □ *RfAc on P$_N$';* ▲ *RfAc on P(RfAc);* △ *RfAc on P$_N$*

The results the frontal analysis clearly confirm the observations made after chromatographic analysis of the polymers. **P(RfAc)'** shows both higher affinity and capacity for its template, compared to **P(RfAc)**, while **P$_N$'** exhibits significantly less affinity for **RfAc** than **P$_N$**, providing a first indication of a decrease in non-specific binding.

Similarly to **P(RfAc)**, the obtained data curves fit best to the Freundlich model, since the logarithmic plot of the experimental data is a straight line (Figure 4.45).
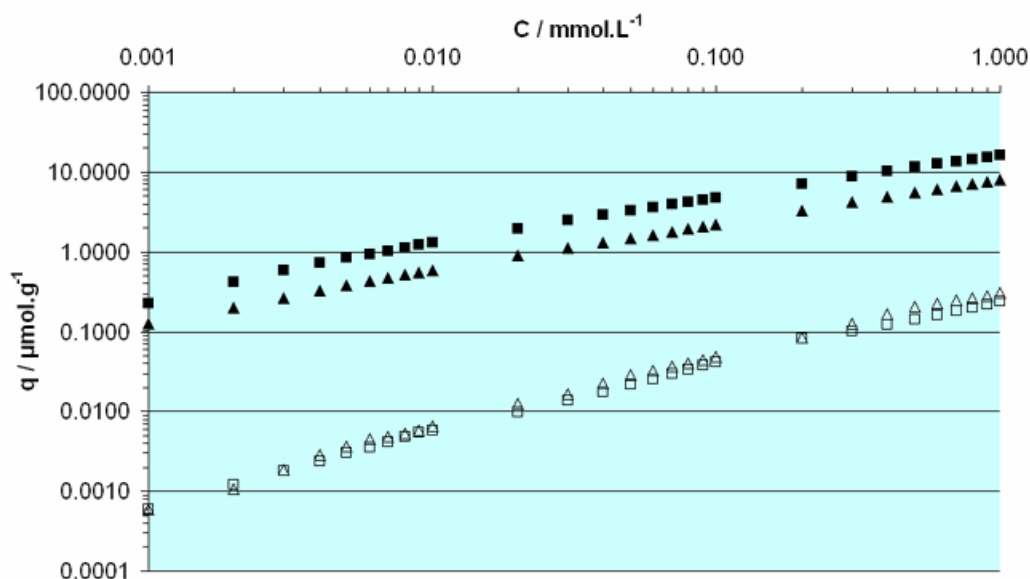
Figure 4.45: *Log-Log plot of the data obtained by frontal analysis:* ■ *RfAc on P(RfAc)';* □ *RfAc on P_N';* ▲ *RfAc on P(RfAc);* △ *RfAc on P_N*

Thus, the data points were fitted to the Freundlich isotherm, using Origin 7.0, and the parameters displayed in Table 4.15, together with the corresponding parameters for **P(RfAc)** for direct comparison, were obtained.

Polymer	a	m	K_a (M^{-1})	N ($\mu mol.g^{-1}$)
P(RfAc)	3.996	0.558	2.60×10^4	1.13×10^{-1}
P_N	0.158	0.774	1.29×10^4	5.98×10^{-4}
P(RfAc)'	8.256	0.539	2.80×10^4	2.76×10^{-1}
P_N'	0.120	0.757	1.36×10^4	5.46×10^{-4}

Table 4.15: *Fitting parameters of the frontal analysis data to the Freundlich isotherm (q=a×C^m) and calculated average association constants and average number of binding sites*

Confirming the previous observations, **P(RfAc)'** appears to have almost double the amount of binding sites compared to **P(RfAc)** and a slightly higher association constant, which explains the differences in the performance of the two polymers in chromatography. On the other hand, the parameters calculated for the two control polymers are to a great extent similar, with **P_N'** showing marginally lower affinity constant and number of sites.

Based on the above derived thermodynamic data, the following affinity distribution plot was generated, showing that in the studied window of affinity constants, **P(RfAc)'** has a significantly higher number of binding sites both in the low and the high affinity area.
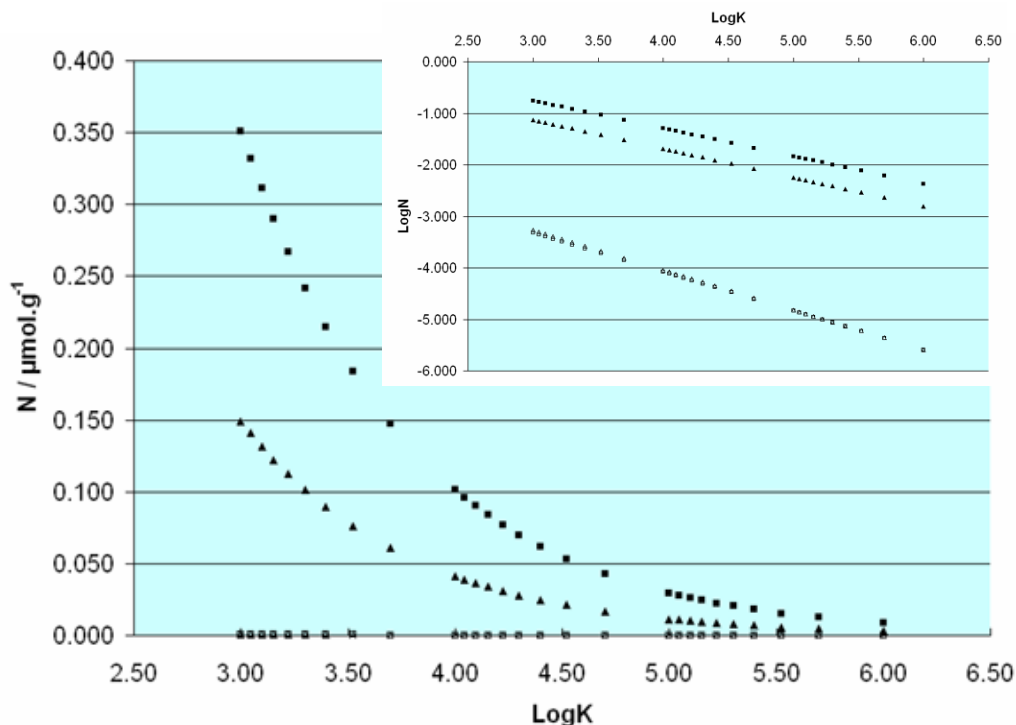
Figure 4.46:   *Semi-log plot of the affinity distribution obtained by fitting of the frontal analysis data to the Freundlich isotherm (■ RfAc on P(RfAc)'; □ RfAc on P_N'; ▲ RfAc on P(RfAc); △ RfAc on P_N); Insert: corresponding log-log plot*

So far, **P(RfAc)'** has proven its superiority to the previously synthesised polymers in both selectivity and association strength for its template in organic mobile phases. The next step is to investigate whether these very attractive features can be exploited for the selective recognition of riboflavin in aqueous systems.

4.3.8.d Performance of the materials in aqueous environments

Chromatographic evaluation of the polymers in aqueous mobile phases further emphasises the supremacy of **P(RfAc)'** compared to **P(RfAc)**. Thus, the retention time for riboflavin is increased by ~60% on the imprinted polymer, while it is decreased by ~30% on the non-imprinted polymer.
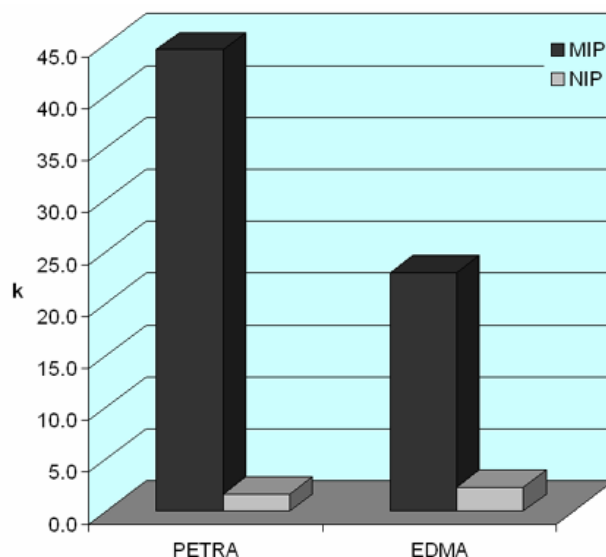
Figure 4.47:   *Retention factors of 0.5mM riboflavin on **P(RfAc)'** and **P(RfAc)** imprinted polymers (mobile phase: 10% MeCN – 90% (H_2O-5%EtOH); injection: 5μL; flow rate: 1mL/min; detection: DAD @ 260nm)*

Thermodynamic evaluation of the materials by means of frontal analysis in H_2O-5%EtOH (Figure 4.48) reveals the potential of the polymers to selectively recognise riboflavin in almost pure aqueous environments.
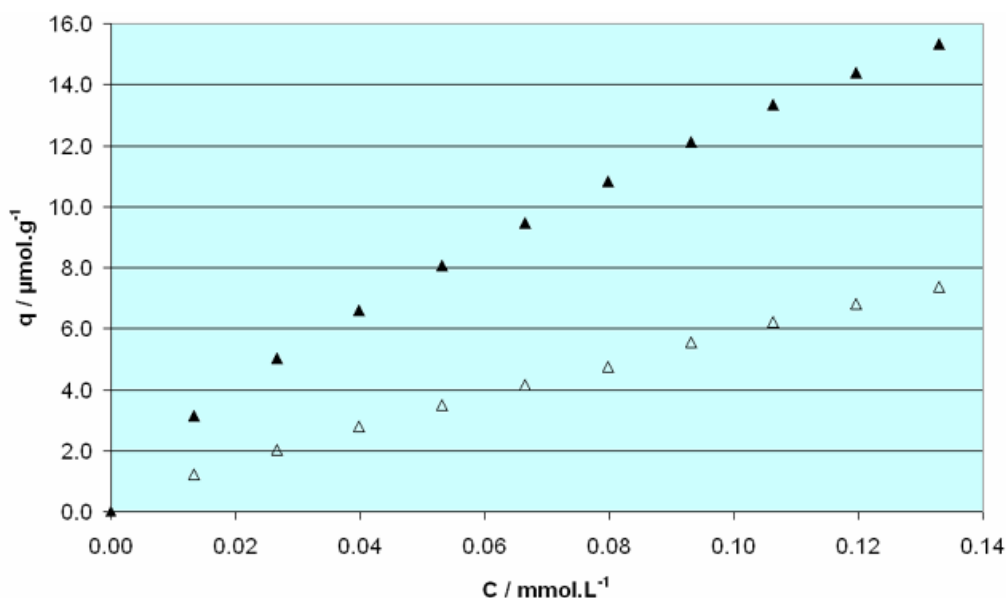
Figure 4.48:   *Binding isotherms of obtained by frontal analysis of **P(RfAc)'** polymers (▲ riboflavin on **P(RfAc)'**; △ riboflavin on **P_N'**) in H_2O-5%EtOH*

94

Unfortunately, due to solubility limitations, the range of concentrations that could be studied is narrow, not allowing the extraction of accurate thermodynamic parameters, is however enough for a qualitative evaluation of the materials.

4.3.9   Use of alternative cross-linkers III – PEDMA

Inspired by the outstanding performance of PETRA, a more hydrophilic cross-linker was used, with the hope that it would lead to further improvement of the polymer performance.
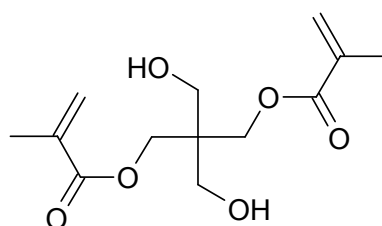
Scheme 4.17: Structure of pentaerythritol dimethacrylate (PEDMA)

Thus, the di-functional cross-linking monomer PEDMA was incorporated in the polymerisation recipe in a 1:1:20 ratio of template : monomer : cross-linker (Table 4.16), similar to the one used for the EDMA-based polymers.

Polymer	RfAc	Functional Monomer *1*	Cross-linker (PEDMA)
P(RfAc)PEDMA	0.546g / 1mmol	0.218g / 1mmol	4.4g / 20mmol

*Table 4.16:   Composition of **P(RfAc)**PEDMA polymers (5.1mL of CHCl$_3$ used as porogenic solvent; initiator: AIBN; T=60°C for 24h)*

However, as seen from the results of the chromatographic evaluation of the polymers, the retention time for **RfAc** is significantly lower than the one measured on **P(RfAc)'** or **P(RfAc)**. This is possibly due to the reduced percentage of cross-linking offered by the di-functional cross-linker compared to the tri-functional PETRA, in concert with its higher polarity which could interrupt the formation of the monomer-template complexes in the pre-polymerisation solution.
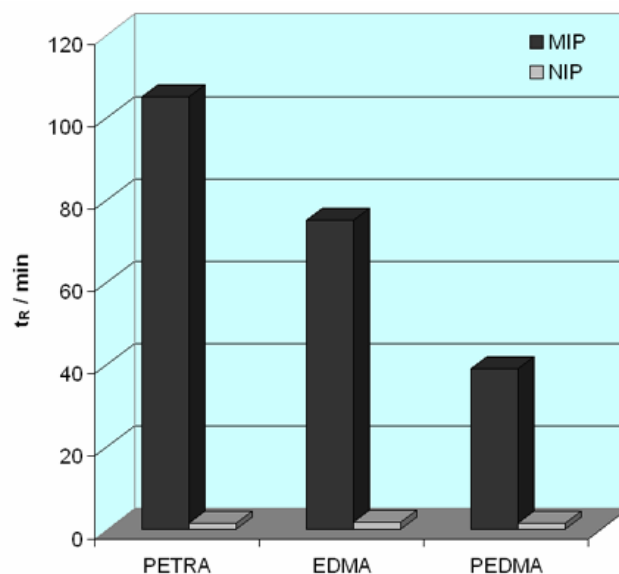
Figure 4.49:   *Retention times of **RfAc** (1mM) on **P(RfAc)'**, **P(RfAc)** and **P(RfAc)$_{PEDMA}$** imprinted polymers (mobile phase: MeCN-1% CH$_3$COOH; injection: 5µL; flow rate: 1mL/min; detection: DAD @ 260nm)*

Similarly, when evaluated in aqueous environments, **P(RfAc)$_{PEDMA}$** shows reduced affinity for riboflavin and an unexpected increase in the retention time on the non-imprinted polymer.
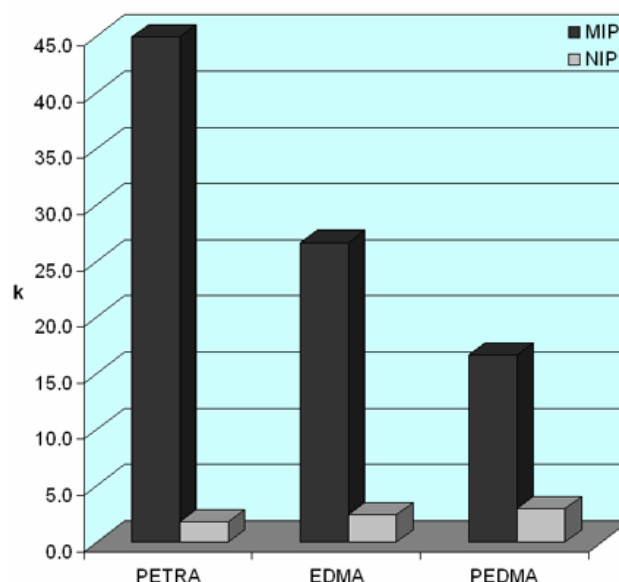
Figure 4.50:   *Retention factors of 0.5mM riboflavin on **P(RfAc)'**, **P(RfAc)** and **P(RfAc)$_{PEDMA}$** imprinted polymers (mobile phase: 10% MeCN – 90% (H$_2$O-5%EtOH); injection: 5µL; flow rate: 1mL/min; detection: DAD @ 260nm)*

96

This could be attributed to the interactions between the ribose chain of riboflavin and the excess of hydroxyl groups in the polymer matrix, especially since no increase in the non-specific binding is observed for the template in the organic mobile phase. If this is the case, PETRA could be considered as the optimal cross-linker for this system, since it comprises both structural rigidity leading to robust binding sites and enough functionality to facilitate the binding event without interrupting the main hydrogen bonding interaction between monomer **1** and riboflavin.

4.3.10   Incorporation of π – stacking co-monomers

A closer look at the binding site of the riboflavin binding protein (**RfBP**) reveals the importance of aromatic amino acids in the recognition process. In particular, the iso-alloxazine ring is stacked between the parallel planes of Tyr75 and Trp156, which also leads to the complete quenching of riboflavin fluorescence upon binding.[113]
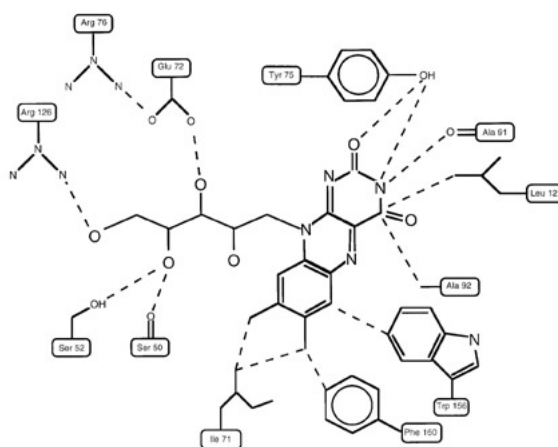
Figure 4.51:   *Schematic representation of the interaction taking place in the binding site of RfBP*

Thus, inspired by the natural receptor, a series of polymers was synthesised, each containing a different aromatic co-monomer, aiming to increase the number of interactions locking the template in position during the imprinting process, leading to binding sites of higher fidelity.
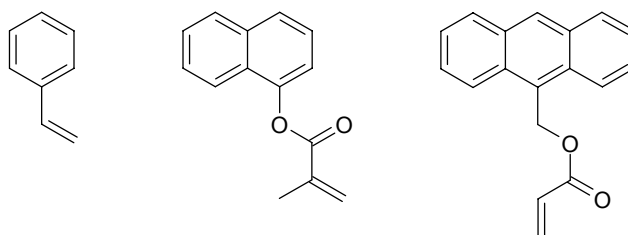
Scheme 4.18: Structures of the used π-stacking co-monomers

The base recipe used was the same as the one that led to **P(RfAc)'** and is described in detail in Table 4.17.

Polymer	Co-monomer	
P(RfAc)'$_{STYR}$	styrene	1mmol (0.104g)
P(RfAc)'$_{NAPH}$	naphthalen-1-yl methacrylate	1mmol (0.212g)
P(RfAc)'$_{ANTH}$	anthracen-10-ylmethyl acrylate	1mmol (0.262g)

*Table 4.17: Composition of π-monomer containing polymers (**RfAc**: 1mmol (0.546g); monomer **1**: 1mmol (0.218g); CHCl$_3$: 3.5mL; AIBN: 0.036g)*

Figure 4.52 depicts the performance of the synthesised polymers in chromatography. Retention factors for 1mM **RfAc** are decreasing with the increase of the size of the aromatic monomer, an effect observed also on the non-imprinted polymers, indicating increased non-specific binding. This could be due to either π-π interactions between the aromatic rings of the monomers and the iso-alloxazine ring of the flavin system, or due to preferable partitioning of a non-polar compound on a non-polar stationary phase, a process similar to reversed phase chromatography.
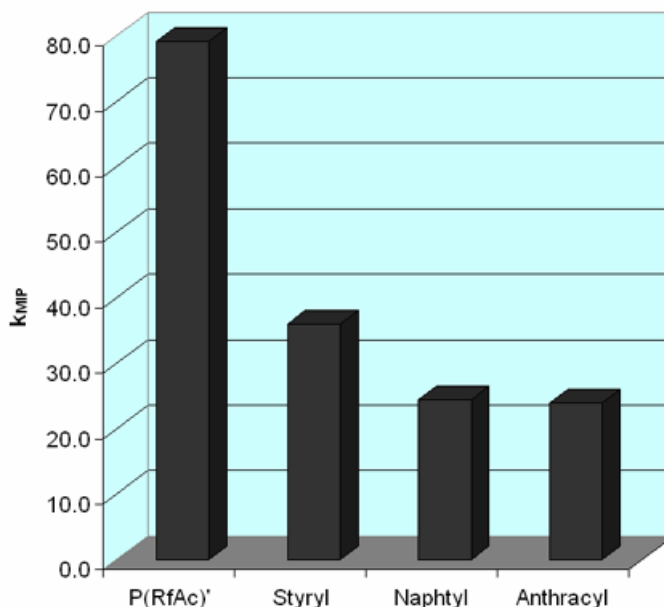
Figure 4.52:   *Retention factors of **RfAc** (1mM) on **P(RfAc)'**, **P(RfAc)'**$_{STYR}$, **P(RfAc)'**$_{NAPH}$ and **P(RfAc)'**$_{ANTH}$ imprinted polymers (mobile phase: MeCN-1% CH$_3$COOH; injection: 5µL; flow rate: 1mL/min; detection: DAD @ 260nm)*

Similarly, hydrophobic interactions are likely to take place in aqueous environments since all three used co-monomers are expected to increase the hydrophobic character of the polymers. Indeed, an increase in the retention time of riboflavin on the non-imprinted polymers is observed with the increase in the size of the used co-monomer, with the exception of the anthracyl based polymers, which show almost no retention for riboflavin on either imprinted or non-imprinted polymer. This very interesting effect could be attributed to a collapse of the hydrophobic polymer matrix when brought in contact with aqueous mobile phases, thus not allowing access of riboflavin into the binding sites under these conditions.
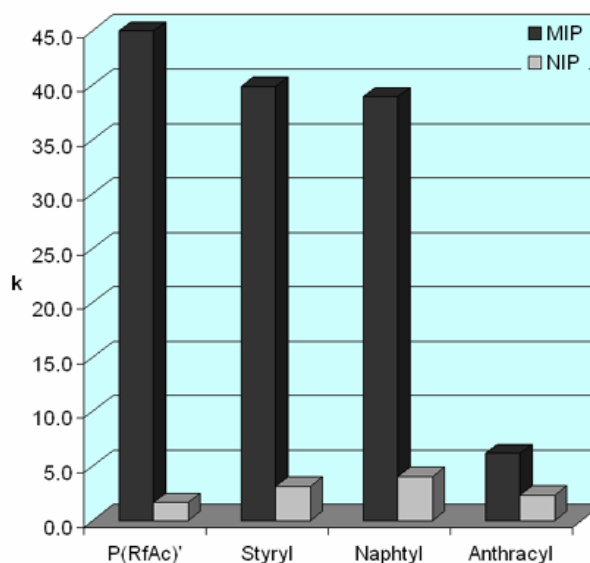
Figure 4.53:   *Retention factors of 0.5mM riboflavin on **P(RfAc)'**, **P(RfAc)'$_{STYR,}$** **P(RfAc)'$_{NAPH}$** and **P(RfAc)'$_{ANTH}$** imprinted polymers (mobile phase: 10% MeCN – 90% (H_2O-5%EtOH); injection: 5μL; flow rate: 1mL/min; detection: DAD @ 260nm)*

Further insight in the affinity of the above synthesised polymers was gained by batch rebinding experiments, which this time were performed in the solvent in which the polymers were synthesised, namely chloroform, in order to reveal any weak π-π interactions present.
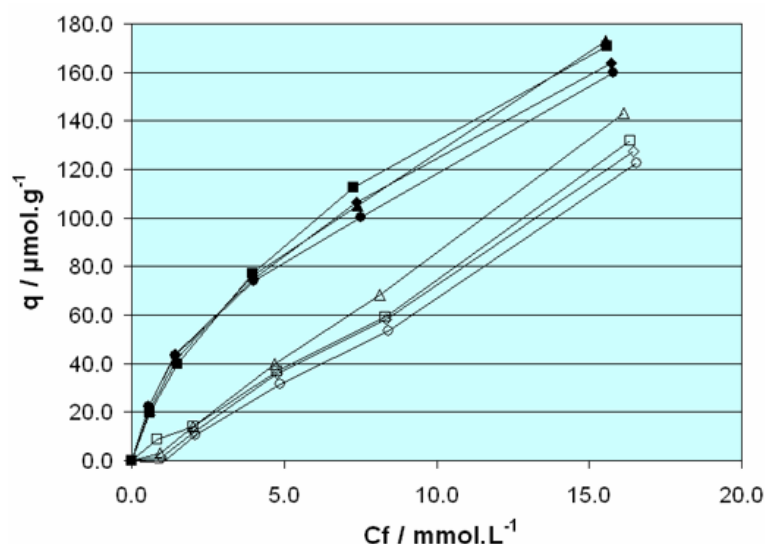
Figure 4.54:   *Binding isotherms obtained by batch rebinding in chloroform (RfAc on: ▲ **P(RfAc)'**; △ **P$_N$'**; ◆ **P(RfAc)'$_{STYR}$**; ◇ **P$_N$'$_{STYR}$**; ● **P(RfAc)'$_{NAPHT}$**; ○ **P$_N$'$_{NAPHT}$**; ■ **P(RfAc)$_{ANTHR}$**; □ **P$_N$'$_{ANTHR}$***)

The rebinding results paint a completely different picture to the one obtained by chromatographic evaluation in both organic and aqueous based mobile phases. All three π-monomer based polymers appear to have similar affinity and capacity with the original hydrophilic polymer **P(RfAc)'** when tested in a low polarity solvent. Furthermore, the extent of non-specific binding is significantly increased, especially in the high concentration range.

Overall, the incorporation of π-monomers in the polymerisation protocol appears to lead to a general reduction of the binding strength of the resulting polymers and an increase in the non-specific binding compared to **P(RfAc)'**, even though in non-polar environment all materials show similar behaviour.

4.3.11   *Post-hydrolysis of the imprinted polymers*

It is generally accepted that most synthetic protocols for the preparation of imprinted polymers by bulk free radical polymerisation, lead to a final material which contains 5-10% of unreacted double bonds.[80] This percentage varies depending on the way the polymerisation was initiated, the temperature and the type of monomers participating. The presence of these unreacted double bonds also affects the rigidity of the final material hence thermal curing of the materials has been employed in order to push the polymerisation reaction to completion, resulting in a more rigid polymer matrix.[79, 140] However, the presence of unreacted double bonds offers also a potential advantage. Hydrolysis of these pending functional groups would usually result in the exposure of hydroxyl groups, essential elements for a hydrophilic polymer backbone. This hydrolysis can be performed by mild base solutions, e.g. 0.1M KOH or TBA^{+-}OH in isopropanol.

In a first attempt to partially hydrolyse the pendant double bonds present in **P(RfAc)'** and **P$_N$'**, 1M NaOH or TBA^{+-}OH solutions were added to a small amount of polymer and allowed to shake for 1, 6 or 24 hours. The resulting materials were then washed and the wash solutions were analysed by ^{1}H-NMR. A similar pattern was detected in the spectra of all the hydrolysis samples, where signals matching the ones found also in a small extent in the original cross-linker spectrum and could not be assigned due to lack of

information about the exact composition of the commercially available cross-linker.
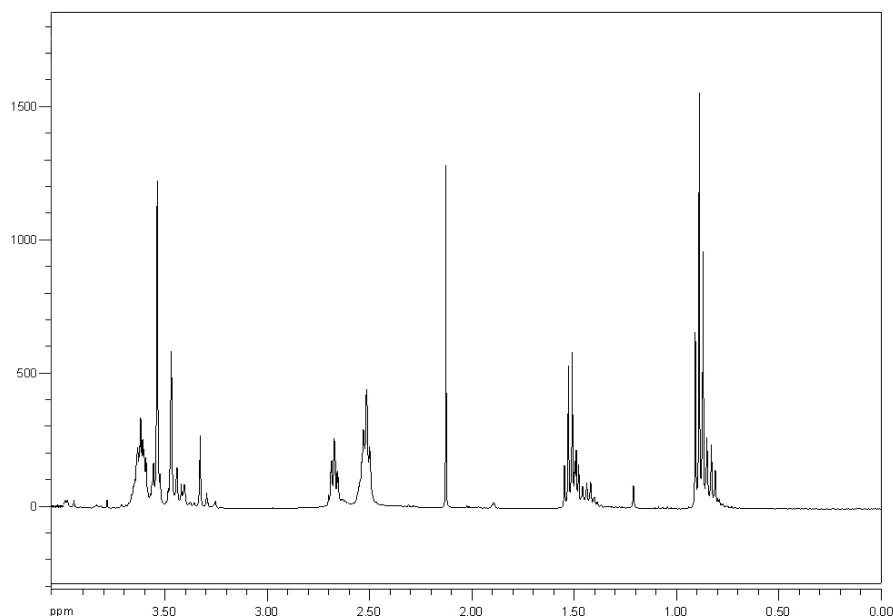
Figure 4.55: ^{1}*H-NMR (CDCl$_3$) spectrum of PETRA (0-4 ppm)*

Interestingly however, no vinyl peaks were detected, leading to the conclusion that the used conditions are too harsh for the double bonds to survive the hydrolysis process.
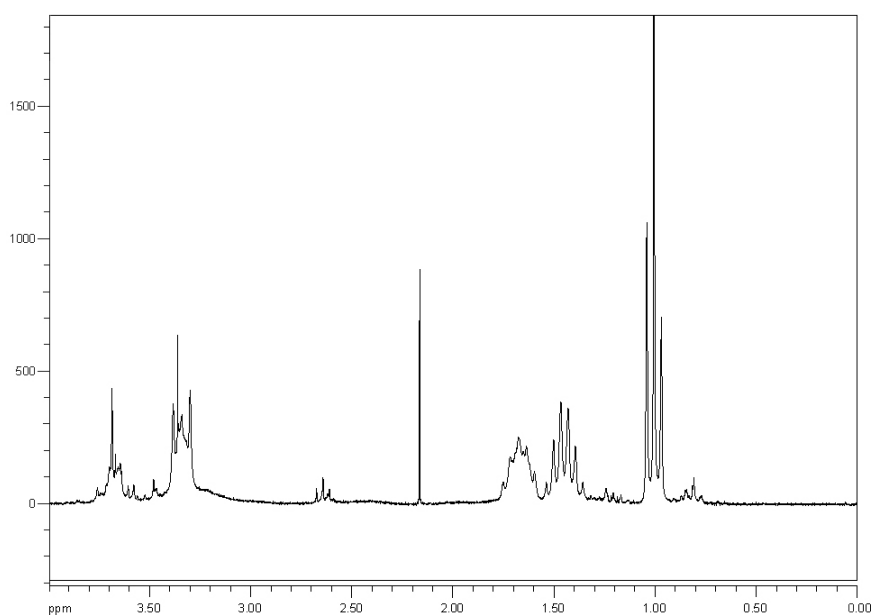
Figure 4.56: ^{1}*H-NMR (CDCl$_3$) spectrum of hydrolysis sample (0-4 ppm)*

Subsequent rebinding of the hydrolysed polymers with 0.1mM solutions of riboflavin was inconclusive due to the destruction of the polymer matrix by the strong base solution, especially after 6 or 24 hours, which led to interference in the analysis of the supernatant solutions by semi-soluble polymer.

In order to overcome this problem, a milder hydrolysis experiment was designed, combined with direct subsequent measurement of riboflavin retention by HPLC. Thus, after injection of 100μL of 0.1M KOH in methanol on a 30mm column packed with **P(RfAc)'** or **P$_N$'** polymer particles at a low flow-rate (0.1mL/min), the columns were washed and 0.5mM riboflavin was injected, using the standard analysis method. This cycle was repeated five times on both imprinted and non-imprinted polymers. After this, two further cycles were performed, in which the column was filled with the above base solution and the flow was stopped for 15 or 30 minutes. The column was then washed, equilibrated with the mobile phase used for the analysis of riboflavin, and then the latter was injected.
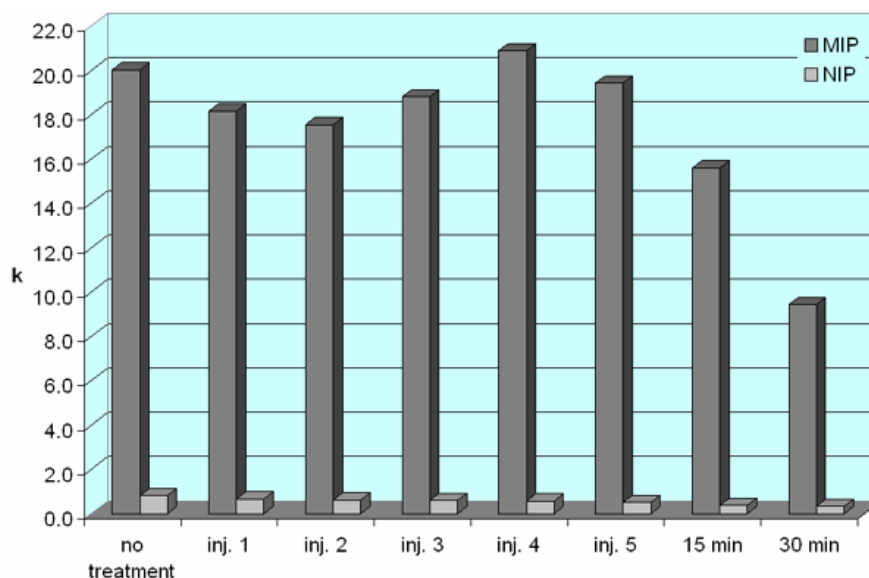
Figure 4.57:   *Retention factors of 0.5mM riboflavin on **P(RfAc)'** after the KOH hydrolytic cycles (mobile phase: 10% MeCN – 90% (H$_2$O-5%EtOH); injection: 5µL; flow rate: 1mL/min; detection: DAD @ 260nm)*

As expected, the retention time of riboflavin decreased gradually on the non-imprinted polymer as the number of base injections increased, indicating a reduction in the non-specific binding. Interestingly however, a reverse effect

was observed on the imprinted polymers. Here, the retention times increased and each hydrolysis wash was accompanied by release of template detected by the DAD-UV detector. This indicates that previously entrapped template molecules were freed-up, subsequently revealing more accessible binding sites in the polymer matrix.
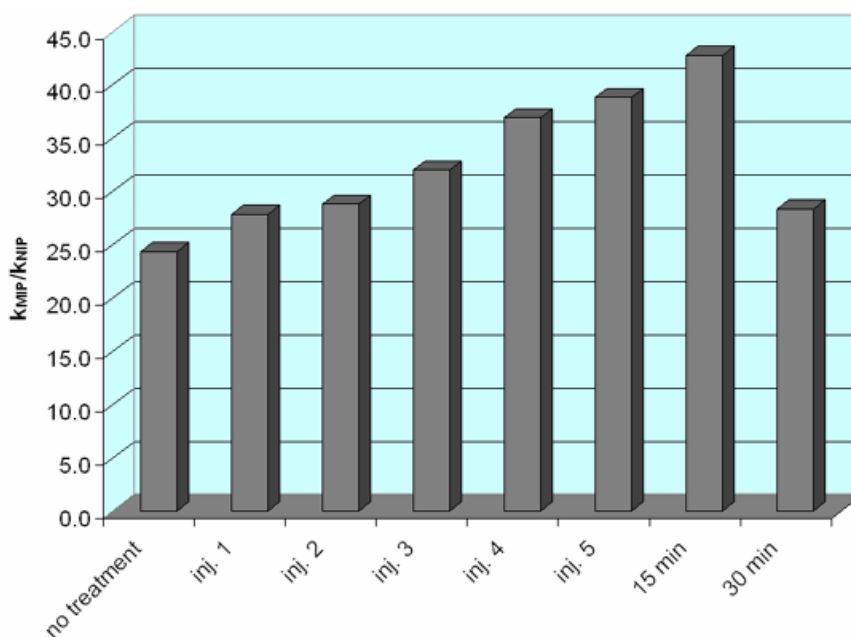
Figure 4.58: k_{MIP}/k_{NIP} values obtained after each KOH hydrolytic cycle as described above

Overall, by the fifth injection of base on both polymers, the k_{MIP}/k_{NIP} value was almost doubled. Making the conditions of hydrolysis harsher by increasing the contact time and quantity of base with the polymers, leads to a dramatic decrease in their binding strength, signalling the collapsing of the polymer matrix. Nevertheless, the loss is relatively smaller on the imprinted polymer than on the non-imprinted, leading to a net increase in the k_{MIP}/k_{NIP} value after 15 minutes of hydrolysis.

A further hydrolysis experiment was performed, similar to the one described above, this time using $TBA^{+-}OH$ (0.1M), a weaker and bulkier base, which should act only on the "outer" surface of the polymers and not access the binding sites.
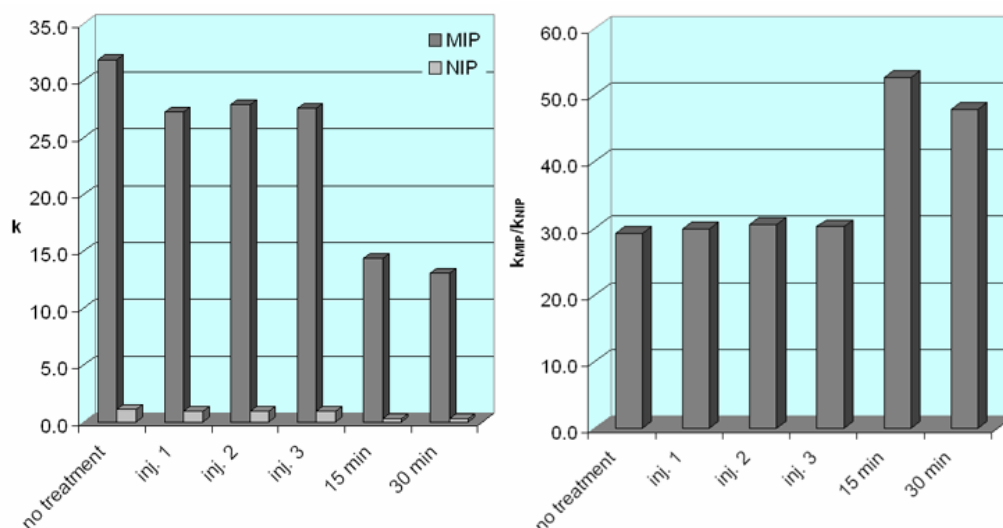
Figure 4.59: *Retention factors and* k_{MIP}/k_{NIP} *values of 0.5mM riboflavin on P(RfAc)' after the TBA^{+-}OH hydrolytic cycles (mobile phase: 10% MeCN – 90% (H$_2$O-5%EtOH); injection: 5µL; flow rate: 1mL/min; detection: DAD @ 260nm)*

Clearly, the hydrolysis using TBA^{+-}OH is much milder than the one using KOH. On both imprinted and non-imprinted polymer, only a small decrease in the retention time is observed after injection of 100μL of base at 0.1mL/min and the changes are proportional, thus the k_{MIP}/k_{NIP} values remain unaffected. This could mean that only the outer surface of the polymer is modified under these conditions and no hydrolysis takes place near or at the binding sites.

Allowing more contact time to the base with the polymer, leads to a significant decrease in the retention times of riboflavin on both polymers, yet the non-imprinted polymer is much more affected. Overall, the k_{MIP}/k_{NIP} value is maximal after 15 minutes of hydrolysis and decreases slightly after 30 minutes. After the last hydrolytic step with TBA^{+-}OH, a frontal analysis experiment was performed in aqueous environment, in order to verify the decrease in the non-specific binding in the equilibrium mode. Indeed, as seen on Figure 4.60, the difference between imprinted and non-imprinted materials has significantly increased, compared to Figure 4.48, mainly due to a decrease in the non-specific binding.
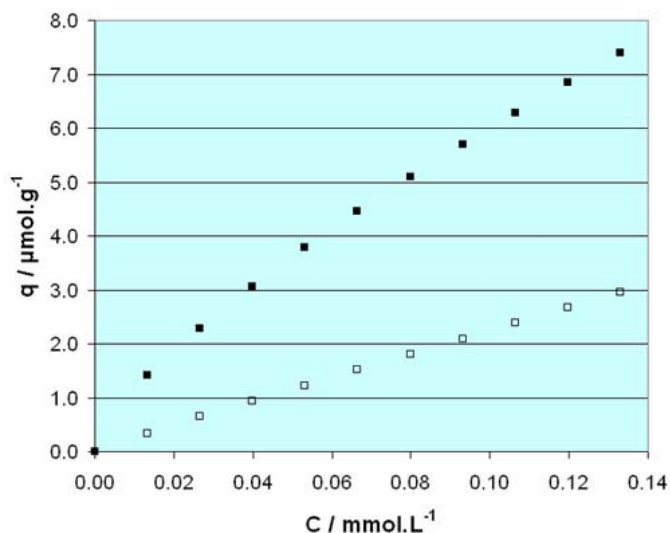
Figure 4.60:   *Binding isotherms of obtained by frontal analysis of partially hydrolysed **P(RfAc)'** polymers (■ riboflavin on **P(RfAc)'**; □ riboflavin on **P_N'**) in H_2O-5%EtOH*

This series of experiments indicates the importance of a post-polymerisation modification to the properties of the imprinted material. TBA^{+-}OH is certainly a better choice compared to KOH, since it comprises weaker basic character, thus allowing the preservation of the polymer integrity, and bulkier size, facilitating hydrolysis of the outer surface of the polymers, leading to hydrophilisation of the materials.

4.3.12   Extraction of riboflavin from real samples

A series of experiments were designed and performed in order to establish the water compatibility of the best performing imprinted polymers, **P(RfAc)'**. These include extraction of riboflavin from a large volume of "academic" aqueous solution of the vitamin, a mixture of 7 water-soluble vitamins, beer and milk. The results are presented in the following paragraphs. The detailed setup for each experiment is described in § 6.7-6.8 of the Experimental Part.

4.3.12.a   Extraction of riboflavin from aqueous solutions

Scope of this experiment has been the determination of the amount of riboflavin that **P(RfAc)'** and **P$_N$'** can bind in a flow-through experiment, mimicking a potential application of on-line extraction of large volume samples. Standard solutions (500μg/L) of the vitamin in three different solvent systems were prepared, namely pure water and water containing 5% ethanol in neutral and acidic pH (pH=4), a solvent mixture similar to the composition of beer. These solutions were passed through a 12.5cm column packed with **P(RfAc)'** or **P$_N$'** with a flow-rate of 1mL/min and the time until breakthrough was measured. This time corresponds to the volume of solution from which all the riboflavin has been extracted, an indirect measure of the polymer's capacity. The results are presented in Table 4.18.

Solvent	Extracted volume (mL)		Ratio
	P(RfAc)'	**P$_N$'**	
H_2O	210	60	3.5
H_2O – 5% EtOH	200	30	6.7
H_2O – 5% EtOH (pH=4)	200	30	6.7

Table 4.18

The performance of the imprinted polymer is minimally affected by either the presence of organic modifier or the pH. In all three cases approximately 100μg of riboflavin could be bound on the column. Contrariwise, the amount of vitamin bound on the non-imprinted polymer decrease by 50% upon

addition of 5% ethanol, but remains unaffected by the change of the pH value to 4. In conclusion, this experiment verifies the potential of the synthesised materials as riboflavin-selective sorbents although the importance of an organic modifier in order to reduce the non-specific binding is pointed-out.

4.3.12.b Extraction of riboflavin from a mixture of water-soluble vitamins

Taking the evaluation of the synthesised materials one step further, extraction of riboflavin from a commercially available multivitamin tablet was attempted. Unfortunately, the background of the solution was too high, due to the additives and sugars present in the tablet, and it did not allow the detection of riboflavin by the available DAD-UV detector. Thus, an "academic" aqueous mixture of the vitamins was prepared with the following composition:

Vitamin	$C / \mu mol.L^{-1}$
Thiamine	100
Ascorbic acid	100
Pyridoxine	100
Nicotinic acid	100
Nicotinamide	100
Folic acid	10[a]
Riboflavin	10[a]

Table 4.19: *Composition of the aqueous vitamin solution ([a]concentration was lower due to limited solubility)*

Similarly to the previous experiment, the solution of the water soluble vitamins was pumped through an HLPC column packed with **P(RfAc)'** or **P$_N$'** and the time until breakthrough of riboflavin was monitored using the DAD-UV detector recording the signal at 480nm, at which wavelength only riboflavin exhibits absorbance.
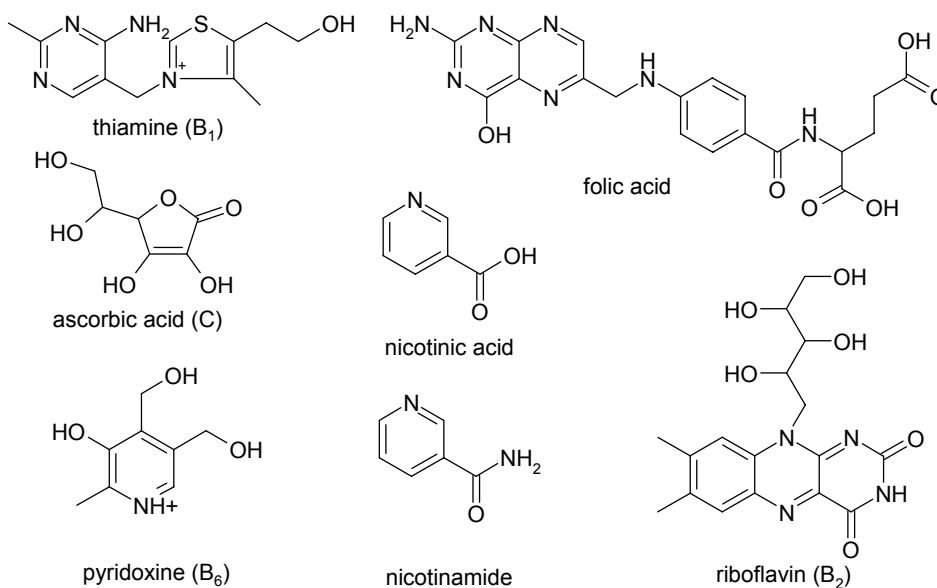
Scheme 4.19: Structures of the analysed vitamins

The following curves were recorded showing the breakthrough of riboflavin at ~100 minutes on the imprinted polymer and at ~40 minutes on the non-imprinted. The concentration of riboflavin in this experiment is approximately 8 times higher than the one in the previous experiment, thus the shorter time until breakthrough is expected.
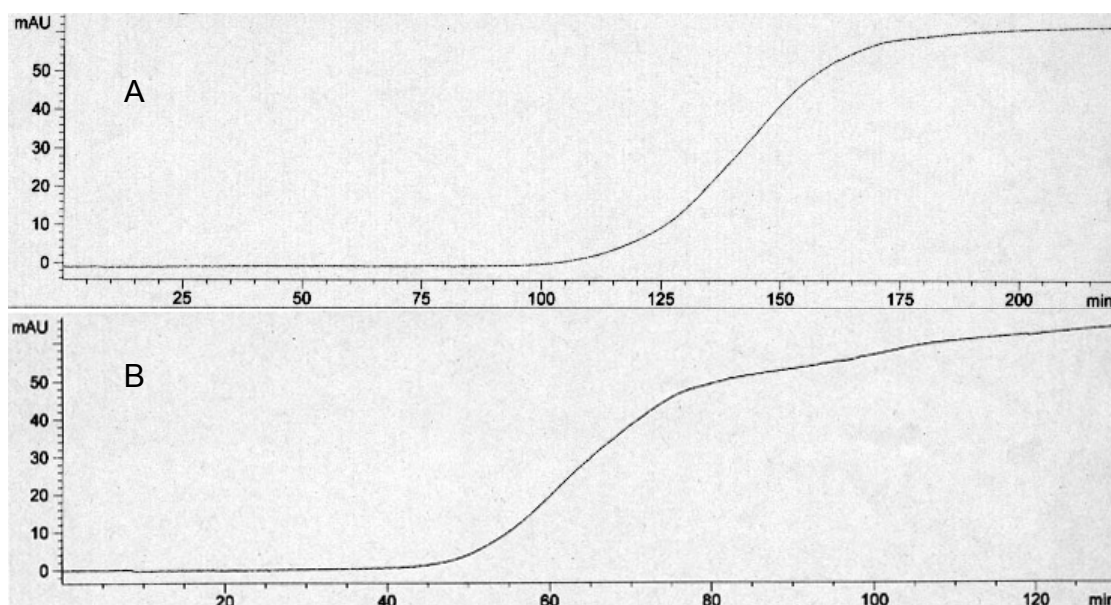
*Figure 4.61:   Breakthrough curves for the extraction of riboflavin from a mixture of 7 water-soluble vitamins. A: on **P(RfAc)'**; B: on **P$_N$'***

A sample of the mixture was analysed as reference before passing through the columns (Figure 4.62).
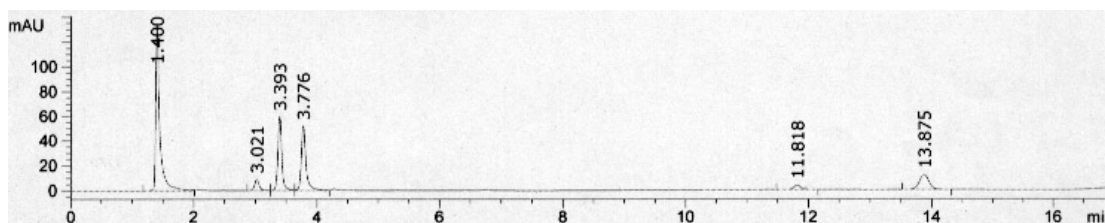
Figure 4.62:   Chromatographic separation of 7 water soluble vitamins (elution profile: thiamine 1.40min; ascorbic acid 2.80min (not marked); pyridoxine 3.02min; nicotinic acid 3.93min; nicotinamide 3.77min; folic acid 11.81min; riboflavin 13.87min)

The composition of the extracted solution after the column was monitored by collecting fractions and parallel analysis thereof with the developed HPLC method.

In the example shown here, Figure 4.63 depicts the composition of the solution extracted by **P(RfAc)'** as it eluted from the column at t = 30 minutes. Clearly, all vitamins elute apart from the selectively bound riboflavin.
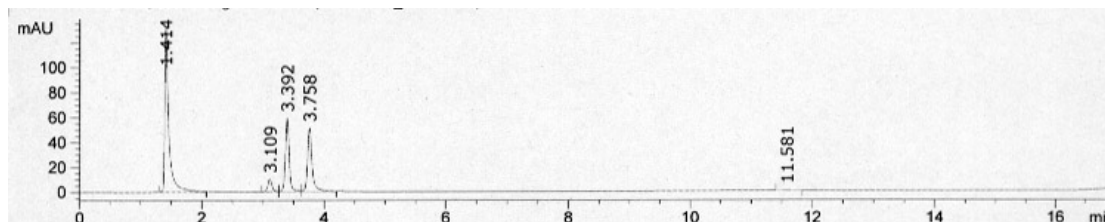
Figure 4.63:   Composition of the extracted solution after 30 minutes

Once the breakthrough has been reached, e.g. at t = 200 minutes, all vitamins elute from the column, which has at this point reached its saturation for riboflavin (Figure 4.64).
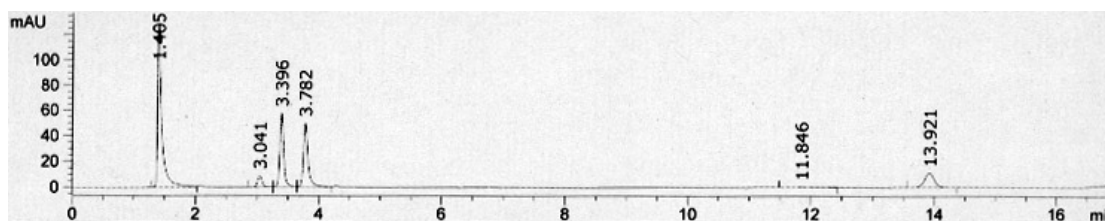
Figure 4.64:   Composition of the extracted mixture after 200 minutes

110

The column is subsequently washed with water in order to empty the interstitial volume from the vitamin solution, and finally washed with acetonitrile containing 1% acetic acid, to disrupt the binding of riboflavin and elute it from the column. Figure 4.65 shows the composition of this wash solution, which appeared bright orange-yellow, an indication of the high concentration in riboflavin that is confirmed by the chromatographic analysis of the fraction.
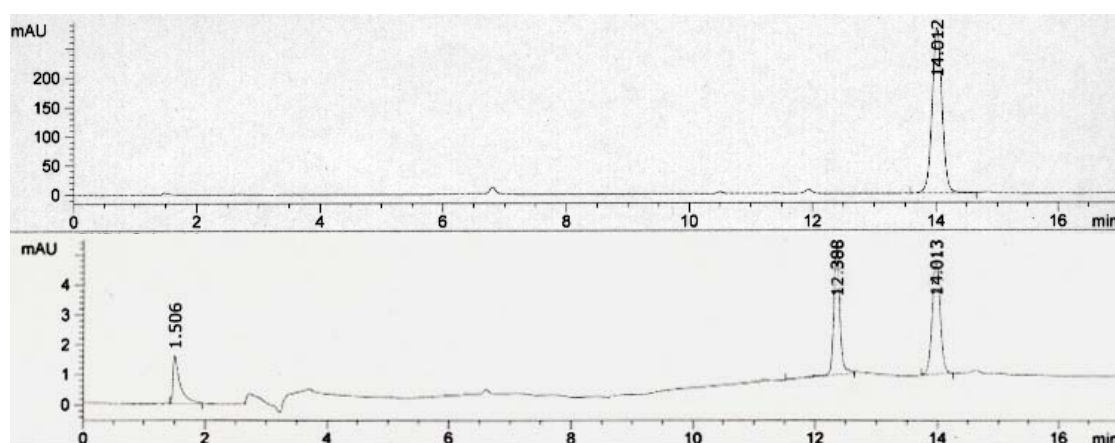
Figure 4.65:   *Composition of the wash fraction from the imprinted (top) and non-imprinted (bottom) polymers*

The area corresponding to the riboflavin peak (~14min) extracted by the imprinted polymer is at least 60 times larger than the one corresponding to the amount of the vitamin extracted by the non-imprinted polymer, proving the selectivity of **P(RfAc)'** for riboflavin, in a very competitive medium and in the presence of other competing analytes, and has opened the way for testing the polymers in real samples.

4.3.12.c *Extraction of riboflavin from beer*

In order to study the performance of the synthesised imprinted polymers in the extraction of riboflavin from beer, a reverse batch rebinding experiment was designed, whereby increasing amounts of **P(RfAc)'** and **P_N'** polymer particles (2.5-50mg) were equilibrated with a standard volume of beer, which was previously sonicated in order to remove CO_2. After 24h, the fluorescence emission of the supernatants at 525nm was recorded after excitation at

450nm. At this wavelength only riboflavin and similar flavins are emitting fluorescent light.

As displayed in Figure 4.66, the fluorescence intensity of the beer sample decreases with the increase of the amount of added polymer.
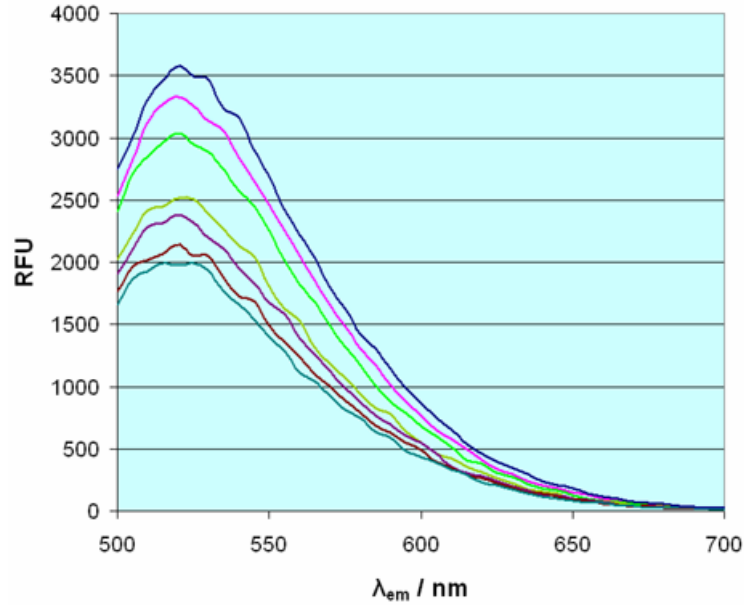
Figure 4.66: *Quenching of beer sample fluorescence with the increase of the amount of added polymer (top (pure beer); bottom (50mg))*

Plotting the percentage of "lost" fluorescence *vs.* the amount of added polymer, the following binding isotherm is produced (Figure 4.67).
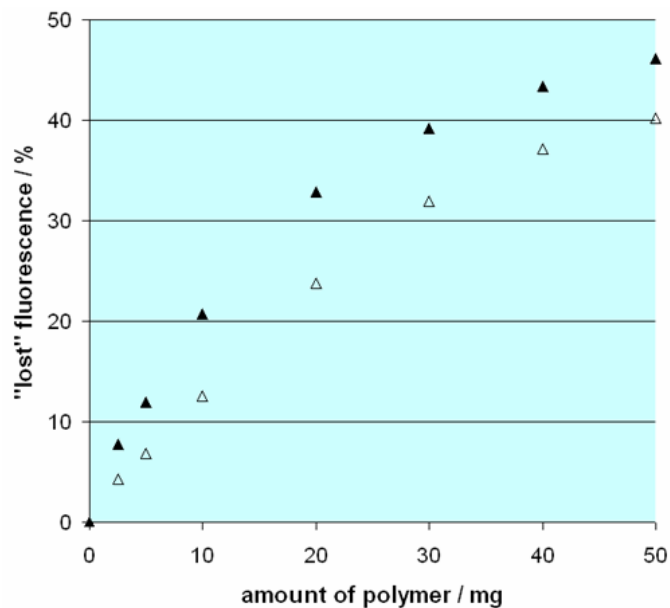
Figure 4.67: *Binding isotherms for the extraction of riboflavin from beer using **P(RfAc)'** (▲) and **P$_N$'** (△)*

112

Approximately 45% of the total beer fluorescence is lost when 50mg of imprinted polymer are added and 40% upon extraction with the non-imprinted polymer. Thus, it appears that under these conditions, the selectivity of **P(RfAc)'** diminishes and there is a significant increase in the binding on **P_N'**. This is however expected, since beer is a very complicated mixture of compounds, many of which could interfere with the binding event. The remaining fluorescence after extraction is probably due to other flavin containing molecules, e.g. FAD or FMN, which due to their size cannot fit in the binding sites generated by **RfAc**.

Further experiments were performed in collaboration with InBev (former Interbrew) brewing company. Hence, 150 mg of polymer were added to 4.5 ml of beer and stirred for a period of 24 hours. Then, the supernatants were analysed by HPLC – fluorescence and the amount of extracted riboflavin was established (Table 4.20).

Riboflavin in Stella Artois	P_N'	P(RfAc)'
Initial level (ppb)	323	323
After treatment (ppb)	123	36
Riboflavin removal (%)	60	90

Table 4.20

90% of riboflavin present in beer was extracted by the imprinted polymer, a percentage significantly higher that what was estimated by direct fluorescence measurement in the batch-type extraction. Furthermore, the difference in the performance of imprinted and non-imprinted polymer is much higher. These observations confirm the interference of other flavins in the direct measurement of fluorescence, which leads to underestimation of the polymer performance, and further highlight the potential of the imprinted materials for applications in real samples.

4.3.12.d   Extraction of riboflavin from milk

A solid phase extraction (SPE) protocol for the extraction of riboflavin in milk was developed. Thus, 25mg of **P(RfAc)'** were packed in a 10mL SPE

cartridge and conditioned with 1mL of methanol followed by 1mL of water. Then, 1mL of milk was loaded on the column and the latter was subsequently dried for 10 minutes under vacuum. Non-specifically bound compounds were washed out of the column with 1mL of water, followed by another drying step. Finally, riboflavin was eluted from the column with 3×1mL acetonitrile / water 7/3, applying gentle vacuum between the washes. The wash solutions were combined, evaporated to dryness and reconstituted in 150μL of water containing 1% acetic acid.
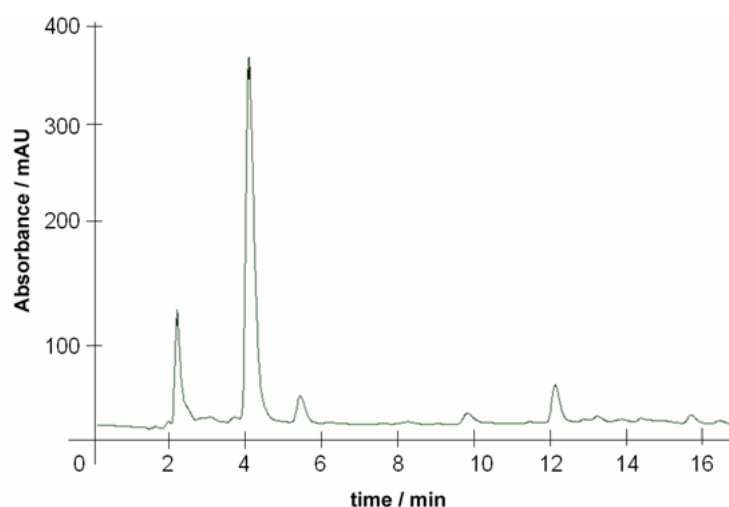
Figure 4.68:   *Chromatogram obtained by analysis of the reconstituted milk extract. Riboflavin elutes at 4.5min and lumiflavin at 12.5min (HPLC conditions described in Experimental Part)*

The reconstituted sample was analysed by HPLC. With the optimised analytical method, riboflavin elutes at 4.5 minutes while it is possible to detect lumiflavin in the same run, eluting at 12.5 minutes.

As seen on Figure 4.68, the above method of milk extraction leads to a remarkably clean extract where riboflavin is the major compound, with recoveries ranging between 75-90% of the total riboflavin content given by the milk provider.

4.3.13 Isothermal Titration Calorimetry

P(RfAc)' was finally subjected to a thermodynamic investigation using isothermal titration calorimetry (ITC). This technique has proven extremely versatile for the thermodynamic characterisation of receptor–ligand interactions,[141] including an imprinted system,[142] and is based on the measurement of the heat changes occurring upon titration of a receptor (or a ligand) with its binding partner. The addition of a dilute solution of riboflavin to a suspension of the polymer particles (0.9mg/mL) in a beverage-mimicking solution (water/formic acid/ethanol: 90.6/4.7/4.7 (v/v/v)) led to exothermic heat pulses, thus indicating non-covalent interactions between the titrant and the suspended polymer particles. The heat generated per addition was calculated by integrating the heat pulses and thereafter plotted against the total concentration of riboflavin in the cell (Figure 4.69).
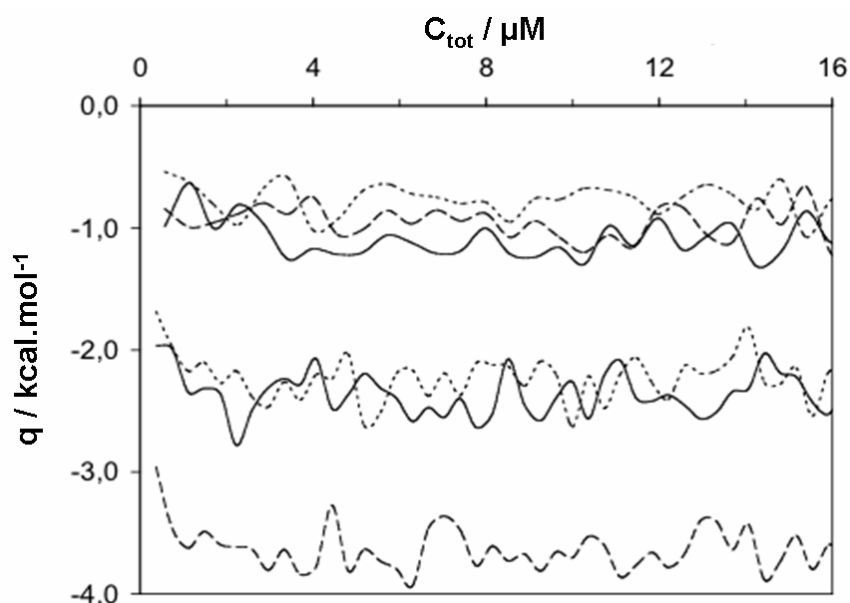
Figure 4.69:   ITC titration profiles showing the energy released (q) versus the total concentration of the titrant in the cell (C_{tot}) for the titration of **P(RfAc)'** (dashed lines), **P$_N$'** (solid lines), or blank (dotted lines) with riboflavin (lower three profiles) or uridine (upper three profiles) in water/ethanol/formic acid: 90.6/4.7/4.7 (v/v/v)

Within this small concentration interval, limited by the analyte solubility, the heat generated per addition was constant, with no evidence of saturation. Nevertheless, clear differences between the polymers were observed.

115

Interaction of riboflavin with the imprinted polymer was exothermic, exceeding that with the non-imprinted polymer by more than 1.3 kcal/mol, with the latter signal coinciding with the background signal obtained by addition of riboflavin in the absence of polymer.

The presence of highly discriminating imprinted sites was further supported by the absence of any such effect when the control analyte uridine was added. Uridine, which contains both the imide and ribose substructures, could be expected to cross-react with sites designed to bind riboflavin. However, the signal observed when this analyte was added to the different polymers did not differ from the blank runs.

Unfortunately, the limited solubility of riboflavin meant that only a fraction of the binding sites could be investigated in these experiments. Thus, none of the thermodynamic quantities typically furnished by this type of experiment could be estimated. However, the presence of a specific exotherm at a low total concentration of analyte (<400nM) implies that binding sites with affinities >10^6 M^{-1} are present. The absence of saturation effects further indicates that the sites within this population are relatively uniform.
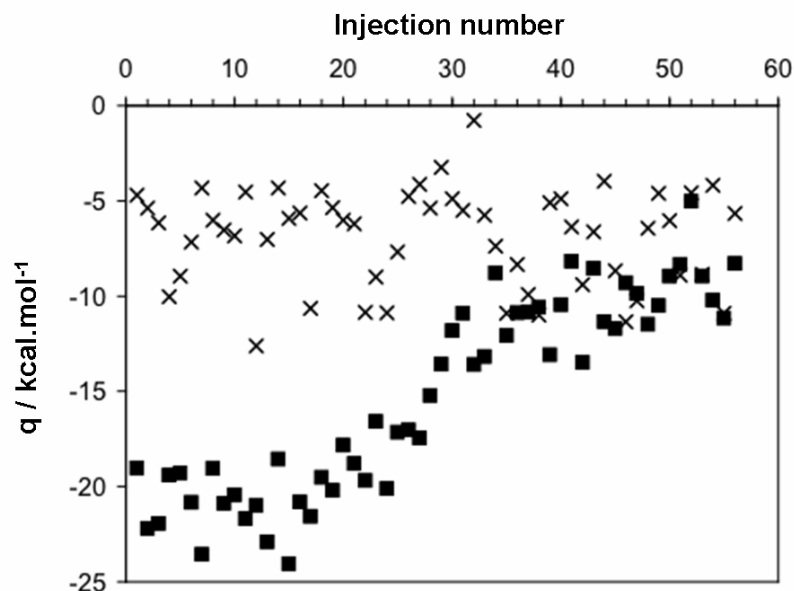
Figure 4.70:   *ITC titration profiles showing the energy released (q) versus the injection number for the titration of solutions of riboflavin (■) or U (✕) (1mM in 50 mM aqueous sodium phosphate buffer pH 7) by **RfBP**.*

Finally, the imprinted receptor was compared with its biological counterpart, riboflavin binding protein (**RfBP**). This protein was titrated by the classical technique in two different solvent systems. Pronounced exothermic heat pulses were observed under neutral conditions, with saturation clearly occurring close to a receptor : ligand stoichiometry of 1:1. Analysis of the saturation curve provided a binding constant of ~9.0×10^5 M^{-1}, with an associated enthalpy of ~9.4kcal/mol.

Similar to the situation with the imprinted receptor, no signal was observed when the control analyte uridine was used as the titrant. A different picture emerged when the protein was assessed in the beverage-mimicking solution used to evaluate the imprinted polymer. A pronounced exotherm was observed under these conditions upon each addition, with no apparent binding-related signals, which implies that the protein denatures under conditions where the imprinted polymer retains its ability to bind the target. Notably, this occurs in a solvent system which resembles that found in common alcoholic beverages, highlighting the superior properties of the synthesised materials and their potential use as substitutes for natural receptors.

4.3.14 Conclusions

A stepwise approach was followed that led to the generation of materials able to selectively bind riboflavin in highly aqueous media. The recognition event is based on a three point hydrogen bond interaction between 2,6-bis(acrylamido)pyridine and the imide moiety of the flavin. The first generation of materials was based on EDMA, the most commonly used cross-linker in molecular imprinting. From this first screening the best template analogue was selected, that was used in all subsequent studies. At this point, the focus of the research was diverted towards the synthesis of more hydrophilic materials that would comprise strong binding for riboflavin in highly aqueous media as well as reduced non-specific binding. After several different attempts, the use of PETRA as cross-linker instead of EDMA was found to be mostly appealing. The binding properties of the thus synthesised materials were tested in real samples, where riboflavin was selectively extracted from aqueous mixtures of

water-soluble vitamins as well as milk and beer. Furthermore, the polymers outperformed the natural receptor of riboflavin in conditions similar to the ones typically present in food and beverages, as indicated by ITC measurements. A step towards further decrease in the non-specific binding appears to be the partial hydrolysis of the surface confined unreacted double bonds. Preliminary results show a significant decrease in the binding of riboflavin on the non-imprinted polymers, after hydrolysis with $TBA^{+-}OH$, accompanied by an increase in the selectivity of the imprinted polymers for riboflavin, expressed by the calculated imprinting factors.

4.4 Recognition of carboxylate anions

As part of an ongoing effort in the working group in collaboration with the University of Pavia, Italy, for the recognition of dihydrofolate reductase inhibitors via the substructure approach,[143] several polymerisable receptors that could recognise the glutamic acid moiety were synthesised. The part of the work that was assigned to the author was mainly to evaluate the binding characteristics of the available receptors, thus selecting the optimum monomer that was subsequently used for the imprinting of N-Z-L-glutamic acid. This was performed by means of ^{1}H-NMR as well as UV-Visible and fluorescence titrations. In addition to this, batch rebinding experiments were performed using the synthesised materials, in order to estimate their enantio-selectivity and capacity.

4.4.1 Monomer design

The design of the monomers has been based on substituted mono- or bis-ureas, since it has been well established in the literature[144-148] that the latter are very capable receptors for anions, carboxylates included. Thus, one bis-urea[15] and seven mono-urea based monomers[16, 35] were synthesised by simple one-step synthesis in moderate to good yields by commercially available amines (or diamines) and isocyanates.

4.4.2 The mono-urea monomers

The structures of the studied mono-ureas are depicted in Scheme 4.20. In order to estimate the binding strength of the synthesised monomers towards the carboxylate anion, tetrabutylammonium benzoate (**TBA-Bz**) was selected as the model "guest". The respective association constants were measured in DMSO-d_6, a competitive polar solvent. Self-association of the monomers and/or the guest does not take place in these systems.
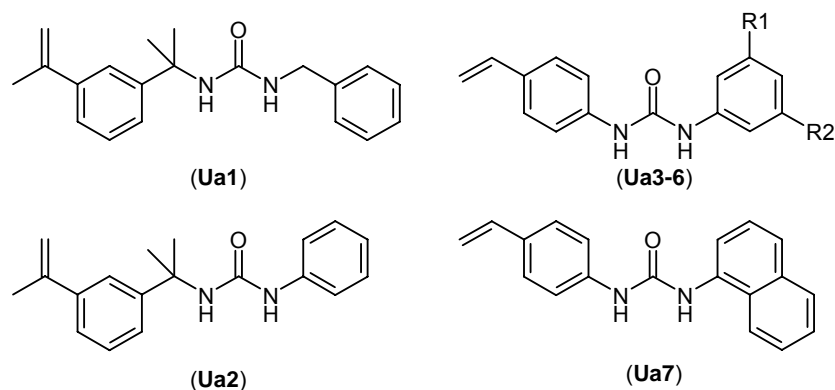
Scheme 4.20: Structures of the synthesised mono-ureas. **Ua3**: R1=R2=H, **Ua4**: R1=CF$_3$, R2=H, **Ua5**: R1=NO$_2$, R2=H, **Ua6**: R1=R2=CF$_3$

The measured association constants are displayed in Table 4.21.

Monomer	K_a $(M^{-1})^a$	CIS (ppm)
Ua1	30 ± 4	1.21
Ua2	121 ± 6	2.34
Ua3	1322 ± 48	3.28
Ua4	6520 ± 1099	3.48
Ua5	6498 ± 170	3.54
Ua6	8820 ±1600	3.39
Ua7	613 ± 61	2.31

Table 4.21: Association constants (K_a) and Complexation Induced Shifts (CIS) for the interaction of the synthesised ureas with TBA-benzoate in DMSO-d$_6$. ^{a}CIS of both urea protons were monitored (K_a refers to the average of the individual values)

The stoichiometry of binding of the urea monomers with the carboxylate anion was confirmed to be 1:1 by Job plot analysis, as shown on Figure 4.71, for the case of **Ua5**.
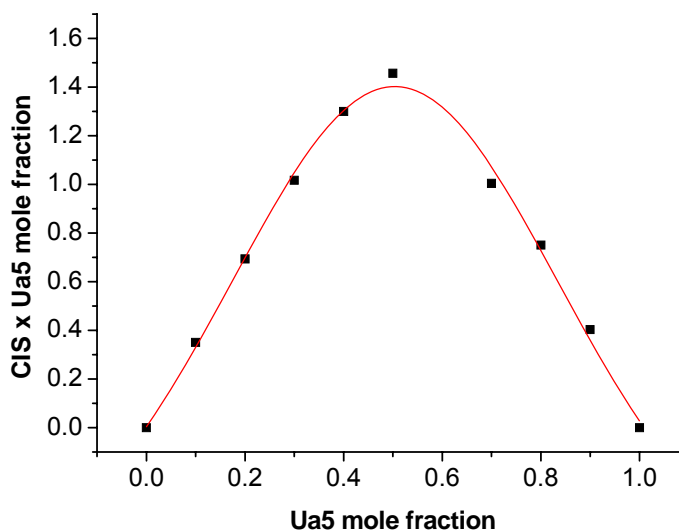
Figure 4.71: *Job plot for the binding of **Ua5** with TBA-benzoate in DMSO-d$_6$*

In agreement with previous reports,[149] dramatic increases in the binding strengths of the monomers are observed on varying the substitution of these simple mono-urea systems. These are attributed to the nature of the urea substituents, which leads to increases in the acidity of the urea protons and, hence, increased magnitudes of association with the carboxylate guest. *Meta*-substitution furthermore enhances the acidity of the *ortho-* aromatic ring proton, which in turn enhances its ability to act as a hydrogen bond donor towards the carbonyl oxygen. This effect is important in the crystalline state leading it to co-crystallise with Lewis basic solvents but is likely to be of less importance in solution.[150]

As reported for similar low molecular weight host molecules,[146, 148] the binding of **Ua5** with TBA-benzoate was accompanied by a bathochromic shift of 15nm leading to a clearly visible increase in the yellow colour intensity (Figure 4.72).

0   0.5   1   5   10

Equivalents of TBA-benzoate
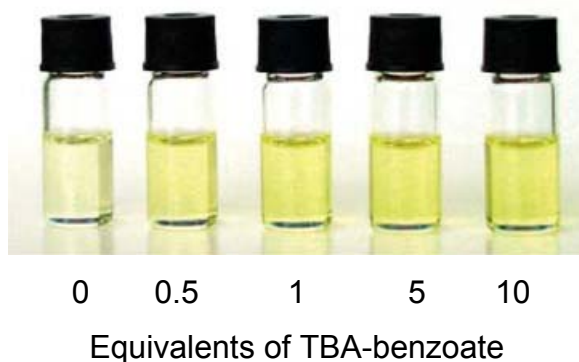
Figure 4.72:   *Solutions of **Ua5** (10 mM in DMSO) in the presence of, from*
             left to right, 0, 0.5, 1, 5 and 10 equivalents of TBA benzoate,
             respectively

A UV-Vis titration of **Ua5** with TBA-benzoate was performed in DMSO (see §
6.3.2). Thus, solutions of the receptor with increasing concentrations of added
guest were prepared and their UV-Vis spectra were recorded using a UV-Vis
spectrophotometer. The overlaid spectra are displayed in Figure 4.73.
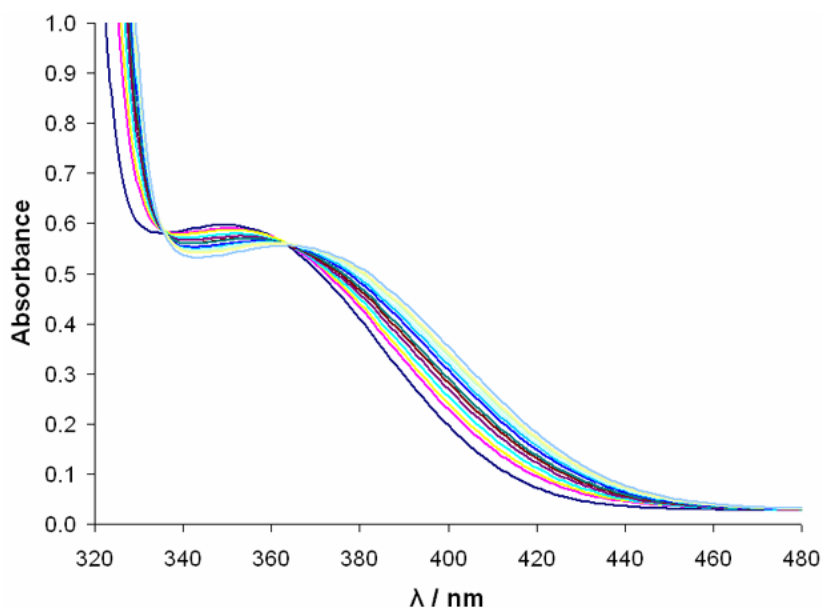
Figure 4.73:   *UV–Vis spectra of **Ua5** (0.33mM in DMSO) in the presence of*
             increasing concentrations of TBA-benzoate (details available
             in the Experimental Part)

In order to estimate the binding constant for the complexation of **Ua5** with
TBA-benzoate a wavelength at which maximum change in the absorbance
had to be selected. 400 nm appeared to be a good choice since the difference
between the absorbance of the pure monomer and in the presence of 10

equivalents of TBA-benzoate was ~0.2mAU, greater than at any other wavelength.

Thus, the difference in absorbance intensities at 400nm (ΔA) were plotted against the calculated concentration of "free" template in solution to yield the binding isotherm displayed in Figure 4.74.
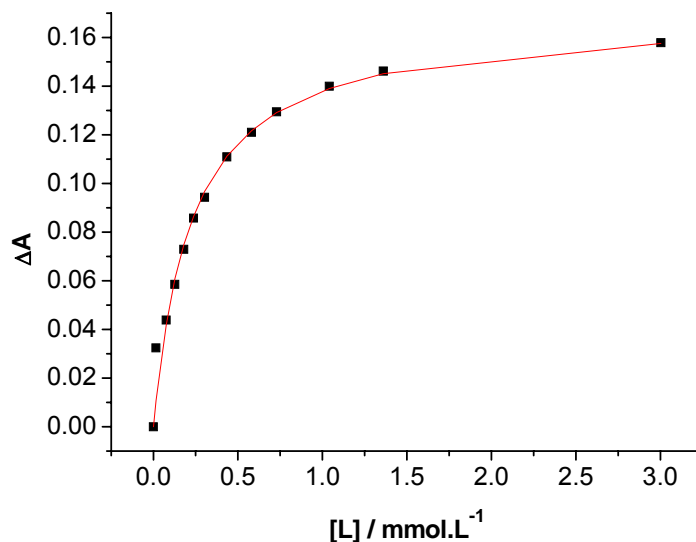
*Figure 4.74:   UV-Vis titration data for the binding of **Ua5** with TBA-benzoate*

An association constant of ~4400 M^{-1} was derived by non-linear regression fit of the experimental data to the 1:1 binding model.

Alternatively, generating the double reciprocal Benesi-Hildebrand plot (Figure 4.75) a value of Ka = 4660 M^{-1} is obtained, a value slightly lower than the one obtained by the ^{1}H-NMR titration (Table 4.21).
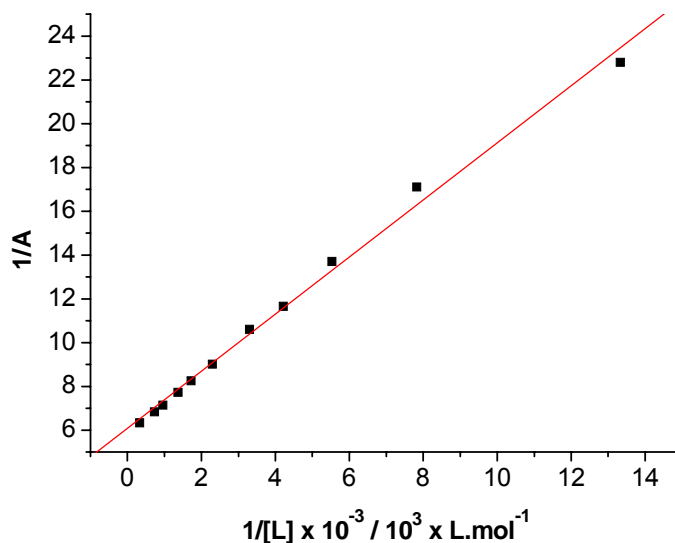
Figure 4.75: *Benesi-Hildebrand plot for the binding of **Ua5** with TBA-benzoate (linear fit: y=1.304x+6.082; b/a=4.664)*

Monomer **Ua7** is fluorescent, thus enabling an alternative way to study its complexation with TBA-benzoate. A fluorescence titration experiment was performed in DMSO as described in § 6.3.3 of the Experimental Part.
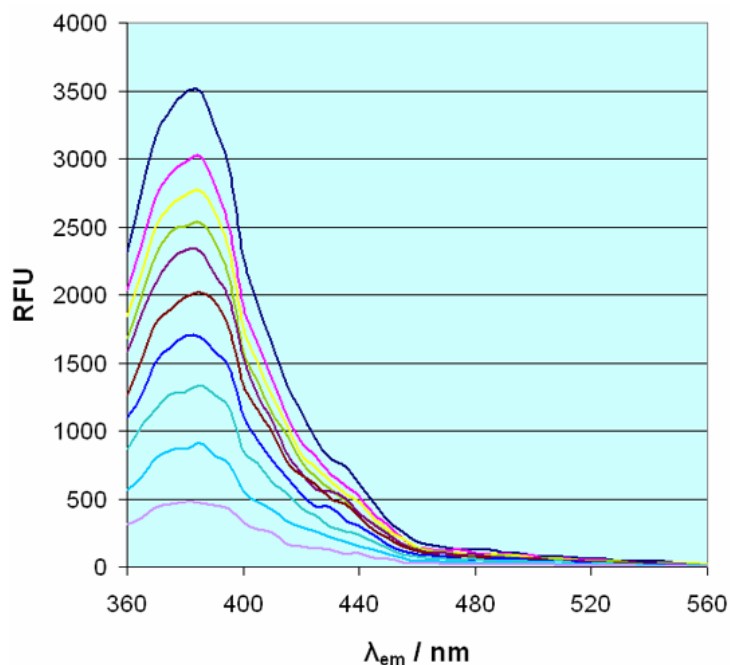
Figure 4.76: *Fluorescence emission spectra (λ_{ex}=330nm) obtained by titration of **Ua7** (1mM) with TBA-benzoate (0 (top)-10mM (bottom)) in DMSO*

124

A clear fluorescence quenching phenomenon can be observed on Figure 4.76 upon addition of TBA-benzoate in a solution of **Ua7**. Mathematic elaboration of the acquired data leads to the Stern-Volmer plot (Figure 4.77).
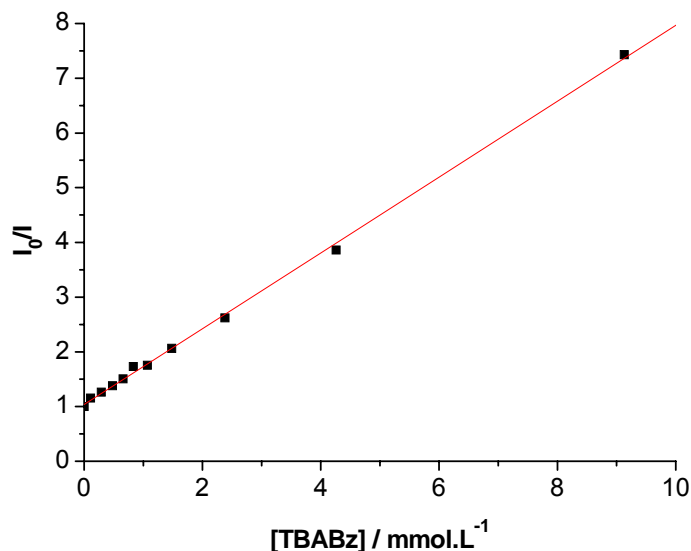
Figure 4.77:   *Stern-Volmer plot for the titration of **Ua7** with TBA-benzoate (linear fit: y= 0.6924x + 1.039)*

The slope of the fitted data points corresponds to the association constant between the two studied compounds. This value is found to be approximately 700 M^{-1}, in very good agreement with the result obtained by ^{1}H-NMR titration.

4.4.3   *Imprinting of N-Z-L-Glutamic acid*

Molecularly Imprinted Polymers were subsequently prepared using **Ua5** and EDMA as cross-linker, in the presence of Z-(D or L)-Glu and two equivalents of triethylamine in DMF. Elemental analysis performed on the polymers after Soxhlet extraction indicated that the monomer conversion was high, that the monomers had been stoichiometrically incorporated into the polymers and that the template had been successfully removed from the polymer. The molecular recognition properties of the materials were then investigated chromatographically, comparing the retention of the template, Z-glutamic acid, with that of more complex biologically active molecules such as methotrexate

(MTX), containing the glutamic acid substructure, and structurally related analogues Z-Asp and Z-Gly.[35]

Interestingly, the bathochromic shift that was observed upon binding of **Ua5** to TBA-benzoate is directly translated to a bathochromic change in the colour of the Z-glutamic acid imprinted polymers. As seen in Figure 4.78, binding of the template on the imprinted polymers induces a colour change. Although this change is small, the yellowish polymers adopt a more intense yellow colour in presence of added template (Z-L-Glu). Thus, prior to template removal, **PU5** exhibited a more intense yellow colour than the corresponding non-imprinted polymer **PU_N**.
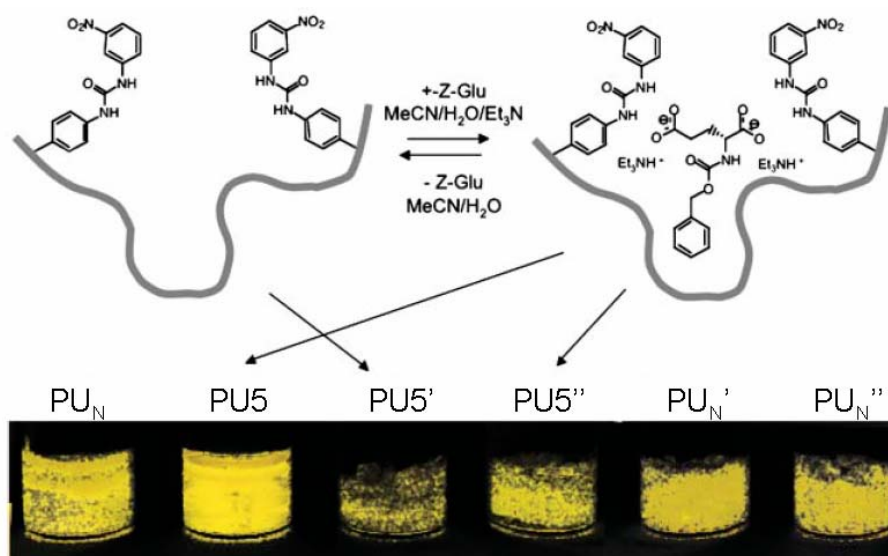
Figure 4.78: *Photographs after tone adjustment and with blackened background of polymer monoliths illuminated with a 60W light bulb. The monoliths were prepared by co-polymerisation of **Ua5** with EDMA in absence (**PU_N**) and presence (**PU5**) of Z-L-Glu. **PU5'** is an imprinted polymer (**PU5**) after template removal by extensive washing and **PU5''** is a washed polymer (**PU5'**) incubated with Z-L-Glu. **PU_N'** and **PU_N''** are non-imprinted polymers subjected to the same treatments*

Extensive washing of **PU5** resulted in polymer **PU5'**, which showed a lighter colour, indicating removal of the glutamate guest. The washed polymer was then incubated with the template Z-L-Glu in MeCN/H$_2$O/TEA: 92/7/1 (v/v/v) for 5 days giving **PU5''**. As seen from the tone adjusted photographs, **PU5''** exhibits a significantly more intense yellow colour than **PU5'**. Interestingly,

these binding induced changes were not observed for the corresponding non-imprinted polymer **PU_N**, indicating that the colour changes originate from the template occupying imprinted sites in the polymer.[16]

To gain insight into the binding energy and site density of the polymers we measured the equilibrium binding isotherm on a Z-D-Glu imprinted polymer in the optimum solvent system described above and in MeCN/TEA (99/1 v/v) where Z-D-Glu is expected to bind strongly to both the imprinted and non-imprinted polymers (Figure 4.79A). Z-D-Glu interacts strongly (Ka ~ 1000 M^{-1}) with both polymers in the latter system and the difference between the uptake of the solute by them is small. Interestingly, the curve levels off at a value close to the theoretical capacity of **PU5** based on the amount of template added to the monomer mixture. This shows that the matrix urea groups are functional and fully accessible.
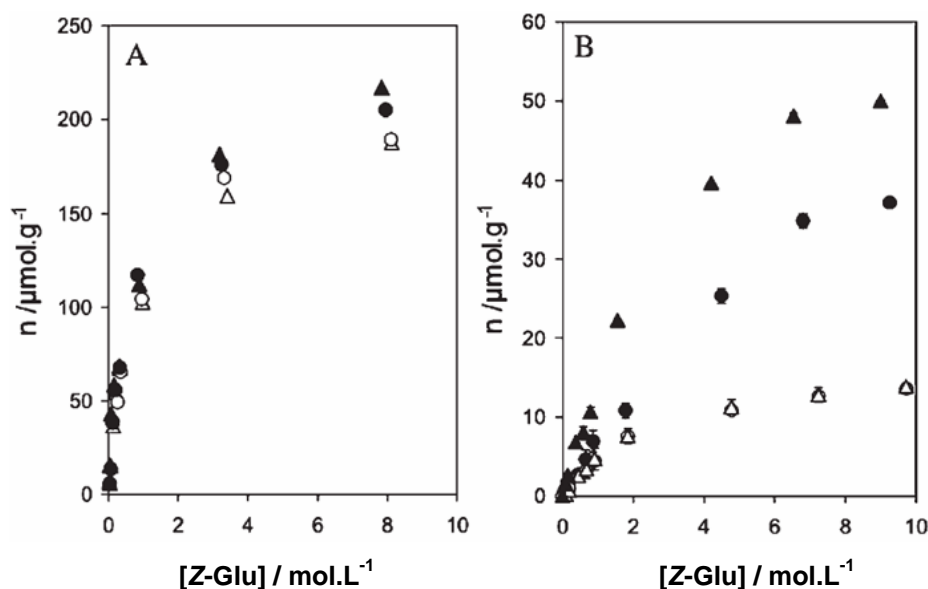
Figure 4.79: *Adsorption isotherms of Z-D-Glu on **PU5** (▲) or **PU_N** (△) and Z-L-Glu on **PU5** (●) or **PU_N** (○) as solutions in (A) MeCN/TEA: 99/1 (v/v) and (B) MeCN/H₂O/TEA: 92/7/1 (v/v/v)*

The association to **PU_N** could be selectively suppressed by addition of water, resulting in a large difference in adsorption properties between the materials. Thus, in addition to a preferential weakening of the binding to **PU_N**, the difference in the adsorbed amount of Z-D-Glu to imprinted and non-imprinted polymers amounted to *ca.* 35μmol/g and the imprinted polymer then exhibited

a pronounced enantio-selectivity with the adsorbed amount of *Z*-D-Glu exceeding that of *Z*-L-Glu by *ca.* 13μmol/g (Figure 4.79B).

Further chromatographic evaluation of the materials as well as investigation of the selectivity of the polymers for larger related structures containing the carboxylate moiety, were performed by the collaborating group of *Prof. E. de Lorenzi* in Pavia, Italy and the results have been recently published.[35]

4.4.4 The bis-urea monomer

The polymerisable bis-urea receptor (**Ua8**) was readily prepared in one step, from p-xylylene diamine and 3-isopropenyl-R,R-dimethylbenzyl isocyanate, in 67% yield. The design of this monomer was based on a previously reported receptor, which encompassed a suitably spaced bis-urea and exhibited an affinity constant with bis-TBA-glutarate of ~790 M^{-1} in DMSO-d$_6$.[145, 151]

In order to determine the binding abilities of **Ua8,** ^{1}H-NMR titrations were performed using bis-TBA-glutarate as model di-carboxy anion guest. Addition of increasing amounts of bis-TBA glutarate (0-10 equiv.) to DMSO-d$_6$ solutions of **Ua8** (5mM) led to significant downfield complexation-induced shifts (CIS) of both the "inner" and "outer" urea proton signals (CIS 1.8 ppm in each case) (Figure 4.80).
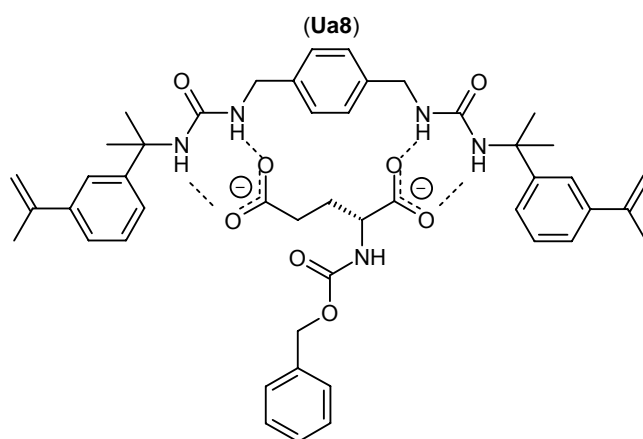
*Scheme 4.21: Binding of **Ua8** with the bis-anion of N-Z-L-glutamic acid*

A Job plot titration (Figure 4.80-insert), performed to establish the stoichiometry of the interaction revealed a small deviation from the expected 1:1 monomer/guest stoichiometry (maximum at mole fraction **Ua8** ~0.45).

Indeed, the data obtained in the first titration exhibited deviation from the theoretical 1:1 binding isotherm at higher guest concentrations (7.5 and 10 equiv.); this is indicative of the formation of higher order complexes. Exclusion of the deviant points led to a good fit to the 1:1 binding isotherm, and an apparent association constant of 1500 M^{-1} was extracted.
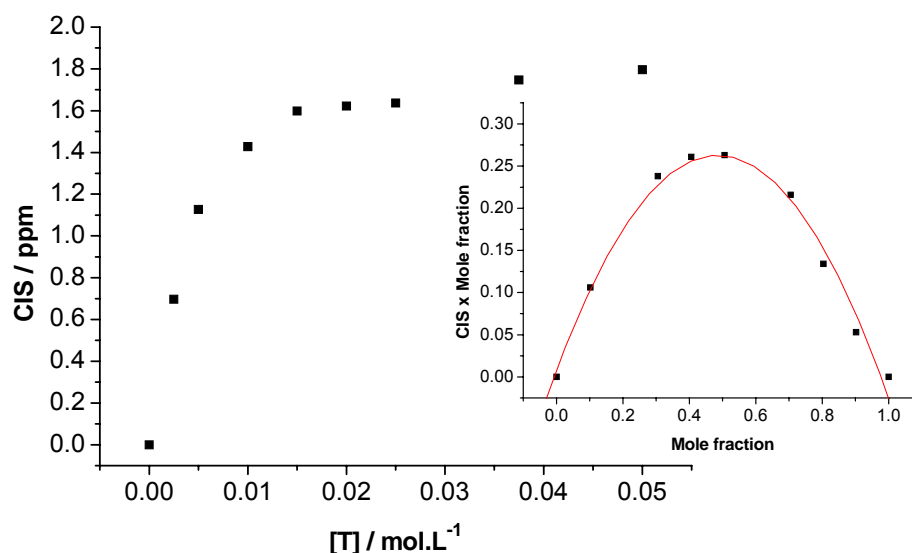
Figure 4.80: *Binding isotherm and Job plot for the association of **Ua8** with bis-TBA-glutarate*

Monomer **Ua8** was subsequently used in the preparation of a MIP using bis-TBA-N-Z-L-glutamate (prepared by the reaction of N-Z-L-glutamic acid with 2 equiv. of TBA hydroxide in methanol) as the template and DMSO as the polymerisation solvent. Thermally initiated polymerisation at 40°C was allowed to continue for 24 hours. Following the polymerisation, the template was removed by extraction with methanol in a Soxhlet apparatus. The polymer was then crushed and sized to yield particles of size 25-50μm. A control, non-imprinted polymer was prepared under identical conditions, but with the omission of the template molecule. The recognition properties of the respective polymers toward the template, its optical antipode, and other amino acids were examined via HPLC using mobile phases based on acetonitrile and modified with triethylamine.

Imprinting effects are observed only when the analyte is in the de-protonated state, thus confirming the mode of binding to the pendant polymer

129

functionality. The MIP is selective for N-Z-L-Glu over N-Z-L-Asp and N-Z-L-Gly and is furthermore able to bind the drug methotrexate, providing further evidence that substructure approaches to molecular imprinting offer a viable alternative to the imprinting of the entire target structure.[15]

4.4.5   Conclusions

A series of aliphatic and aromatic urea based host monomers, as well as a bis-urea monomer was put together. The binding characteristics of the monomers with a model carboxylate anion were primarily estimated by means of ^{1}H-NMR titrations. A difference in binding strength was observed, depending on the substitution pattern around the urea core. Thus, it was concluded that increasing the electron-deficiency of the aromatic ring attached to the urea moiety leads to an increase to the binding strength of the monomer. In addition to this, valuable spectroscopic properties were present in two of the studied monomers. These were utilised in order to confirm the association constant values obtained by ^{1}H-NMR. Both techniques yielded results that were in good agreement.

The polymers synthesised subsequently using the optically active urea, displayed colour changes upon binding of the template similar to those observed in solution, thus indicating potential sensory applications. Following a thorough optimisation of the mobile phase, maximum selectivity and enantio-selectivity were achieved, in presence of 7% water.

4.5 Recognition of carboxylic acids

An alternative route towards the recognition of carboxylic acids is by designing monomers that bind to the neutral acid functional group, instead of the carboxylate anion. This project was also in collaboration with the University of Pavia, Italy, thus the work undertaken by the author was the characterisation of the different synthesised monomers by means of ^{1}H-NMR. The results are presented in the following paragraphs.

Five amidopyridine-based functional monomers with different substitution patterns were synthesised in order to tune their binding strength and select the best host monomer for the target of interest. The structures of the synthesised monomers are shown in Scheme 4.22.

(AP1)   (AP2)

(AP3)   (AP4)

(AP5)
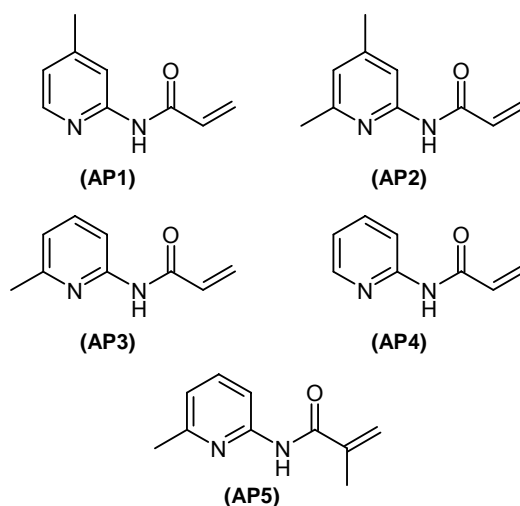
Scheme 4.22

It should be mentioned that N-(2-pyridyl)methacrylamide[152] and **AP5**[32] have been used previously in an imprinting context. In neither the latter example nor here have the effects of host and/or guest self-association been de-convoluted from the association constants determined. Thus, the values reported herein are referred to as "apparent" association constants (K_{app}).

The amidopyridine Donor-Acceptor (D-A) hydrogen bond array is complementary to the A-D array of the protonated carboxyl group. These two moieties can associate in a 1:1 complex as it has been proven by a Job plot analysis (Scheme 4.23). Propionic acid was selected as a model carboxylic

acid, since it is commercially available and its pK_a lies close to the average of those of most amino acids.
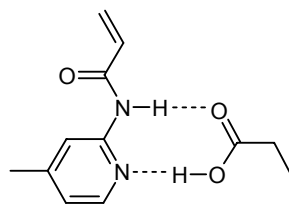
Scheme 4.23

The association constants for the binding of each of the above host monomers with propionic acid were estimated by ^{1}H-NMR titration experiments in $CDCl_3$. The results are displayed in Table 4.22.

Monomer	K_{app} (M^{-1})		CIS (ppm)
AP1	777	± 83	2.82
AP2	704	± 44	3.01
AP3	650	± 111	2.71
AP4	540	± 53	2.68
AP5	160	± 26	1.26

Table 4.22:   Example of 1:1 complex between an amidopyridine based monomer and propionic acid

Out of the five monomers, four are acrylamides (**AP1-AP4**) and one is a methacrylamide (**AP5**). **AP5** appears to have the weakest binding with propionic acid, possibly due to the presence of the methyl group which probably repels the carbonyl of the acid, therefore not allowing the two molecules to come together. This fact is reflected in the big difference in binding strength between this methacrylamide and the acrylamides. All four acrylamides contain the same core, which is essentially monomer **AP4**, which binds with moderate strength to propionic acid. Adding a methyl group in the *ortho-* to the ring nitrogen position makes the pyridine core slightly more electron rich, which in its turn makes the pyridine N more basic and thus the amide proton more acidic, leading to an overall increase in the binding strength of the monomer. However, if this methyl group is placed in the *para-*

instead of the *ortho-* position to the pyridine nitrogen (monomer **AP1**), the effect is much more enhanced. This is probably due to the fact that an *ortho-* methyl group slightly repels the hydroxyl group of the acid, decreasing in this manner the overall binding constant. This hypothesis is supported by the result from the titration of monomer **AP2** with the same guest. The binding constant is found to lay in between the ones of monomers **AP1** and **AP3**, indicating lowering effect of the methyl group in the *ortho-* position to the ring nitrogen.

Imprinted polymers synthesised using monomer **AP2** were evaluated by the collaborating group in Pavia, Italy, and their recognition properties for N-*Z*-L-glutamic acid as well as larger structures containing the glutamic acid substructure have been assessed in the chromatographic mode.[153]

5 Conclusions and Outlook

During this work, considerable knowledge has been gained with regards the design and optimisation of Molecularly Imprinted Polymers for applications in aqueous environments. It has been demonstrated that by designing the host monomers used in molecular imprinting and optimising the polymer backbone, one can achieve significant enhancement in the binding selectivity of the resulting material in competitive and complicated matrices. Furthermore, the synthesised binding elements can be provided with additional interesting features, e.g. optical or fluorescent response upon binding, which are then transferred to the final polymer.

In this chapter, the author would like to draw a few conclusions regarding the performed research and discuss potential steps towards further enhancement in the performance of the systems studied during this doctoral work.

During the initial stages of this work, it has been shown that incorporation of a seemingly weaker host monomer for uracils in molecularly imprinted polymers reveals its superior inherent binding strength, which is supported by solution studies including ^{1}H-NMR and fluorescence dilution experiments and in depth study of the monomer characteristics using IR spectroscopy.

Further improvement in the binding strength could be achieved by using 4-substituted pyridines instead of pyrimidines. A potentially successful route leading to such monomers could be adapted by a publication by Lehn *et al.*[130] starting by chelidamic acid and following a multiple step synthesis.
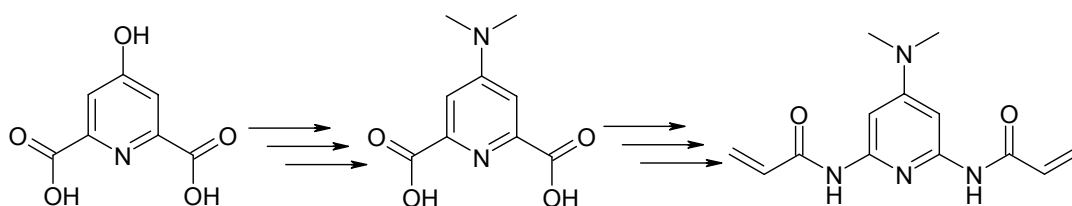
Scheme 5.1

The recognition of riboflavin proved to be a significantly more challenging project, since the template itself is not sufficiently soluble in any of the organic solvents used in molecular imprinting. Hence, a series of analogues were synthesised and tested to lead to the final selection of riboflavin tetraacetate

as the template substituent. Achievement of selective binding and entrapment of riboflavin in aqueous systems was essential for this project, since the aim was to remove it from sensitive food samples such as milk and beer. A step towards this goal was made using a hydrophilic cross-linker (PETRA) in the place of the commonly used EDMA, thus not only achieving higher selectivity, but also reducing the non-specific binding. The synthesised materials were successfully applied in the extraction of riboflavin from milk and beer samples, as well as from commercial and home-made multivitamin drinks. The capacity of the polymers was not high enough as far as large scale applications are concerned, but this problem could be tackled by further tuning of the polymerisation and different formulation of the materials.

Isothermal Titration Calorimetry measurements provided further proof of the binding strength and selectivity of the materials, which outperformed the natural receptor of riboflavin (**RfBP**) under the acidic conditions found in foodstuffs.

An effort towards the improvement of these polymers has already been initiated, following mainly two different approaches; enhancement of the binding strength and capacity and improvement of the water compatibility of the polymers. Thus, the incorporation of π-stacking monomers in the polymer matrix was expected to lead to further increase in the binding strength, since such components are found in the binding site of the natural receptor (tryptophan amino acid units). Initial tests show no significant improvement in the performance of the imprinted polymers, but a slight increase in the non-specific binding has been observed.

The use of an indole based co-monomer could be a good alternative to the commercially available π-stacking monomers as it provides functionality more similar to the one present in the protein binding site. Furthermore, tuning of the polymerisation conditions (temperature, solvent) to facilitate the weak π-π interactions is essential.
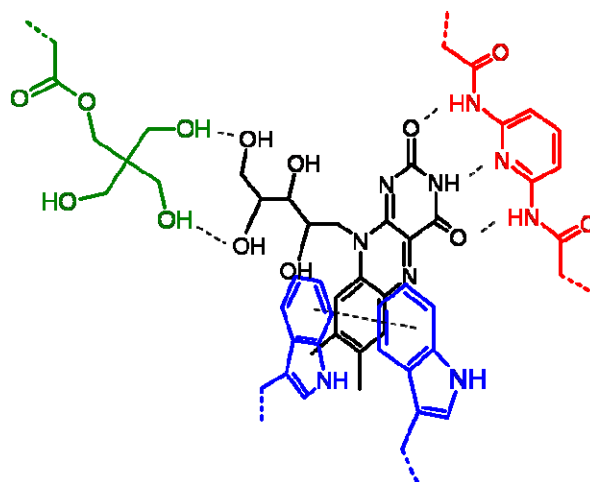
Figure 5.1: *Envisaged riboflavin binding site, encompassing 3-point hydrogen bonding by the functional monomer, hydrogen bonding of the ribose –OH groups with polymer backbone hydroxyl groups and π-π interactions with an indole based functional monomer*

Secondly, partial hydrolysis of the remaining un-reacted double bonds leading to the introduction of hydroxyl groups on the polymer surface, thus increasing the hydrophilic character of the materials, is currently underway. Preliminary results indicate a significant decrease in the retention time of riboflavin on the non-imprinted polymer, while the retention times increase on the imprinted polymer, as a result of the release of trapped template and thus an increase in the number of available binding sites. Further evaluation of the hydrophilised materials and test of their properties in real samples is essential in order to prove the importance of the partial hydrolysis.

A third step towards the enhancement in the water compatibility of the synthesised materials could be the grafting of hydrophilic branched polymer chains on the surface of the imprinted polymers. By careful balancing of the size of the polymer chains, the polymers are expected to display improved hydrophilic character, without losing their selectivity or capacity due to decreased accessibility to the binding sites caused by pore filling.

The format in which the polymer is prepared and used plays an important role in its binding characteristics. Different approaches are currently under investigation, including synthesis of riboflavin specific polymers by precipitation polymerisation, grafting of polymer layers on silica based supports and incorporation of imprinted micro-particles, produced during the

crushing of the bulk monoliths, in membranes prepared by phase inversion. In view of a potential need for larger quantities of material for commercial use, other polymerisation techniques are under investigation, including precipitation and suspension polymerisation.
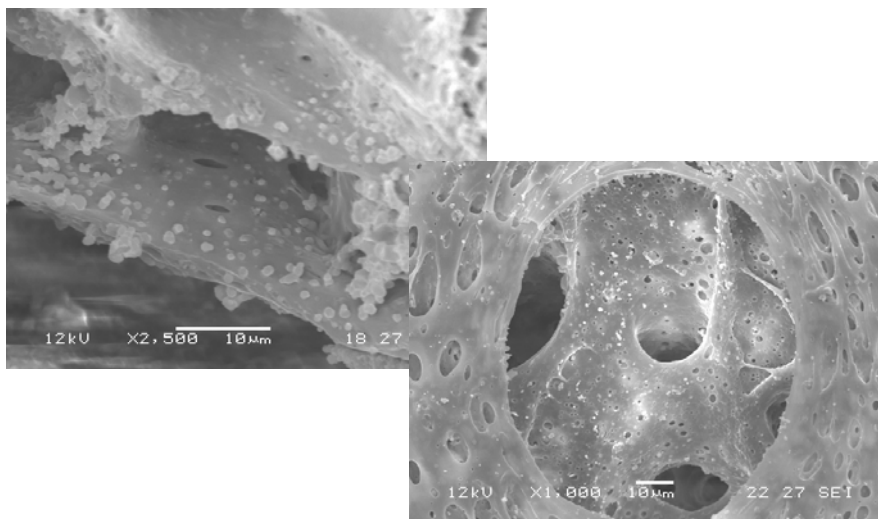
Figure 5.2:   *SEM micrographs of membranes prepared by phase inversion, including imprinted micro-particles*

Regarding the recognition of carboxylate anions, a good start has been made with the screening and selection of the best performing monomers. The so far synthesised materials show some water compatibility, but further improvement is necessary in order for the materials to be used in biomedical or sensing applications. Enhanced water compatibility can be achieved by combination of the urea based monomers with the hydrophilic cross-linkers used for the recognition of riboflavin (e.g. PETRA). Additionally, taking advantage of the higher affinity and solubility of the **Ua6** monomer, materials with superior recognition properties can be attained, using less polar solvents and higher concentrations of monomer : template complexes in the pre-polymerisation solution.

Such materials can be employed in the solid phase extraction of carboxylates from biological fluids and in array format for the detection of anions, taking advantage of their optical properties (colour change, fluorescence).

6 Experimental Part

In the following paragraphs, all the experimental details of the present project will be discussed.

6.1 Synthesis of Functional Monomers

Whereas in Molecular Imprinting the use of commercially available monomers is widely spread, all functional monomers used during this work have been synthesised in house. In the following paragraphs the synthetic protocols for each of the synthesised monomers will be presented. For the compounds that have been synthesised previously, the related bibliographic reference(s) will be provided.

6.1.1 Synthesis of 9-(3/4-vinylbenzyl)adenine

Reaction:
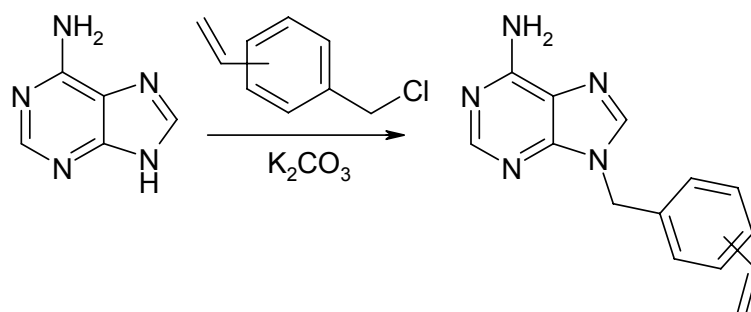
Synthetic procedure:

9-(3/4-vinylbenzyl)adenine was synthesised in 45% yield *via* the reaction of adenine and 3/4-vinylbenzyl chloride in the presence of potassium carbonate in dimethylformamide.[126]

Compound characterisation:

^{1}H-NMR (DMSO-d$_6$): δ (ppm): 5.23 (d, 1H), 5.38 (s, 2H), 5.63 (s, br, 2H), 5.75 (d, 1H), 6.70 (m, 1H), 7.20 - 7.40 (m, 4H), 7.80 (s, 1H), 8.40 (s, 1H).

6.1.2 Synthesis of 9-(3/4-vinylbenzyl)-2,6-diaminopurine

Reaction:
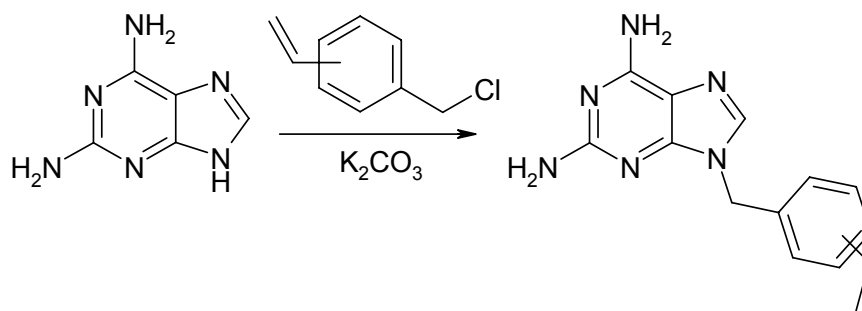
Synthetic procedure:

9-(3/4-vinylbenzyl)-2,6-diaminopurine was obtained by modification of a published procedure[128] for the synthesis of 9-benzyl-2,4-diaminopurine, in ~50% yield.

Compound characterisation:

^{1}H-NMR (CDCl$_3$): δ (ppm): 4.71 (s, 2H), 5.18 (s, 2H), 5.25 (q, 1H), 5.35 (s, br, 1H), 5.74 (d, 1H), 7.2 (d, 1H), 7.27 (t, 2H), 7.35 (t, 2H), 7.46 (t, 2H).

6.1.3 Synthesis of 2,6-bis(acrylamido)pyridine

Reaction:
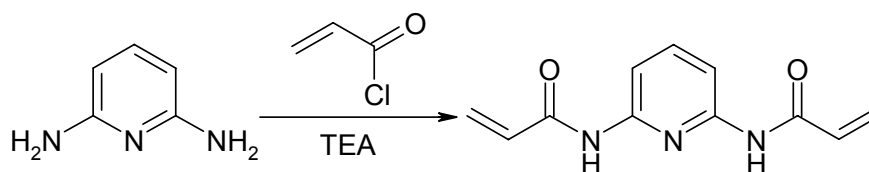
Synthetic procedure:

Modified from a published procedure,[127] as follows: 20mmol (2.18g) of 2,6-diaminopyridine and 50mmol (5.05g) of TEA are dissolved in 100 mL of dry THF. The flask is connected to the flow of N$_2$ and cooled in an ice-water bath. 44mmol (3.98g) of acryloyl chloride are diluted with 10mL of solvent in a pressure equilibrated dropping funnel and the addition begins slowly and under vigorous stirring of the reaction mixture. After the addition is complete the ice-water bath is removed and the reaction mixture is stirred for an

additional 2 hours. Then, 50mL of distilled H_2O are added to it in order to quench the excess of acryloyl chloride and dissolve the TEA.HCl that is formed during the reaction, followed by 100mL of $CHCl_3$. The layers are separated and the aqueous phase is washed with additional 100mL of $CHCl_3$. The organic layers are combined, washed with saturated $NaHCO_3$ and water and finally concentrated under reduced pressure. The crude product is isolated in the form of a grey-yellow solid and is subsequently recrystallised from toluene to yield the pure monomer in yellow crystalline form (50%).

Compound characterisation:

^{1}H-NMR ($CDCl_3$): δ (ppm): 5.81 (d, 2H), 6.25 (q, 2H), 6.45 (d, 2H), 7.68 (s, br, 1H), 7.74 (t, 1H), 7.99 (d, 2H).

^{13}C-NMR (DMSO-d_6): δ (ppm): 99.4, 127.4, 131.3, 140.5, 150.3, 166.2.

6.1.4 Synthesis of 2,6-bis(propylamido)pyridine

Reaction:
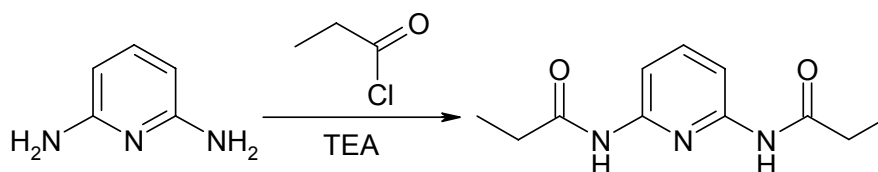
Synthetic procedure:

The compound was synthesised according to a published procedure,[154] in 40% yield.

Compound characterisation:

^{1}H-NMR (DMSO-d_6): δ (ppm): 1.00 (t, 6H), 2.23 (q, 4H), 7.67 (m, 3H), 9.92 (s, 2H).

^{13}C-NMR (DMSO-d_6): δ (ppm): 9.8, 29.7, 109.2, 140.2, 150.7, 173.2.

Exact mass: Calculated: 221.1164, Found (HRMS): 221.1188

M. P.: 149°C.

6.1.5 Synthesis of 2-propylamido-6-aminopyridine

Reaction:
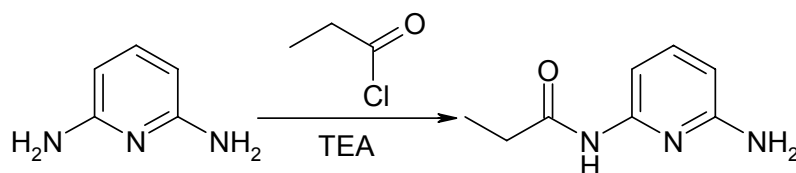
Synthetic procedure:

Monoacylation of 2,6-diaminopyridine with propionic acid chloride was achieved following a published method.[155] Column chromatography (acetone/n-hexane 4/6) yielded 2-propylamido-6-aminopyridine as a white solid in 50% yield.

Compound characterisation:

^{1}H-NMR (DMSO-d$_6$): δ (ppm): 0.96 (t, 3H), 2.25 (q, 2H), 5.65 (s, 2H), 6.09 (d, 1H), 7.17 (d, 1H), 7.25 (t, 1H), 9.72 (s, 1H).

^{13}C-NMR (DMSO-d$_6$): δ (ppm): 9.3, 29.0, 100.5, 102.9, 138.5, 150.2, 158.1, 172.1.

Exact mass: Calculated: 165.0902, Found (HRMS): 165.0875.

M. P.: 142-143 °C.

6.1.6 Synthesis of 2-acrylamido-6-(propylamido)pyridine

Reaction:
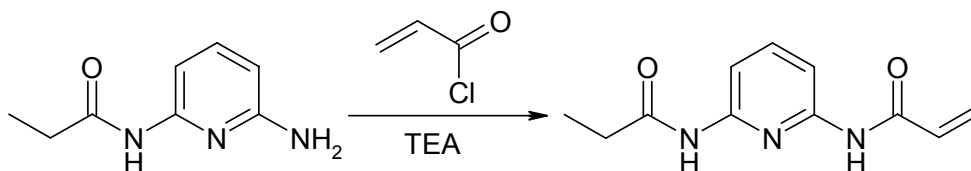
Synthetic procedure:

1mmol of the monoacylated compound synthesised as described in paragraph 6.1.5, was reacted with 1.1mmol acryloyl chloride in the presence of 1.1mmol of triethylamine in 50mL dry THF. The compound was obtained as a white solid in 40% yield.

Compound characterisation:

^{1}H-NMR (DMSO-d$_6$): δ (ppm): 1.01 (t, 3H), 2.34 (q, 2H,), 5.72 (d, 1H), 6.23 (d, 1H), 6.58 (q, 1H), 7.70 (m, 3H), 9.95 (s, 1H), 10.25 (s, 1H).

^{13}C-NMR (DMSO-d$_6$): δ (ppm): 9.2, 29.1, 108.9, 109.1, 127.4, 131.3, 139.7, 149.9, 150.2, 163.4, 172.6.

Exact mass: Calculated: 219.1008, Found (HRMS): 219.0984

M. P.: 158-159 °C.

6.1.7 Synthesis of 6-(piperidin-1-yl)pyrimidine-2,4-diamine

Reaction:
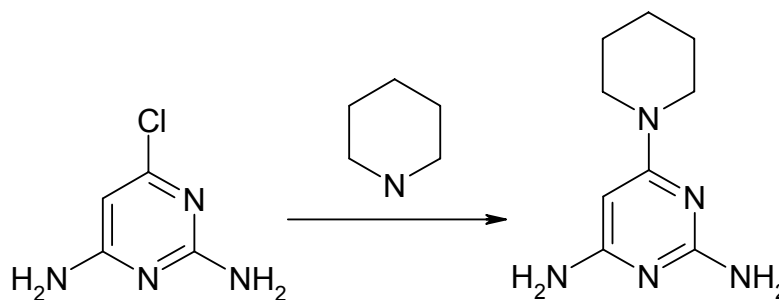
Synthetic procedure:

The compound was synthesised according to a published procedure by reflux of 2,4-diamino-6-chloropyrimidine in piperidine.[156]

Compound characterisation:

^{1}H-NMR (DMSO-d$_6$): δ (ppm): 1.49 (m, 4H), 1.60 (m, 2H), 3.53 (t, 4H), 4.98 (s, 1H), 5.38 (s, 2H), 5.58 (s, 2H)

^{13}C-NMR (DMSO-d$_6$): δ (ppm): 24.0, 25.0, 44.6, 85.4, 161.2, 163.1, 164.4.

6.1.8 Synthesis of 2,4-bis(acrylamido)-6-(piperidino)pyrimidine

Reaction:
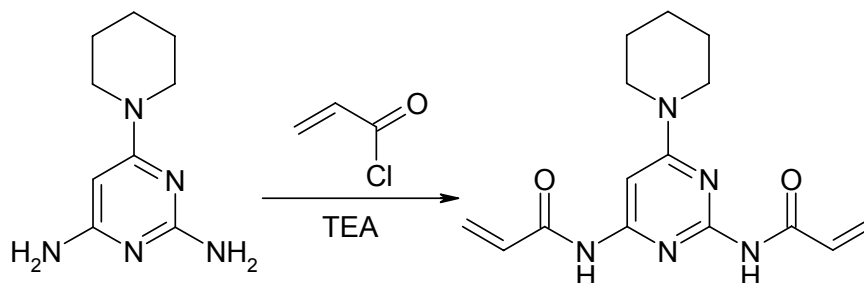
Synthetic procedure:

20mmol (3.86g) of 6-(piperidin-1-yl)pyrimidine-2,4-diamine (see previous paragraph) and 50mmol (5.05g) of TEA are dissolved in 100mL of dry THF. The flask is connected to the flow of N_2 and cooled in an ice-water bath. 44mmol (3.98g) of acryloyl chloride are diluted with 10mL of solvent in a pressure equilibrated dropping funnel and the addition begins slowly and under vigorous stirring of the reaction mixture. After the addition is complete the ice-water bath is removed and the reaction mixture is stirred for an additional 2 hours. Then, 50mL of distilled H_2O are added to it in order to quench the excess of acryloyl chloride and dissolve the TEA.HCl that is formed during the reaction, followed by 100mL of $CHCl_3$. The layers are separated and the aqueous phase is washed with additional 100mL of $CHCl_3$. The organic layers are combined, washed with saturated $NaHCO_3$ and water and finally concentrated under reduced pressure. The yellow solid that is obtained is recrystallised from ethanol. Typical yields range from 30-50%.

Compound characterisation:

^{1}H-NMR (DMSO-d$_6$): δ (ppm): 1.49 (m, 4H), 1.60 (m, 2H), 3.53 (t, 4H), 5.67 (q, 2H), 6.18 (q, 2H), 6.60 (q, 2H), 7.25 (s, 1H), 9.97 (s, 1H), 10.38 (s, 1H).

^{13}C-NMR (DMSO-d$_6$): δ (ppm): 24.0, 25.0, 44.6, 85.4, 127.2, 128.1, 131.3, 131.9, 156.4, 158.1, 163.1, 163.2, 164.4.

Exact mass: Calculated: 301.1539, Found (HRMS): 301.1501.

M. P.: 213°C.

6.1.9 Synthesis of 2,4-bis(propylamido)-6-(piperidino)pyrimidine
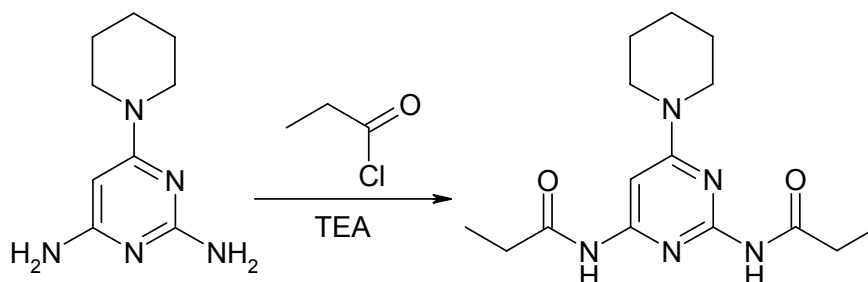
Reaction:

Synthetic procedure:

Synthesis is performed as described in paragraph 6.1.4, starting from 6-(piperidin-1-yl)pyrimidine-2,4-diamine (§ 6.1.7). The crude reaction product is recrystallised from ethanol.

Compound characterisation:

^{1}H-NMR (DMSO-d$_6$): δ (ppm): 0.97 (m, 6H), 1.47 (m, 4H), 1.56 (m, 2H), 2.32 (q, 2H), 2.46 (q, 2H), 3.49 (t, 4H), 7.11 (s, 1H), 9.54 (s, 1H), 10.03 (s, 1H).

^{13}C-NMR (DMSO-d$_6$): δ (ppm): 8.9, 9.0, 23.9, 24.8, 29.2, 29.3, 44.5, 84.2, 159.3, 158.0, 163.0, 172.6, 173.6.

Exact mass: Calculated: 305.1852, Found (HRMS): 305.1952.

M. P.: 223-224°C.

6.1.10 Synthesis of 2,4-diamino-6-ethoxypyrimidine

Reaction:
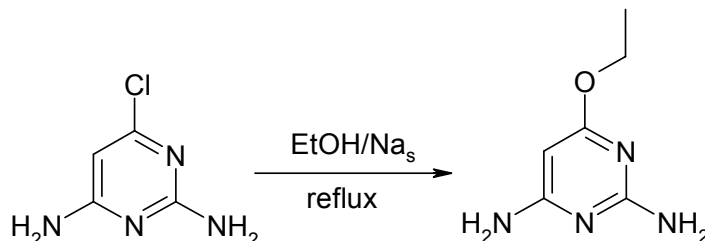
Synthetic procedure:

The synthetic protocol is adapted from a published procedure, whereby 2,4-diamino-6-chloropyrimidine was refluxed in a solution of sodium ethoxide prepared by dissolution of Na_s in methanol.[157]

Compound characterisation:

^{1}H-NMR (DMSO-d_6): δ (ppm): 1.20 (t, 3H), 3.35 (s, 1H), 4.10 (q, 2H), 5.00 (s, 1H), 5.85 (s, 2H), 5.98 (s, 2H).

^{13}C-NMR (DMSO-d_6): δ (ppm): 15.4, 60.9, 76.8, 163.6, 166.6, 170.7.

6.1.11 Synthesis of 2,4-bis(acrylamido)-6-ethoxypyrimidine

Reaction:
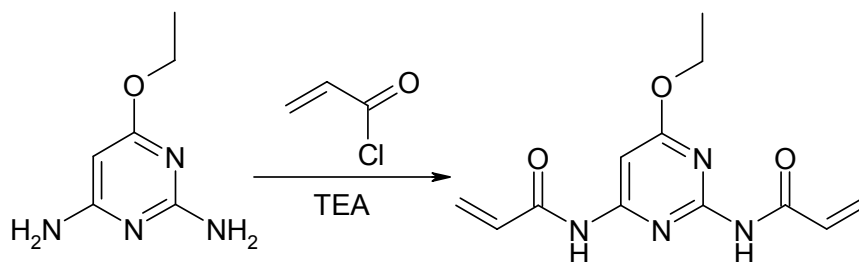
Synthetic procedure:

Synthesis is performed as described in § 6.1.8 starting from 2,4-diamino-6-ethoxypyrimidine. The yellow solid that is obtained is recrystallised from ethanol. Yield: ~65%.

Compound characterisation:

^{1}H-NMR (DMSO-d$_6$): δ (ppm): 1.27 (t, 3H), 4.29 (q, 2H), 5.73 (q, 2H), 6.22 (q, 2H), 6.61 (m, 2H), 7.20 (s, 1H), 10.41 (s, 1H), 10.73 (s, 1H).

^{13}C-NMR (DMSO-d$_6$): δ (ppm): 14.7, 62.7, 90.2, 129.3, 131.3, 156.8, 159.5, 165.0, 171.1.

Exact mass: Calculated: 262.1066, Found (HRMS): 262.1049.

M. P.: 217°C.

6.2 Synthesis of Templates

Most of the templates used for imprinting during this doctoral work were commercially available. However, since riboflavin is not soluble in any of the non-polar solvents used in Molecular Imprinting, model compounds and template analogues had to be synthesised in order to replace the original target. The synthetic procedures towards these compounds are discussed below.

6.2.1   Synthesis of 1-benzyluracil

Reaction:
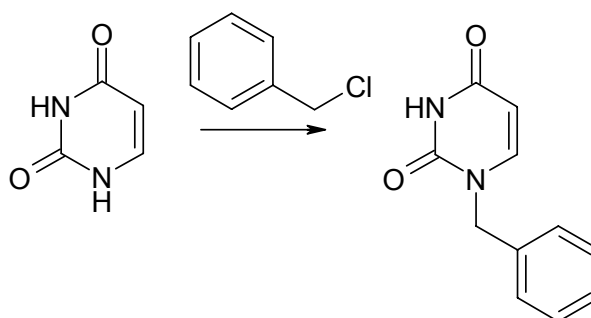
Synthetic procedure:

1-(benzyl)uracil was synthesised according to a previously published procedure and its characterisation data match the ones reported in literature.[125] 1,3-dibenzyluracil was isolated as a by-product of the same reaction.

Compound characterisation:

^{1}H-NMR (CDCl$_3$): δ (ppm): 7.34 (t, 1H), 7.73 (t, 1H), 8.30 (d, 1H), 8.70 (d, 1H), 11.35 (s, 1H).

6.2.2 Synthesis of 10-isobutylbenzo[g]pteridine-2,4(3H,10H)-dione (IBF)

6.2.2.a Synthesis of N-(2-nitrophenyl)trifluoroacetamide

Reaction:
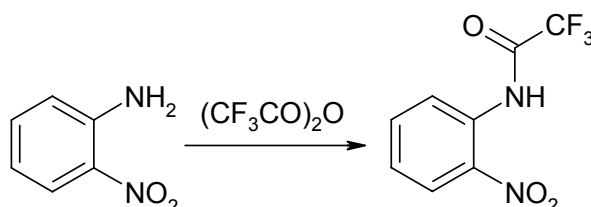
Synthetic procedure:

100mmol (13.8g) of 2-nitroaniline and 150mmol (21mL) of triethylamine are dissolved in 100mL of dry chloroform. The reaction mixture is cooled in an ice bath and stirred using a magnetic stirrer. Inert atmosphere is obtained above the reaction mixture by a gentle N_2 stream which is kept throughout the process. To the solution described above, 120mmol (17mL) of trifluoroacetic acid anhydride are added drop-wise, using a pressure equalised dropping funnel, over a period of 1 ½ hours. Once the addition is complete, the ice bath is removed and the reaction is allowed to proceed overnight.

The reaction mixture is then transferred in a separation funnel and washed with 100mL of H_2O. The two layers are allowed to separate and the organic layer is collected. The aqueous layer is washed with 2x50mL of chloroform. The organic phases are combined and dried over $MgSO_4$, filtered and concentrated under reduced pressure. The crude reaction product is finally recrystallised from n-hexane and N-(2-nitrophenyl)trifluoroacetamide is collected in the form of yellow needle-like crystals in ~70% yield.

Compound characterisation:
^{1}H-NMR (CDCl$_3$): δ (ppm): 7.34 (t, 1H), 7.73 (t, 1H), 8.30 (d, 1H), 8.70 (d, 1H), 11.35 (s, 1H).

6.2.2.b   Synthesis of N-isobutyl-N-(2-nitrophenyl)amine

Reaction:
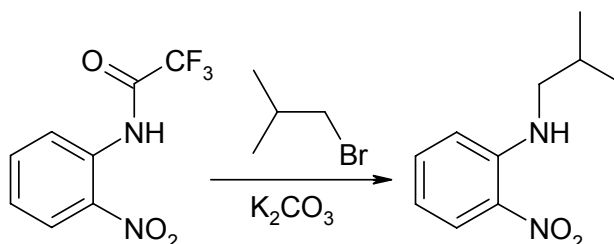
Synthetic procedure:

15mmol (3.5g) of N-(2-nitrophenyl)trifluoroacetamide and 57mmol (7.8g) of K_2CO_3 are suspended under vigorous stirring in 50mL of DMF. 42 mmol (4.6mL) of isobutyl bromide are added drop-wise to the above suspension, while the whole is heated up to 100°C in an oil bath. After the addition is completed, the reaction mixture is allowed to reflux for 90 minutes. After this time, and while the reaction mixture is still warm, the solvent is removed under reduced pressure. The residual solid is taken up in 100mL of H_2O. The resulting solution is extracted with 3x100mL of chloroform and the combined organic layers are dried over $MgSO_4$ and concentrated under reduced pressure and subsequently chromatographed (SiO_2, toluene). N-isobutyl-N-(2-nitrophenyl)amine is collected as a red liquid in 50% yield.

Compound characterisation:

^{1}H-NMR (CDCl$_3$): δ (ppm): 0.85 (d, 3H), 0.94 (d, 3H), 1.83 (m, 1H), 2.82 (q, 2H), 4.16 (q, 1H), 7.38 (d, 1H), 7.60 (t, 1H), 7.70 (t, 1H), 8.10 (d, 1H).

6.2.2.c   Synthesis of N-(2-aminophenyl)-N-isobutylamine

Reaction:
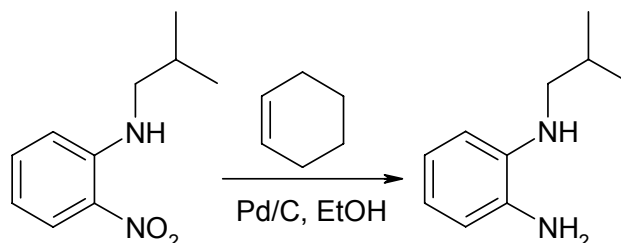
Synthetic procedure:

5mmol (1g) of N-isobutyl-N-(2-nitrophenyl)amine is mixed with 0.5g of Pd/C (10% Pd) powder and 3mL of cyclohexene in 15mL of ethanol.[158] The suspension is refluxed for 24h, at which point no starting material could be detected during TLC analysis of the reaction mixture. At this point, the reaction mixture was filtered through a celite pad to remove the Pd/C powder. The colourless filtrate (indicative of the disappearance of the nitro aniline) was then concentrated under reduced pressure and was used without further characterisation (due to the sensitivity of the product).

6.2.2.d   Synthesis of 10-isobutylbenzo[g]pteridine-2,4(3H,10H)-dione

Reaction:
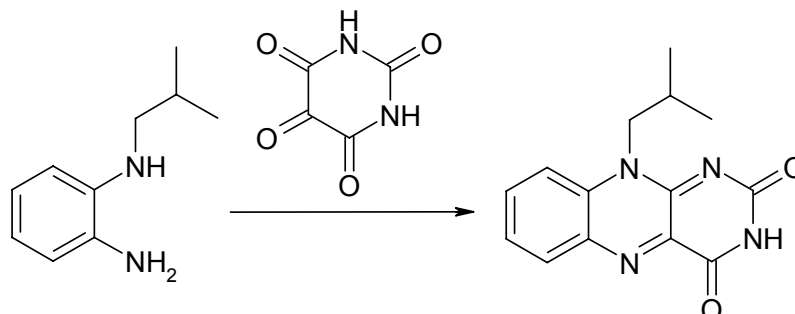
Synthetic procedure:

The product of the previous step (N-(2-aminophenyl)-N-isobutylamine) was mixed with 20mmol (3g) of alloxane monohydrate and 6g of boric acid in 20mL of acetic acid. The mixture was stirred at room temperature for 3 hours. Then, 250mL of H_2O were added to the reaction mixture and the whole was extracted with 3x100mL of chloroform. The combined organic phases were dried over $MgSO_4$, filtered and concentrated under reduced pressure and recrystallised from acetic acid to yield 1g of the product (70%).

Compound characterisation:

^{1}H-NMR (CDCl$_3$): δ (ppm): 1.02 (d, 3H), 1.04 (d, 3H), 2.42 (m, 1H), 4.62 (s, 2H), 7.62 (d, 1H), 7.64 (d, 1H), 7.88 (t, 1H), 8.30 (d, 1H), 8.6 (s, 1H).

^{13}C-NMR (DMSO-d$_6$): δ (ppm): 20.0, 27.1, 50.5, 117.1, 126.2, 132.1, 133.1, 135.0, 135.2, 139.0, 151.3, 155.9, 160.1.

6.2.3 Synthesis of 10-isopentyl-benzo[g]pteridine-2,4(3H,10H)-dione (IPF)

Reaction:
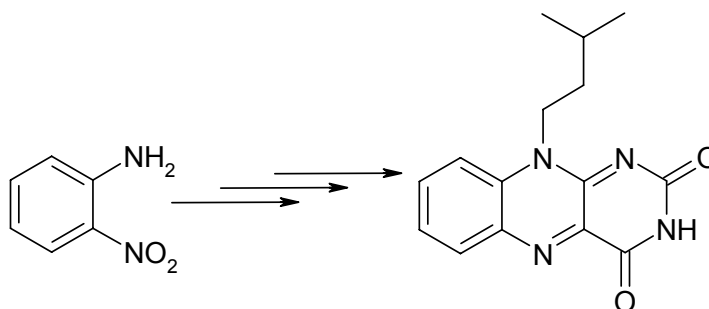
Synthetic procedure:

The synthetic protocol was identical to the one for isobutyl flavin, starting from 2-nitroaniline and using isopentyl instead of isobutyl bromide at the alkylation step.

Compound characterisation:

^{1}H-NMR (CDCl$_3$): δ (ppm): 1.02 (d, 3H), 1.04 (d, 3H), 1.48 (m, 2H), 2.42 (m, 1H), 4.62 (t, 2H), 7.62 (d, 1H), 7.64 (d, 1H), 7.88 (t, 1H), 8.30 (d, 1H), 8.6 (s, 1H).

^{13}C-NMR (DMSO-d$_6$): δ (ppm): 20.0, 27.1, 37.4, 50.5, 117.1, 126.2, 132.1, 133.1, 134.9, 135.1, 139.0, 151.3, 155.9, 160.1.

6.2.4 Synthesis of riboflavin tetraacetate (RfAc)

(acetic acid 2,3,4-triacetoxy-1-(7,8-dimethyl-2,4-dioxo-3,4-dihydro-2H-benzo[g]pteridin-10-ylmethyl)-butyl ester)

Reaction:
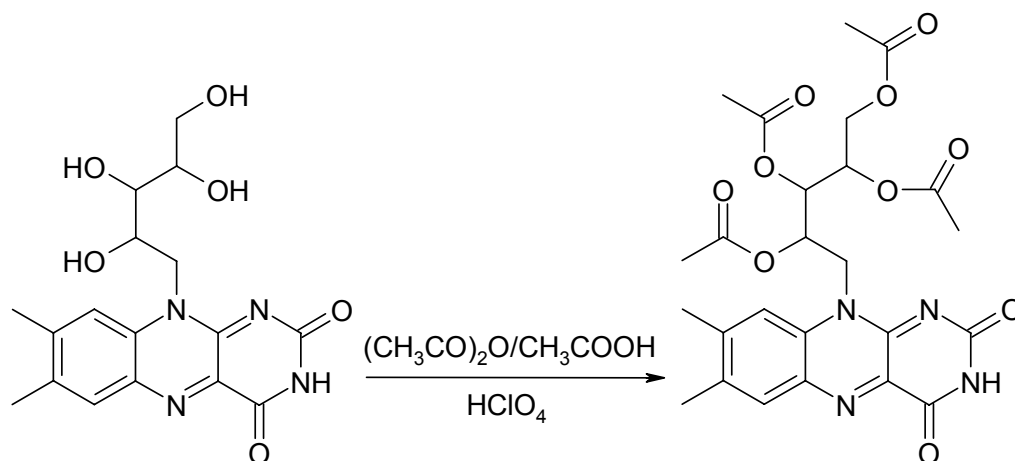
Synthetic procedure:

20mmol (7.52g) of riboflavin are suspended in 100mL of a 1:1 mixture of acetic acid and acetic acid anhydride, in an oil bath equipped with a stirring/heating apparatus. Approximately 1mL of $HClO_4$ (70% aqueous solution) is added to the suspension (until a clear solution is obtained). The solution is then heated up to 80°C for 2 hours. After this time, 100mL of distilled water are added to the reaction mixture and are stirred overnight (in order for the excess of the anhydride to be destroyed). The mixture is extracted 3x100mL with chloroform and the organic layers are combined, washed with $NaHCO_3$, then water, and dried over $MgSO_4$. The desiccant is then filtered-off and the filtrate is evaporated under reduced pressure. The resulting orange solid is re-dissolved in the minimum amount of methanol and then precipitated into water. The product is filtered and dried under vacuum to yield a bright orange solid (90%).[159]

Compound characterisation:

^{1}H-NMR (DMSO-d$_6$): δ (ppm): 1.55 (s, 3H), 1.96 (s, 3H), 2.15 (d, 6H), 2.36 (s, 3H), 2.47 (s, 3H), 4.19 (m, 1H), 4.32 (m, 1H), 4.82 (m, 1H), 5.27 (m, 1H), 5.45 (m, 2H), 7.70 (s, 1H), 7.85 (s, 1H), 11.36 (s, 1H)

^{13}C-NMR (DMSO-d$_6$): δ (ppm): 19.12, 20.47, 20.86, 20.94, 21.10, 21.15, 61.85, 61.09, 116.70, 131.43, 133.96, 136.22, 137.25, 146.62, 155.67, 160.07, 169.78, 170.02, 170.13, 170.48.

6.2.5 Synthesis of riboflavin tetrapropionate (RfPr)

(propionic acid 1-(7,8-dimethyl-2,4-dioxo-3,4-dihydro-2H-benzo[g]pteridin-10-ylmethyl)-2,3,4-tris-propionyloxy-butyl ester)

Reaction:
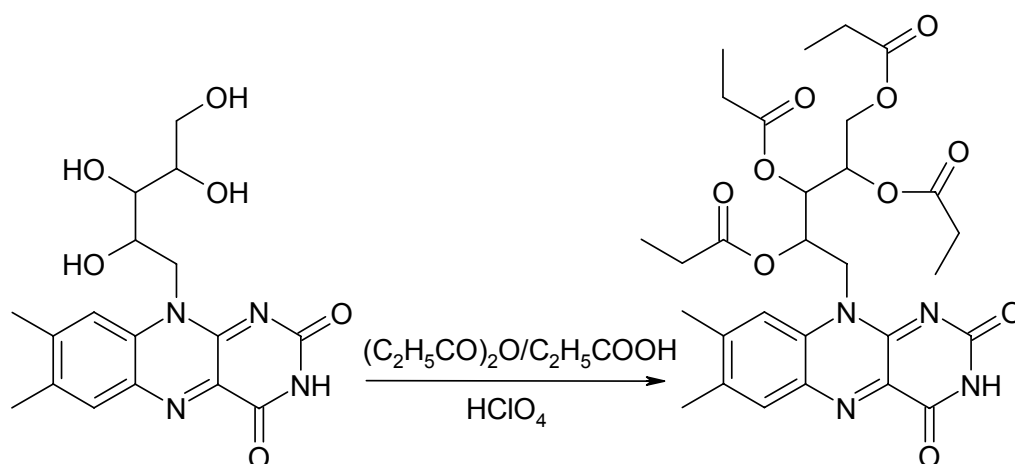
Synthetic procedure:

The synthetic protocol was identical to the one for riboflavin tetraacetate (see 6.2.4), using propionic acid and the corresponding acid anhydride instead of acetic acid and acetic acid anhydride.

Compound characterisation:

^{1}H-NMR (DMSO-d$_6$): δ (ppm): 1.55 (s, 3H), 1.96 (s, 3H), 2.15 (d, 6H), 2.36 (s, 3H), 2.46 (d, 6H), 4.19 (m, 1H), 4.32 (m, 1H), 4.82 (m, 1H), 5.27 (m, 1H), 5.45 (m, 2H), 7.70 (s, 1H), 7.85 (s, 1H), 11.36 (s, 1H)

6.2.6   Synthesis of N-3-methyl riboflavin tetraacetate

(acetic acid 2,3,4-triacetoxy-1-(3,7,8-trimethyl-2,4-dioxo-3,4-dihydro-2H-benzo[g]pteridin-10-ylmethyl)-butyl ester)

Reaction:
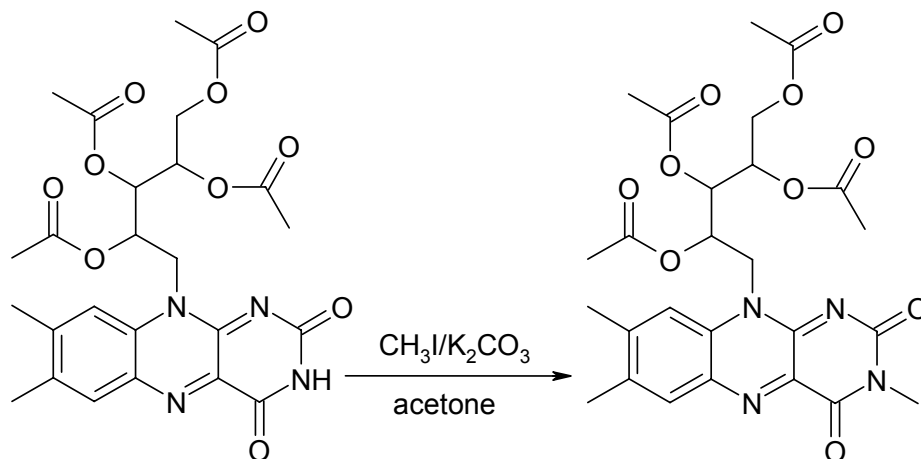
Synthetic procedure:

The synthesis was adapted from the literature.[160] 1g of riboflavin tetraacetate was mixed with 2.5g of K_2CO_3 in 50mL of dry acetone. 5mL of methyl iodide were diluted to a total volume of 30mL with acetone and added to the above mixture under vigorous stirring and the reaction was allowed to proceed overnight.

Compound characterisation:

^{1}H-NMR (DMSO-d_6): δ (ppm): 1.55 (s, 3H), 1.96 (s, 3H), 2.15 (d, 6H), 2.36 (s, 3H), 2.47 (s, 3H), 3.16 (s, 3H), 4.19 (m, 1H), 4.32 (m, 1H), 4.82 (m, 1H), 5.27 (m, 1H), 5.45 (m, 2H), 7.70 (s, 1H), 7.85 (s, 1H), 11.36 (s, 1H)

6.3 Spectroscopic Techniques

Several spectroscopic techniques have been utilised during this project with main focus on the study of the binding between the synthesised monomers and templates in solution and the subsequent rebinding of the templates on the corresponding synthesised imprinted polymers.

In this paragraph, all the used techniques will be discussed briefly and the mode in which they were applied will be explained.

6.3.1 NMR spectroscopy

NMR spectroscopy has proven to be a valuable tool for the supramolecular chemist in the recent years as it is broadly used for the assessment of the strength and type of interactions in general host-guest chemistry. Examples of applications are protein-ligand, antibody-antigen or soluble receptor-ligand binding. The main NMR based experiments that have been utilised in the attempt to screen and select the best monomer/receptor for the template/guest of interest are ^{1}H-NMR titrations, NMR based dilution studies and NOE spectroscopy. Here, only a brief description of the methods will be presented, as they are all well described in the literature.

6.3.1.a ^{1}H-NMR titration

The NMR titration experiment, as any titration experiment, is based on the monitoring of the "change" in a system, which is triggered by the stepwise modification of the system composition. In this case, the "change" is the complexation of the host/functional monomer with the guest/template, trigger is the stepwise addition of higher amount of one of the two components in a standard solution of the other (the order of addition varies depending on the examined system) and monitoring is achieved by following the *Complexation Induced Shift* (CIS) of a relevant proton in the bimolecular mixture.[161]

As an example, the experimental procedure for the calculation of the association constant between 2,6-bis(acrylamido)pyridine (M) and 1-benzyluracil (T), will be described in detail.

Two standard solutions are prepared in $CDCl_3$: A 2mM solution of T (5mL) and a 20mM solution of M. Different amounts of these solutions in 9 different NMR tubes are mixed and diluted to the same final volume (0.600mL) with $CDCl_3$. In the following table the composition of the prepared samples is presented. $(T)_{std.}$ and $(M)_{std.}$ correspond to the standard solutions of T and M respectively.

Sample	T:M ratio	$(T)_{std.}$ (mL)	$(M)_{std.}$ (mL)	$CDCl_3$ (mL)
1	1:0.0	0.300	0.000	0.300
2	1:0.5	0.300	0.015	0.285
3	1:1.0	0.300	0.030	0.270
4	1:2.0	0.300	0.060	0.240
5	1:3.0	0.300	0.090	0.210
6	1:4.0	0.300	0.120	0.180
7	1:5.0	0.300	0.150	0.150
8	1:7.5	0.300	0.225	0.075
9	1:10.0	0.300	0.300	0.000

Table 6.1

The samples are then scanned and the CISs of the uracil imide proton are plotted against the concentration of "free" M and the curve that is produced is fitted to the 1:1 binding isotherm, which is described by equation 6.1:

$$\Delta\delta = \frac{K_C \cdot [M]}{1 + K_C \cdot [M]} \cdot \Delta_{TM} \qquad\qquad 6.1$$

Where $\Delta\delta$ is the CIS, $[M]$ is the concentration of "free" M, Δ_{TM} is the CIS at 100% complexation between T and M, and K_c is the binding constant. The detailed mathematical derivation of equation 6.1 is displayed in § 8.4 of the Appendix.

The experimental details of all the NMR titrations as well as the result of each evaluation are presented in § 8.5. The methodology for each titration is as described above.

6.3.1.b ^{1}H-NMR dilution studies

While studying the binding characteristics of a binary system, comprising of a guest (template) and a host (functional monomer), it is possible that two or more equilibriums take place at the same time. The simplest case of multiple equilibriums is when one of the two components of the studied system forms dimers to a significant extent in the same experimental environment. In this case the ^{1}H-NMR proves again to be a valuable tool for the estimation of the degree of self-association of the studied compound.

As an example of the experimental setup of a dilution study, the case of 2,4-bis(acrylamido)-6-(piperidino)pyrimidine will be described in detail.

A 10mM solution of 2,4-bis(acrylamido)-6-(piperidino)pyrimidine in $CDCl_3$ is prepared and subsequently, by serial dilutions, 8 additional solutions are prepared, and are transferred to NMR tubes.

Sample	[M] (M)	(M) $_{std.}$ (mL)	$CDCl_3$ (mL)
1	0.0100	0.600	0.000
2	0.0083	0.500	0.100
3	0.0067	0.400	0.200
4	0.0050	0.300	0.300
5	0.0033	0.200	0.400
6	0.0017	0.100	0.500
7	0.0008	0.050	0.550
8	0.0002	0.010	0.590
9	0.0001	0.005	0.595

Table 6.2

The samples are scanned and the shifts of the imide NH protons are plotted against the concentration of free monomer [M], calculated by equation 6.2.

$$[M] = M_t \times (1 - \frac{\delta_{S_2}}{\delta_0}) \hspace{3cm} 6.2$$

Where M_t is the concentration of monomer in each solution, δ_{S_2} is the shift of the followed proton measured in each sample and δ_0 is the shift of the followed protons in the "free" state.

158

The plotted data are fitted to the 1:1 binding isotherm and the self-association constant is derived.[161]

6.3.1.c   Job plots

In order to determine the stoichiometry of a complex formed in solution, meaning the number of host and guest units taking part in a single complex molecule, or confirm an expected ration of host : guest, a Job plot needs to be prepared. The experimental design will be explained through the study of the complex formed between urea-based monomer **Ua5** and TBA-benzoate.

Two standard solutions are prepared: A 2mM solution of the monomer (M) and a 2mM solution of TBA-benzoate (T), in the appropriate deuterated solvent (in this case DMSO-d_6). The solutions are mixed in different ratios as shown on Table 6.3, where X_i corresponds to the respective mole fraction of the monomer (M) or template (T).

Sample	(T) $_{std.}$ (mL)	(M) $_{std.}$ (mL)	X_T	X_M
1	0.600	0.000	1.0	0.0
2	0.540	0.060	0.9	0.1
3	0.480	0.120	0.8	0.2
4	0.420	0.180	0.7	0.3
5	0.360	0.240	0.6	0.4
6	0.300	0.300	0.5	0.5
7	0.240	0.360	0.4	0.6
8	0.180	0.420	0.3	0.7
9	0.120	0.480	0.2	0.8
10	0.060	0.540	0.1	0.9
11	0.000	0.600	0.0	1.0

Table 6.3

The samples are scanned and the mole fraction of either the template or the monomer is plotted against the CIS of a selected proton multiplied by the corresponding mole fraction (CIS × X_i). A bell-shaped curve is obtained. If the maximum of the curve is situated at X_i=0.5, then a 1:1 complex is formed

between the participating species. If the maximum is at 0.33 or 0.66, then a 1:2 or a 2:1 complex is formed respectively, and so on (Figure 6.1).
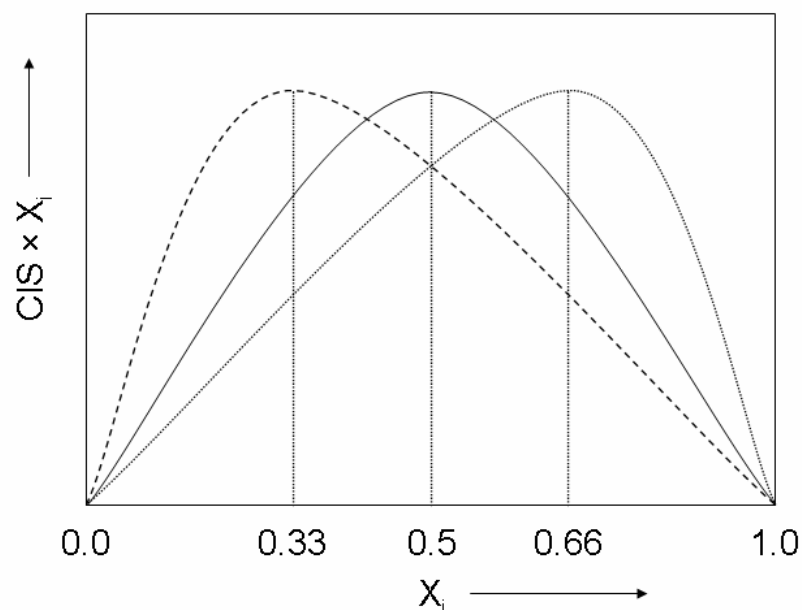
Figure 6.1:   *Schematic representation of a Job plot*

6.3.2   UV-Visible titrations

During this project, UV-Vis spectroscopy has been utilised in several different applications, ranging from the detection and identification of compounds after being injected on an imprinted column (diode-array detector) to the titration of the UV-Vis active urea monomer **Ua5** and the derivation of its association constant with TBA-benzoate in solution.

Here the methodology for this latter experiment will be presented. Thus, similarly to the ^{1}H-NMR titration, two standard solutions of the host (monomer; 1mM) and the guest (template; 5mM) are prepared in DMSO. Then, 1mL of the monomer standard solution is mixed with increasing volumes of the template solution and diluted to a total volume of 3mL thus, keeping the concentration of the monomer constant to 0.33mM, as shown in Table 6.4.

The UV-Vis spectrum of each sample is then recorded using a UV-Vis spectrometer and the recorded spectra are overlaid in order to visualise the changes observed upon binding of the studied monomer to the template. In the case of a 1:1 binding between the studied compounds, at least one

isosbestic point should be observed in the overlaid spectra, which has been the case for all the monomers studied here.

Sample	[T] (M)	(T) $_{std.}$ (mL)	DMSO (mL)
1	0.000000	0.000	2.000
2	0.000083	0.050	1.950
3	0.000167	0.100	1.900
4	0.000250	0.150	1.850
5	0.000333	0.200	1.800
6	0.000417	0.250	1.750
7	0.000500	0.300	1.700
8	0.000667	0.400	1.600
9	0.000833	0.500	1.500
10	0.001000	0.600	1.400
11	0.001333	0.800	1.200
12	0.001667	1.000	1.000
13	0.003333	2.000	0.000

Table 6.4: *Composition of samples used for the UV-Vis titration experiment (volume of monomer added = 1mL per sample)*

Finally, the wavelength at which the maximum change in the absorbance is observed is selected and the *ΔA* at this wavelength is plotted against the corresponding concentration of "free" template ([L]) in the sample to yield the binding isotherm, which is described by equation 6.3:

$$\frac{\Delta A}{b} = \frac{S_t \cdot K_a \cdot \Delta\varepsilon \cdot [L]}{1 + K_a \cdot [L]} \qquad 6.3$$

The concentration of "free" ligand can be calculated from equation 6.4.

$$[L] = L_t - S_t \cdot \frac{\Delta A}{\Delta A_{max}} \qquad 6.4$$

Where L_t is the total concentration of ligand in the sample, S_t is the total concentration of host in solution (=constant) and ΔA_{max} the maximum change in absorbance observed at 100% complexation (~ last point of the titration).

The corresponding linear double reciprocal plot (1/ΔA vs. 1/[L]) is the Benesi-Hildebrand plot ($y=ax+b$), where b/a is equal to the K_a.

It should be noted here that in order to draw safe conclusions by a UV-Vis titration, minimal to zero absorbance of the template (in the case of UV-Vis active monomer or *vice versa*) is a prerequisite.

6.3.3 Fluorescence titrations

The fluorescence titration is another powerful tool for the determination of the association constant of fluorescent molecules, especially in the case where the study needs to be performed in the low concentration range, e.g. when high association constants are expected or the solubility of the components taking part in the binding event is limited. The methodology for the performance of the fluorescence titration is identical to the one for the UV-Vis titration.

Thus, to a standard solution of the fluorescent component (in this study monomer **Ua7**) an increasing volume of the template (TBA-benzoate) is added and the samples are then diluted to the same final volume. 200μL of each sample are then transferred into the wells of a 96 well-plate and their fluorescence emission spectra are recorded at the optimum wavelength (in this case λ_{ex}= 330nm). The spectra collected are overlaid for a better visualisation of the quenching effect upon binding. The change in the fluorescence intensity at the maximum emission wavelength (ΔI) is then used to generate the binding isotherm (ΔI vs. [L]). A plot of I_0/I vs. [L], where I is the fluorescence intensity of the corresponding sample, I_0 the fluorescence intensity of the free monomer and [L] the concentration of the "free" template in the sample, is the Stern-Vollmer plot, from which the K_a is derived (equation 6.5).

$$\frac{I_0}{I} = 1+K_a \cdot [L] \qquad\qquad 6.5$$

Similarly to the UV-Vis titration, the fact that the non-fluorescent component of the titration does not absorb light at the excitation wavelength used in the experiment has to be established in order to draw solid conclusions.

6.3.4   Attenuated Total Reflectance Infrared Spectroscopy (ATR-IR)

Harrick and co-workers[162] with their pioneering efforts, developed a technique called Attenuated Total Reflectance (ATR) spectroscopy, in which IR spectra of the thin films/plates can be obtained from near surface region. In ATR-IR, the IR light passes through the optically denser crystal and reflects at the surface of the sample as shown in the figure. According to Maxwell's theory, "*when the propagation of light takes place through an optically thin, non absorbing medium, it forms a standing wave perpendicular to the total reflecting surface. If the sample absorbs a fraction of this radiation, the propagating wave interacts with the sample and (its energy or frequency) becomes attenuated, giving rise to a reflection spectrum, very similar to the absorption spectra*". In other words, in order to determine the chemical composition of a surface, (i.e., surface of a leaf, petal or an unknown object) it can be done using the ATR accessory in the IR spectrophotometer (Figure 6.2).
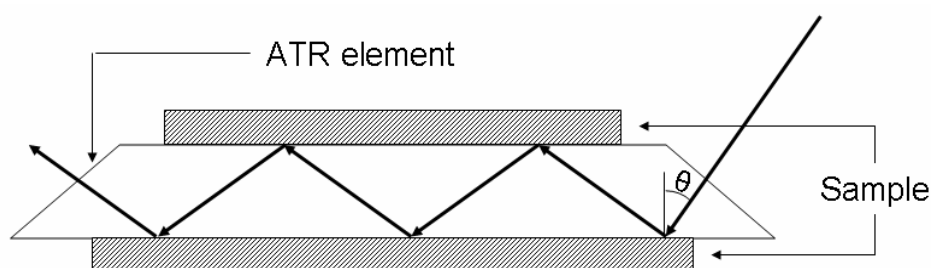
Figure 6.2:   Schematic representation of the ATR module

The infrared radiation is reflected from the surface of the sample, and the resultant spectrum reveals the functional groups present on the surface. Using this technique it is possible to determine the composition of a multilayered sample up to the sampling depth of ~ 5μm.

Here, a small volume of equimolar solutions of monomers **1** and **4** with **1-BU** is evaporated on the surface of the ATR crystal and the IR spectra were recorded. The spectra are subsequently compared with the ones recorded for the solutions of monomers alone and conclusions are drawn with regards to the changes in the conformation of the monomers upon binding to **1-BU**.

6.4 Preparation of Imprinted Polymers

The general protocol for the synthesis and work-up of Molecularly Imprinted Polymers, according to the non-covalent approach, is described in the following paragraphs. The detailed composition of each synthesised polymer is presented in the corresponding paragraph of the Results and Discussion chapter.

6.4.1 Monomer and initiator purification

Commercially available monomers contain small amounts of polymerisation inhibitors to prevent polymerisation during the storage period. In order to ensure reproducibility in the composition of the polymers, the most commonly used monomers were purified before use. Ethyleneglycol dimethacrylate was washed with 10% NaOH, followed by brine wash, dried over magnesium sulphate and subsequently distilled under reduced pressure. Methacrylic acid and 2-hydroxyethyl methacrylate were distilled under reduced pressure prior to use. The purified monomers were stored in the freezer.

Free radical polymerisation initiators, 2,2'-azobis(2-methylbutyronitrile) (AIBN) and 2,2'-azobis(2,4-dimethylvaleronitrile) (ABDV) were recrystallised from methanol before use.

All synthesised monomers and templates were recrystallised and dried under vacuum prior to use.

6.4.2 Polymer preparation

The amounts of solid chemicals calculated for each polymerisation recipe (except for the initiator) are first weighed in a 20mL scintillation vial and dissolved with the required amount of dry solvent. Then, the liquid components are added and finally the free radical initiator. The mixture is then transferred to the polymerisation ampoule, which is subsequently placed in an ice-bath. The pre-polymerisation solution is purged with N_2 for 5min, the ampoule is sealed using a micro burner and placed in a water-bath thermostatted at the proper initiation temperature, depending on the initiator used. The polymerisation reaction is allowed to proceed for 24 hours.

After this time, the polymerisation ampoules are smashed and the polymer monoliths are crushed down to smaller pieces, transferred into paper thimbles, and extracted using a Soxhlet apparatus for 24-48 hours with a good solvent for the template and monomers (usually methanol or mixtures thereof with acetic/formic acid).

Once the polymers are extracted, they are crushed using laboratory mortar and pestle, and sieved using sieves of the desired mesh-size, depending on the application for which the materials are intended. Crushing and sieving takes place in an alternating manner, rather than in a continuous one, to minimise the amount of fine (< 25μm) particles and maximise the yield in useful particle sizes (Figure 6.3).
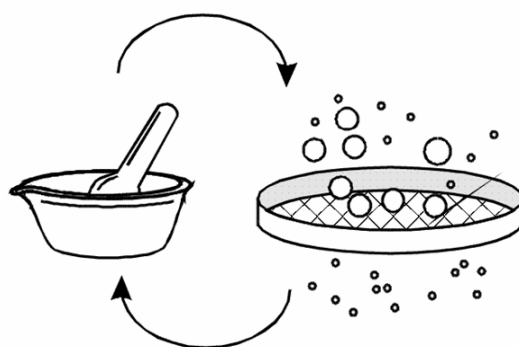
Figure 6.3:   *Crushing and sieving cycles*

Typically, particles with size 25-50μm (or 25-36μm) are used as packing material in HPLC columns and batch rebinding experiments, and 50-100μm for solid phase extraction.

Once the crushing-sieving cycles have been completed, the desired fraction of particles is sedimented from a mixture of methanol/water (80/20 v/v) in order to remove any fine particles present to avoid blocking of the frits in subsequent HPLC evaluation and to obtain clear supernatant solutions in batch-type experiments.

6.4.3   Post-treatment of the imprinted polymers

After the polymerisation time allowed for the synthesis of an imprinted polymer has been completed, a significant amount of unreacted double bonds is left in the polymer matrix. These pending acryl- or methacryl- groups can be

hydrolysed to yield free hydroxyl groups in the most common case of ester-based monomers (EDMA, PETRA). Thus, the hydrophilic character of the polymer should increase and, provided that the hydrolysis is performed under controlled conditions, the recognition properties of the polymer should remain unaffected.

The following experiment was designed in order to investigate the effect of hydrolysis to the performance of the synthesised imprinted polymers:

100mg of polymer particles (25-50μm) were suspended in 4mL of a 1M solution of either NaOH or TBA^{+-}OH in methanol and allowed to shake for different periods of time. The first hydrolysis was allowed to proceed for 1h, the second for 6 hours and the third for 24 hours. The reaction was stopped with addition of 5mL 1M HCl$_{aq}$ solution (end pH ~ 3). The polymers were well shaken in order to wash all formed salts from the polymer matrix and subsequently washed with 20mL of methanol. The methanolic-aqueous supernatants were extracted with 5mL of chloroform and each organic phase was dried with MgSO$_4$ and concentrated to dryness. The remaining solids were finally reconstituted each in 1mL of CDCl$_3$ and ^{1}H-NMR spectra are recorded. The performance of the hydrolysed polymers is evaluated by means of batch rebinding.

Additionally, an on-line hydrolysis experiment was performed. Thus, two 30mm HPLC columns were packed with **P(RfAc)'** or **P$_N$'** particles and 100μL aliquots of 0.1M base solution (KOH or TBA^{+-}OH) were injected and allowed to flow through the column in a small flow rate (0.1mL/min). The effect of the hydrolysis was monitored by subsequent wash of the column and injection of 0.5mM riboflavin samples.

6.5 Chromatographic Evaluation of Imprinted Polymers

One of the easiest and most straightforward ways to evaluate an imprinted material is to pack it into an HPLC column and subsequently estimate its binding properties by injecting different analytes on the column (dynamic mode).

6.5.1   Packing an imprinted material into an HPLC column

The system used for packing an imprinted polymer in an HPLC column is presented in Figure 6.4:
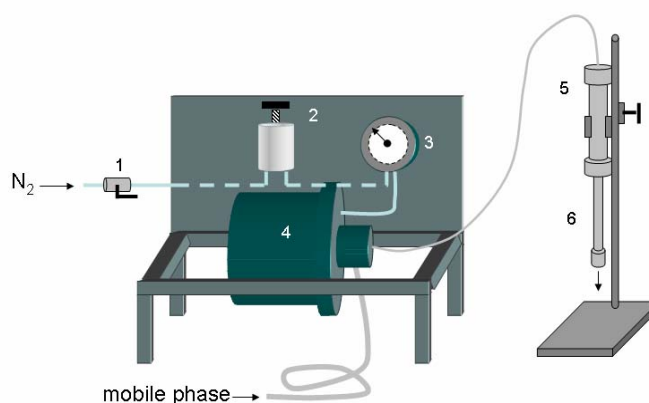
Figure 6.4:   Graphic representation of the packing equipment

The packing equipment used throughout this work consists of a gas (air) piston pump (4), which is used to pull the mobile phase from a solvent container and push it through the system, a pressure regulator (2) and a manometer (3), and a stainless steel vessel of 40mL volume (5), which is filled with the material suspension before the later is forced by the solvent flow to be packed into the HPLC column (6) attached at the bottom of this vessel.

Initially, the whole system is filled with the mobile phase (80% methanol – 20% water) (Figure 6.5a). The gas supply is then interrupted closing valve 1 and the bottom end of the HPLC column is closed with a screw cap.
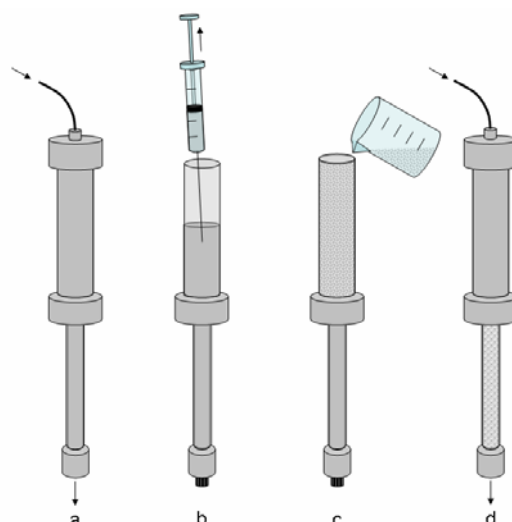
Figure 6.5:   *Graphic representation of the packing process*

Approximately 1g of the sized (usually 25-50μm) and sedimented material is suspended in 20mL of the above mentioned mobile phase. The top screw-head of the vessel is opened and 20mL of solvent are removed with a syringe (Figure 6.5b). The suspension is transferred in the vessel and the system is closed again (Figure 6.5c). The gas supply is opened again from valve 1 and the solvent starts flowing through the system, forcing the polymer particles to be packed in the HPLC column, whose bottom exit is blocked by a frit that prevents the particles from passing through (Figure 6.5d). After approximately 120mL (3 times the volume of vessel 5) have passed through the system, the gas flow is interrupted again, the packed column is removed from the bottom of the vessel and the top frit is screwed on it. The direction of packing is marked and the column is sealed on both ends with screw caps in order to avoid drying of the packed material.

6.5.2   Derivation of retention and imprinting factors

The columns containing the imprinted polymers are connected to an HPLC instrument and equilibrated with the mobile phase in which the evaluation is required. The change in the mobile phase from methanol-water to the evaluation mobile phase is performed step-wise and in reduced flow, to avoid sudden changes in the pressure of the system, as well as generation of gas bubbles from the mixing of different solvents, or the precipitation of salts on

the column in the case of buffered mobile phases. The columns need to be equilibrated for at least 30 minutes, after which time, in most cases, a stable baseline is obtained.

The analysis usually begins with an injection of a void marker (a non-retained compound, e.g. acetone), which is necessary for the calculation of the retention and imprinting factors, the two main measures of the imprinting effect that can be obtained by chromatographic analysis. The shape of the peak of the non-retained analyte is also an indication of the packing quality of the column. Symmetric, sharp peaks indicate homogeneous packing throughout the column and good equilibrated column, while asymmetric, fronting or tailing peaks, or peak splitting is an indication of inhomogeneous packing and/or need for further equilibration of the column.

Once the void volume of the column has been measured, the evaluation proceeds with the injection of the different analytes selected, namely the analyte used as the template during polymerisation and template analogues or other related analytes. As a general rule, at least 3 injections of each analyte should be performed and the average of the retention times should be used in the further data elaboration. These minimum 3 injections should not be performed subsequently, but in a rotating manner, completing a full series of injections of the different analytes and then re-initiating the sequence. Additionally, in case a range of different concentrations of a given analyte need to be tested, low concentration samples are injected first to avoid overloading the binding sites, thus obtaining inaccurate retention times for the subsequent injected analytes.

When all the analyses are completed, the columns are washed carefully with an appropriate solvent (usually acetonitrile or methanol), sealed and stored in dry and clean environment.

The retention data are collected and retention factors for the imprinted and non-imprinted polymers are calculated using equation 6.6:

$$k = \frac{t_R - t_0}{t_0} \qquad \text{6.6}$$

Where t_R is the retention time of each analyte and t_0 is the retention time of the void marker.

Imprinting factors are a measure of the imprinting effect and therefore should be quoted only for the imprinted molecule, as calculated using equation 6.7:

$$I.F. = \frac{k_{MIP}}{k_{NIP}} \qquad\qquad 6.7$$

However, imprinting factors are in most cases calculated for all the injected analytes and used as a further measure of the imprinting selectivity.

6.5.3 Frontal analysis

Frontal analysis is considered to be the ideal technique for a quantitative study of the interactions between solutes and a stationary phase[163] and there are several examples of its application for the determination of the binding of an analyte on an imprinted stationary phase.[164-166] In contrast to simple HPLC analysis where a small volume of sample is injected in the column, in frontal analysis a constant flow of analyte-containing mobile phase is allowed to pass through the column until breakthrough and subsequent equilibration of the column is achieved. There are two different modes of frontal analysis, each with its advantages and disadvantages. In the simple step frontal analysis, after recording the breakthrough time of one concentration of analyte, the column is washed before changing to the next concentration. The amount of analyte bound on the column in each step can be calculated either by the retention time of the step (Figure 6.6) or by integration of each step.
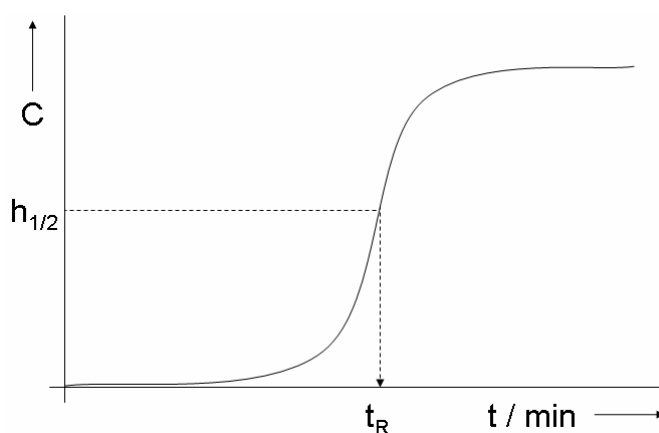
Figure 6.6:   Schematic representation of a frontal analysis chromatogram showing the calculation of the retention time of the breakthrough step

In staircase frontal analysis, after each breakthrough is recorded, the mobile phase is changed without washing the column, leading to a chromatogram with several steps, a staircase (Figure 6.7).
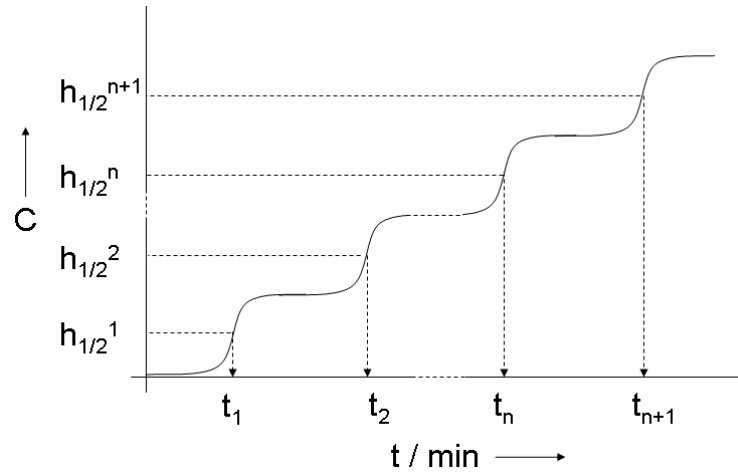
Figure 6.7: *Schematic representation of a staircase frontal analysis chromatogram showing the calculation of the retention times of each breakthrough step*

The amount of bound analyte is calculated using equation 6.8.

$$q^*_{n+1} - q^*_n = \frac{(C_{n+1} - C_n)}{F} \cdot \frac{(t_{R,n+1} - t_0)}{t_0}$$
6.8

Where $t_{R,n+1}$ is the retention time of the $(n+1)^{th}$ step, C_{n+1} and C_n the corresponding concentrations of each step, F the phase ratio and t_0 the void volume of the column corrected for the hold-up and extra-column volumes.

After all required points of the isotherm are recorded, the amount of bound analyte of each step is plotted against the corresponding concentration of the mobile phase and the resulting curve is fitted to the best binding model, by e.g. non-linear regression, and the binding constant and capacity of the column material are calculated.

6.5.4 Binding isotherm models

The most commonly used models that describe the binding of an analyte on an imprinted column are:

a) The Langmuir Isotherm:

$$q*(C) = \frac{a_1 \cdot C}{1 + b_1 \cdot C}$$ 6.9

Where a single type of binding sites is considered to be present in the polymer, which all have the same binding strength and whose number is given by the ratio a_1/b_1.

b) The bi-Langmuir Isotherm:

$$q*(C) = \frac{a_1 \cdot C}{1 + b_1 \cdot C} + \frac{a_2 \cdot C}{1 + b_2 \cdot C}$$ 6.10

Where two distinct types of binding sites are considered to be present in the polymer, each with a single binding constant, and their corresponding number given by the ratios a_1/b_1 and a_2/b_2.

c) The Freundlich Isotherm (FI):

$$q*(C) = a \cdot C^m$$ 6.11

Where a distribution of sites of different binding strength is present in the polymer. The Freundlich Isotherm does not have a saturation capacity.

There are two fitting parameters, *a* and *m*, that both yield a measure of physical binding parameters. The pre-exponential factor *a* is a measure of the capacity (N_T) and average affinity (K_0). However, the individual contributions of N_T and K_0 to the pre-exponential factor cannot be directly extracted without additional experiments or assumptions. Therefore, this Freundlich fitting parameter is of lesser value. The second fitting parameter *m* is also known as the heterogeneity index, the value of which varies from zero to one, with one being completely homogeneous and values approaching zero being increasingly heterogeneous. Recently, Shimizu and co-workers[167] have developed an analytically derived expression for the affinity distribution for a

Freundlich Isotherm which requires only the experimentally derived Freundlich fitting parameters, *a* and *m*:

$$N(K) = 2.303 \cdot a \cdot m \cdot (1 - m^2) \cdot K^{-m} \qquad \textit{6.12}$$

Expressions for two additional binding parameters can be derived from equation 6.12. These are the number of sites, N_{K1-K2}, and the weighted average affinity, K_{K1-K2} (equations 6.13 and 6.14). As the subscripts on N_{K1-K2} and K_{K1-K2} imply, these expressions yield values that represent only a subset of the entire distribution from K_1 to K_2. These limits are set by the concentration range over which the experimental binding isotherm was measured. The binding parameters N_{K1-K2} and K_{K1-K2} can be measured for any set for K_1 of K_2 values that are within the boundaries $K_{min}(=1/C_{max})$ and $K_{max}(=1/C_{min})$. Further in comparing binding parameters N_{K1-K2} and K_{K1-K2}, it is important to calculate them over the same range of binding sites (K_1 and K_2):

$$N_{K_1-K_2} = a \cdot (1 - m^2) \cdot (K_1^{-m} - K_2^{-m}) \qquad \textit{6.13}$$

$$\overline{K}_{K_1-K_2} = \frac{m}{m-1} \cdot \frac{K_1^{1-m} - K_2^{1-m}}{K_1^{-m} - K_2^{-m}} \qquad \textit{6.14}$$

The Freundlich model is most easily applied by re-plotting the experimental binding isotherm in Log*q* versus Log*C* format. In this form, systems that fit to the FI will fall on a straight line, having a slope of *m* and a y-intercept of Log*a*. The Freundlich model has been shown to be generally applicable to most non-covalently imprinted polymers[168].

6.6 Equilibrium Rebinding Experiments

Batch type experiments are a quick and reliable method to study the binding characteristics of an imprinted material and calculate valuable parameters, such as association constants, (enantio-) selectivity factors and binding capacity, at equilibrium. During this work the traditional batch rebinding has been used, as well as fluorescence-monitored rebinding, in the case of the uracil imprinted polymers, which encompassed fluorescent monomers.

6.6.1 Batch rebinding

An exact amount of imprinted and non-imprinted polymer (usually 10-50mg) is weighed accurately into HPLC vials, the number of which depends on the extent of the performed experiment, but should not be less than eight. A fixed volume (0.5-1mL) of analyte containing solutions of increasing concentrations is then pipetted into each of the vials, which are then shaken and allowed to equilibrate at room temperature for 24 hours. The supernatant solutions are removed carefully and their concentration in analyte is measured by HPLC analysis or by direct absorbance / fluorescence measurement using a UV-Vis and/or fluorescence reader or simple spectrophotometer. The measured concentration is then used to calculate the amount of bound analyte on the polymer (in μg/g of polymer). The latter is then plotted against the concentration of "free" analyte to yield the binding isotherm. Finally, by non-linear curve fitting or Scatchard analysis the affinity constant(s) of the polymer for the analyte as well as the number of binding sites corresponding to each binding site type, are calculated. This elaboration is only effective when the experimental data correspond to a finite number of binding sites, most commonly one- (Langmuir model) or two-type binding sites (bi-Langmuir model). In all other cases, more advanced mathematic elaboration of the data is required.

6.6.2 Fluorescence-monitored batch rebinding

Using the 96 well-plate reader, that was available in the working group, the possibility of monitoring the rebinding process of an analyte on the imprinted polymers, by recording the changes in the fluorescence properties of the materials, was exploited. In order to be able to perform such experiments, it is necessary to use a polymer that contains fluorescent units. It was discovered that both monomers **1** and **4**, used for the recognition of **1-BU**, are indeed fluorescent and in addition to this their fluorescent properties were also present in the polymer.

Hence, 10mg of each polymer are weighed and transferred into a row of wells of the quartz plate used for the fluorescence measurements. The wells are subsequently filled with 200μL of solutions of the template with increasing

concentrations. The instrument is setup to the "kinetic measurement" mode, thus each well is scanned repeatedly over a period of time in fixed intervals. Depending on the experiment, whole spectra or single wavelength emission data are obtained. The fluorescence response of the polymers at the optimum wavelength of emission is plotted against the time, resulting to a diagram depicting the kinetics of adsorption of each polymer.
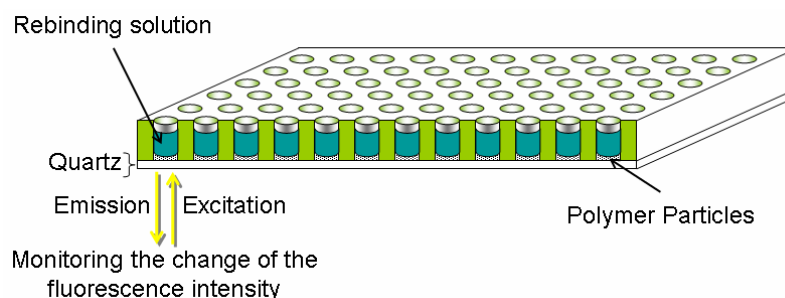
Figure 6.8:   *Schematic representation of the fluorescence monitored rebinding experiment*

Once equilibrium has been reached (the fluorescence reading remains constant), $100\mu L$ of the supernatant solution are carefully pipetted into a neighbouring well and their concentration is calculated by measurement of the UV absorbance. Subsequently, the amount of analyte bound on the polymer is calculated by simple subtraction and thus a fluorescence intensity *vs.* concentration of free analyte is constructed (Stern-Volmer plot), giving valuable information about fluorescence change upon binding.

6.7   Online MIP – Solid Phase Extraction

A method for the direct monitoring of the extraction of an analyte has been developed based on the continuous feed of a MIP or NIP column with a solution containing the analyte and recording the UV signal of the solution after passing through the column, utilising an HPLC instrument.

6.7.1 Extraction of riboflavin from aqueous solutions

A solution of riboflavin (500μg/L in a) H_2O, b) H_2O - 5% EtOH and c) H_2O - 5% EtOH, pH=4) is continuously pumped through a MIP or NIP packed HPLC column and the time until breakthrough is measured by following the UV signal at 480nm. Taking into account the flow-rate (1mL/min), the concentration of the solution and the weight of material packed in each column, this time is then converted to amount of riboflavin bound per unit of mass of polymer (μg/g or μmol/g of polymer)

6.7.2 Extraction of riboflavin from a water-soluble vitamins mixture

A solution of seven water-soluble vitamins in H_2O with the composition shown on Table 6.5 is passed through a MIP or NIP packed HPLC column. The UV signal of the mixture exiting the column is recorded at 480nm. Samples are collected every set time intervals and their composition is measured in a separate experiment using HPLC. The chromatographic method for the separation / quantification of the water soluble vitamins is displayed schematically in Figure 6.9.

By analysing all the collected fractions, it is possible to draw conclusions about the selectivity of the column for the template (riboflavin) over the other vitamins, as well as the competition effects taking place during the loading of the column.

Additional information are extracted by the subsequent wash of the column with mobile phases of different polarity, leading to complete wash of the non-specifically bound vitamins and final selective elution of pure riboflavin from the selective binding sites of the imprinted material.
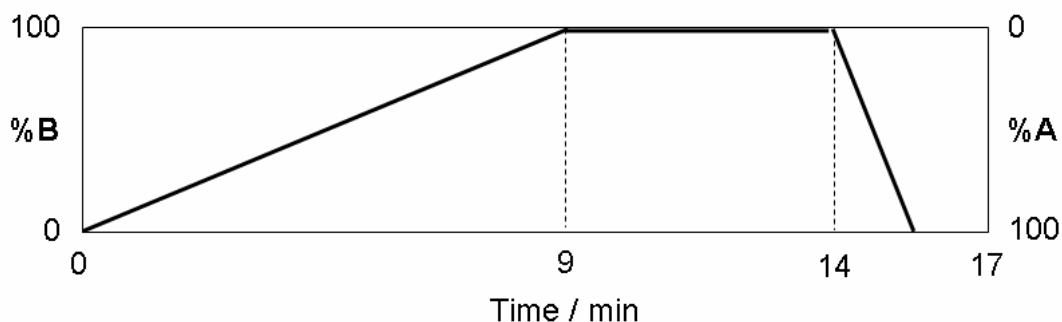
Figure 6.9: *Gradient programme developed for the separation of the water-soluble vitamins (A: H_2O-1%AcOH; B: 30% MeOH - 70% (H_2O-1%AcOH); Phenomenex Luna C-18 (150mm x 4.6mm - 5µm); flow-rate: 1mL/min)*

Under the conditions of the analysis, the vitamins eluted at the following times:

Vitamin	C (µmol.L^{-1})	Retention time[b] (min)
Thiamine	100	1.400
Ascorbic acid	100	2.800
Pyridoxine	100	3.021
Nicotinic acid	100	3.393
Nicotinamide	100	3.776
Folic acid	10[a]	11.820
Riboflavin	10[a]	13.875

Table 6.5: *Composition of the multivitamin solution and vitamin elution times ([a]the concentration was lower due to limited solubility; [b]conditions as described in Figure 6.9)*

6.8 Offline Extractions

Apart from the online extractions, offline experiments were performed in the cases of real samples, where the matrix was too complicated to allow the separation / detection of the analyte of interest by an HPLC system.

6.8.1 Extraction of riboflavin from beer samples

An increasing amount of polymer particles (2.5-50mg) are weighed accurately into HPLC vials, followed by the addition of a standard volume of beer (1.5mL) that has previously been degassed by sonication. The mixtures are shaken and allowed to equilibrate for 24 hours. After this time, a small volume of each supernatant solution is transferred into the wells of a quartz 96 well-plate and its content in riboflavin is measured directly by fluorescence at the specific for riboflavin wavelength (λ_{ex}: 450nm; λ_{em}: 525nm).

6.8.2 Extraction of riboflavin from milk samples

25mg of imprinted polymer are packed into a 10mL SPE cartridge. The column is conditioned with 1mL of methanol followed by 1mL of water. 1mL of milk is applied on the cartridge and the column is subsequently dried using a slight vacuum. Non-specifically bound compounds are washed with 1-2mL of water and riboflavin is finally eluted with 3×1mL acetonitrile/water: 7/3. The fractions collected are evaporated to dryness and reconstituted to 150μL of water containing 1% acetic acid. The sample is then analysed using HPLC with UV detector using the following gradient method.
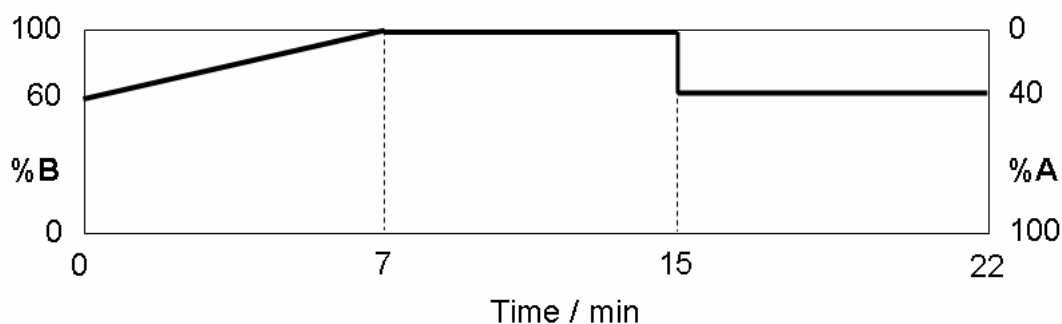
Figure 6.10:   Gradient programme developed for the quantification of riboflavin after extraction from milk (A: H_2O-1%AcOH; B: 50% MeOH - 50% (H_2O-1%AcOH); Thermo Hypersil Keystone BetaBasic (150mm x 4.6mm - 5μm); flow-rate: 0.25mL/min); temperature: 35°C; injection volume: 80 μL

Under the conditions of the experiment, riboflavin elutes at 4.5 minutes and lumiflavin at 12.5 minutes.

6.9 Isothermal Titration Calorimetry (ITC)

Isothermal Titration Calorimetry (ITC) is a thermodynamic technique for monitoring any chemical reaction initiated by the addition of a binding component, and has become the method of choice for characterising biomolecular interactions. When substances bind, heat is either generated or absorbed. Measurement of this heat allows accurate determination of binding constants (K_B), reaction stoichiometry (n), enthalpy (ΔH) and entropy (ΔS), thereby providing a complete thermodynamic profile of the molecular interaction in a single experiment.

In ITC, a syringe containing a "ligand" solution is titrated into a cell containing a solution of the "macromolecule" at constant temperature. When ligand is injected into the cell, the two materials interact, and heat is released or absorbed in direct proportion to the amount of binding. As the macromolecule in the cell becomes saturated with ligand, the heat signal diminishes until only background heat of dilution is observed.

Typically, an ITC system a Cell Feedback Network (CFB) to differentially measure heat produced or absorbed between the sample and reference cell. Twin coin-shaped cells are mounted in a cylindrical adiabatic environment, and connect to the outside through narrow access tubes (Figure 6.11).
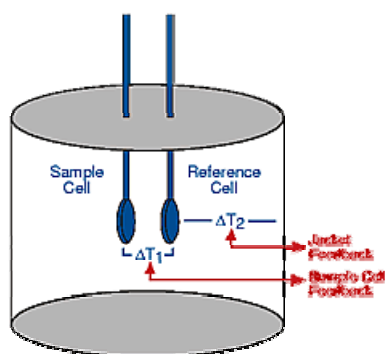
Figure 6.11:   Schematic drawing of the ITC cell

A thermoelectric device measures the temperature difference between the two cells and a second device measures the temperature difference between the cells and the jacket. As chemical reactions occur in the sample cell, heat is generated or absorbed. The temperature difference between the sample and

reference cells (ΔT_1) is kept at zero by the addition of heat to the sample or reference cell, as appropriate, using the CFB system. The integral of the power required to maintain $\Delta T_1 = 0$ over time is a measure of total heat resulting from the process being studied.

7 Bibliography

[1]   Plato, *Cratylus*.
[2]   C. R. Darwin, *The Origin of Species*, **1859**.
[3]   J. D. Watson, F. H. C. Crick, *Nature* **1953**, *171*, 737.
[4]   H. Dugas, in *A Chemical Approach to Enzyme Action*, 3rd ed.,
        Springer-Verlag, New York, **1996**.
[5]   J.-M. Lehn, *Supramolecular Chemistry: Concepts and Perspectives*,
        VCH, Verlagsgesellschaft mbH, Weinheim, **1995**.
[6]   A. D. Buckingham, A. C. Legon, S. M. Roberts, *Principles of Molecular
        Recognition*, Blackie Academic and Professional, London, UK, **1993**.
[7]   J. J. Rebek, *Chem. Soc. Rev.* **1996**, *25*, 255.
[8]   J. Kang, J. J. Rebek, *Nature* **1996**, *382*, 239.
[9]   J. J. Rebek, *Angew. Chem. Int. Ed. Engl.* **2005**, *44*, 2068.
[10]   J.-M. Lehn, *Rep. Prog. Phys.* **2004**, *67*, 249.
[11]   B. Sellergren (Ed.), *Molecularly imprinted polymers. Man made mimics
        of antibodies and their applications in analytical chemistry*, Techniques
        and instrumentation in analytical chemistry, *Vol. 23*, Elsevier Science
        B.V., Amsterdam, **2001**.
[12]   M. Yan, O. Ramström (Eds.), *Molecularly Imprinted Polymers: Science
        and Technology*, Marcer Dekker/CRC Press, New York, **2005**.
[13]   B. Sellergren, *Anal. Chem.* **1994**, *66*, 1578.
[14]   B. Sellergren, B. Ekberg, K. Mosbach, *J. Chromatogr.* **1985**, *347*, 1.
[15]   A. J. Hall, L. Achilli, P. Manesiotis, M. Quaglia, E. de Lorenzi, B.
        Sellergren, *J. Org. Chem.* **2003**, *68*, 9132.
[16]   P. Manesiotis, A. J. Hall, M. Emgenbroich, M. Quaglia, E. de Lorenzi,
        B. Sellergren, *Chem. Commun.* **2004**, 2278.
[17]   I. Idziak, A. Benrebouh, *Analyst* **2000**, *125*, 1415.
[18]   A. E. Rachkov, S.-H. Cheong, A. V. El'skaya, K. Yano, I. Karube,
        Polym. Adv. Technol. **1998**, *9*, 511.
[19]   L. Ye, P. A. G. Cormack, K. Mosbach, *Anal. Commun.* **1999**, *36*, 35.
[20]   R. Say, E. Birlik, A. Ersoz, F. Yilmaz, T. Gedikbey, A. Denizli, *Anal.
        Chim. Acta* **2003**, *480*, 251.
[21]   A. Cui, A. Singh, D. L. Kaplan, *Biomacromolecules* **2002**, *3*, 1353.
[22]   A. Ersoz, R. Say, A. Denizli, *Anal. Chim. Acta* **2004**, *502*, 91.
[23]   J. Matsui, I. A. Nicholls, T. Takeuchi, K. Mosbach, I. Karube, *Anal.
        Chim. Acta* **1996**, *335*, 71.
[24]   A. Rachkov, N. Minoura, *Biochim. Biophys. Acta* **2001**, *1544*, 255.
[25]   G. Theodoridis, G. Konsta, C. Bagia, *J. Chromatogr. B* **2004**, *804*, 43.
[26]   M. M. Titirici, B. Sellergren, *Anal. Bioanal. Chem.* **2004**, *378*, 1913.
[27]   O. Hayden, R. Bindeus, C. Haderspock, K.-J. Mann, B. Wirl, F. L.
        Dickert, *Sensors and Actuators, B: Chemical* **2003**, *91*, 316.
[28]   D. Silvestri, C. Cristallini, G. Ciardelli, P. Giusti, N. Barbani, *Journal of
        Biomaterials Science, Polymer Edition* **2004**, *15*, 255.
[29]   A. Rachkov, M. Hu, E. Bulgarevich, T. Matsumoto, N. Minoura, *Anal.
        Chim. Acta* **2004**, *504*, 191.
[30]   M. M. Titirici, Ph.D. thesis, University of Dortmund **2005**.
[31]   L. Pauling, *J. Am. Chem. Soc.* **1940**, *62*, 2643.

[32]   J. Y. Ju, C. S. Shin, M. J. Whitcombe, E. N. Vulfson, *Biotech. Bioeng.* **1999**, *64*, 232.

[33]   G. Wulff, R. Schoenfeld, *Adv. Mater.* **1998**, *10*, 957.

[34]   K. Yano, K. Tanabe, T. Takeuchi, J. Matsui, K. Ikebukuro, I. Karube, *Anal. Chim. Acta* **1998**, *363*, 111.

[35]   A. J. Hall, P. Manesiotis, M. Emgenbroich, M. Quaglia, E. de Lorenzi, B. Sellergren, *J. Org. Chem.* **2005**, *70*, 1732.

[36]   P. Manesiotis, A. J. Hall, J. Courtois, K. Irgum, B. Sellergren, *Angew. Chem. Int. Ed.* **2005**, *44*, 3902.

[37]   P. Manesiotis, A. J. Hall, B. Sellergren, *J. Org. Chem.* **2005**, *70*, 2729.

[38]   G. Wulff, A. Sarhan, *Angew. Chem. Int. Ed.* **1972**, *11*, 341.

[39]   R. Arshady, K. Mosbach, *Macromol. Chem.* **1981**, *182*, 687.

[40]   K. J. Shea, D. Y. Sasaki, *J. Am. Chem. Soc.* **1989**, *111*, 3442.

[41]   K. J. Shea, E. A. Thompson, *J. Org. Chem.* **1978**, *43*, 4253.

[42]   A. Beckett, P. Andersson, *J. Pharm. Pharmacol.* **1959**, *11*, 258T.

[43]   F. H. Dickey, *Proc. Natl. Acad. Sci.* **1949**, *35*, 227.

[44]   K. Mosbach, in *Affinity Chromatography and Biological Recognition. Part IV: Affinity Methods - Design and Development* (Eds.: I. M. Chaiken, M. Wilchek, I. Parikh), Academic Press, Orlando, FL, **1983**, pp. 209.

[45]   P. A. G. Cormack, A. Z. Elorza, *J. Chromatogr. B* **2004**, *804*, 173.

[46]   L. Andresson, B. Sellergren, K. Mosbach, *Tetrahedron Lett.* **1984**, *25*, 5211.

[47]   M. J. Whitcombe, M. E. Rodriguez, P. Villar, E. N. Vulfson, *J. Am. Chem. Soc.* **1995**, *117*, 7105.

[48]   M. M. Titirici, A. J. Hall, B. Sellergren, *Chem. Mater.* **2003**, *15*, 822.

[49]   A. G. Mayes, in *Molecularly Imprinted Polymers: Man made mimics of antibodies and their applications in analytical chemistry, Vol. 23* (Ed.: B. Sellergren), Elsevier Science B. V., Amsterdam, **2001**, pp. 305.

[50]   A. Strikovsky, J. Hradil, G. Wulff, *React. Funct. Polym.* **2003**, *54*, 49.

[51]   H. Kempe, M. Kempe, *Macromol. Rap. Commun.* **2004**, *25*, 315.

[52]   M. Yoshida, K. Uezu, M. Goto, S. Furusaki, *J. Appl. Polym. Sci.* **1999**, *73*, 1223.

[53]   N. Perez, M. J. Whitcombe, E. N. Vulfson, *J. Appl. Polym. Sci.* **2000**, *77*, 1851.

[54]   B. Sellergren, *J. Chromatogr. A* **1994**, *673*, 133.

[55]   G. E. M. Tovar, I. Kraeuter, C. Gruber, *Top. Cur. Chem.* **2003**, *227*, 125.

[56]   J. Wang, P. A. G. Cormack, D. C. Sherrington, E. Khoshdel, *Angew. Chem. Int. Ed. Engl.* **2003**, *42*, 5336.

[57]   C. Sulitzky, B. Rückert, A. J. Hall, F. Lanza, K. Unger, B. Sellergren, *Macromolecules* **2002**, *35*, 79.

[58]   N. Perez, M. J. Whitcombe, E. N. Vulfson, *Macromolecules* **2001**, *34*, 830.

[59]   A. G. Mayes, K. Mosbach, *Anal. Chem.* **1996**, *68*, 3769.

[60]   M. Ulbricht, *J. Chromatogr. B* **2004**, *804*, 113.

[61]   K. Das, J. Penelle, V. M. Rotello, *Langmuir* **2003**, *19*, 3921.

[62]   M. Ramamoorthy, M. Ulbricht, *J. Membrane Sci.* **2003**, *217*, 207.

[63]   S. A. Piletsky, H. Matuschewski, U. Schedler, A. Wilpert, E. V. Piletska, T. A. Thiele, M. Ulbricht, *Macromolecules* **2000**, *33*, 3092.

[64]   R. Suedee, C. Songkram, A. Petmoreekul, S. Sangkunakup, S. Sankasa, N. Kongyarit, *J. Pharm. Biomed. Anal.* **1999**, *19*, 519.

[65]   J. Nilsson, P. Spegel, S. Nilsson, *J. Chromatogr. B* **2004**, *804*, 3.

[66]   J. M. Lin, T. Nakagama, K. Uchiyama, T. Hobo, *Chromatographia* **1996**, *43*, 585.

[67]   K. Nilsson, J. Lindell, O. Norrlöw, B. Sellergren, *J. Chromatogr. A* **1994**, *680*, 57.

[68]   O. Brüggemann, R. Freitag, M. J. Whitcombe, E. N. Vulfson, *J. Chromatogr. A* **1997**, *781*, 43.

[69]   Z. J. Tan, V. T. Remcho, *Electrophoresis* **1998**, *19*, 2055.

[70]   M. Quaglia, E. De Lorenzi, C. Sulitzky, G. Massolini, B. Sellergren, *Analyst* **2001**, *126*, 1495.

[71]   M. Quaglia, E. De Lorenzi, C. Sulitzky, G. Caccialanza, B. Sellergren, *Electrophoresis* **2003**, *24*, 952.

[72]   R. J. Ansell, K. Mosbach, *J. Chromatogr. A* **1997**, *787*, 55.

[73]   X. Huang, H. Zou, X. Chen, Q. Luo, L. Kong, *J. Chromatogr. A* **2003**, *984*, 273.

[74]   B. Sellergren, A. J. Hall, in *Molecularly imprinted polymers. Man-made mimics of antibodies and their applications in Anal. Chem., Vol. 23* (Ed.: B. Sellergren), Elesevier Science B.V., Amsterdam, **2001**, pp. 21.

[75]   B. Sellergren, *J. Chromatogr. A* **2001**, *906*, 227.

[76]   J.-M. Lin, T. Nakagama, K. Uchiyama, T. Hobo, *J. Pharm. Biomed. Anal.* **1997**, *15*, 1351.

[77]   M. Kempe, K. Mosbach, *J. Chromatogr. A* **1995**, *691*, 317.

[78]   O. Ramström, I. A. Nicholls, K. Mosbach, *Tetrahedron: Asymmetry* **1994**, *5*, 649.

[79]   B. Sellergren, *Chirality* **1989**, *1*, 63.

[80]   B. Sellergren, K. J. Shea, *J. Chromatogr.* **1993**, *635*, 31.

[81]   L. Ye, O. Ramstroem, K. Mosbach, *Anal. Chem.* **1998**, *70*, 2789.

[82]   L. Schweitz, L. I. Andersson, S. Nilsson, *J. Chromatogr. A* **1997**, *792*, 401.

[83]   M. Kempe, K. Mosbach, *J. Chromatogr. A* **1994**, *664*, 276.

[84]   L. Fischer, R. Mueller, B. Ekberg, K. Mosbach, *J. Am. Chem. Soc.* **1991**, *113*, 9358.

[85]   F. Lanza, B. Sellergren, *Adv. Chromatogr.* **2001**, *41*, 137.

[86]   G. Theodoridis, P. Manesiotis, *J. Chromatogr. A* **2002**, *948*, 163.

[87]   G. Theodoridis, A. Kantifes, P. Manesiotis, N. Raikos, H. Tsoukali-Papadopoulou, *J. Chromatogr. A* **2003**, *987*, 103.

[88]   N. Lavignac, C. J. Allender, K. R. Brain, *Anal. Chim. Acta* **2004**, *510*, 139.

[89]   G. Vlatakis, L. I. Andersson, R. Mueller, K. Mosbach, *Nature* **1993**, *361*, 645.

[90]   M. T. Muldoon, L. H. Stanker, *J. Agric. Food Chem.* **1995**, *43*, 1424.

[91]   M. Siemann, L. I. Andersson, K. Mosbach, *J. Agric. Food Chem.* **1996**, *44*, 141.

[92]   C. J. Allender, K. R. Brain, C. M. Heard, *Prog. Med. Chem* **1999**, *36*, 235.

[93]   O. Ramström, L. Ye, K. Mosbach, *Chem. Biol.* **1996**, *3*, 471.

[94]   G. Wulff, A. Biffis, in *Molecularly Imprinted Polymers: Man made mimics of antibodies and their applications in analytical chemistry, Vol.*

23 (Ed.: B. Sellergren), Elsevier Science B. V., Amsterdam, **2001**, pp. 71.

[95] J.-q. Liu, G. Wulff, *Angew. Chem. Int. Ed. Engl.* **2004**, *43*, 1287.

[96] J.-q. Liu, G. Wulff, *J. Am. Chem. Soc.* **2004**, *126*, 7452.

[97] L. Ye, K. Haupt, *Anal. Bioanal. Chem.* **2004**, *378*, 1887.

[98] F. L. Dickert, O. Hayden, *Anal. Chem.* **2002**, *74*, 1302.

[99] F. L. Dickert, O. Hayden, P. Lieberzeit, C. Haderspoeck, R. Bindeus, C. Palfinger, B. Wirl, *Synthetic Metals* **2003**, *138*, 65.

[100] D. Kriz, O. Ramstroem, A. Svensson, K. Mosbach, *Anal. Chem.* **1995**, *67*, 2142.

[101] J. Matsui, M. Higashi, T. Takeuchi, *J. Am. Chem. Soc.* **2000**, *122*, 5218.

[102] L. Ye, Y. Yu, K. Mosbach, *Analyst* **2001**, *126*, 760.

[103] P. T. Vallano, V. T. Remcho, *J. Chromatogr. A* **2000**, *888*, 23.

[104] M. A. E. Bouman, C. J. Allender, K. R. Brain, C. M. Heard, *Methodol. Surv. Bioanal. Drugs* **1998**, *25*, 37.

[105] D. A. Spivak, K. J. Shea, *Macromolecules* **1998**, *31*, 2160.

[106] D. Spivak, M. A. Gilmore, K. J. Shea, *J. Am. Chem. Soc.* **1997**, *119*, 4388.

[107] A. Kugimiya, T. Mukawa, T. Takeuchi, *Analyst* **2001**, *126*, 772.

[108] H. Y. Wang, S. L. Xia, H. Sun, Y. K. Liu, S. K. Cao, T. Kobayashi, *J. Chromotogr. B* **2004**, *804*, 127.

[109] I. Caelen, A. Kalman, L. Wahlström, *Anal. Chem.* **2004**, *76*, 137.

[110] P. F. Heelis, in *Chemistry and Biochemistry of Flavoenzymes* (Ed.: F. Müller), CRC Press, Boca Raton, FL, **1991**.

[111] M. G. Duivis, R. Hilhorst, C. Laane, D. J. Evans, D. J. M. Schmedding, *J. Agric. Food Chem.* **2002**, *50*, 1548.

[112] C. Laane, G. de Roo, E. van den Ban, M.-W. Sjauw-en-Wa, M. G. Duyvis, W. A. Hagen, W. J. H. van Berkel, R. Hilhorst, D. J. M. Schmedding, D. J. Evans, *J. Inst. Brew.* **1999**, *105*, 392.

[113] H. L. Monaco, *EMBO J.* **1997**, *16*, 1475.

[114] J. Wang, D.-B. Luo, P. A. M. Farias, J. S. Mahmoud, *Anal. Chem.* **1985**, *57*, 158.

[115] H. Sawamoto, *J. Electroanal. Chem.* **1985**, *186*, 257.

[116] M. Nishikimi, Y. Kyogoku, *J. Biochem.* **1973**, *73*, 1233.

[117] V. M. Kodentsova, O. A. Vrzhesinskaya, V. B. Spirichev, *Ann. Nutr. Metab.* **1995**, *39*, 355.

[118] A. Kozik, *Analyst* **1996**, *121*, 333.

[119] C. Zhang, H. Qi, *Anal. Sci.* **2002**, *18*, 819.

[120] H. Ushijima, H. Okamura, Y. Nishina, K. J. Shiga, *Biochem.* **1989**, *105*, 467.

[121] J. Becvar, G. J. Palmer, *Biol. Chem.* **1982**, *257*, 5607.

[122] R. L. Simon, D. A. Spivak, *J. Chromatogr. B* **2004**, *804*, 203.

[123] B. Dirion, Z. Cobb, E. Schillinger, L. I. Andersson, B. Sellergren, *J. Am. Chem. Soc.* **2003**, *125*, 15101.

[124] A. G. Strikovsky, D. Kasper, M. Gruen, B. S. Green, J. Hradil, G. Wulff, *J. Am. Chem. Soc.* **2000**, *122*, 6295.

[125] N. G. Kundu, S. Sikdar, R. P. Hertzberg, S. A. Schmitz, S.G. Khatri, *J. Chem. Soc. Perkin I* **1985**, 1295.

[126] A. J. Hall, P. Manesiotis, J. T. Mossing, B. Sellergren, *Mat. Res. Soc. Symp. Proc.* **2002**, *723*, M1.3.1.

[127] E. Oikawa, K. Motomi, T. Aoki, *J. Polym. Sci.: Part A: Polym. Chem.* **1993**, *31*, 457.

[128] J. A. Montgomery, K. Hewson, *J. Am. Chem. Soc.* **1960**, *82*, 463.

[129] K. Hoogsteen, *Acta Crystalogr.* **1963**, *16*, 907.

[130] M. Kotera, J.-M. Lehn, J.-P. Vigneron, *Tetrahedron* **1995**, *51*, 1953.

[131] F. H. Beijer, H. Kooijman, A. L. Speck, R. P. Sijbesma, E. W. Meijer, *Angew. Chem. Int. Ed.* **1998**, *37*, 75.

[132] N. B. Colthup, L. H. Daly, S. E. Wiberly, *Introduction to IR and Raman Spectroscopy, 3rd ed.*, Academic Press, New York, **1990**.

[133] K. J. Shea, D. Y. Sasaki, G. J. Stoddard, *Macromolecules* **1989**, *22*, 1722.

[134] P. Turkewitsch, B. Wandelt, G. D. Darling, W. S. Powell, *Anal. Chem.* **1998**, *70*, 2025.

[135] *The Merck Index*.

[136] R. Kuhn, F. Weygand, *Chem. Ber.* **1935**, *68*, 1282.

[137] R. Epple, E.-U. Wallenborn, T. Carell, *J. Am. Chem. Soc.* **1997**, *119*, 7440.

[138] M. Kempe, *Anal. Chem.* **1996**, *68*, 1948.

[139] X. Dong, H. Sun, X. Lue, H. Wang, S. Liu, N. Wang, *Analyst* **2002**, *127*, 1427.

[140] B. Sellergren, *Makromol. Chem.* **1989**, *190*, 2703.

[141] I. Jelesarov, H. R. Bosshard, *J. Mol. Recognit.* **1999**, *12*, 3.

[142] A. Weber, M. Dettling, H. Brunner, G. E. M. Tovar, *Macromol. Rapid Commun.* **2002**, *23*, 824.

[143] M. Quaglia, K. Chenon, A. J. Hall, E. de Lorenzi, B. Sellergren, *J. Am. Chem. Soc.* **2001**, *123*, 2146.

[144] P. A. Gale, *Coord. Chem. Rev.* **2003**, *240*, 191.

[145] B. R. Linton, M. S. Goodman, E. Fan, S. A. van Arman, A. D. Hamilton, *J. Org. Chem.* **2001**, *66*, 7313.

[146] R. Kato, S. Nishizawa, T. Hayashita, N. Teramae, *Tetrahedron Lett.* **2001**, *42*, 5052.

[147] D. H. Lee, H. Y. Lee, K. H. Lee, J.-I. Hong, *Chem. Commun.* **2001**, 1188.

[148] M. Mei, S. Wu, *New J. Chem.* **2001**, *25*, 471.

[149] C. S. Wilcox, E. Kim, D. Romano, L. H. Kuo, L. B. Burt, D. P. Curran, *Tetrahedron* **1995**, *51*, 621.

[150] M. C. Etter, T. W. Panunto, *J. Am. Chem. Soc.* **1988**, *110*, 5896.

[151] E. Fan, S. A. van Arman, S. Kincaid, A. D. Hamilton, *J. Am. Chem. Soc.* **1993**, *115*, 369.

[152] D. Spivak, K. J. Shea, *J. Org. Chem.* **1999**, *64*, 4627.

[153] A. J. Hall, M. Quaglia, P. Manesiotis, E. de Lorenzi, B. Sellergren, *manuscript in preparation*.

[154] B. Feibush, A. Figueroa, R. Charles, K. D. Onan, P. Feibush, B. L. Karger, *J. Am. Chem. Soc.* **1986**, *108*, 3310.

[155] V. Berl, M. Schmutz, M. J. Krische, R. G. Khoury, J.-M. Lehn, *Chem.-Eur. J.* **2002**, *8*, 1227.

[156] B. Roth, J. M. Smith, J. M. E. Hulquist, *J. Am. Chem. Soc.* **1950**, *72*, 1914.

[157]   B. Roth, J. M. Smith, J. M. E. Hulquist, *J. Am. Chem. Soc.* **1951**, *73*, 2864.

[158]   I. D. Entwistle, R. A. W. Johnstone, T. J. Povall, *J. Chem. Soc. Perkin I* **1975**, 1300.

[159]   D. McCormick, *J. Heterocyclic Chem.* **1970**, *7*, 447.

[160]   D. McCormick, *J. Heterocyclic Chem.* **1974**, *11*, 969.

[161]   K. A. Connors, *Binding Constants: The Measurement of Molecular Complex Stability*, J. Wiley & Sons, New York, **1987**.

[162]   H. J. Harrick, *Internal reflection spectroscopy*, Interscience, New York, **1967**.

[163]   G. Guiochon, S. Goishan-Shirazi, A. Katti, *Fundamentals of Preparative and Nonlinear Chromatography*, Academic Press, New York, **1994**.

[164]   P. Sajonz, M. Kele, G. Zhong, B. Sellergren, G. Guiochon, *J. Chromatogr. A* **1998**, *810*, 1.

[165]   Y. Chen, M. Kele, P. Sajonz, B. Sellergren, G. Guiochon, *Anal. Chem.* **1999**, *71*, 928.

[166]   Y. Chen, M. Kele, I. Quinones, B. Sellergren, G. Guiochon, *J. Chromatogr. A* **2001**, *927*, 1.

[167]   R. J. Umpleby, S. C. Baxter, A. M. Rampey, G. T. Rushton, Y. Chen, K. D. Shimizu, *J. Chromatogr. B* **2004**, *804*, 141.

[168]   R. J. Umpleby, S. C. Baxter, M. Bode, J. K. Berch, R. N. Shah, K. D. Shimizu, *Anal. Chim. Acta* **2001**, *435*, 35.

8 Appendix

This appendix contains information about the abbreviations contained in this manuscript, details about chemicals, solvents and equipment used during this work, as well as the theory behind the ^{1}H-NMR titration and the results of the titrations performed for the different studied systems.

8.1 List of Abbreviations

1,3-DBU	1,3-dibenzyluracil
1-BU	1-benzyluracil
5-FU	5-fluorouracil
ABDV	2,2'-azobis(2,4-dimethylvaleronitrile)
A-D-A	Acceptor-Donor-Acceptor
AIBN	2,2'-azobis(2-methylbutyronitrile)
ATR-FT-IR	Attenuated Total Reflection Fourier Transform Infrared
AZT	3-azido-3´-deoxythymidine
CHU	cyclohexyluracil
CIS	Complexation Induced Shift
DAD/DAD-UV	Ultraviolet Diode Array Detector
D-A-D	Donor-Acceptor-Donor
DMF	dimethyl formamide
DMSO	dimethyl sulfoxide
EDMA	ethyleneglycol dimethacrylate
EtOH	ethanol
HEMA	2-hydroxyethyl methacrylate
HPLC	High Performance Liquid Chromatography
HRMS	High Resolution Mass Spectroscopy
IBF	isobutyl flavin
IF	Imprinting Factor
IPF	isopentyl flavin
LC	lumichrome
LF	lumiflavin
M	monomer

MAA	methacrylic acid
MeCN	acetonitrile
MeOH	methanol
MIP	Molecularly Imprinted Polymer
NIP	Non-Imprinted Polymer
NMR	Nuclear Magnetic Resonance
NOE	Nuclear Overhauser Effect
PEDMA	pentaerythritol dimethacrylate
PETRA	pentaerythritol triacrylate
PF	phenyl flavin
RfAc	riboflavin tetraacetate
RfBP	riboflavin binding protein
RfBu	riboflavin tetrabutyrate
RfPr	riboflavin tetrapropionate
RFU	Relative Fluorescence Units
SPE	Solid Phase Extraction
T	template
TBA	tetrabutylammonium
TEA	triethylamine
THF	tetrahydrofurane
TRIM	trimethylolpropane trimethacrylate
Z	Carbobenzyloxy protecting group

8.2 Chemicals and Solvents

Chemicals and solvents were provided by the following sources:

8.2.1   Chemicals and solvents for synthesis

2,4-diaminopurine	Acros Chemicals, Geel, Belgium
2,6-diaminopyridine	Acros Chemicals, Geel, Belgium
2-nitroaniline	Acros Chemicals, Geel, Belgium
3/4-vinylbenzyl chloride	Acros Chemicals, Geel, Belgium
4-chloro-2,6-diaminopyrimidine	Acros Chemicals, Geel, Belgium

4-methoxy-2-nitroaniline	Acros Chemicals, Geel, Belgium
Acetic acid anhydride	Merck KGaA, Darmstadt, Germany
Acetic acid	Fluka, Deisenhofen, Germany
Acetone, p.a.	Merck KGaA, Darmstadt, Germany
Acryloyl chloride	Acros Chemicals, Geel, Belgium
Adenine	Acros Chemicals, Geel, Belgium
Alloxane monohydrate	Acros Chemicals, Geel, Belgium
Aniline	Sigma-Aldrich, Steinheim, Germany
Benzyl chloride	Acros Chemicals, Geel, Belgium
Chloroform, p.a.	Merck KGaA, Darmstadt, Germany
Cyclohexene	Acros Chemicals, Geel, Belgium
Dichloromethane, (dry)	Fluka, Deisenhofen, Germany
Ethanol, p.a.	Merck KGaA, Darmstadt, Germany
Perchloric acid, 70% in water	Acros Chemicals, Geel, Belgium
Isobutyl chloride	Sigma-Aldrich, Steinheim, Germany
Isopropyl bromide	Sigma-Aldrich, Steinheim, Germany
Isopentyl bromide	Sigma-Aldrich, Steinheim, Germany
Magnesium sulphate monohydrate	Fluka, Deisenhofen, Germany
Methanol, p.a.	Merck KGaA, Darmstadt, Germany
Methyl iodide	Merck KGaA, Darmstadt, Germany
Piperidine	Acros Chemicals, Geel, Belgium
Potassium carbonate	Acros Chemicals, Geel, Belgium
Propionic acid	Acros Chemicals, Geel, Belgium
Propionic acid anhydride, p.a.	Acros Chemicals, Geel, Belgium
Propionyl chloride	Acros Chemicals, Geel, Belgium
Riboflavin	Acros Chemicals, Geel, Belgium
Riboflavin tetrabutyrate	Lancaster, Frankfurt a.M., Germany
Tetrahydrofuran, (dry)	Fluka, Deisenhofen, Germany
Toluene, p.a.	Merck KGaA, Darmstadt, Germany
Triethylamine	Sigma-Aldrich, Steinheim, Germany
Trifluoroacetic acid anhydride	Sigma-Aldrich, Steinheim, Germany
Uracil	Sigma-Aldrich, Steinheim, Germany

8.2.2 Chemicals and solvents for HPLC

Acetic acid, biochemical grade	Fluka, Deisenhofen, Germany
Acetonitrile, gradient grade	Merck KGaA, Darmstadt, Germany
L-(+)-ascorbic acid	Acros Chemicals, Geel, Belgium
3'-Azido-3'-deoxythymidine	The Wellcome Corp. Ltd. London, UK
Folic acid	Acros Chemicals, Geel, Belgium
N-Z-L-glutamic acid	Sigma-Aldrich, Steinheim, Germany
N-Z-D-glutamic acid	Sigma-Aldrich, Steinheim, Germany
Lumichrome	Sigma-Aldrich, Steinheim, Germany
Lumiflavin	Sigma-Aldrich, Steinheim, Germany
Methanol, gradient grade	Merck KGaA, Darmstadt, Germany
Nicotinamide	Acros Chemicals, Geel, Belgium
Nicotinic acid	Acros Chemicals, Geel, Belgium
D-pantothenic acid, calcium salt	Fluka, Deisenhofen, Germany
Pyridoxine	Acros Chemicals, Geel, Belgium
Thiamine hydrochloride	Acros Chemicals, Geel, Belgium
Water, HPLC grade	Merck KGaA, Darmstadt, Germany

8.2.3 Solvents for NMR spectroscopy

Acetonitrile, d_3 (CD_3CN)	Merck KGaA, Darmstadt, Germany
Chloroform, d_1 ($CDCl_3$)	Deutero GmbH, Kastellaun, Germany
Deuterated water (D_2O)	Merck KGaA, Darmstadt, Germany
Dimethylsulfoxide, d_6 (DMSO-d_6)	Deutero GmbH, Kastellaun, Germany

8.2.4 Chemicals for polymer synthesis

2,2'-azobis(2,4-dimethylvaleronitrile)	Wako GmbH, Neuss, Germany
2,2'-azobis(2-methylbutyronitrile)	Wako GmbH, Neuss, Germany
2-hydroxyethyl methacrylate	Sigma-Aldrich, Steinheim, Germany
Ethyleneglycol dimethacrylate	Sigma-Aldrich, Steinheim, Germany
Methacrylic acid	Sigma-Aldrich, Steinheim, Germany
Pentaerythritol dimethacrylate	ABCR GmbH & Co. KG, Karlsruhe, Germany

| Pentaerythritol triacrylate | Polysciences Europe GmbH, Eppelheim, Germany |
| Trimethylolpropane trimethacrylate | Sigma-Aldrich, Steinheim, Germany |

8.3 Equipment

NMR spectra were recorded at 400 MHz using a Brucker DRX400 spectrometer. Elemental analyses were performed using a Heraeus CHN rapid analyser. High resolution mass spectra were obtained using a JEOL JMS-SX-102A mass spectrometer. Infrared spectra were recorded with use of a NEXUS FT-IR spectrometer (Thermo Electron Corporation) equipped with an ATR module. UV and fluorescence measurements were performed using a SAFIRE 96 well-plate reader (TECAN) and quartz 96 well-plates (HELMA). HPLC evaluation of the materials was performed on HP1050 and HP1100 Liquid Chromatographs equipped with autosamplers and controlled by computer (Agilent ChemStation).

8.4   The 1:1 binding isotherm equation for ^{1}H-NMR titrations

When looking at the interaction between two compounds, the peaks observed in the ^{1}H-NMR spectrum are dependent on the rate of the association and dissociation of the studied complex. Following a proton which is directly affected by the association, it is possible to observe three different situations: If the interaction is slow, one can observe, for the same proton(s), a peak for the complexed and a peak for the "free" ones. If the interaction is moderately slow one will see these two peaks broadening towards each other. Finally there is the possibility of very fast complex association / dissociation; in this case it is only possible to observe a weighted average of the two situations (Figure 8.1).
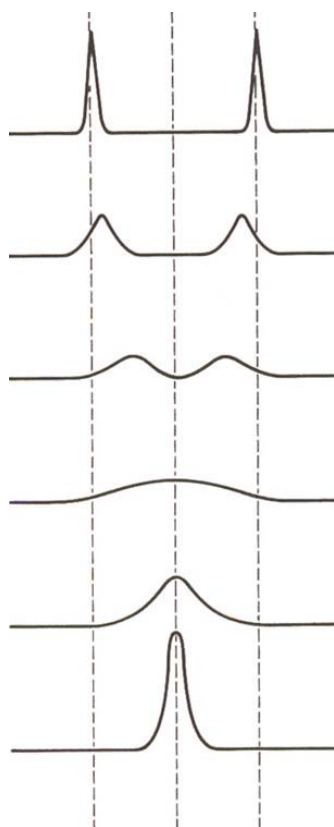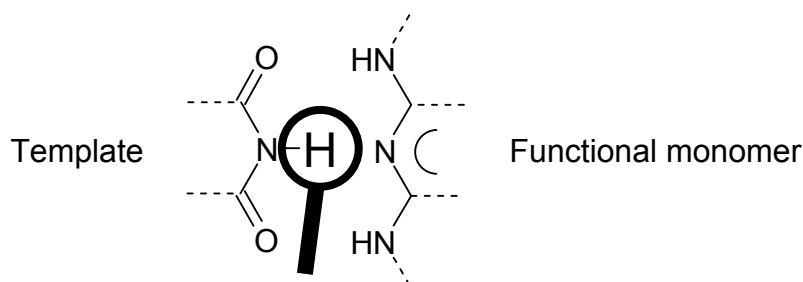

Figure 8.1:   *From top to bottom: Slow exchange, moderately slow exchange, coalescence, very fast exchange*

This last phenomenon was observed during these experiments. In the example below, the proton followed is the imide proton of 1-benzyluracil.

Template ⋯ Functional monomer

Scheme 8.1

The observed chemical shift, δ, for the selected proton, will be the weighted average of the two extremes, δ_T and δ_{TM}, which are the chemical shift of the template (T) in the free state and of the template-monomer (TM) complex.

$$\delta = \delta_T \cdot x_T + \delta_{TM} \cdot x_{TM} \qquad 8.1$$

Where x_T and x_{TM} are the molar fractions.

When the volume of solvent is kept constant in every NMR measurement, we have:

$$\delta = \frac{\delta_T \cdot [T] + \delta_{TM} \cdot [TM]}{[T] + [TM]} \qquad 8.2$$

If one then looks at the difference between the observed shift for the complex at a given concentration of monomer (M) and the peak corresponding to the "free" template, their difference is given by $\Delta\delta = \delta - \delta_T$, with δ from above and δ_T written as:

$$\delta_T = \frac{\delta_T ([T] + [TM])}{[T] + [TM]} \qquad 8.3$$

This becomes:

$$\Delta\delta = \frac{[TM]\Delta_{TM}}{[T] + [TM]} \qquad 8.4$$

where $\Delta_{TM} = \delta_{TM} - \delta_T$.

Inserting [TM] = K_C.[T].[TM] from the equilibrium in a 1:1 stoichiometric complex we get the 1:1 binding isotherm for NMR:

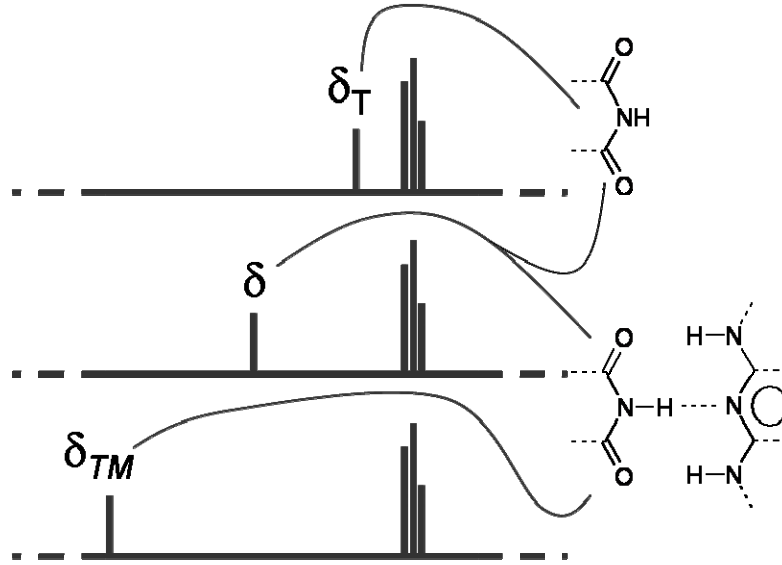$$\Delta\delta = \frac{K_C[M]}{1 + K_C[M]} \cdot \Delta_{TM} \qquad 8.5$$

193

Figure 8.2: *Schematic representation of the CIS in fast exchange between free and bound T.*

The fraction of complexed template (f_{TM}) can be written as:

$$f_{TM} = \frac{[TM]}{C_T} = \frac{[TM]}{[T]+[TM]} = \frac{K_C[M]}{1+K_C[M]} \qquad 8.6$$

When inserting $K_C.[T].[M]$ for [TM] again. Identifying this as a part of the binding isotherm, it can be deduced that:

$$f_{TM} = \frac{\Delta\delta}{\Delta_{TM}} \qquad 8.7$$

A graph of the shift change *Δδ vs.* the concentration of "free" functional monomer [M] can then be fitted to give the association constant (K_C) and the maximum shift change (Δ_{TM}). Since the formal concentration of the monomer in these experiments is much different from the actual, a correction has to be made.

The concentration of "free" monomer can be written as:

$$[M]=C_M -[TM]=C_M - f_{TM}C_T \qquad 8.8$$

Where C_M and C_T are the formal concentrations of monomer (C_M = [M] + [TM]) and template (C_T = [T] + [TM]) respectively.

Therefore the concentration of "free" monomer can be calculated from:

$$[M]=C_M -\frac{\Delta\delta}{\Delta_{TM}}C_T \qquad 8.9$$

When fitting the measured data points to the *1:1 binding isotherm for NMR* one obtains an approximate value for K_C and Δ_{TM}. Then the concentrations have to be recalculated using the obtained Δ_{TM} and the fitting done again with the new values for K_C and Δ_{TM} until they converge. This method and related other ones have been widely used to estimate the parameters K_C and Δ_{TM} for molecular complexes.

The elaboration described above provides us with an apparent association constant (K_{app}). Monomer or template self-association has not been taken into account. The association constants for different modes of binding have also not been taken into account. The apparent association constant therefore only gives an impression of how much of the template is complexed with the monomer in the solvent in which the experiment was carried out. A true binding constant can give a deceivingly high estimate of the actual binding and can be misleading when used with molecular imprinting.

8.5   ^{1}H-NMR titrations

In this part of the Appendix, all ^{1}H-NMR titration experimental designs will be presented in detail, as well as all the obtained binding curves and the curve-fitting results.
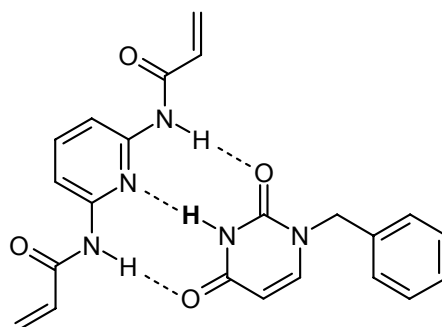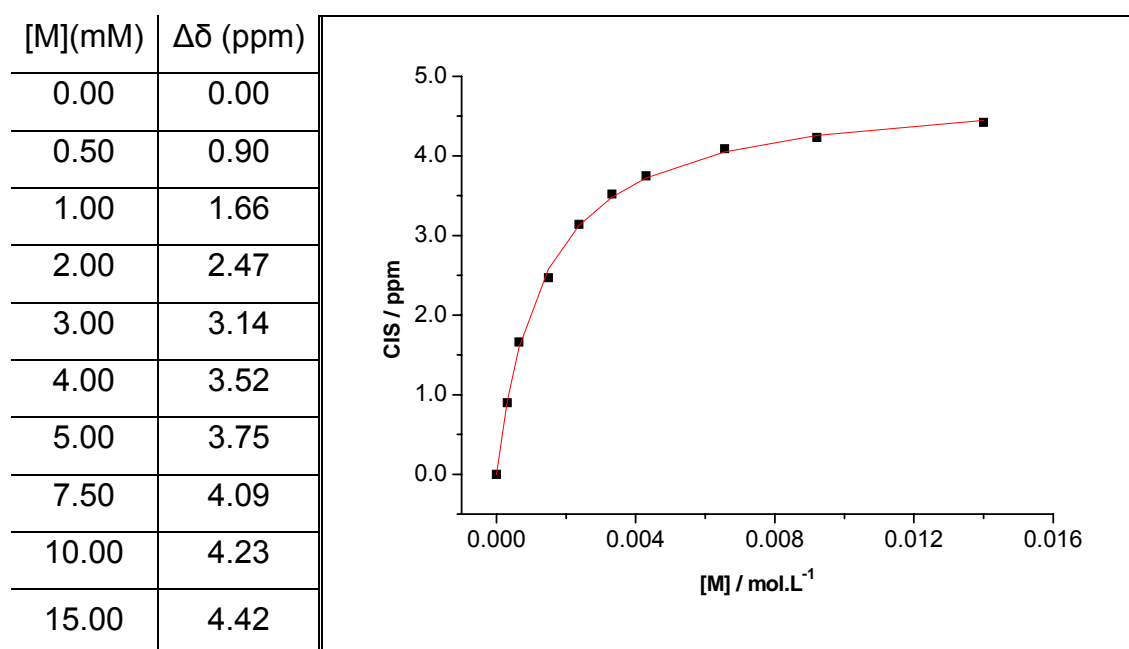
8.5.1   Imide recognition

The imide functionality, the main "handle" on which the recognition of riboflavin is based, is present also in the RNA base uracil. Initial studies for the selection of the monomer that would provide the best recognition for this functional group where based on 1-benzyluracil, which comprises functionality and sufficient solubility in organic solvents, a perquisite for the determination of binding constants by NMR. Additionally, one titration experiment has been performed using one of the first organic soluble riboflavin analogues. The results of the screening of different monomers against the imide moiety by means of NMR titrations will be presented in this paragraph.

8.5.1.a

Host (Template): 1-benzyluracil (1mM)

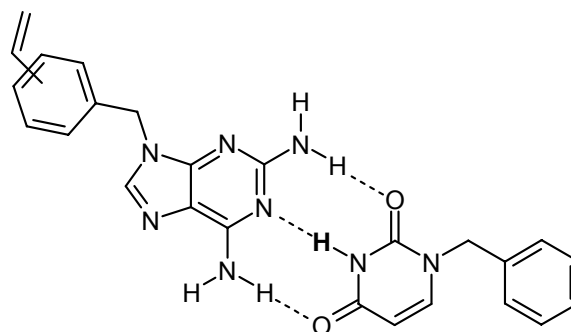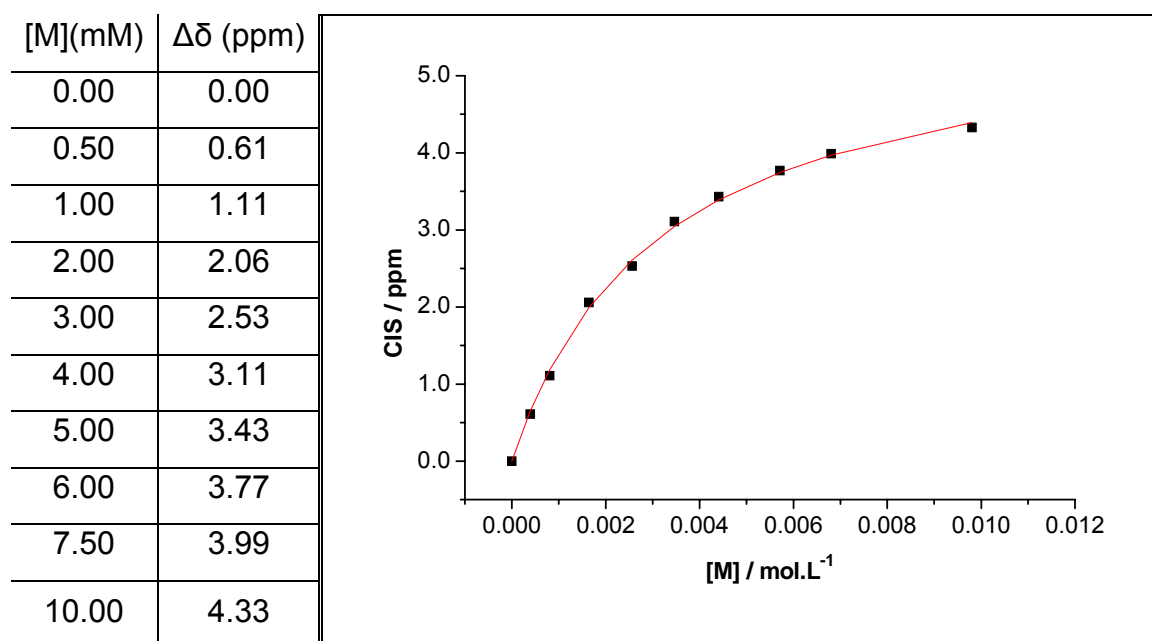Guest (Monomer): 2,6-bis(acrylamido) pyridine (varied from 0-15mM)

Solvent: $CDCl_3$.

Figure 8.3: Proposed complexation mode. (Followed proton in bold)

[M](mM)	Δδ (ppm)
0.00	0.00
0.50	0.90
1.00	1.66
2.00	2.47
3.00	3.14
4.00	3.52
5.00	3.75
7.50	4.09
10.00	4.23
15.00	4.42

The above curve was fitted by non-linear regression using Origin 5.0 and the association constant for this complex was calculated K_a= 757±28 M^{-1}, in $CDCl_3$.

NMR dilution studies of 2,6-bis(acrylamido)pyridine in $CDCl_3$ indicate no self-association of the molecule since no shift of the amide protons was observed upon increasing the concentration of the monomer.

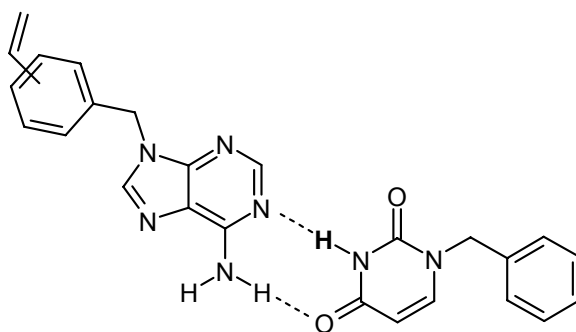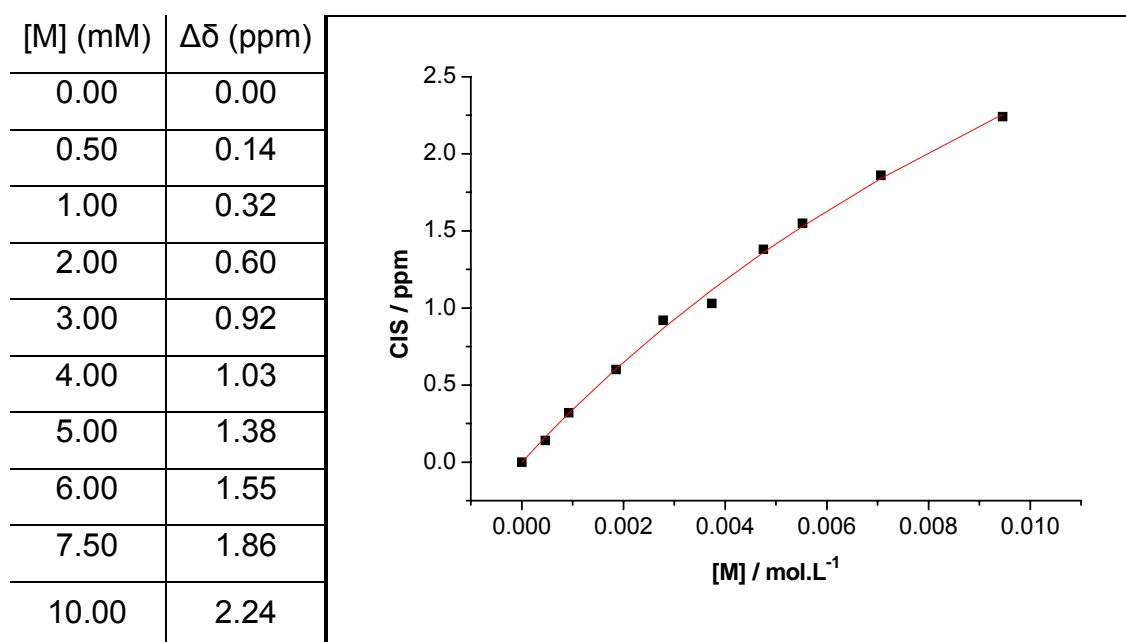### 8.5.1.b

Host (Template): 1-benzyluracil (1mM)

Guest (Monomer): 9-(3,4-vinylbenzyl)-2,6-diaminopurine

(varied from 0-10mM)

Solvent: CDCl$_3$.

Figure 8.4: Proposed complexation mode. (Followed proton in bold)

[M](mM)	Δδ (ppm)
0.00	0.00
0.50	0.61
1.00	1.11
2.00	2.06
3.00	2.53
4.00	3.11
5.00	3.43
6.00	3.77
7.50	3.99
10.00	4.33

An association constant of K_a= 320±16 M^{-1} was calculated for the above complex, in CDCl$_3$.

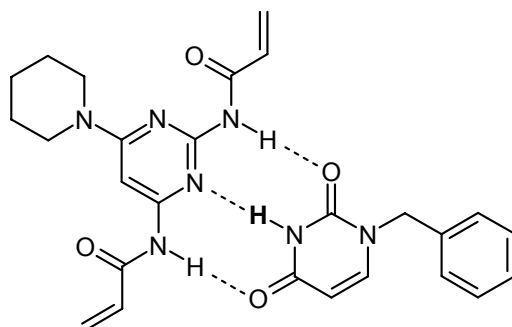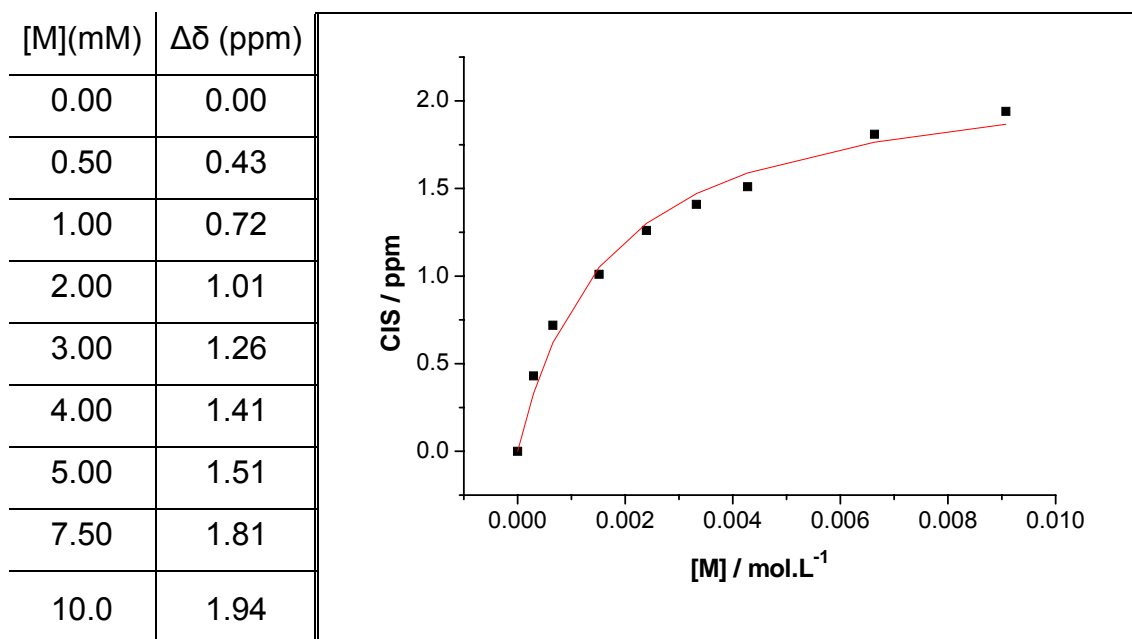*8.5.1.c*

Host (Template): 1-benzyluracil (1mM)

Guest (Monomer): 9-(3,4-vinylbenzyl) adenine (varied from 0-10mM)

Solvent: $CDCl_3$.

Figure 8.5: Proposed complexation mode. (Followed proton in bold)

[M] (mM)	Δδ (ppm)
0.00	0.00
0.50	0.14
1.00	0.32
2.00	0.60
3.00	0.92
4.00	1.03
5.00	1.38
6.00	1.55
7.50	1.86
10.00	2.24

The binding here is much weaker than the previous systems and the association constant was calculated K_a= 53±7.5 M^{-1}, in $CDCl_3$.
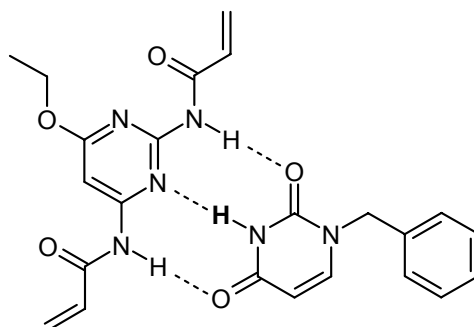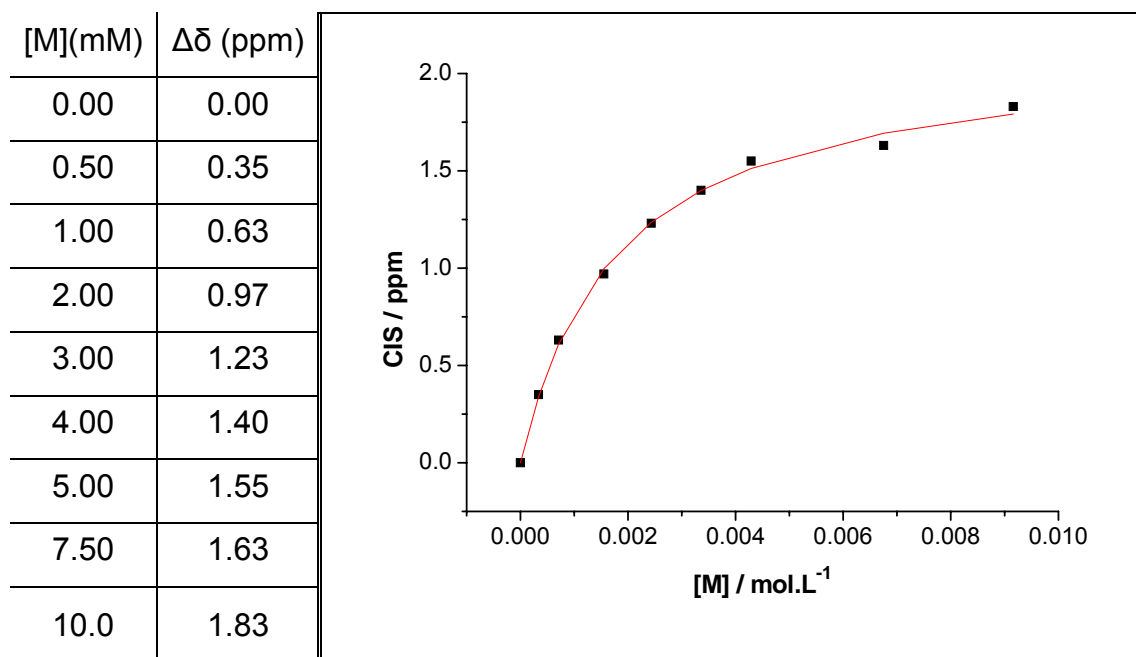
8.5.1.d

Host (Template): 1-benzyluracil (1mM)

Guest (Monomer): 4-piperidino-2,6-bis(acrylamido)pyrimidine
(varied from 0-10mM)

Solvent: CDCl$_3$.

Figure 8.6: Proposed complexation mode. (Followed proton in bold)

[M](mM)	Δδ (ppm)
0.00	0.00
0.50	0.43
1.00	0.72
2.00	1.01
3.00	1.26
4.00	1.41
5.00	1.51
7.50	1.81
10.0	1.94

The curve was fitted by non-linear regression using Origin 5.0 and the association constant for this complex was found to be K$_a$= 596±85 M^{-1}, in CDCl$_3$. However, it was discovered that this monomer self-associates to a significant extent, therefore dilution study experiments were performed to estimate the degree of self-association and to derive the exact value of the binding constant.

8.5.1.e
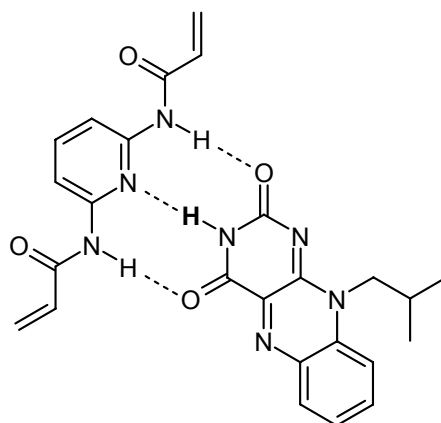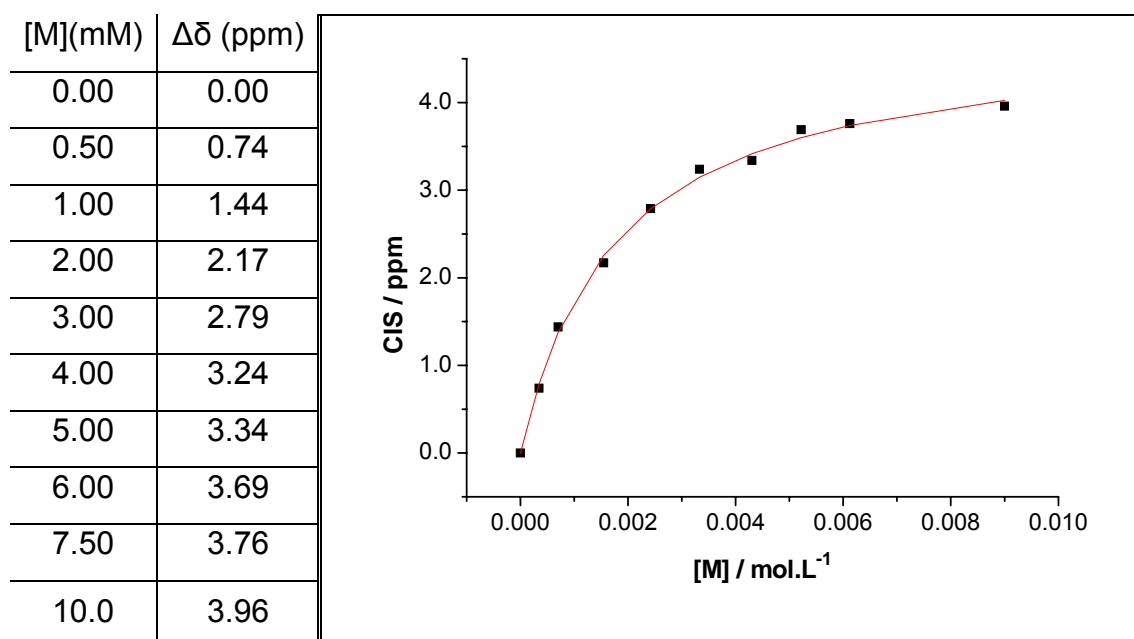
Host (Template): 1-benzyluracil (1mM)

Guest (Monomer): 4-ethoxy-2,6-bis(acrylamido)pyrimidine

(varied from 0-10mM)

Solvent: CDCl$_3$.

Figure 8.7: Proposed complexation mode. (Followed proton in bold)

[M](mM)	Δδ (ppm)
0.00	0.00
0.50	0.35
1.00	0.63
2.00	0.97
3.00	1.23
4.00	1.40
5.00	1.55
7.50	1.63
10.0	1.83

An association constant of K$_a$= 561±37 M^{-1} was derived by non-linear regression of the data above. Similarly to the previous system, it was found that this monomer also self-associates to a significant extent. Therefore dilution study experiments were performed to estimate the degree of self-association and to derive the exact value of the binding constant.

201

8.5.1.f

Host (Template): isobutyl flavin (1mM)

Guest (Monomer): 2,6-bis(acrylamido)pyridine (varied from 0-10mM)

Solvent: $CDCl_3$.

Figure 8.8: Proposed complexation mode. (Followed proton in bold)

[M](mM)	Δδ (ppm)
0.00	0.00
0.50	0.74
1.00	1.44
2.00	2.17
3.00	2.79
4.00	3.24
5.00	3.34
6.00	3.69
7.50	3.76
10.0	3.96

The curve was fitted by non-linear regression using Origin 5.0 and the association constant for this complex was calculated K_a= 570±35 M^{-1}, in $CDCl_3$.
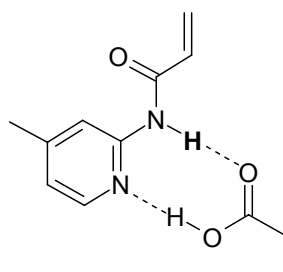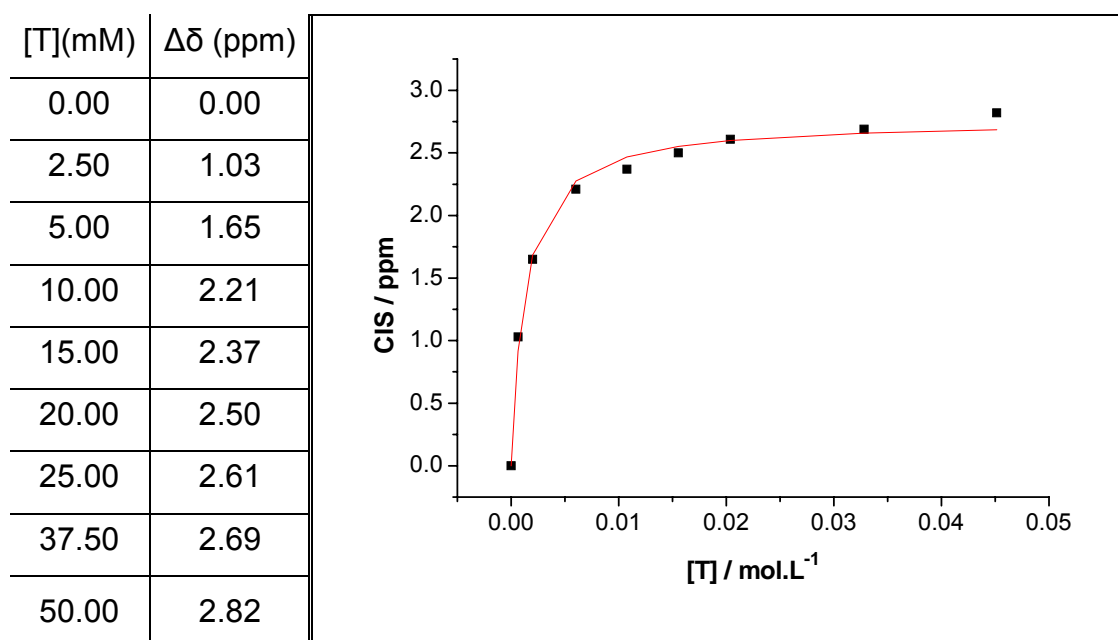
202

8.5.2 Carboxylic acid recognition

The approach taken towards the binding of carboxylic acids is based on a library of amido-pyridines. Since it is not possible to follow the acid proton of propionic acid, these titrations were performed in the "reverse" mode, namely by adding the template T to a standard solution of monomer M and following the amide proton of the latter. The results of this screening are presented in the following paragraphs.

8.5.2.a

Host (Monomer): 2-acrylamido-4-methylpyridine (5mM)

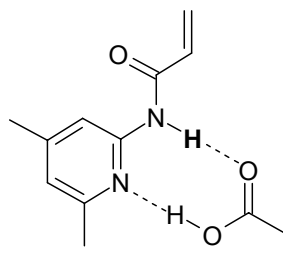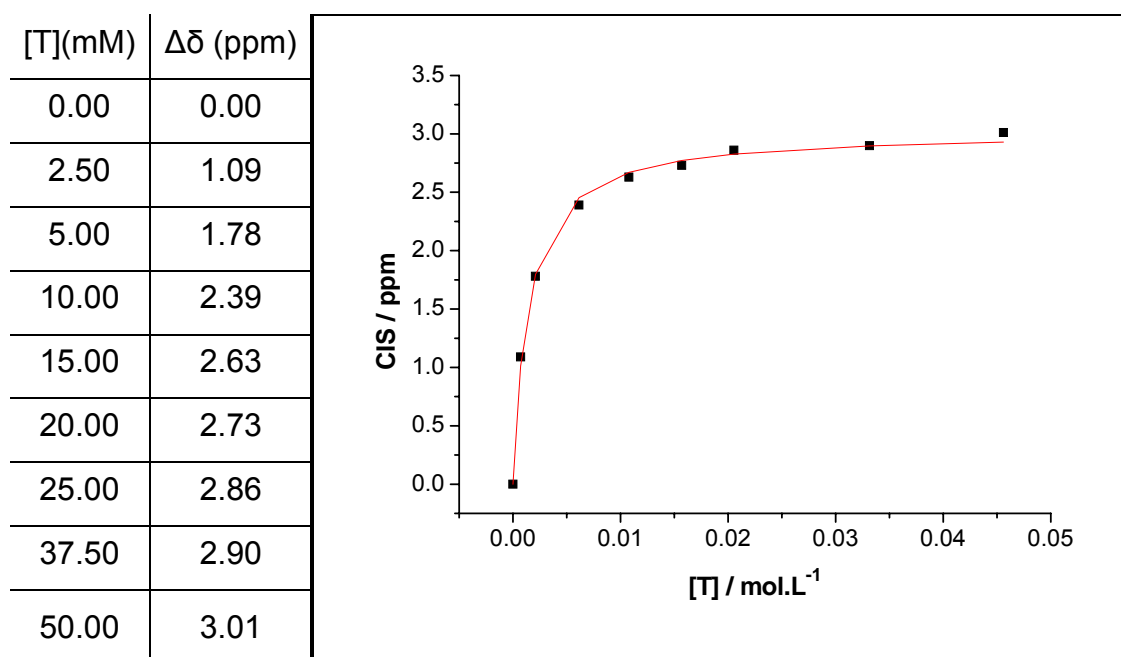Guest (Template): propionic acid (varied from 0-50mM)

Solvent: $CDCl_3$.

Figure 8.9: Proposed complexation mode. (Followed proton in bold)

[T](mM)	Δδ (ppm)
0.00	0.00
2.50	1.03
5.00	1.65
10.00	2.21
15.00	2.37
20.00	2.50
25.00	2.61
37.50	2.69
50.00	2.82

The curve was fitted by non-linear regression using Origin 5.0 and the association constant for this complex was calculated K_a= 777±83 M^{-1}, in $CDCl_3$.

8.5.2.b

Host (Monomer): 2-acrylamido-4,6-dimethylpyridine (5mM)
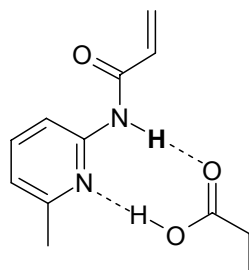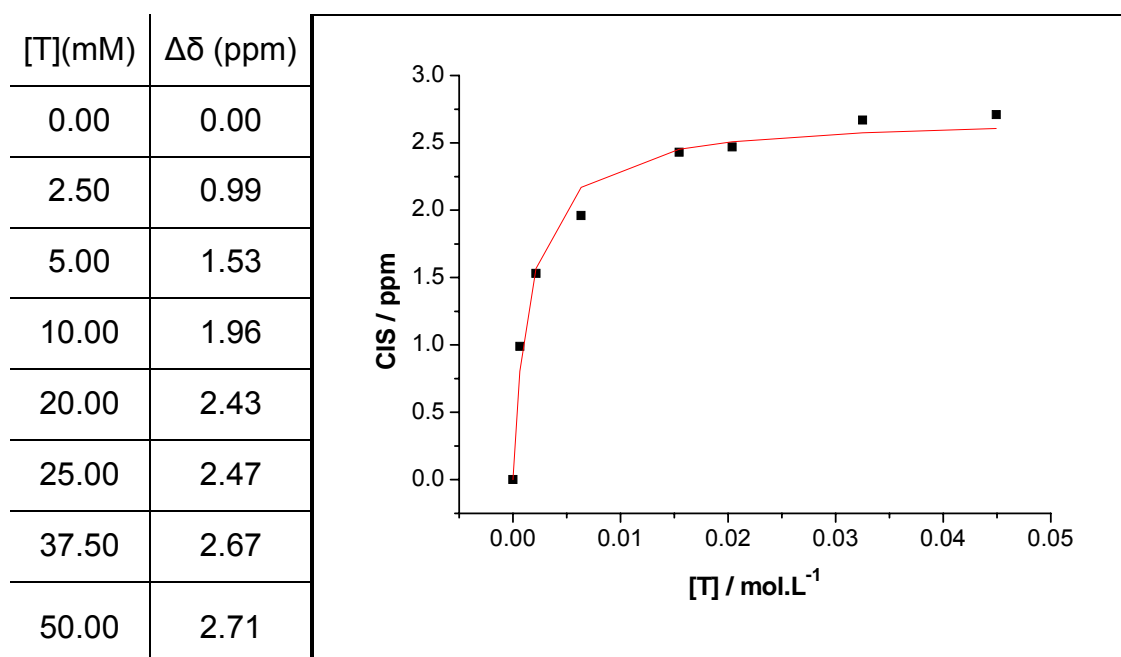
Guest (Template): propionic acid (varied from 0-50mM)

Solvent: CDCl$_3$.

Figure 8.10: Proposed complexation mode. (Followed proton in bold)

[T](mM)	Δδ (ppm)
0.00	0.00
2.50	1.09
5.00	1.78
10.00	2.39
15.00	2.63
20.00	2.73
25.00	2.86
37.50	2.90
50.00	3.01

The curve was fitted by non-linear regression using Origin 5.0 and the association constant for this complex was calculated K_a= 704±44 M^{-1}, in CDCl$_3$.

8.5.2.c

Host (Monomer): 2-acrylamido-6-methylpyridine (5mM)
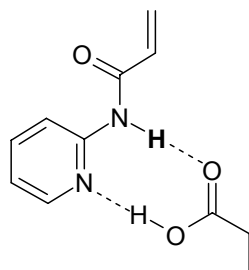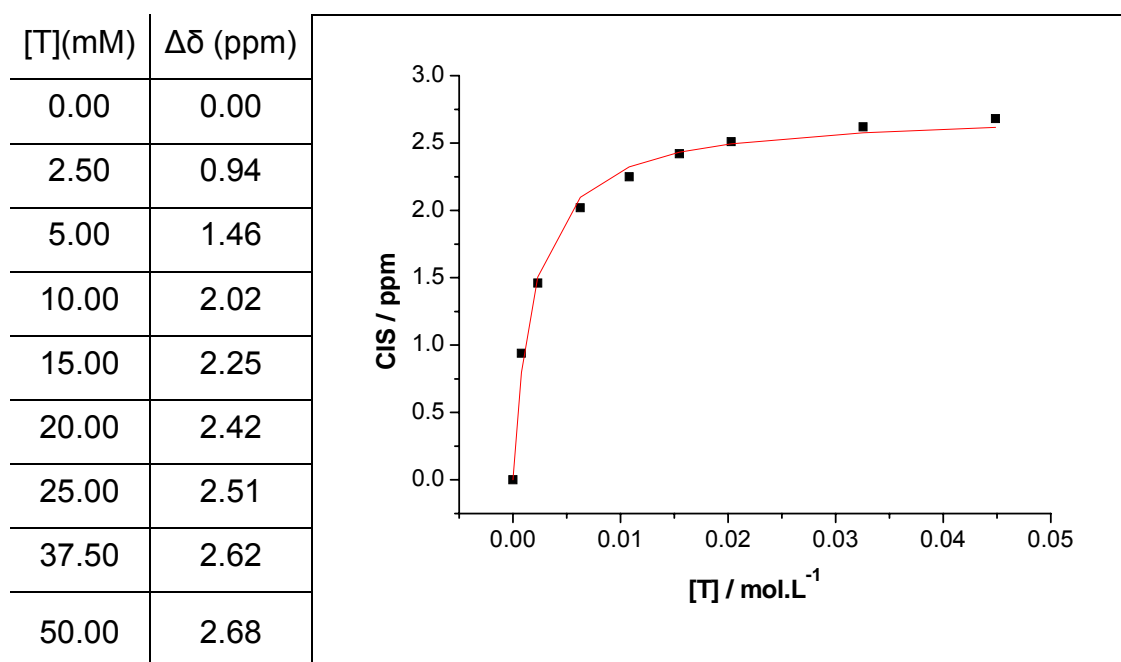
Guest (Template): propionic acid (varied from 0-50mM)

Solvent: CDCl$_3$.

Figure 8.11: Proposed complexation mode. (Followed proton in bold)

[T](mM)	Δδ (ppm)
0.00	0.00
2.50	0.99
5.00	1.53
10.00	1.96
20.00	2.43
25.00	2.47
37.50	2.67
50.00	2.71

The curve was fitted by non-linear regression using Origin 5.0 and the association constant for this complex was calculated K$_a$= 650±111 M^{-1}, in CDCl$_3$.

206

8.5.2.d

Host (Monomer): 2-acrylamido pyridine (5mM)
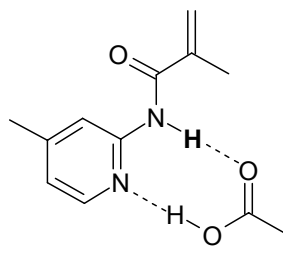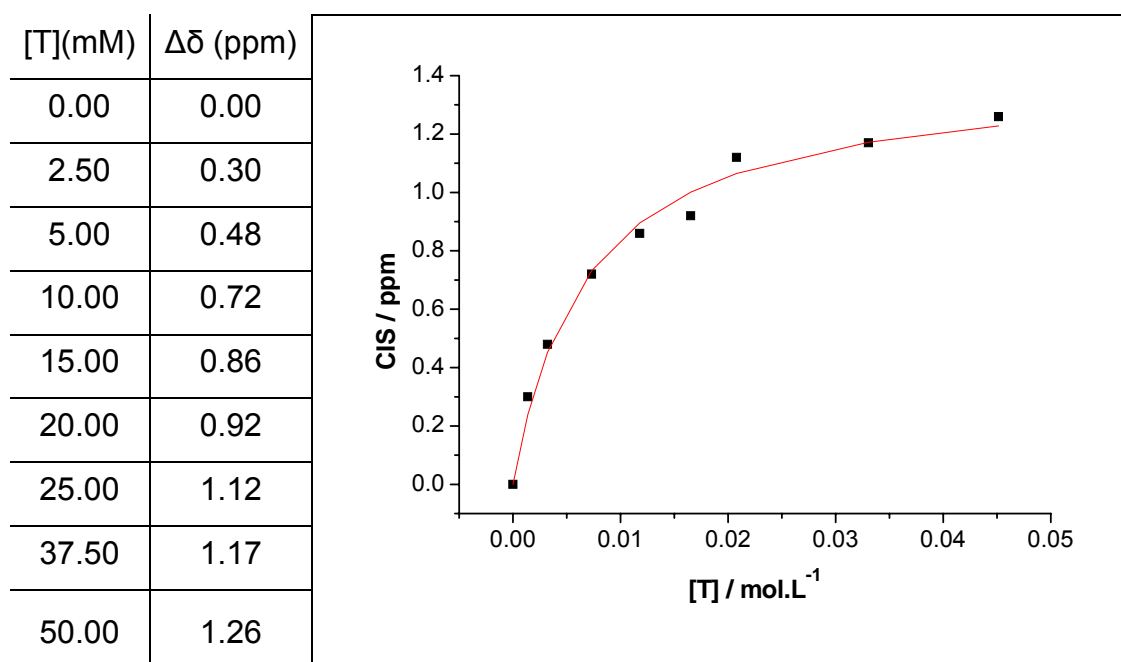
Guest (Template): propionic acid (varied from 0-50mM)

Solvent: $CDCl_3$.

Figure 8.12: Proposed complexation mode. (Followed proton in bold)

[T](mM)	Δδ (ppm)
0.00	0.00
2.50	0.94
5.00	1.46
10.00	2.02
15.00	2.25
20.00	2.42
25.00	2.51
37.50	2.62
50.00	2.68

The curve was fitted by non-linear regression using Origin 5.0 and the association constant for this complex was calculated K_a= 540±53 M^{-1}, in $CDCl_3$.

207

8.5.2.e

Host (Monomer): 2-methacrylamido-4-methylpyridine (5mM)

Guest (Template): propionic acid (varied from 0-50mM)

Solvent: $CDCl_3$.

Figure 8.13: Proposed complexation mode. (Followed proton in bold)

[T](mM)	$\Delta\delta$ (ppm)
0.00	0.00
2.50	0.30
5.00	0.48
10.00	0.72
15.00	0.86
20.00	0.92
25.00	1.12
37.50	1.17
50.00	1.26

The curve was fitted by non-linear regression using Origin 5.0 and the association constant for this complex was calculated K_a= 160±26 M^{-1}, in $CDCl_3$.

8.5.3 Carboxylate recognition

Similarly with the carboxylic acids, the carboxylate anion does not offer a proton that can be followed in an NMR titration experiment; therefore it was necessary to perform "inverse" titrations, following the urea protons of the monomers. The concentration of the monomer M was kept constant while varying the concentration of the anion.

8.5.3.a

Host (Monomer): 1-(3-Isopropenyl-α,α-dimethylbenzyl)-3-(benzyl)urea (5mM)

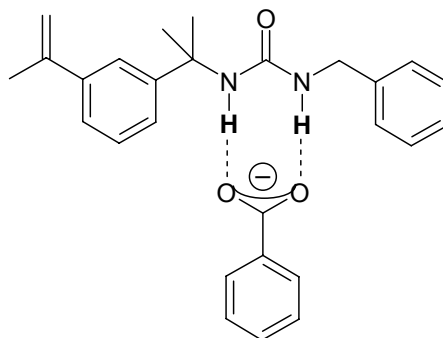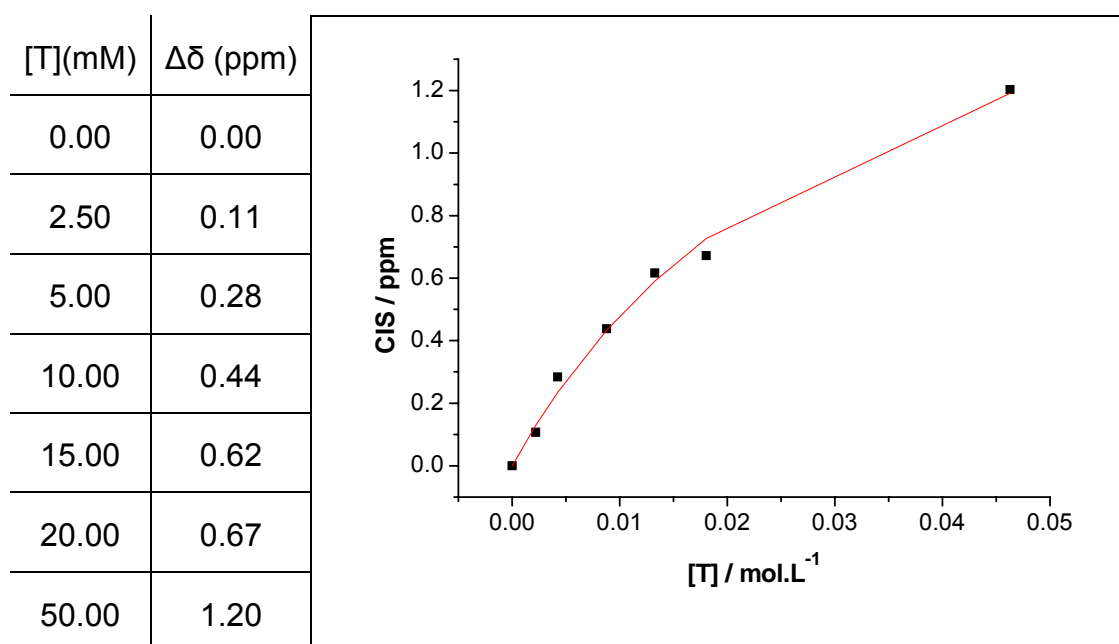Guest (Template): tetrabutylammonium benzoate (varied from 0-50mM)

Solvent: DMSO-d_6.

Figure 8.14:   Proposed complexation mode. (Followed protons in bold)

[T](mM)	Δδ (ppm)
0.00	0.00
2.50	0.11
5.00	0.28
10.00	0.44
15.00	0.62
20.00	0.67
50.00	1.20

The curve was fitted by non-linear regression using Origin 5.0 and the association constant for this complex was calculated K_a= 31±4.6 M^{-1}, in DMSO-d_6.

8.5.3.b

Host (Monomer): 1-(3-Isopropenyl-α,α-dimethylbenzyl)-3-(phenyl)urea (5mM)

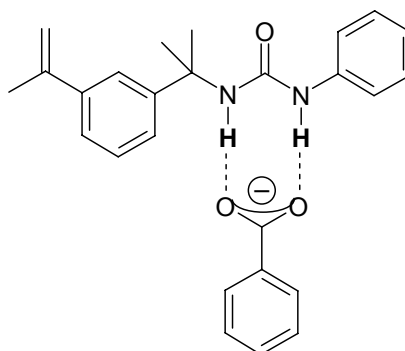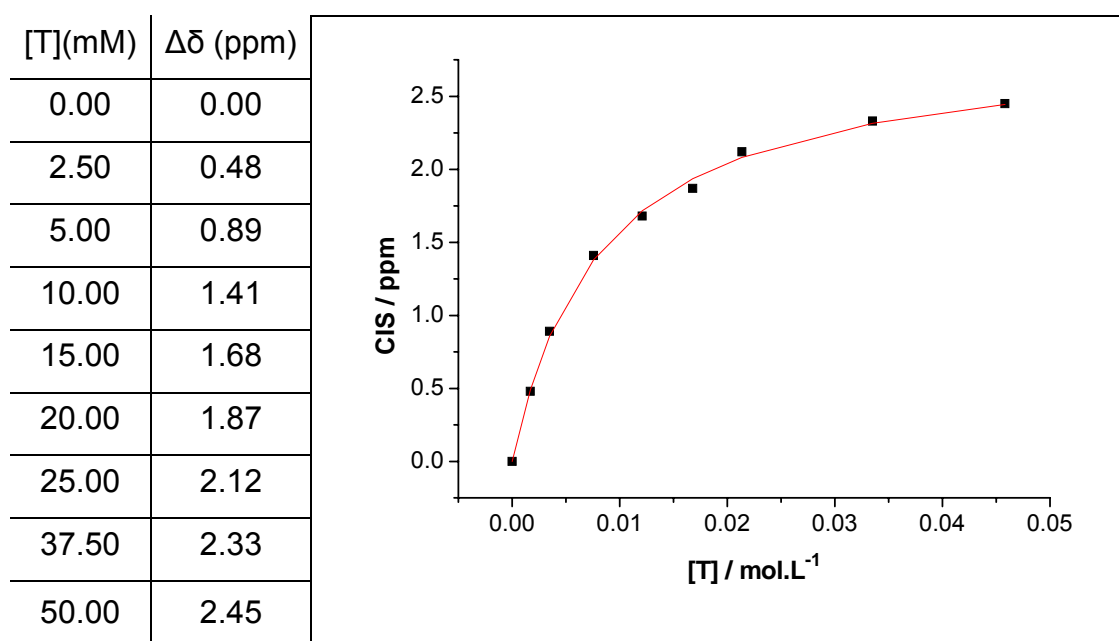Guest (Template): tetrabutylammonium benzoate (varied from 0-50mM)

Solvent: DMSO-d_6.

Figure 8.15:   Proposed complexation mode. (Followed protons in bold)

[T](mM)	Δδ (ppm)
0.00	0.00
2.50	0.48
5.00	0.89
10.00	1.41
15.00	1.68
20.00	1.87
25.00	2.12
37.50	2.33
50.00	2.45

The curve was fitted by non-linear regression using Origin 5.0 and the association constant for this complex was calculated K_a= 121±6.3 M^{-1}, in DMSO-d_6.

211

8.5.3.c

Host (Monomer): N-(3-nitrophenyl)-N'-(4-vinylphenyl)urea (5mM)

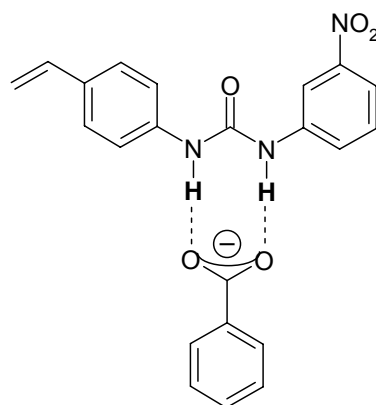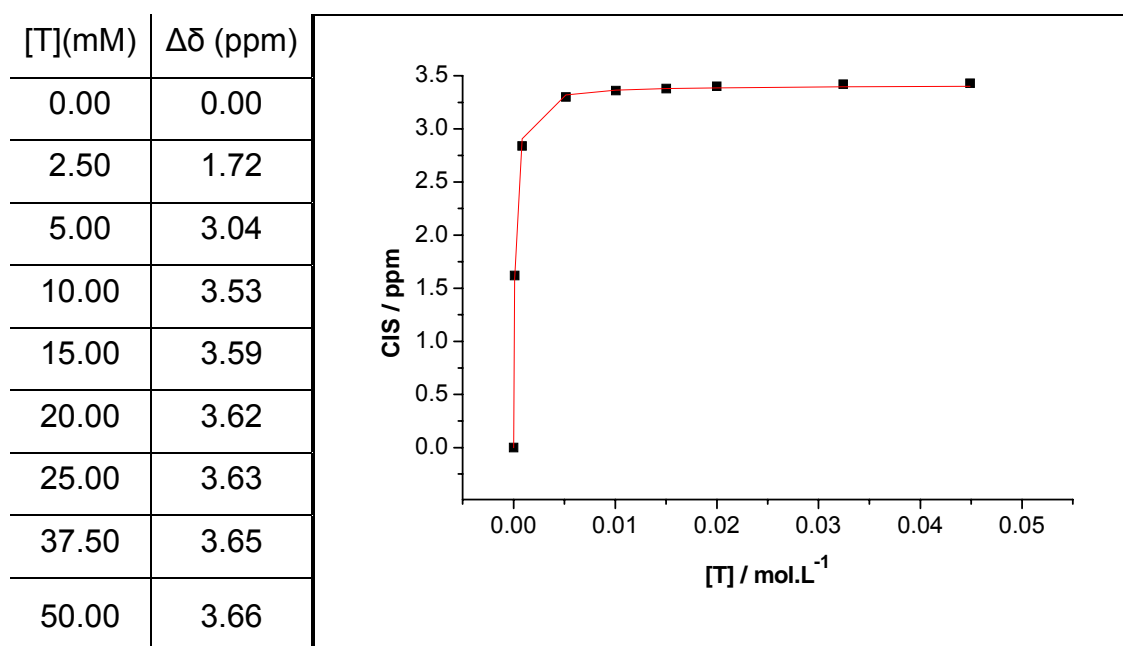Guest (Template): tetrabutylammonium benzoate (varied from 0-50mM)

Solvent: DMSO-d_6.

Figure 8.16: Proposed complexation mode. (Followed protons in bold)

[T](mM)	Δδ (ppm)
0.00	0.00
2.50	1.72
5.00	3.04
10.00	3.53
15.00	3.59
20.00	3.62
25.00	3.63
37.50	3.65
50.00	3.66

The curve was fitted by non-linear regression using Origin 5.0 and the association constant for this complex was calculated K_a= 6890±258 M^{-1}, in DMSO-d_6.

Following the second urea proton a binding constant of 6105±81 M^{-1} was obtained, a value that within the error of the measurement is considered very similar to the first one. Finally, by monitoring the shift of the aromatic H that is

situated in ortho- position to the nitro group pointing towards the urea carbonyl, we obtain a value of 9135±985 M^{-1} (CIS = 0.26ppm).

An additional experiment was performed in order to estimate the effect of a more competitive solvent in the binding strength of the examined monomer. Thus, the whole experiment was repeated this time using as solvent DMSO-d$_6$ containing 10% D$_2$O. As expected, a dramatic decrease in the association constant value was observed, namely the obtained value was 247±8.6, although, considering the environment in which the experiment was performed, this can be considered as significant binding strength.

8.5.3.d

Host (Monomer): N-(3-trifluoromethylphenyl)-N'-(4-vinylphenyl)urea (5mM)

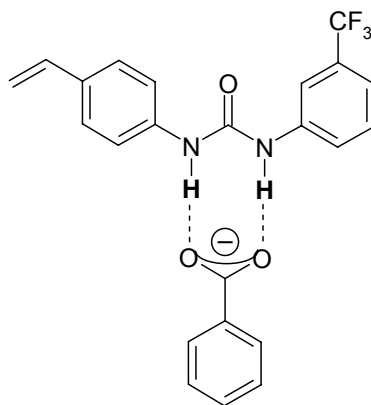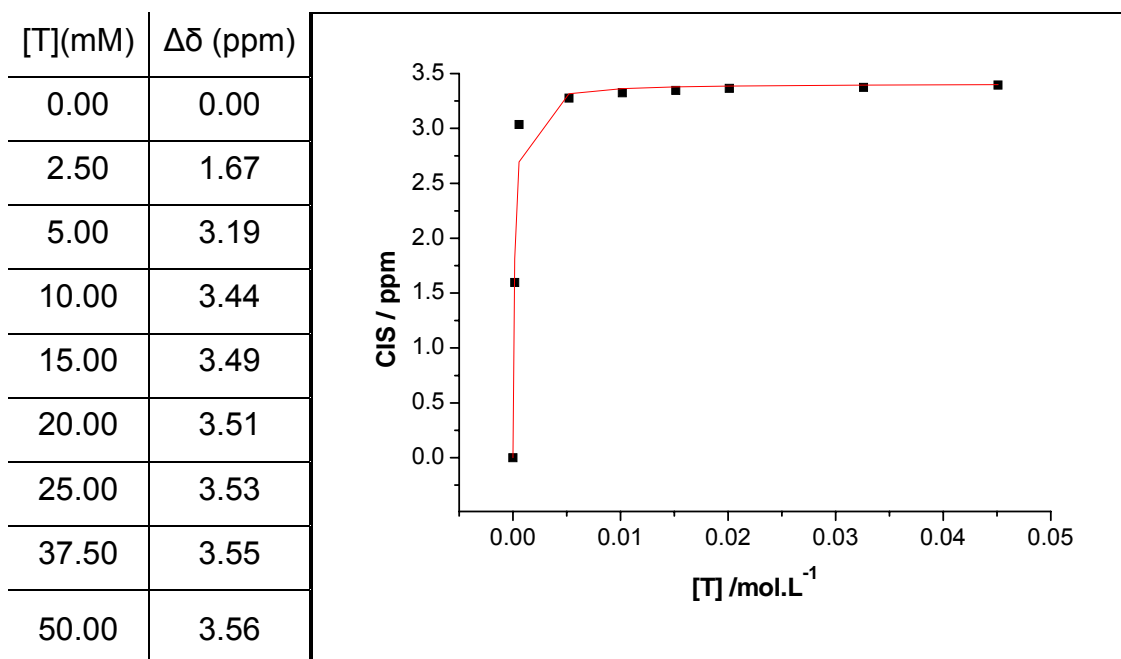Guest (Template): tetrabutylammonium benzoate (varied from 0-50mM)

Solvent: DMSO-d$_6$.

Figure 8.17: Proposed complexation mode. (Followed protons in bold)

[T](mM)	Δδ (ppm)
0.00	0.00
2.50	1.67
5.00	3.19
10.00	3.44
15.00	3.49
20.00	3.51
25.00	3.53
37.50	3.55
50.00	3.56

The curve was fitted by non-linear regression using Origin 5.0 and the association constant for this complex was calculated K$_a$= 6460±1133 M^{-1}, in DMSO-d$_6$. The result obtained by following the CIS of the second urea proton is 6580±1097 M^{-1}, in very good agreement with the result obtained by following the first proton.

8.5.3.e

Host (Monomer): N-phenyl-N'-(4-vinylphenyl)urea (5mM)

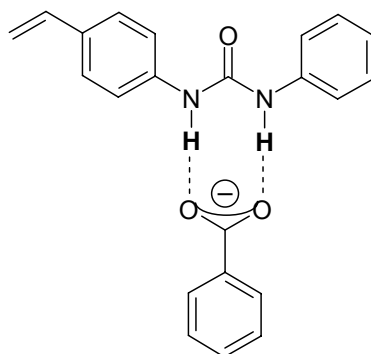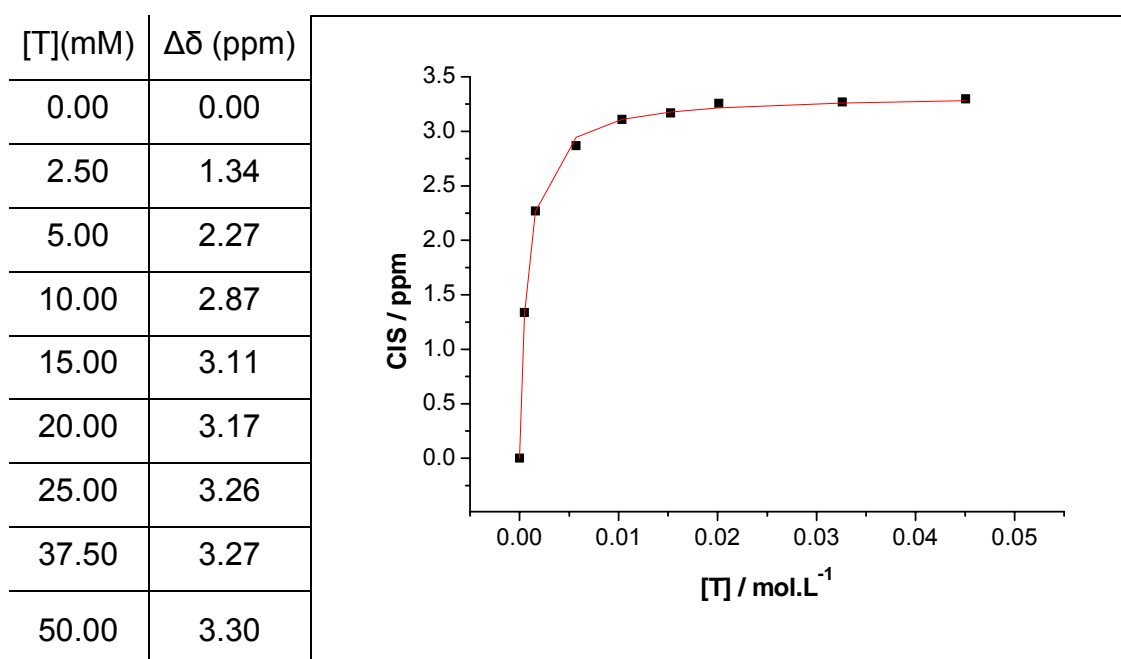Guest (Template): tetrabutylammonium benzoate (varied from 0-50mM)

Solvent: DMSO-d_6.

Figure 8.18: Proposed complexation mode. (Followed protons in bold)

[T](mM)	Δδ (ppm)
0.00	0.00
2.50	1.34
5.00	2.27
10.00	2.87
15.00	3.11
20.00	3.17
25.00	3.26
37.50	3.27
50.00	3.30

The curve was fitted by non-linear regression using Origin 5.0 and the association constant for this complex was calculated K_a= 1318±49 M^{-1}, in DMSO-d_6. The result obtained by following the CIS of the second urea proton is 1327±47 M^{-1}, in very good agreement with the result obtained by following the first proton.

8.5.3.f

Host (Monomer):

1-[1-(3-Isopropenylphenyl)-1-methylethyl]-3-[4-[3-[1-(3-isopropenylphenyl)-1-methylethyl]ureidomethyl]benzyl]urea (5mM)

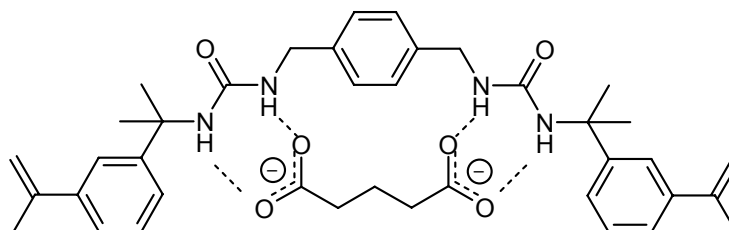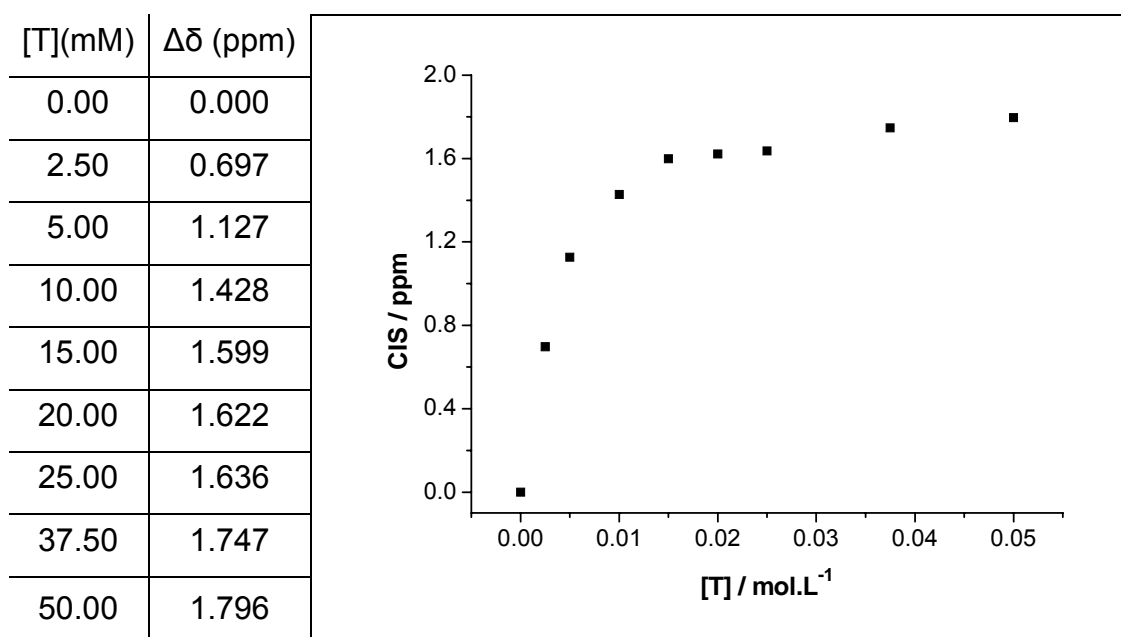Guest (Template): bis-tetrabutylammonium glutarate (varied from 0-50mM)

Solvent: DMSO-d$_6$.

Figure 8.19:   *Proposed complexation mode.*

[T](mM)	Δδ (ppm)
0.00	0.000
2.50	0.697
5.00	1.127
10.00	1.428
15.00	1.599
20.00	1.622
25.00	1.636
37.50	1.747
50.00	1.796

The curve was fitted by non-linear regression using Origin 5.0 and the association constant for this complex was calculated K_a= 1500±200 M^{-1}, in DMSO-d$_6$. The same result was obtained following both the "inner" and the "outer" urea protons.